ISSN: 2164-5388 Volume 11, Number 1, January 2021

Scientific Research Publishing

Open Journal of Biophysics

ISSN: 2164-5388

https://www.scirp.org/journal/ojbiphy

Journal Editorial Board

ISSN Print: 2164-5388 ISSN Online: 2164-5396
https://www.scirp.org/journal/ojbiphy

Associate Editors

Editorial Board

Scientific Research Publishing

Open Journal of Biophysics, 2021, 11, 1-132
https://www.scirp.org/journal/ojbiphy
ISSN Online: 2164-5396
ISSN Print: 2164-5388

Table of Contents

Volume 11 Number 1 January 2021

Open Journal of Biophysics (OJBIPHY)
Journal Information

SUBSCRIPTIONS

The *Open Journal of Biophysics* (Online at Scientific Research Publishing, https://www.scirp.org/) is published quarterly by Scientific Research Publishing, Inc., USA.

Subscription rates:
Print: $79 per issue.
To subscribe, please contact Journals Subscriptions Department, E-mail: sub@scirp.org

SERVICES

Advertisements
Advertisement Sales Department, E-mail: service@scirp.org

Reprints (minimum quantity 100 copies)
Reprints Co-ordinator, Scientific Research Publishing, Inc., USA.
E-mail: sub@scirp.org

COPYRIGHT

PRODUCTION INFORMATION

For manuscripts that have been accepted for publication, please contact:
E-mail: ojbiphy@scirp.org

Scientific Research Publishing

Open Journal of Biophysics, 2021, 11, 1-67
https://www.scirp.org/journal/ojbiphy
ISSN Online: 2164-5396
ISSN Print: 2164-5388

A Bioelectromagnetic Proposal Approaching the Complex Challenges of COVID-19

Andras Szasz

Biotechnics Department, St. Istvan University, Godollo, Hungary
Email: szasz.andras@gek.szie.hu

How to cite this paper: Szasz, A. (2021) A Bioelectromagnetic Proposal Approaching the Complex Challenges of COVID-19. *Open Journal of Biophysics*, **11**, 1-67.
https://doi.org/10.4236/ojbiphy.2021.111001

Received: November 11, 2020
Accepted: December 21, 2020
Published: December 24, 2020

Abstract

The COVID-19 pandemic has experienced unprecedented limitations and extraordinary scientific efforts to address this exceptional situation. Despite blanket closures that have resulted in significant financial constraints and losses around the world, research has an "unlimited" budget, with an exceptional concentration of medical and scientific care on a single topic: understanding the mechanisms for overcoming the disease. A large number of clinical trials have been launched with different drugs that have been behind different concepts and solutions. I would like to focus on the complexity aspect of COVID-19. Living systems are organized in a complex way, which implies dynamic stochastic phenomena, and deterministic reductionism can mislead research. When research focuses on individual molecules or pathways as products, it is distracted from the processes in which these products operate, thus neglecting the complex interactions between regulations and feedback controls. Common problems in product-oriented research are articulated as "double-edged swords", "Janus behavior", "two-sided action", with a simple question: "friend or foe?" I focus on the missing complexity. I propose a bioelectromagnetic process that can maintain a complex approach, affecting processes rather than products. This hypothetical proposal is not a comprehensive solution. Complexity itself limits the overall effects of causing "miracles". Well-designed electromagnetic effects can support current efforts and, in combination with intensively developed pharmaceuticals, bring us closer to a pharmaceutical solution against COVID-19.

Keywords

SARS-Cov-2, Homeostasis, Feedback Mechanisms, Biophysical Selection, Modulated-Electro-Hyperthermia, mEHT, Oncothermia, Vaccination

Graphical Abstract: Targeting the well-known and measured hallmarks of the infection does not deliver a cure. The process which produces "hallmarks" has to be considered in its dynamism. Instead of "products", we have to concentrate on the "processes".

1. Introduction

Human coronavirus-induced severe acute respiratory syndrome (SARS-CoV) first appeared in March 2003 [1] [2]. The current global pandemic is a disease called COVID-19. It is caused by severe acute respiratory syndrome coronavirus 2 (SARS-CoV-2). It is the third known coronavirus disease, probably zoonotic, after SARS-CoV-1 and the Middle East respiratory syndrome (MERS). The new coronavirus strain was recognized for the first time in Wuhan, China [3]. It is classified as SARS-CoV-2, and the COVID-19 pandemic was declared on March 11 by the WHO [4]. The number of people affected by COVID-19 is exceptional. The epidemiological investigation shows the validity of the networking complexity (long-tail distribution). SARS-CoV-2 follows approximately the 80/20 law [5], which means that 80% of transmissions occur by 20% of infected individuals, "super-spreaders" contagious" [6]. The analyses of the network show how "super-spreader" individuals spread the disease, locating "super-susceptible sites" [7]. Viruses appear active for quite some time on various surfaces [8], promoting the potency of pandemic danger [9]. The SARS-CoV-2 has much in common with previous coronaviruses, but their essential characteristics clearly differ [10]. The similarities allow us to use some experiences from previous viruses, such as slowing down the host's inflammatory response or using some antibodies or compounds that neutralize cytokines, but the essential challenge of complete therapy remains unresolved today.

The tipping point of the COVID-19 pandemic was seriously underestimated at the onset of the disease [11]. The SARS-CoV-V2 coronavirus behind the pandemic is a "great imitator" [12] showing symptoms of other simple diseases. You may be asymptomatic, or you may have simple symptoms like a runny nose.

However, it differs completely from an upper respiratory tract infection (URI). Later, when the disease develops, you may have more severe symptoms such as loss of smell, fatigue, vomiting, diarrhea, abdominal pain, muscle aches, and even whole-body symptoms such as rashes or redness. Severe organic damage (heart failure, kidney damage, liver damage, etc.) is also possible, which usually occurs as a complication after the period of curative treatment. The long incubation period and mild symptoms of URI do not alert the patient, and many times when the disease worsens, it is too late to avoid harm. It should be noted that the relative "weakness" of SARS-Cov-2 compared to other viral infections that manifest its possible asymptomatic or misdiagnosed cold symptoms is also the strength of this virus. Asymptomatic and unrecognized presymptomatic individuals promote viral shedding by improving community transmission. URIs' symptoms do not alert the patient, and, many times, when the disease becomes severe, it is too late to prevent transmission. Since the long, possibly asymptomatic incubation period allows the virus to multiply in large numbers in the subject, the virus will inadvertently spread to other people and accelerate the pandemic.

Massive research has begun with the advent of the COVID-19 disease to understand the causal effects of SARS-CoV-2 and other related viruses [13]. The goal of elucidating its infection mechanism is vivid, and, unfortunately, the solution is still waiting. 8764 publications (Aug. 10, 2020) had been published on the subject [14], including the record start of several clinical trials [15], and 68 ongoing clinical trials (Sep. 27, 2020) are also attempting to develop appropriate prevention and treatment [16]. Our knowledge is expanding day by day, and probably when this article appears, we will have more vital information on the subject than we have now. This is why I focus more on the general challenges, mainly on the on-demand hypothesis of the paradigm shift of SARS research.

The central request for successful clinical therapy is an accurate understanding of the infection mechanism, given its complexity, which is determined by the interrelated physiological feedback mechanisms of human homeostatic regulation. The human body has developed defense mechanisms to prevent the growth and multiplication of invading pathogens. One of the oldest immune response types is the termination of cells infected with bacterial pathogens by apoptosis [17]. In plants, pathogens elicit a hypersensitivity response (HR), which induces systemic acquired resistance (SAR) [18] as a form of apoptosis. In animals and humans, dynamic homeostatic processes regulate the activation of apoptosis in a highly controlled manner. In both animals and plants, apoptosis is promoted by the production of anti-inflammatory molecules that are associated with tissue development and homeostasis [19]. Despite the differences, both types of apoptosis are associated with the induction of similar morphological characteristics, including membrane blowing, cytosolic fragmentation, nuclear condensation, and fragmentation, as well as biochemical events such as degradation of genomic DNA, proteolysis, and lipid redistribution of membrane [20] [21]. These changes are mainly due to the activation of a family of cysteine proteases, cas-

pases [22] [23]. Furthermore, infected host cells produce defensins, innate immune host protection peptides [24], and induce anti-inflammatory cytokines that play an important role in eliminating the invading pathogen.

Proper vaccination could be decisive in preventing infection and stopping the pandemic, but it could also be an effective curative therapy tool for patients at different stages of the disease. So far, many solutions have been proposed to overcome the pandemic [25]. Many drugs are proposed for therapies [26], but none have currently been shown to be successful. The use of various virus-specific antibodies for active treatment is currently being tested more intensively [27]. Many companies compete in the race to develop antiviral drugs and vaccines to defeat the pandemic [28]. Research on basic vaccines, such as nucleic acid-based vaccines (RNA or DNA vaccine), recombinant protein vaccines, and viral vector-based vaccines, has not produced the results expected so far [14].

Inhibition of coronavirus cell penetration (e.g., Hydroxycoquine [29], Umifenovir (arbidol) [30], etc.), inhibition of virus replication (e.g., Remdesivir [31] [32], Ritonavir [33], Ribavirin [34], Oseltamivir (Tamiflu) [35], Favipiravir [30], etc.), the synthesis of bacterial proteins, the use of antiparasitic agents (Ivermectin), the rethinking of other drugs previously used against the virus (Lopinavir [36], Ritonavir [37]), or plasma extracts from people who have recovered (immunoglobulins [38]), or monoclonal antibodies that enhance general immunity (interferon) (for example, tocilizumab [39]), have achieved clinical phase. However, many of them fail to the point of expectations [14]. The method that had superheated hopes, convalescent plasma from patients, who developed effective antibodies and transferred it as passive antibody treatment to patients in the intensive care unit (ICU), has not yet been tested [40], and the decision on the validity of the "hopes" could not be made [41]. The drug hydroxycoquine, despite enormous political and financial support, was unable to produce satisfactory efficacy as the Cochrane meta-analysis had shown [42]. A new trend to develop vaccines is related to interferons [43] [44]. The intranasal application of recombinant interferon (rINF-α-2b) effectively shortened the duration and reduced the severity of coronavirus cold symptoms. A comprehensive summary of the activities in vaccine development reviews the actualities [45].

Numerous drugs were tested in preclinical experiments with additional expectations, but most did not pass safety tests. One of the recent is that the University of Pittsburgh has published some fascinating information about its success with one component (Ab8) of the antibody. It had been successfully tested in animal experiments as a possible viral vaccine [46]. However, it has yet to reach any human research, so in our opinion, the "news flash" is too early. Vector-based heterologous prime-boost immunization (Gam-COVID-Vac, [Sputnik-V]) is presently the first approved drug in the world [47]. The international professional community has serious doubts about this approval for security reasons [48]. Experts explain the irresponsible side of the decision to certify this treatment [49]. Currently, we do not have enough knowledge about its effects, but doubts are increasing. A promising drug (AZD1222) and its clinical trial de-

veloped in collaboration with Astra-Zeneca and the University of Oxford [50]. However, the studies were stopped due to serious side effects [51] and then partially reauthorized, but doubts remain [52].

The meta-analysis of the clinical trials of new, hopeful medications (Remdesivir, Hydroxychloroquine, Lopinavir, and Interferon) had little or no effect on hospitalized patients with COVID-19 [53]. The evaluation was based on overall mortality, initiation of ventilation, and duration of hospital stay. No drug reduced the mortality (in unventilated patients or any other subgroup of entry characteristics), initiation of ventilation, or hospitalization duration. 405 hospitals in 30 countries 11.266 adults were randomized, with 2750 allocated Remdesivir, 954 Hydroxychloroquine, 1411 Lopinavir, 651 Interferon plus Lopinavir, 1412 only Interferon, and 4088 no study drugs were involved in the analysis. Presently (middle of October 2020) two extensive clinical studies are on halt because of safety concerns [54] [55].

The currently known curative support (not vaccination) proven in clinical trials are glucocorticosteroids and corticosteroids [28]. Dexamethasone (a corticosteroid) with respiratory support is the first drug that has been shown to improve survival in COVID-19 disease [56]. These steroids are anti-inflammatory immunosuppressants. Immunosuppression is required to suppress overstimulated immune responses. This is very helpful against a cytokine storm that occurs late in the disease. Despite the apparent contradiction to steroids' success, immune system support provides the best means when we consider the complex integration of immune effects into the body's regulatory system. The immune effects could cause prevention to escalate the disease while blocking autoimmune reactions with steroids is needed in the severe stages when cytokine storm appears to be the most challenging danger.

The task is to regulate the complex processes rather than control individual molecular products. The disease's complexity can only be managed through the therapy's appropriate complexity. With a unique molecular healing effect, a "miracle drug", we can expect total success, that hope is unrealistic. The possibility of a paradigm shift lies in the tracking of physiological complexity, which essentially seeks to restore control at the system level rather than control individual threads. For this, the use of the immune system is more pronounced, which can best be achieved by a combination of chemical and physical methods.

2. Challenges of the Complexity

Medical history strikes a balance between two comprehensive but competing sets of methodologies: the inductive and deductive approaches. The inductive studies the details of the system, like the organs, tissues, cells, organelles, etc. and builds the whole body based on data from the parts and their function. The deductive view focuses on the whole body as a unit, taking it into its environmental interactions and deduces from them the to the parts, to organs and their functions. The two approaches build the diagnosis oppositely. The inductive is up from parts to the whole, while the deductive is down, from whole to details. The in-

ductive system builds the complete system as workers do; the walls are built with bricks, while the engineer makes a general plan and breaks down deductively in detail how to connect the bricks to a functional structure. Both processes require professionals, and only together can they get the job done correctly. In medicine, a very similar situation occurs when an organ specialist studies the organ to determine a patient's health. We are well aware that having perfect organs does not mean that the system is organized healthily. Conversely, as the deductive practitioner claims, having a perfectly organized system does not mean that all the system's organs are functioning properly. Both approaches and their cross-talks and regulations are necessary to ensure healthy functioning, Figure 1.

Unfortunately, the current clinical paradigm is very unbalanced in terms of inductive/deductive attitudes. Well-developed and educated medical knowledge characterizes the organ and its functions in the description of professionally well-trained organ specialists; but the whole system, the patient, does not receive as much attention. The same can be observed in the field of therapies: the focus is on the actual local disease drugs, paying less attention to the patient as a whole.

Biological complexity is a well-proven fact based on physical and physiological principles [57]. The stochastic approach is fundamental in biological dynamism, including RNA polymerization and the most basic gene exchanges [58]. Darwin developed the uncertain (non-deterministic) idea through the theory of evolution that introduces probability in biological species development. This idea drives biological development everywhere. Contrary to the complexity of human organisms, the paradigm of modern medical research loses it. The concept of homeostasis is ignored, and reductionist attempts to become the central dogma. This approach reduces the focus of medical actions to a set of the whole in almost isolated parts, components smaller and simpler than network interconnections, and hoping that the sum of these parts can explain the complete

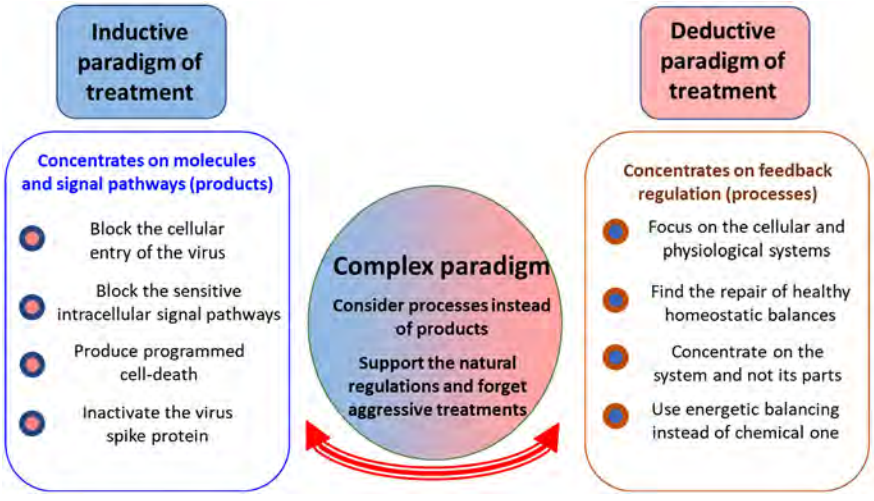

Figure 1. The complex thinking is the key to solve the problem of the present COVID-19 viral infection.

system. This reductionism contradicts the concept of physiology and also science in general.

The reductionist management and control of the disease are based on influencing, inhibiting, or assisting molecular interactions, mainly leading to adequate medication through the creation of the effects of known drugs or through physical intervention (such as ionizing radiation) to modify the chosen molecular task. The forcing influence of certain molecules and signaling pathways strongly determines the research's objective; complex interactive network processes are out of the majority of studies. However, living matter has a dynamic equilibrium (homeostasis) that implies a balance of sensitively adjusted feedback controls, showing the complexity of this highly organized material [59]. Complexity does not mean complication, but the intertwining of processes, which at each step seeks to have a dynamic and interconnected balance of suppressor-promoter pairs of the regulatory process [60]. Predominantly negative feedback characterizes these mechanisms. Homeostasis is often ignored and used as a static framework for effects [61]. The challenge is the complexity of living organs, the highly interconnected interactions between the parts. The demand to understand and use dynamic equilibrium develops a new paradigm for investigating the living matter, which requires a stochastic approach (probability of events dependent on time) instead of conventional thinking that requires deterministic changes [62]. The dynamic homeostatic equilibrium keeps the system in a stable but constantly changing state. The first efforts to show this complexity were made at the beginning of the last century by von Bertalanffy with general systems theory [63] emphasizing the openness of the living organisms, the deep embedment in the environmental interactions, Figure 2. All living organisms

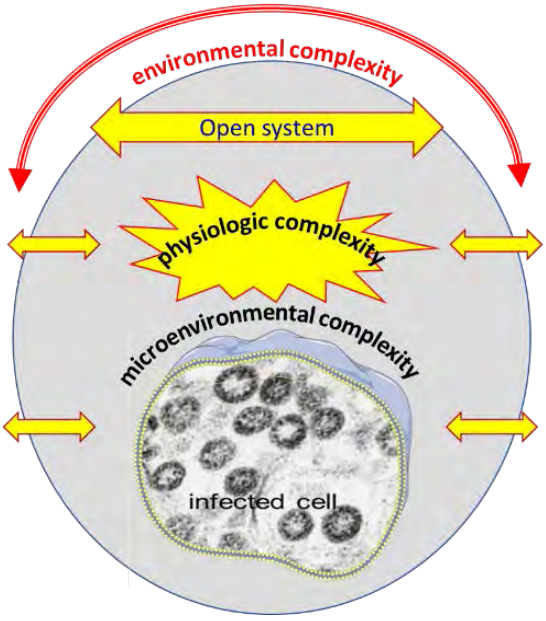

Figure 2. The viral infection is embedded in a complex network of interactions and species.

are open systems, taking energy from the environment, and emitting waste there. A living subject's environment is a network of the non-living and living objects that relate to the subject and connected with each other. The lives modify the environment, and vice versa. The environment modifies the lives. The infections are excellent examples of this complex interconnection. The infected cells are deeply embedded in the complex interactions, so the attempt to stop the infection with a simple one-to-one deterministic approach is a mistake.

The research objective of drug development's actions is to modify the imbalanced inhibitor-promoter system with agonist-antagonist molecules [64]. Turing's pioneering work on complexity established the first exact discipline of the life sciences, "decoded of the life, the mathematical biology [65]. The formulation of morphogenesis was the first complex description, which could explain the chemical basis of dynamical interactions, and successfully predicted the oscillating chemical reactions. Most of the pharma products miss Turing's dynamism, ignoring the fundamental complexity. Agonist ligands bind to a receptor, while antagonist ligands prevent an agonist from binding to a receptor, trying to balance a dynamic equilibrium. Most of the researches miss the dynamical feedback mechanisms which make the agonis/antagonist relations complex. One part of the complex network appears in the adverse effects of the difference in agonist-antagonist pair drugs.

In most cases, the enzyme inhibition could occur due to the modification of homeostatic regulation [66]. The important principle is the feedback mechanism, which controls the balance within a predetermined range around the reference value. It is usually well modeled with fuzzy logic, an approach to counting "degrees of truth" rather than the usual "true or false" decisions [67]. This logic governs homeostatic equilibria in all ranges of space and time in living systems. This uncertain value is undoubtedly in a controlled reference interval, where strongly interconnected negative feedback loops regulate the balance in the micro and macro ranges, forming the system's dynamic stability. Due to this dynamism, the proposed paradigm shift towards the living system's complexity is not an easy turn.

The disease damages the network's complexity in the human body, forming local or systemic sub-units, which declines from the equilibrium of the entire body. The homeostatic dynamic equilibrium is at least partially out of control. Restoring healthy complex mechanisms requires a careful balance of actions. The chosen treatment has to fit the complex challenges of the patient's individual conditions, the environmental loads, and the physiologic (homeostatic) control **Figure 3**. It is easy to make an agonist or antagonist change the faulty mechanisms, but it is not easy to keep the system's balance. The unstable spatio-temporal regulation and the variation of doses of infection destroy the homeostatic balance of the healthy dynamics of the infected region. In this way, the repairing process in a focused part of the system can induce adverse effects in whole, challenging safety. Many experiments went through rigorous testing in the preclinical phase, and some drugs made it possible for clinical trials. These

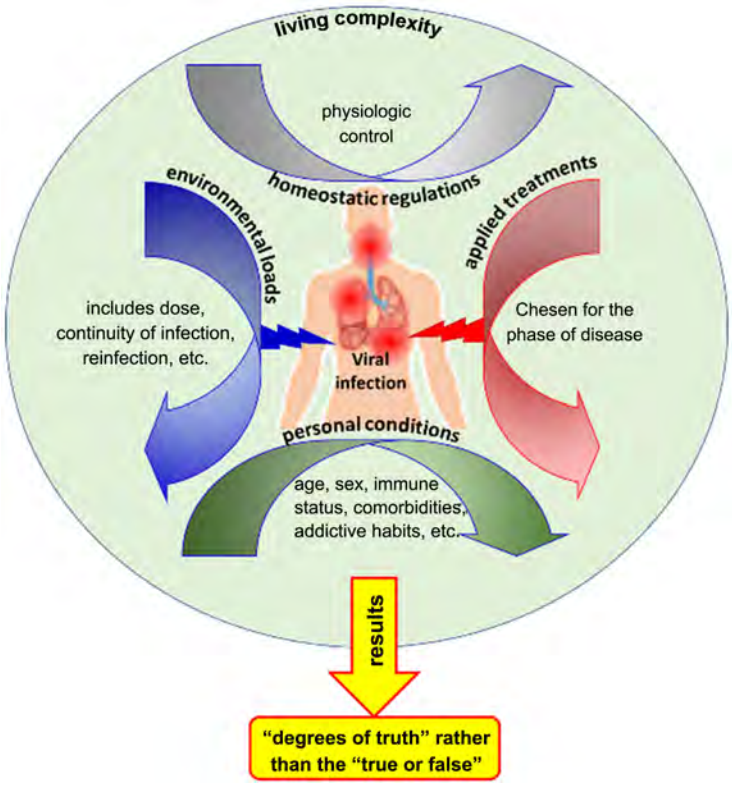

Figure 3. The complex control of the living state has to be counted at the chosen treatment.

trials require long periods of time because safety and side effects need to be monitored in a large patient cohort population and over a long follow-up period. Furthermore, the dosing and practice protocol takes time to fix, considering that "there is only one difference between the drug and the poison: the dose".

Serious side effects can occur when drug rebalancing does not pay enough attention to the relationships built into the balances, which are often dose-related. The often serious side effects of chemotherapies depend in part on the imbalance situation, and the risk/benefit ratio decides their applicability [68]. Pharmacodynamics offers a mixed-effect agonist/antagonist (selective receptor modulation) approach, acting as an agonist for some types of receptors or some tissues and an antagonist for others. Correcting one side of the scale by a drastic regulation, side effects appear as a whole because the unbalance appears in the unfocused subsystem [69]. The need to move the paradigm towards the pharmaceutical industry has also been explicitly articulated in Science Magazine [70].

A fundamental reason is why the transfer of research results cannot find a faster path from laboratory to clinical applications. The problem is that the present investigation paradigm is losing complexity due to our reductionism, leading the investigation in the wrong direction. The question is addressed: "where did the medicine go wrong" and in the response of B. West, the chief scientist of the United States Army laboratory, formulates the necessary task: "rediscover the path to complexity" [71].

Our task is to assist the patient's natural dynamic homeostasis, which again underscores the importance of patient-oriented therapies. Patient orientation involves using the patient's homeostatic capacity, regulating the patient to drive processes and establish general control. For this, it is not enough to administer an agonist or antagonist; regulation of the processes is needed that balances the dynamic agonist-antagonist balance in healthy control. The promoter-suppressor circles characterize all the dynamical changes in the organism from the molecular to the systemic level. These controlling circles are deeply interconnected, and a modification in one could affect multiple, directly not connected, but networked regulations (Figure 4).

When the research identifies a defect of one of the particular regulating circles, a severe challenge occurs. Various solutions could be applied to correct the damaged regulation in an isolated circle (Figure 5). Albeit the study and modification of one regulating ring in isolated conditions offer a relatively easy solution, the consequences in the complex network are unconditionally out of control. The lack of complexity in the research concepts in practice regularly shows its negative side: it is easy to develop a drug that eradicates the virus. Unfortunately, it is also often harmful to human lives. The reason is simple: when the

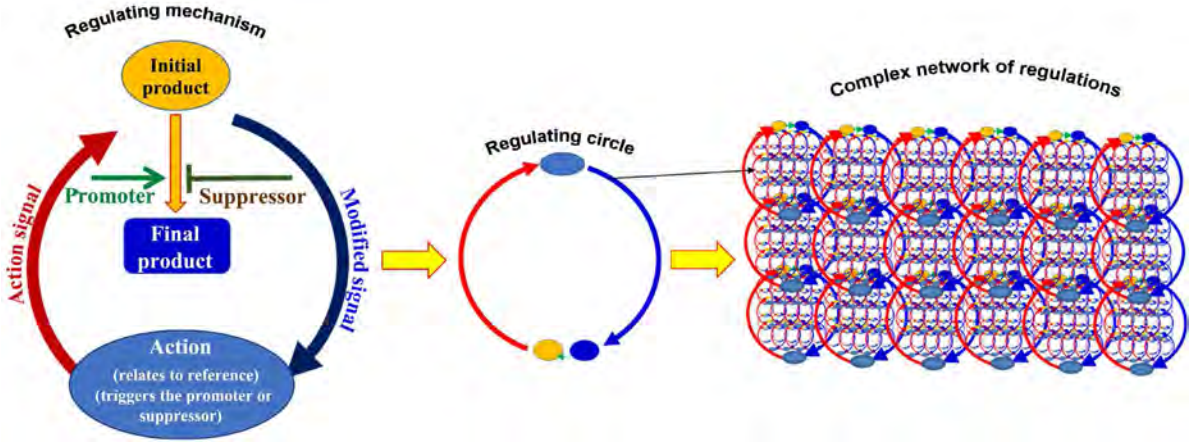

Figure 4. The regulation circle of promoter-suppressor balance guides all the processes in the body. These are interconnected in a large complex network, and any individual change could cause an unexpected and unpredictable "avalanche" of the changes.

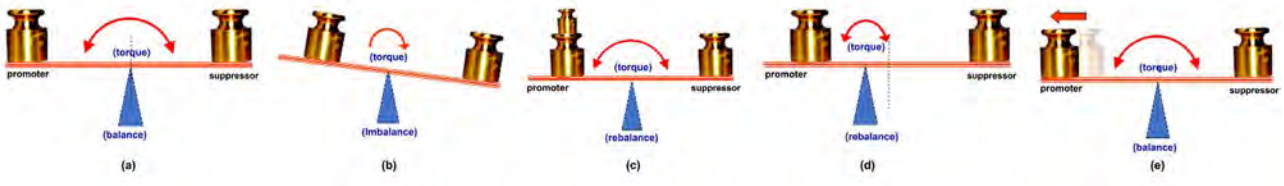

Figure 5. The balancing corrections of one certain promoter/suppressor pair. (a) A healthy balance of a certain process (a part of normal homeostasis); (b) A pair of promoter/suppressor is out-balanced; (c) Rebalancing of a certain process, but the extra "weight" unbalances other regulatory pairs, where the promoters are also involved; (d) Resetting the reference value for rebalancing, but it disturbs all the regulatory links, connected to both, promoter and suppressor; (e) Rebalancing by catching the complex process in a network, where the certain pair is involved.

drug produces an imbalance in complex dynamic regulation, it could help in the desired part (killing the viral infection), but the preference suppresses other processes, and the system goes haywire.

Our research task starts being complex, and new ideas are necessary for going over the obstacles. The focus changes. Re-establishing the regulation does not work correctly when we make rebalancing by the kind of extra promoter (like in **Figure 5(c)**), or by shifting the reference value of regulation (like in **Figure 5(d)**), due to the complex network reacts making the complete homeostatic control effective. The physiological changes can cause unexpected consequences and appear new symptoms, called adverse effects. The task is to correct the regulation by taking care of the complexity and re-establishing the regulation circle smoothly with the natural homeostatic mechanisms (like in **Figure 5(e)**). Note our aggressive actions based on the high scientific ego leads us to a dead-end. We have to recognize the natural complexity and help these natural interconnections to correct the regulatory fault. Ignoring this humble serving of natural process forces the complex control to fight against the actual fault to repair and against our aggressive "invasion"-like action.

We rarely recognize that the current dominant medical paradigm often ignores patient homeostasis [61], even though it is the central theory of physiology that unifies knowledge about the system's self-regulatory processes. Hierarchical process control enables a wide range of dynamic adaptation to changing internal and external conditions. The center of the new paradigm is the homeostasis of the organism. It is bad news that life's dynamic processes are probabilistic, but good news that this "chaos" is by no means the category that has no order [72]. The well-organized harmonic hierarchy of dynamic complexity manifests itself well in the entire organism's interconnectedness and follows a bioscaling [73], which is universal for life [74].

The dominant universality shows multiple-scale behavior at all levels, from the molecular to the organism [75], emphasizing the importance of interconnected and interacting networks. The spatio-temporal self-similarity [76] creates a self-organized network [77]. Learning this, a new science is emerging: the "fractal physiology" [78] [79]. The fractal-based biological scale could serve as a model of developmental dynamism by describing the main characteristics of the clinical stages of viral disease [80]. Fractal analysis gives a structural idea of viral rearrangement in infected tissue [81]. In a matter of time, dynamic interactions have a long-range correlation time lag, composing harmony in the system [82]. External stimuli must conform to homeostatic harmony [83].

Instead of deterministic expectations of each molecular change, complex considerations must focus on the dynamic process and not on the resulting or artificially introduced substances. Understanding the living dynamism of deeply interconnected events implies a necessary paradigm shift in modern medicine, moving from conventional deterministic methodology to complex approaches, considering stochastic processes [84].

The missing homeostatic harmony disrupts the healthy state and leads to dis-

ease. The homeostatic balance of promotion and inhibition is activated in parallel "like twins" [85]. Deterministic "one-sided" actions alter homeostasis's balance and reduce the chances of success by causing adverse reactions. Effective therapy attempts to restore the lost dynamic balance in harmony with and without imposing restrictions against natural personal abilities. This approach allows individualized therapy, taking into account the specific characteristics of the patient [85]. Proper diagnosis finds interrupted control of regulatory mechanisms and points to the damage of self-organizing mechanisms [62]. The therapeutic intention launches modifications that help the natural repair mechanisms find the self-controlled and self-organized homeostatic state.

The medical task must be focused on controllable regulations, so thinking on one side of the action could have serious consequences. Curing the patient as a complete organism has to be in the center of medical efforts, and the local infection is only a part of it. The focus on the patient's defective part should be shifted to a patient-oriented approach (Figure 6). The patient is a complex system, so medical therapy must concentrate on this dynamic equilibrium.

The missing complexity is well illustrated by the fluctuating evaluation of AZD1222, [50] [51] [52]. We have to evaluate all sides of complex phenomena before medical actions [86]. Similar challenges have appeared in other large, well

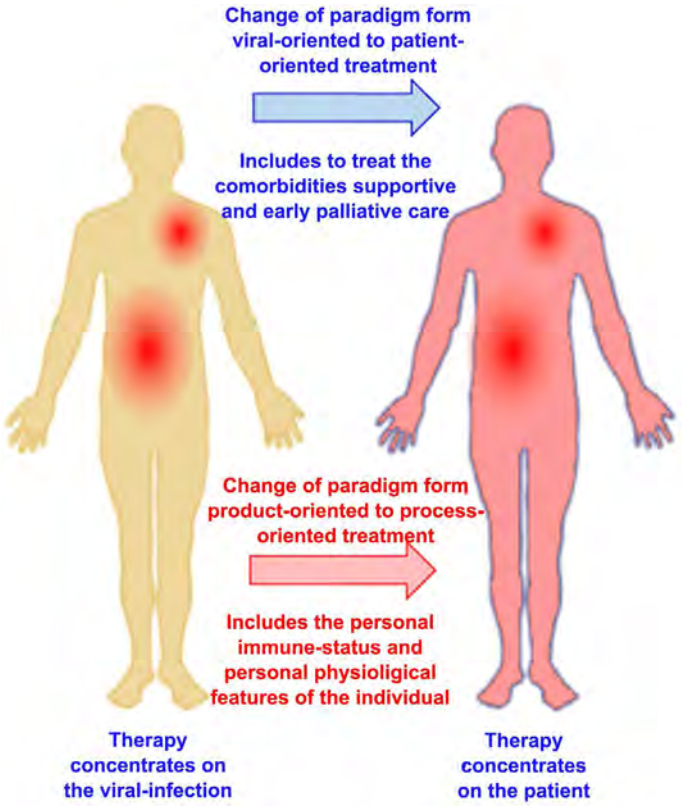

Figure 6. The main clinical focus has to be on the entire patient with their actual personal conditions. The viral-oriented clinical approach must be shifted to the patient oriented one, concentration of the developing processes more than on the developed products of these.

supported clinical trials [54] [55], too. The strictly deterministic clinical decisions must be differentiated. Even though the symptoms are similar, the complete unification of patients' collected cohort does not result in success. The individual homeostatic regulation affects the actual principal treatment protocol, and it could develop complications.

Here is a key issue. How can we ensure homeostatic equilibrium if we artificially interfere with a complex stochastic system's functioning? How can we direct natural processes towards the solution? The solution is probably to support the existing complexity of the living matter, removing the complex balance disorder as harmoniously as possible. The treatment strategy has to be formed as the army leads a war: Attacking the enemy's weakest points and avoiding being embroiled in a conflict with their most potent forces. In this medical "war", we could follow the winning strategy. The most powerful forces of the virus are in its process of replication. Of course, it could be the goal of stopping replication initiated within cells, as many of the drug developments (e.g. Lopinavir, GRL0617, Ribavirin, Remdesivir, Favipiravir, Alisporivir, etc.). Thus drive the blocking of various signal pathways intracellularly [87]; however, it is arduous work, and we must expect many adverse effects due to unwanted changes in general cellular mechanisms. We have to focus on processes rather than products [70]. It nicely shows the problem of complexity when the successful use of immunosuppressive steroids has caused some surprises when the mainstream of viral research favors immune enhancement.

The expansion of COVID-19 clearly divides clinical actions into three interconnected parts. The first period of clinical care begins when the first symptoms appear. In the first period of the infection the focus has to block the further aggravation of the disease. The innate immune actions are in the front of the fight against the virus. Intent to stabilize the patient's condition was unsuccessful, and the patient experiences a more severe illness, the task changes. The patient needs medical help in severe symptoms like shortness of breath, fatigue, and other quality of life suppressants. In the third period, when the previous two could not block development, emergency medicine, mostly in the intensive care unit (ICU) continues the treatment to prevent death. All three periods have some specialties, which we will discuss below in this article.

2.1. Challenges of the Physiologic Regulation and Control

The first coronavirus pandemic (SARS-CoV-1) had shown a fundamental role of the angiotensin-converting enzyme-2 (ACE2) in the cellular invasion of the virus [88]. The same had also been observed in the SARS-CoV-2 virus [89] [90]. The enzyme ACE2 converts angiotensin I to angiotensin 1-9, just as ACE converts angiotensin I to angiotensin II, which again ACE2 converts to angiotensin 1-7. ACE inhibitors generally block the conversion of angiotensin I to II, while angiotensin receptor blockers (ARBs) block the angiotensin II receptor.

The invasion process towards internalization in cells fundamentally depends on the peak glycoprotein (S) (fundamentally on the S1 subunit) of the SARS-CoV-2

virus [91]. The cellular entry of SARS-CoV-2 is promoted by type II transmembrane serine proteases (TTSP) [92]. The participation of TTSPs is confirmed in the viral entry of SARS-CoV-2 into cells. The participating TTSPs are the transmembrane serine protease isoform 2 (TMPRSS2) [93], the lysosomal endopeptidase cathepsin-L (CTSL) [94], the proprotein peptidase furin [95]. The heparan sulfate proteoglycans [96] [97], which are potentially membrane-bound in the glycocalyx layer of epithelial cells [98] could be involved as well, as it was proposed earlier, before COVID-19 [99] [100]. Heparan sulfate could block SARS-CoV-2 infection [101], and, consequently, the multiple clinical application of heparin was proposed [102] [103] [104].

TTSPs, firstly TMPRSS2 [94], facilitate binding to ACE2. The virus mainly uses the ACE2 receptor to enter the host cell, with the help of TMPRSS2. When the receptor binds to the SARS spike protein (S), the process is preactivated by furin, cleaving the spike to prepare it for membrane fusion with the host cell. Furin's assistance in binding is a special feature of SARS-CoV-2, which helps the virus to penetrate the cell. These types of shared structures also appeared in highly pathogenic viruses, such as avian influenza. The frequent mutation capability is another risk of SARS-CoV-2 infection, which is usual in cases of RNA-based viruses.

Even though both SARS-CoV-1 and SARS-CoV-2 share the characteristic that the main receptor for viral entry is ACE2, there are essential differences in intensity. The binding affinity of human ACE2 to the receptor-binding domain (RBD, which selectively recognizes ACE2) is significantly higher in CoV-2 than in CoV-1 [105]. Interestingly, RBD's position also differs in the two viruses. The active state (standing) is more frequent in CoV-1 than in CoV-2, which apparently could mean a lower virus binding efficiency in COVID19. Unfortunately, higher binding compensates for hidden RBD, and more importantly, hidden RBD allows immune evasion, greatly improving its binding efficiency [102]. A significant part of the high SARS-CoV-2 infectivity connected with the new mutations in the RBD and the acquisition of a TTSP cleavage site in the S-spike protein. There are some formal, deterministic approaches to stop the viral replication by blocking the entry to the cells (**Figure 7**). These, however, could drastically modify some key steps of the replication mechanisms by homeostatic regulation. These all have attempted to develop drugs without concerns about its complex feedback effects. The feedbacks are considered as side effects only, and so their applications are rather limited. The symptoms of infection or the side effects of drugs correlate with the dysfunction of the complex homeostasis.

The ACE2 receptor has a central role in developing the disease, being the door to the virus's cellular invasion. What would be the medical intervention? The first logical deterministic answer is relatively straightforward: block the most probable "gate" of the ACE2 receiver [106]. Consequently, the application of the anti-ACE2 antagonist seems an optimal medication. In fact, viral infection in the cell could be drastically suppressed by blocking "entry." However, we learned

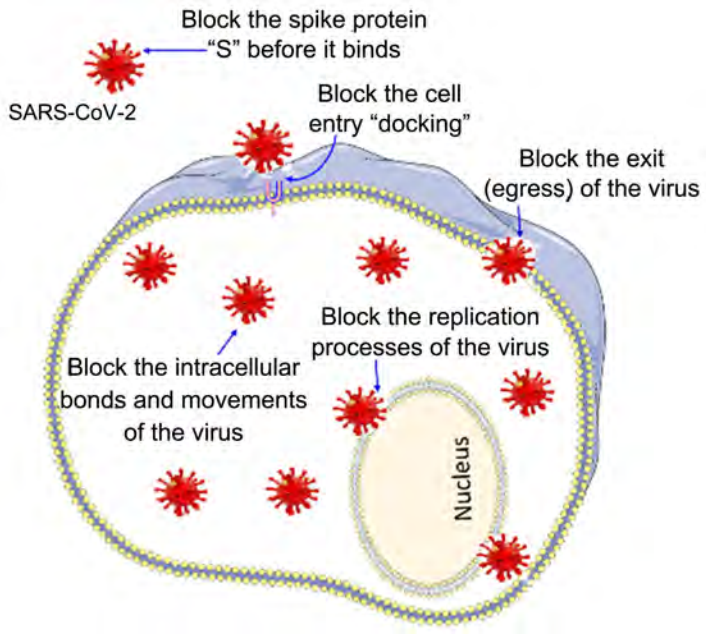

Figure 7. The basic steps to inhibit: neutralize the spike-protein of the virus, block the cellular entry of the virus, block the intracellular moving, bonding, block the RNA replication or block the egress of the newly produced virus from the cell.

that additional ACE2 inhibition could increase the imbalance, leading to the patient becoming critically ill. In many cases, it requires ICU care, and some of these became fatal. Not only is ACE2 a helper for virus invasion, but its double-edged actions address the question "Is it friend or foe?" [107]. The apparent contradiction illustrates the limits of the reductive deterministic thinking when the fundamental physiological knowledge of homeostatic regulation is not involved in the concepts and consequent clinical actions [70].

The series of built-in negative feedback mechanisms ensure the complete equilibrium of all participating molecules. ACE2 viral involvement dysfunction induces an imbalance in the RAS and, through this, involves the immune system (**Figure 8**). The immune connection was recognized at the beginning of the pandemic in China [108]. The massive interconnection of regulatory networks also points to the complexity of COVID and its interaction of the homeostatic system unbalanced by a viral infection. The unbalanced participation of ACE2 in SARS-CoV-2 explains why multiple symptoms can appear during infection, involving different organs that express a considerable amount of ACE and processes regulated by this enzyme.

As usual, in complex systems, ACE2 also has "two faces" [109], which are, in fact, multiple functions, deeply connected to the homeostatic complexity, which must be considered. The complex thinking takes attention to the participation of ACE2 in a wide range of physiological processes [110]. The actions of ACE2 include protecting against inflammation [111], compromising immunity [112], and protecting the active organ against hypertension, diabetes, and cardiovascular disease, as well as protecting against some types of acute lung injury [113].

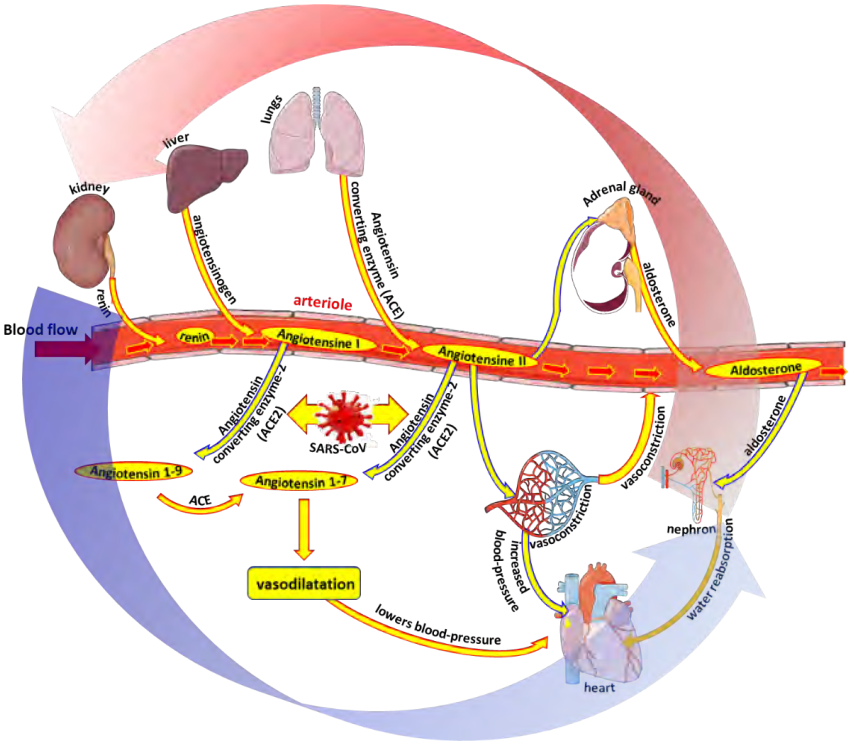

Figure 8. The complex RAS circle shows the interconnections and feedback of the various involved products during the regulation process. The most frequent attack of SARS-CoV is shown in influencing the ACE2 processes.

ACE2 plays an essential role in immune reactions that affect the innate and adaptive immune systems through the action of macrophages and neutrophils [114]. Inhibiting ACE2 could increase dangerous inflammation, grow reactive oxygen species (ROS), create vasoconstriction, and lead to thrombosis. The weakening of immune control could increase the risk of developing a critical condition and need ICU.

The challenge of inhibitors of the ACE enzyme (ACEIs) or angiotensin receptor blockers (ARBs) is reducing the severity of the consequences of virus invasion, reducing their mortality rate [115] [116] or out of balance causing other severe consequences (**Figure 9**). When the ACEI is administered in the wrong time or wrong dose, the regulatory function of ACE2 decreases and the disease may worsen. The patient could develop a severe or critical condition. However, the angiotensin-converting-enzyme gene has polymorphisms [117] capable of forming more than 160 versions [118]. This could cause inequalities in humans in the level of ACE expression [119], requesting more detailed information and consideration of the patient's personal status. On the other hand, a large study showed that ACEIs and ARBs were not associated with the infectivity of SARS-CoV-2. When the dosing of these administered according to the standard protocol for the patients suffering hypertension as comorbidity and had taken the medication regularly as they did before, the viral infection does not exacerbate [120]. These findings support the continuation of ACEI or ARB II among

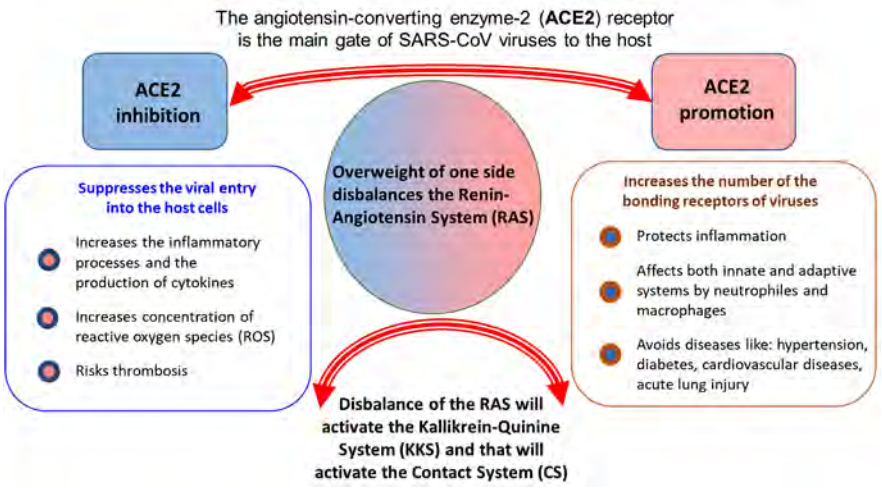

Figure 9. Typical balancing is shown in the most frequently studied ACE2 receptors. Their imbalance drives the RAS processes, which activate the connected KKS and CS circles too.

patients with coexisting hypertension, cardiovascular disease, and COVID-19 [121]. The ACE2 activation has a protective effect on lung injury, including acute respiratory distress syndrome (ARDS), so it could be a potential curative action in COVID-19 [122].

Current statistics show a correlation of COVID-19 with gender [123] [124], and age [125] of infected patients. Comorbidities, such as hypertension [126], diabetes [127], cardiovascular disease [128], asthma, chronic obstructive pulmonary disease (COPD) [129] can lead to serious difficulties. Triggering of comorbidities was also detected in SARS-CoV-1 infection in patients who did not have such damage before [130]. The virus can activate comorbidities like diabetes [131] [132], kidney disease [133] or induce cardiovascular damage [134]. Furthermore, the risk of multi-organ infection by the virus remained a challenge [135] too. An unhealthy lifestyle (such as smoking) and obesity are also risk factors [136] due to weakening the body's healthy physiological regulations. These risks of coronavirus infections have the same root. The virus attacks ACE2 receptors, which have high expression in these organs, causing an increased risk of ACE2 damage.

One of the further challenges in the pathogenesis of SARS-CoV-2 is the imbalance in RAS, which favors severe effects. Viral interstitial pneumonia and diffuse alveolar lung damage appear in early pathologic changes in COVID-19, and pulmonary edema is also commonly seen [137]. The possible extensive cytokine storm could develop the patient's critical condition, an acute lung injury causing an irreversible impairment of restrictive lung function and death. The RAS balance has complex actions on the immune system, and ACE2 may affect antiviral immunity in this context [138]. ACE2 downregulation overstimulates RAS [139], so ACE2 inhibition may decrease viral penetration potential, and altered RAS needs to be balanced. RAS maintains electrolyte and fluid balance and also regulates vascular resistance [140]. RAS imbalance could even cause oxida-

tive stress alone [140], inducing many diverse diseases in clinical practice [141].

The impoverished ACE2 availability with the expansion of the infection or the too intense ACEI/ARB activates the kallikrein-quinine system (KKS), counteracting the RAS [142], *i.e.* that is, any decrease or predominance causes the opposite corrective change in the paired system [143]. The counterbalance action covers multilevel interactions [144]. The RAS-KKS system's effect plays an important role in the entry of SARS-CoV-2 into cells [145]. The virus's extensive invasion causes a shortage of the ACE2 receptors, the widespread viral infection developing the ACE2 dysfunction, and it plays a major role in the induction of the fibrosis [146]. The altered RAS through KKS impacts on bradykinin [147], inducing its overexpression, eliciting an overwhelming action [148]. The central role of bradykinin in the worsening of symptoms as advanced infection binds to ACE2 enzymes to such an extent that its lack can increase bradykinin level. In this phase of the viral infection, the bradykinin leads to the disease's progress, the exhausted immune reaction, and the cytokine storm inevitable. The vast bradykinin expression could cause pulmonary edema [149] and induce pulmonary fibrosis, too [150]. Interestingly, bradykinin's crucial role has recently been "discovered" by programs running on supercomputers [151]. Clinical practice shows that bradykinin-associated angioedema can recover rapidly when the bradykinin pathway is blocked [152].

Another control in complex regulation is the contact system (CS), which is part of the innate immune system and the inflammatory response mechanism against artificial materials [153]. The decision proteins in CS are the members of the coagulation cascades, factor XII (FXII, Hageman factor), prekallikrein (PK, Fletcher factor) and high molecular weight kininogen (HK) that participates in the initiation of the blood coagulation and in the generation of the vasodilator bradykinin with regulation KKS. FXII acts as a growth factor. It promotes angiogenesis and wound repair [154] in healthy conditions; however, pathologically, it can promote pulmonary fibroblasts' proliferation leading to pulmonary fibrosis [155]: COVID-19 can also progress to pulmonary fibrosis. Surfaces that are recognized as "unusual" appear from damaged host cells and will activate CS. Furthermore, damaged cells release characteristic molecules into the extracellular matrix (ECM), forming a damage-associated molecular pattern (DAMP) and a pathogen-associated molecular pattern (PAMS), which could trigger a defense reaction that includes CS activation. The three large regulating feedback mechanisms (RAS, KKS, and CS) are complex themselves and also complexly interconnected, too, **Figure 10**.

It was also recognized that ACE2 alone is insufficient to explain the virus's invasion into the cell [156]. The metalloproteinase inducing receptor (basigin, CD147) was discovered as a new alternative route [157], which is additional to the invasion of ACE2 [157] [158]. Basigin (BSG) is a highly glycosylated single transmembrane protein of the immunoglobulin superfamily. It is relatively small; it has 50 - 60 kDa.

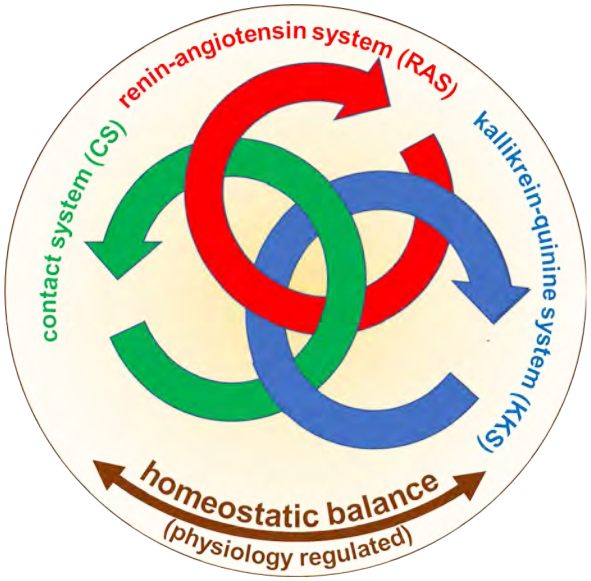

Figure 10. The regulatory feedbacks are profoundly interconnected and undoubtedly modifies the homeostatic balance.

The alternate route of entry of cells through BSG also participates in numerous negative feedback controls, and thus its imbalance re-induces challenges. BSG is widely distributed in the human body with various functions. It is involved in a broad spectrum of interactions [159]: regulates angiogenesis through VEGF, affects inflammation through Matrix metallopeptidases (MMPs), and IL-6, it induces pro-inflammatory cytokines through TRAF6, it is involved in the regulation of the cell cycle with P13K/AKT, etc. While ACE2 and TMPRSS2 are co-expressed in epithelial cell membranes, BSG expression appears in both epithelium and immune cells [136], so BSG inhibition may produce more consequences than in ACE2. In the bronchial biopsy, in the cells of the bronchoalveolar fluid (BAL) and the blood, a greater expression of genes related to ACE2 and BSG was found; and in addition, genes related to BSG were positively correlated with body mass index (BMI) [136].

On the other hand, BSG is involved in multiple physiological regulations. BSG regulates cell proliferation, apoptosis, migration, metastasis, and differentiation of tumor cells, especially under hypoxic conditions [160]. Inhibition of the BSG protein prevents interleukin IL-17 and CD4+ and CD8+ memory T-cells in the peripheral circulation [161]. The activity of BSG (CD147) increases under hypoxic conditions [160], which is usually generated by the massive use of ATP for cellular viral infection. It is well-known that BSG appears in most of the malignant processes [162] that are involved in the production of vascular endothelial growth factor and can promote tumor cell invasion and metastasis. The BSG protein appears to be a hallmark of cancer through metabolic reprogramming. BSG improves glucose metabolism [163] and contributes to immunosuppression by inhibiting the p53-dependent signaling pathway [164]. The BSG is a part of the complex physiological regulation (**Figure 11**). The SARS-CoV-2 virus can

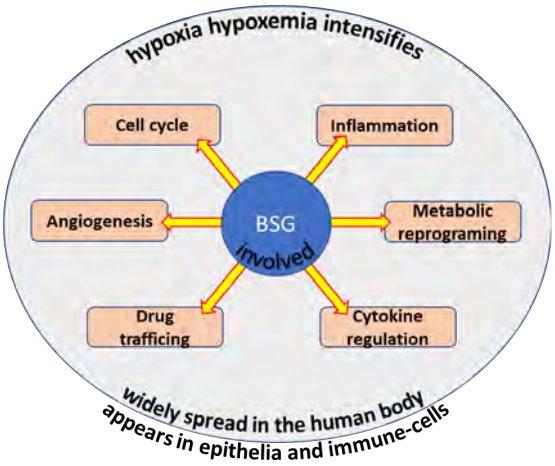

Figure 11. The complex regulatory effects of BSG. BSG is an alternative of the SARS-CoV-2 entering into the host cell, but its presence and change broadly act in the entire body's physiology.

reprogram cell bioenergetics supporting its replication [165]. In such a way, the SARS-CoV-2 virus shifts the cellular metabolic activity activating the simple glycolysis, similarly to the malignant cells. The glycolytic shift induces hypoxia triggering inflammatory changes in the lungs. This regulates the respiratory activity creating hypoxemia, which could support the viral infection by a positive feedback loop.

Importantly other feedback regulations help the extension of the viral infection [166]. The RAS-KKS-CS complex regulation has extensions with evading the immune response (vicious viral loop, "sneaky virus") gaining hyper-inflammation, including T-cell lymphopenia and infiltration of macrophages and polymorphonuclear neutrophils (hyper-inflammatory loop, "gathering storm"), the non-canonical RAS, the ACE2/angiotensin-1-7 loop involving platelet dysfunction and at the end vascular leakage, (loop of the "helpless lung"), and the hypercoagulation loop developing fibrosis ("an epidemic within a pandemic"), [166]. This interconnected networking shows the complexity of the COVID-19 processes, which must be considered in the therapy approaches.

Inhibition of the BSG protein (like the same for ACE) may be a useful strategy in preventing or first-line treatment of infection by the SARS-CoV-2 virus, suppressing the possibility of developing the disease to a severe phase. However, the regulatory action needs a careful choice of the right time with the right dose; otherwise, the treatment could seriously affect other connected functions, causing severe adverse effects or even directly opposite processes than the expected. The involvement of various receptors in SARS-CoV-2 infection shows a wide range in epithelial barriers and immune cells [63], so inhibition of a key player could come at a price broadening the spectrum of the fights during the disease.

The spike proteins of the SARS-CoV-2 are the key in viral entry to the host cell and in the induction of neutralizing-antibody and T-cell responses [167]. Blocking the S-spike protein with a polyclonal antibody is one of the promising

prophylactic neutralizations of the possible viral penetration [168]. Various peptides, antibodies, organic compounds, and short interfering RNAs are also other anti-SARS-CoV therapeutics targeting the S protein [167], developing a vaccine for the prevention of the infection. The S-block, together with the inhibition of the main gates of cellular entries like ACE2 and BSG could be a successful strategy in the early infection period.

2.2. Challenges of the Immune Regulation and Control

The patient-oriented approach involves the detailed measure of the personal patient features, taking care of their individual character. Patients are different in their homeostatic control. Their pre-set "trained" immunity and complete regulatory system depend on the environmental conditions, modified by the diets and habits, as well as the recognized or hidden comorbidities. Every living organism has intrinsic self-time defined by their individual features [169] [170]. One study compared the host immunity of SARS-infected patients directly at the time of admission for care [171]. Differences in host immunity were found when the patient developed mild or severe disease. Host values for ferritin, lactate dehydrogenase, and D-dimer increased as patients develop harsh conditions during care.

Conversely, the absolute number of CD4+ helper T-cells and CD8+ killer T-cells and B cells decreased significantly, and NK cells increased substantially with increasing infection intensity. At the same time, their share-percentage did not change so markedly. The CD4/CD8 cell ratio did not change, while the CD4+ and CD8+ T cell activation markers (HLA-DR and CD45RO) increased, and the costimulatory CD28 decreased as the disease worsened. The percentage of natural regulatory (suppressor) T-cells (Tregs) decreased in the patients' extreme conditions. The rate of interferon-gamma (IFN-γ), a soluble cytokine essential for innate and adaptive immune reactions, is produced predominantly by NK cells and promotes the development of CD8+ and CD4+ T-cells, increases with the development of the illness. Cytokines IL-2R, IL-6, and IL-10 all increased in host immunity in patients who developed extremely severe conditions. Activation of dendritic cells (DC) and B cells decreased in extremely severe stages from the patients. Interestingly, patients' age in severe and extremely severe disease stages did not have a significant influence. Another notable observation is that CD4+ and CD8+ T-cells are involved in the pathogenesis of an extremely severe viral infection [164]. Genetic diversity studies show that mutations interact with host CD8 and CD4 T-cells and could cause simultaneous infections with different genetic compositions [172].

The SARS-CoV-2 virus down-regulates the ACE2 by developing the infection, reducing the anti-inflammatory role of this enzyme. The early lymphopenia observed was possibly associated with a reduction in CD4+ T-cells and some CD8+ cells, which could delay or suppress the immune response and viral shedding. Macrophages and hyper-stimulated neutrophils can produce uncontrolled amplification of cytokine production [173]. Excessive autoimmune reactions wor-

sen symptoms and could lead to a critical condition. A positive side of the inhibition of ACE2 proteins is that their limited availability typically reduces the autoimmune effect [174] and suppresses the cytokine storm, and contributes to alleviating the disease in this way. From this point, the cytokine storm's critical state is highly dependent on the additional expression of bradykinin, regulated by the KKS system as a counteraction of the RAS imbalance.

Most patients who are transferred to the ICU have severe cytokine storm. The storm is an attempt to regulate body homeostasis that reacts to hyper inflammation induced by the SARS spike protein's active binding to ACE2 [175]. The high concentration of various pro-inflammatory interleukins such as IL-1β, IL-4, IL-5, IL-6, IL-17, IL-18, IL-21, IL-22, IL-23, etc. together with chemokines (such as CCL2, CCL3, CCL5, CXCL8, CXCL9, CXCL10 etc.) [176] and GM-CFS is released into the extracellular matrix and into the bloodstream. Due to attempts to regulate weak physiological control, anti-inflammatory cytokines (such as IL10, IL-13, M-CSF, etc.) are produced [177], but their presence is insufficient to rebalance severe inflammatory overload. The situation, together with the blocked ACE2, could lead to pneumonia and associated edema. SARS-CoV-2 develops pulmonary [178] and laryngeal [179] edema associated with pneumonia, also seen in SARS-CoV-1 infection [180]. However, the SARS-CoV-2-induced edema and pneumonia differ from standard high-altitude pulmonary edema (HAPE) [181] [182], even though they both meet the criteria for ARDS [183]. The difference is the vascular endothelial cell injury [184] that the COVID-19 infection presents diffuse alveolar damage and airways inflammation. Medium and small vessels dilate accompanied by perfusion abnormalities in the lung [185]. Both types of ARDS have the risk of being lethal, but HAPE, for the most part, does not need ICU treatment, whereas the consequence of COVID does, frequently developing multiple organ failure [186], even heart failure [187]. Endothelial cells' role is essential in SARS-CoV-2 infection [188], characterizing COVID-19 as an endothelial disease [189].

Another side of the complexity shows the production of cytokines and chemokines. A subclass of cytokines, interferons (INFs, named for their interfering actions) again have double-sided activities. On the one hand, IFNs are usually active in antiviral defenses. IFNs are communication molecules between cells to activate protective [190]. The automatic physiological control releases IFNs by the cells infected "alarming" neighboring cells and prepares them for possible viral invasion, helping the immune system destroy pathogens [191]. IFNs can activate natural killer cells and macrophages, and promote antigen presentation by increasing major histocompatibility complex (MHC) antigens. While IFNs are perfect communicators that help organize a defense against viral infection, it upregulates inflammatory symptoms (fever, muscle pain, flu symptoms) that are also commonly present in COVID-19. The molecular basis for the frequently observed progression of pulmonary fibrosis due to SARS-CoV-2 infection is not yet fully clarified. It is most likely due to multifactorial causes [192]: direct viral

effects, immuno-dysregulation, cytokines (MCP-1; IL-6, IL-8, TGF-β, TNF-α) and increased oxidative stress [193]. IFNs along with IL-1, IL-6, IL-15, IL-17, and tumor necrosis factor (TNF) are pro-inflammatory agents that orchestrate various signaling cascades that lead to the induction of chemokines and, what is more important, they trigger the production of other cytokines, which could cause an emergency in the advanced stage of COVID infection.

Consequently, inhibiting these pro-inflammatory proteins could be one of the winning strategies in the severe phase of COVID, when ARDS formation appears as the number one danger [194]. On the other hand, many cytokines, such as IL-1, IL2, TNF, and colony-stimulating factor (CSF), can also enhance IFN production [195]. Other problems appear to be that type I INF (IFN-I) produces fibroblasts and monocytes, which could favor fibrotic processes in the disease's severe phase. On the other hand, the immediate and efficient production of the same IFN-I helps the viral clearance in a mild or moderate state of COVID-19, and its impaired production and weak activity lead to viral existence and further development of the disease. Homeostatic feedback is also active here. The production of IFN-α type I could be inhibited by IL-10. IL-12 acts directly on CD4+ T-cells to enhance the priming of type II IFN (known as IFN-γ, as immune IFN) [196], which could inhibit viral replication [197]. On the other hand, IFN-γ can spread intravascular coagulation and decrease serum protein, maintaining the balance glucocorticoids regulate, inhibit IFN-γ [198].

The regulatory system completely overlaps, and complex feedback signaling maintains dynamism in balance in healthy homeostasis [199]. Patients' whole blood profile in COVID-19 indicates triggering of the highly dynamic immune response even in early stages [200]. The starting disease dynamically induces most the pro-inflammatory genes, causing a well detectable inflammatory response on the SARS-CoV-2. The T cell involvement is likely while CD4 and CD8 are expressed as a part of the pro-inflammatory response, which could worsen the disease or prolong the infection [200]. These findings could help to make prognosis in the early stages and develop patient-oriented, host-directed therapies.

The interaction of several effects also has consequences in diagnostic strategies, where complexity must be considered adaptively depending on the disease [201] [202]. When we act on one side of the scale, this complex system could be so seriously disturbed that it could not find dynamic equilibrium again through the interaction of negative feedback loops' mechanisms. In this way, the system will be out of regulatory range, out of control, as if shown in the case of IL-17 inhibition [203]. For example, a drug such as azithromycin decreases the expression of BSG. It increases the levels of interferons and interferon-stimulated proteins [203], which are effective antiviral inhibitors in the early phase of infection but could cause a storm of severe cytokines in the second phase. Managing inflammatory processes could be the critical issue in the different stages of the disease, again showing a complex tissue response behavior, requiring an adaptive adjustment of therapies [204].

Interestingly, there is a cross-immunity that had been observed between the

rhinovirus and SARS-CoV-2 [172]. Rhinovirus infection could prepare the immune system's mechanisms against other viral [205] [206] diseases. While possible prevention against common cold coronavirus (CCC) infection was shown more than 30 years ago [207], this research was abandoned. It became a hot topic to investigate again only today whether it has a possible cross-immunity connection with SARS-CoV-2 [208]. The idea of CCC protection had been reexamined, and it was hypothesized that pre-existing immunity in COVID-19 was primarily determined by previous CCC infection [209]. The research could contain exposure to cold without viral load, which was expected to also prepare the immune system for better performance against the viral infection [210] [211]. An exciting idea emerges that the Bacillus Calmette-Guerin (BCG), an attenuated strain of Mycobacterium Bovis, applied against tuberculosis for a century could decrease the mortality rate of COVID-19 [212] [213]. The cross-immunity assumption goes even further. There are assumptions that other live vaccines may have a role to prevent COVID-19 [214]. The mixed injection against measles, mumps, rubella (MMR) or Polio vaccine [215] may be a practical addition to avoid the worst developments of COVID-19 [216]. These theories and ideas well characterize how complex the infection and its consequences, and how much these depend on various personal and conditional factors. Even the oxytocin hormone level, which usually has a social and emotional bonding role, may have part in the prevention [217].

3. The Hypothesis

We propose to apply electromagnetism to defeat coronavirus infection. This idea fits well with the request to lock processes rather than remove some products [70]. The suggested new technology is physical so that it could avoid the pitfalls of the chemical approaches.

The conventional heating could affect the SARS-CoV. However, there is a further challenge: This virus is heat resistant even at higher temperatures, while other coronaviruses are heat sensitive. Complete inactivation of the virus requires a reasonably high temperature, [218], with a phenomenon similar to a phase transition at 56˚C, which is well above the physiological limit of body temperature. Nevertheless, the rising temperature could partially inactivate the viral infection by a long-lasting fever. Fever could alter the complex homeostatic regulation of the human body [219] [220].

We propose to use modulated electrohyperthermia (mEHT, trade name in oncology "oncothermia") [221] as a physical method complemented with appropriate immunostimulants in oncology [222] [223]. This method is not simple heating. It has a double role, heats and excites by absorbed energy of the electric field. The mEHT process has already demonstrated its ability to elicit tumor-specific and selective immune effects [224] and is widely applied in clinical oncology [225]. It has only some contraindications [226] and its adverse effects are minor [227]. The widely published preclinical and clinical [228] results on

tumors clearly show healing processes driven by specific immune functions, [229]. To our knowledge, we also expect successful treatment for viral infections [230]. When the procedure is not effective in a particular virus-infected case, our current experience suggests that we do not harm the patient. It does not increase the intensity of the infection process at any stage. This implies that we expect mEHT treatment to be extremely safe. However, since the method was applied to viral infection by HIV/cancer [230] [231], the transposition of the results of malignancy in COVID cases is hypothetical, although the processes listed confirm the practical applicability of the hypothesis. Technical details discussed elsewhere [232], as well as the practical issues, are shown in detail in protocols [233] [234].

The main task of cellular treatment is to select infected cells without damaging healthy ones. The selection of mEHT uses biophysical differences between malignant and healthy cells [235]. Specialties of the SARS-CoV-2 infection cause the biophysical differences presenting the selection possibility. The metabolic rate of cells loaded with the virus remarkable grows because it needs extra energy to support the replication process [236]. The "hijacking" of the energy resources of the host cell [237] [238] makes recognizable the infected cells from the uninfected ones. The higher metabolic rate needs an intensive exchange of ionic species, frequently forcing the cells to direct glycolysis. This accelerated ATP production makes only two ATPs from the glucose. Still, this quick and straightforward process delivers more ATP in a unit of time than the more complicated citrate (Krebs) cycle in the mitochondria with its 36 ATP/glucose. The result is a high concentration of lactate and other ions near virus-infected cells. This makes the microenvironment of infected cells more conductive, recognized by well-chosen radio frequency (RF) current flowing through the tissues. The distinguished flow increases the electric current around the targeted cells and could excite some transmembrane proteins (**Figure 12**).

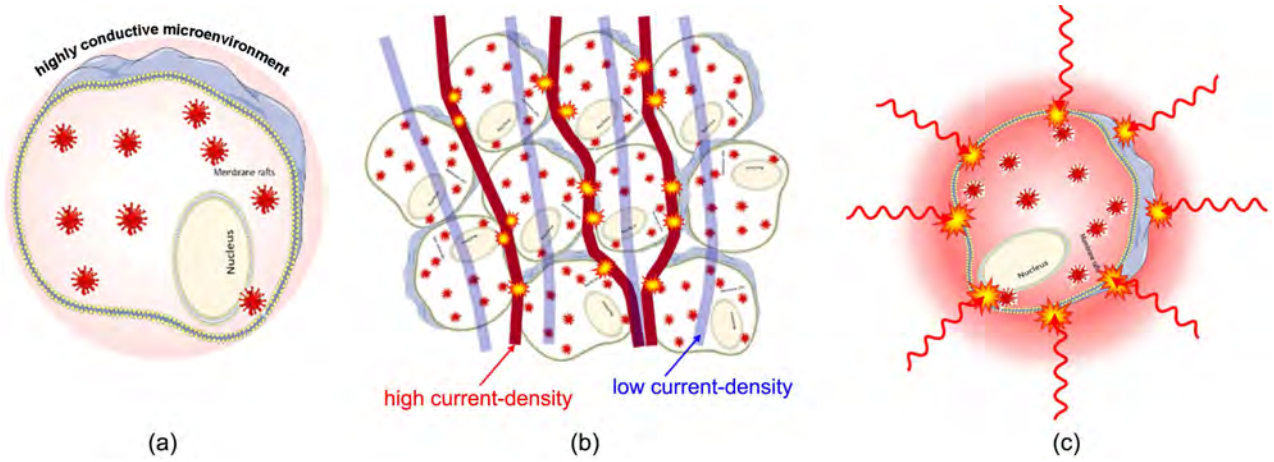

Figure 12. The primary selection of virus infected cells by RF-current, flowing through the tissue. (a) The microenvironment of infected cells is highly conductive due to the high metabolic rate of the cells. (b) The cellular membrane is an isolator (condenser) so the well-chosen current will flow mainly in the extracellular electrolyte. (c) The selected cells are excited by their transmembrane proteins, including the virus-entry points.

The method is centered on electromagnetic action, which synergistically combines the heat and electromagnetic bio-effects on the targeted cells [239], like it is proven and widely used in the similar conditions of malignant cells [240] [241]. Conventional heating also has a general antiviral impact with its thermal effect [242]. The challenge that it heats the tissue equally, but the temperature alone is not selective. However, mEHT is certainly heterogeneous by the non-isothermal electrothermal effect, [243], which precisely attacks only the microenvironments of the target cells [244]. The absorbed electromagnetic energy on selected target cells partly heats them up while the electric field extrinsically excites various signals. The cells' heated microenvironment will increase their conductivity, promoting the selection process in a positive feedback loop. The applied bioelectromagnetic concept chooses the cells that are out of the homeostatic regulation, recognizing where the dynamic equilibrium of homeostatic control is changed. The combination of temperature-dependent and independent factors could provide optimal treatment [245] [246]. Importantly, the lung's intensive cooling with breathing does not modify the process due to the low dependence on the thermal factors.

The relatively low electrical impedance of infected cells' microenvironment allows selection deeply in the body (**Figure 13**); as occurs in cases of malignant neoplasms [247] too.

Cell membranes contain numerous transmembrane proteins, which are connected to the cytoskeleton on one side and act as receptors or intercellular connections (cadherins, junctions) between cells. Some of the transmembrane proteins with the interaction of membrane lipids clump together and form a clustered group. The combination of glycosphingolipids, cholesterol, and protein receptors is organized into lipid microdomains of glycolipoprotein. These clusters (lipid rafts) in the plasma membrane have various functions [248], including signal transmission by group receptors [249], and play an important role in membrane dynamics [250]. Instead of chemical reagents to excite or block the receptors, mEHT targets the selected cells' lipid rafts directly [251]. The membrane

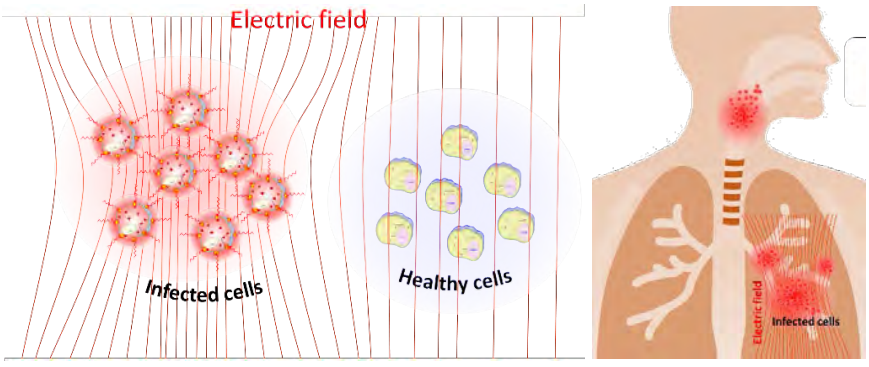

(a) (b)

Figure 13. The electric field directs the radiofrequency current which selects the infected cells. (a) the current flows to the volume where the overall average conductivity is higher (b) the selection could be multilocal, the current flows the electronic rules.

rafts absorb most of the electromagnetic energy (**Figure 14**). It works in nano targeting of the natural nano-units, the rafts [251].

Precise *in silico* models well describe the special energy absorption of the membrane rafts of selected cells [252] (**Figure 15**).

In this way, the mEHT has a double-action (**Figure 16**): the thermal part of mEHT [253] locally heats the membrane rafts of the target cells in the depth of the body, [254], which could cause changes in their structure [255]. It is essential to highlight that the lipid rafts of the cell membrane are involved in the cellular invasion of SARS-CoVs [256] [257] [258], and could have an active reduction of the infectivity of SARS-CoV-2, inhibiting the dependent binding of lipids to host cells [259]. The viral surface's weak temperature dependence could be an additional factor of mEHT action on the selected cellular microenvironments, where the temperature could be locally high [243]. Measurements of viral load in sputum show a small partial inactivation of viral load at 42˚C for 15 min, [260]. Although the virus can recover from severe mechanical disturbances and is unusually resistant to temperature, its surface is progressively stripped of spikes

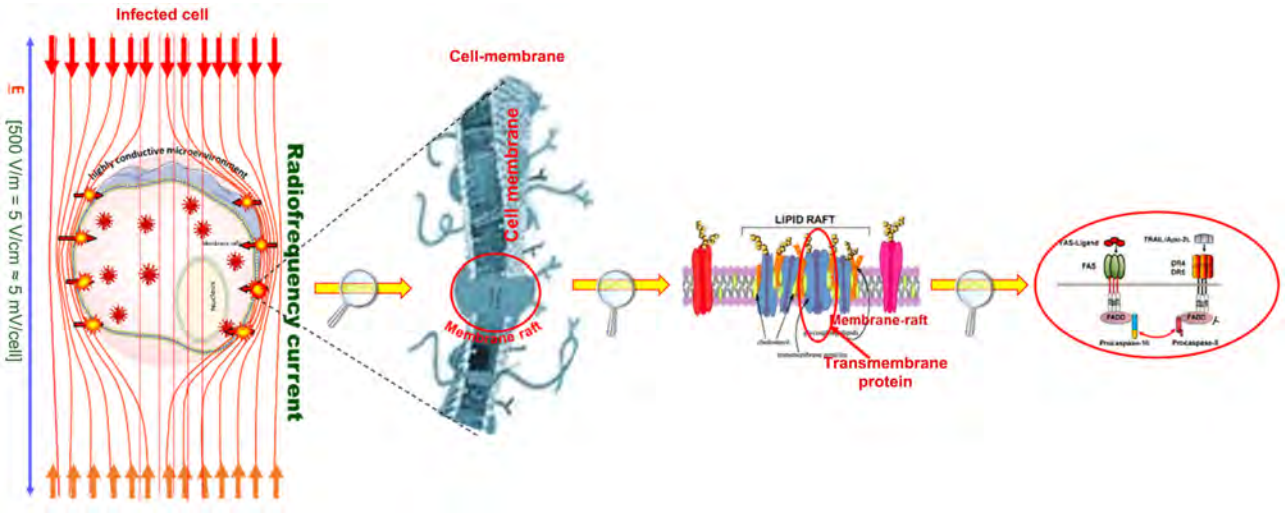

Figure 14. The excitation process in steps: it starts with the transmembrane protein groups (lipid rafts) which absorb more energy than the non-conductive lipid membrane, the proteins are excited in the chosen rafts and at the end the death receptor and its complex molecular set start the apoptotic process.

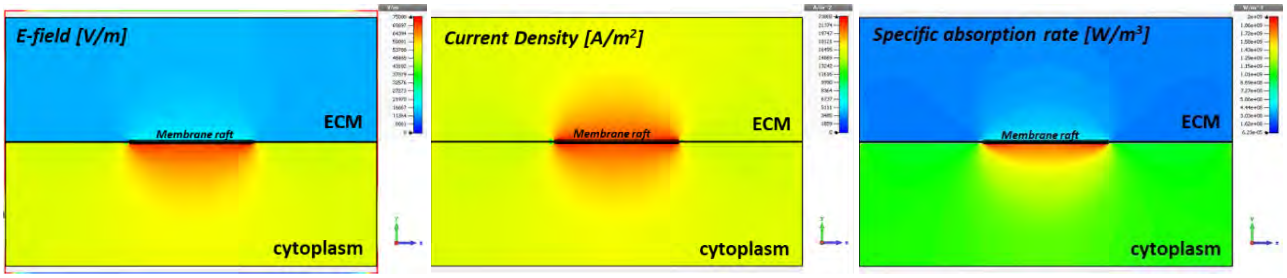

(a) (b) (c)

Figure 15. The energy absorption can be calculated *in silico*, (ECM in upper, cytoplasm in lower parts of the figures divided by the membrane, with a raft in the center: (a) the electric field; (b) the current density; (c) and the specific absorption rate values.

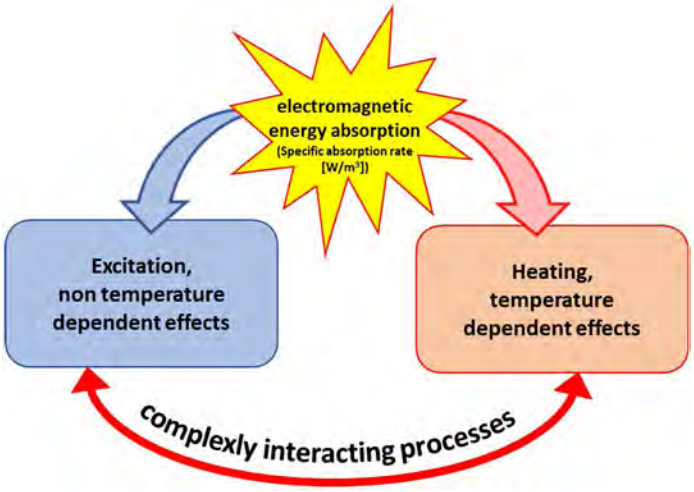

Figure 16. The mEHT uses double effects. The absorbed electric field makes excitation non-thermally, while the absorbed energy heats the absorber, and gives optimal condition for the excitation process.

with thermal exposure. Its dynamism is reduced as measured by atomic force microscopy [261]. Therefore, both the infectivity and the thermal sensitivity of SARS-CoV-2 depend on the stenosis of the superficial peak and dynamics of the virus, and so the growing temperature could decrease the replication speed. The heat affected virus and the observed thermal aggregation may be one reason for the suppressed activity of the SARS-CoV-2 virus by heat [262]. In addition to the effects of the outside temperature, the infection process also generates heat. The infection uses several metabolic pathways in the host, using large amounts of energy, while ATP's amount decreases as early as 3 hours after invasion [263]. This intensive consumption of ATP in a short time causes a sudden increase in temperature, which could reach approximately 4˚C - 5˚C of the host cells [258], which, together with the increase in ionic concentration in the neighboring extracellular electrolyte, decreases impedance also supporting the mEHT selection mechanism.

When cells are exposed to heat shock, they develop protective proteins (heat shock proteins, HSP [264]) in response to exposure to stressful conditions. These proteins also have very complex functions in the cell-life. It was discovered as the protection of cells against thermal stresses [265]. Many HSPs are "chaperones" to stabilize new proteins that fold properly or help to refold proteins damaged by various cell stresses and are found in almost all living organisms. In general, any stress develops HSP [266], including electromagnetic interactions without thermal effects [267]. Under healthy conditions, cell survival modulated by the essential activity of HSP70, repairing the stress damages.

HSPs are very conservative proteins, which are part of general protection at the cellular level. HSPs are involved in stress-induced damage repair mechanisms and are also involved in multiple signal pathways, including many apoptotic signal transmissions. Various HSPs (indicated by their molecular weight in kD) operate to correct the various stress consequences. The most important HSP

members are the 60, 70, and 90 kD proteins (HSP60, HSP70, HSP90). These chaperones are widely used in medicine [268]. Like heat stress induces most of HSP70 [269]; respiratory hyperthermia induces a cytoprotective response to heat shock in vesicular stomatitis virus [270] and rhinovirus-infected cells [271]. The main functions of HSPs as chaperones help repair misfolded or unfolded polypeptides, protect cells from various types of toxic stress, and present immune and inflammatory cytokines that support immune regulations. Merely speaking, HSPs are the guardians of the real dynamic status quo of the system.

Viral infection generally triggers apoptosis or programmed cell death of the infected cell [272]; the cell automatically activates its pathways for programmed cell death [273]. As the oldest cellular immune defense, the natural self-destruction of cells selected by apoptosis can be a significant point to eliminate the virus-infected cells. Despite the normal cellular reactions that induce apoptosis, the "hostile behavior" of HSPs disrupts apoptotic processes, blocks the signal pathways that keep infected cells active [274]. HSP70 has a belligerent activity in viral infection with their protective functions, it cooperates with numerous viruses [275], keeping the host cell alive during the virus's replication and exit. The intrinsic mitochondrial pathway of apoptosis in cells infected with SARS-CoV-2 is positively correlated with the induction of viral pathogenesis of apoptosis and virus replication [276] [277]. The caspase-dependent mitochondrial apoptosis is active in viral pathogenesis [278]. We hypothesize that the complex cellular heat shock and electrical shock presented by mEHT will aid [279] apoptosis of infected cells and induce protective chaperone expression against viral invasion in uninfected cells. The main action of apoptosis by mEHT uses an extrinsic apoptotic pathway, exciting TRAIL (DR) death receptors on the surface of the membrane selected cells [280]. The TRAIL can induce apoptosis in virus-infected cells and can promote immune defense against viral infections [281]. On the other hand, there is evidence of the complexity of the feedback-controlled function of TRIAL in the immune system, helping to kill virus-infected cells or promoting their survival [282], showing the complexity of this effect. Furthermore, the TRAIL is an IFN-dependent mediator. The balance of the IFN/TRIAL signaling response has complex modulation and is essential to balance viral disease promotion or suppression [282]. The IFN-γ could help to develop antitumor immunity in malignancies [283]. The mEHT therapy induces IFN-γ proven *in vivo* [284]. It was measured, that the number of IFN-γ-secreting CD8+ T-cells in mice that were co-treated with DC and mEHT significantly exceeded the corresponding numbers in mice that were treated with DCs alone. The development of IFN-γ supports the systemic abscopal effect of mEHT [285] and helps to avoid the growth of the rechallenged tumor in the animal [284], and so it works like a vaccination. The mEHT developed IFN-γ could promote the appropriate immune-response at the early stages of the viral infection too.

The TRIAL induced extrinsic apoptotic signal goes through caspase (CAS) dependent (CAS-8 → CAS-3, or mitochondria → CAS-9 → CAS-3) and also independent (apoptosis-inducing factor, AIF) pathways [286]. The different apop-

totic processes could usefully suppress viral replication, including the c-Jun N-terminal kinases (JNK) as the dominant factors to induce apoptotic cell death in mEHT [287]. Importantly the radioresistant cells could be forced for apoptosis with mEHT [288] The apoptosis is such a basic feature of mEHT, that its dose could be measured by apoptotic rate [289].

The complex regulation of dynamic equilibrium of homeostatic regulation is active in the role of HSPs too. Their guardian function is a double-edged sword. Processes could express the HSPs on the cell membrane, [290] or release of HSP to the ECM, or secreted in exosomes [291]. The HSPs' function turns to the opposite direction when they are outside of the cytoplasm. In this situation, protection of the "status quo" by HSP activity takes on an opposite meaning outside the cytoplasm: it supports systemic integrity and aids apoptosis of infected cells. The selective stress of the mEHT method expresses HSP70 in the cell membrane and releases these proteins to the ECM [292], well-proven in malignant cases [293]. On this way, the HSP70 out of cytoplasm in oncology induces apoptosis signals and promotes immune effects [294], as well as immune-mediated systemic effects (abscopal) [295] and increases tumor-specific adaptive immune activity [224] in addition to apoptosis. The beneficial immunogenic actions of HSPs could be a helpful tool against COVID-19 too. HSP70 in ECM carries out a transfer of information essential for the specific immune action against the virus. HSPs are crucial components of antigen presentation [296] formed by antigen-presenting cells (APC) and also cross-presentation [291] and autophagy [297]. MEHT induces a complex process that creates a "damage-associated molecular pattern" (DAMP) in ECM [294]. As is usual for all complex regulators, the DAMP has a two-sided behavior: it could be antiviral, causing apoptosis, inhibit virus reproduction, or it could be a promoter of the consequences of infection by enhancing the process of severe inflammation [298]. The DAMP created by mEHT includes calreticulin (CRT), "high mobility group box protein 1" (HMGB1), 70 kDa heat shock proteins (HSP70), and ATP. The members of the pattern that appear in the ECM are separate information carriers: HSP70 carries the genetic information, CRT is the "eat me signal" [299], HGMB1 is the "danger signal" [300], and ATP provides the "find me signal". These pieces of information form a set of spatially and temporally harmonized immune processes in the ECM [301], orchestrated primarily by CDs' maturation to APC [302]. Note the possible shift in DAMP's regulatory direction from suppressor to a promoter, because all the effects of the molecular components have connections embedded in complex ways, and our positive actions could easily be reversed when the system is out of balance. We have to apply mEHT in the mild or moderate phase of the disease when the inflammation and cytokine production promote immune activity and do not lead to an emergency cytokine storm condition. Recurrent in the "double-edged sword" phenomenon also characterizes all elements of DAMP, shown for CRT [303] [304] and for HMGB1 [305] and in HSP70 [275]. ATP as an energy source for dynamic changes could also support viral infection through its energy supply function. DAMP induces immunogenic

cell death (ICD) generating APC [306], with the maturation of DCs [307]. The APC formed by ICD carries specific information about the infected cell and could produce virus-specific killer (CD8+) and helper (CD4+) T-cells (**Figure 17**). An interesting observation in cancer experiments, that mEHT treatment enhances the $\gamma\delta$T-cell migration towards tumor cells even as low temperature as 38˚C [308]. The $\gamma\delta$T-cells link the innate and adaptive immune systems, [309], so could have effective participation in the developing of immune defenses against SARS-CoV-2 invasion.

The virus uses the cell cytoskeleton for all its invasion, movements in the cytoplasm, and leaving the cell for replications [310]. The cytoskeleton components provide a dynamic framework for viral trafficking in the cytoplasm. They are involved in the entire process of the virus in the host, providing efficient elimination, replication, and egress exit [311]. In the first step, the spike protein binds to the cell surface. The docking strategy is universal; it works for all mammals. The binding process rearranges the cytoskeleton in one hour [312]. After this initiation, the intracellular transport of the virus involves both the cytoskeletal filaments of actin and tubulin and their dynamic components dynein, kinesin, and myosin [313]. After transport to the perinuclear region, the coronavirus replicates. With the active promotion of microtubules, the virion is transported to the plasma membrane, "hijacking" the host's cytoskeletal system [314] and helping the viral replication exit. The applied electric field of mEHT also affects intracellular components. The rearrangement of the cytoskeleton by the modulated electric field signal suppresses the viral replication by limiting the intracellular transport by modifying the necessary polymerizing components for viral replication [315]. The structural reorganizing of the microtubules and actin filaments and also limiting the dynamics of cytoskeletal "motors" dynein, kinesin, and myosin [316] distract the correct transports for virus replication.

The hypoxemia caused by the low oxygen availability in later stages of the viral infection help many viruses replicates more easily. Hypoxia leads to inflammation and endothelial activation [317]. Cells adapt to hypoxia and induce cell survival and specifically endothelial cell adaptation (migration, growth, differentiation)

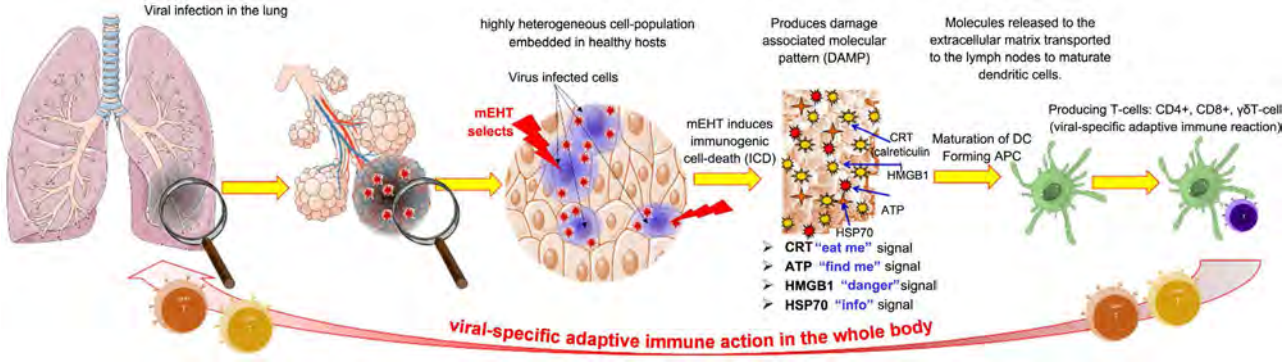

Figure 17. The immunogenic process has a systemic feedback from the local excitement. The clue is the immunogenic action, which makes the genetic information available for the immune-system. The "trained" immune mechanism produces adequate cells (killer cells) to attack and kill the virus infected cells in all over the body.

[318]. The developing hypoxemia in COVID-19 upregulates the hypoxia-inducible factor-1 (HIF-1α), increases the ACE protein expression, while counterbalancing downregulates the ACE2 enzymes [319]. Due to the possible bradykinin overload, the process produces cytokine storm, evolving the patient state to critical.

On the other hand, the hypoxia at the onset of the COVID-19 helps avoid serious infections because ACE2 is the main target of SARS-CoV-2 in pulmonary epithelia. Clear epidemiologic fact among highlander populations supports the positive role of hypoxemia in preventing the COVID-19 [320] [321]. This well emphasizes the double-faces of HIF-1α which could help in prophylactics in early infection stages [322], but oppositely active during development of the disease. A variety of viral pathogens may activate the HIF-1α, as well as the glycolytic supported high metabolic rate, which is induced with viral infection in the host cell, which promotes inflammation, and facilitates viral replication [323]. Suppression of HIF-1α [324] is an additional advantage of mEHT against the development of the symptoms.

Other factors involving mEHT to COVID-19 treatments are that both mEHT and bradykinin promote the activation of TRPV1 receptors [325], which can trigger additional regulatory mechanisms and reduce pain sensation. Although TRP channels have no role in healthy lung function, repair processes use them to promote endothelial permeability, inducing inflammation for immune action, which are normal helper processes. Still, again their activation could become pathological [326], involved in asthma, COPD, and pulmonary fibrosis [327] and pulmonary edema [328].

The KKS induced overregulation of bradykinin due to the RAS disbalance is caused by dysfunctional or downregulated ACE2. This process can be partially corrected by mEHT, producing vasodilation [329] without RAS control. This bradykinin-free action would be a helpful option for the vasocontraction challenge, which additional advantage could be essential in the treatment of patients in the ICU.

Fibrotic processes dangerously risk the survival of the patient and could cause serious harm and reduce the quality of life of the patient even chronically after successful antiviral therapy as well. Those who survived treatment the applied aberrant and excessive treatment in the ICU, sometimes have hardly reversible or irreversible lung damage and fibrosis, resulting in functional disability and a significantly reduced quality of life [330] [331]. The worsening of symptoms could also become chronic without further viral infection. The fibrotic damage in patients during and after a viral infection may cause acute lung injury (ALI), releasing fibrosis mediators [332]. The epithelial-mesenchymal transition (EMT) [333] promotes fibrotic processes [334] [335] derailing the epithelial-fibroblastic crosstalk [336]. The mEHT is feasible for treating fibrotic states due to its electric field effect, which could moderate the EMT [337], so we consider it to treat certain fibrotic conditions. The successful anti-fibrotic effect of mEHT is proven for patients with fibrosis of the penis (Peyronie's disease) [338], and fibrosis of the palm (Dupuytren's contracture) [339]. Furthermore, mEHT treatment in

malignant fibrosarcoma also showed a great benefit to the patient [340]. Note that RF current is widely used for cellulite fibrosis [341], and skin laxity [342], but only for areas near the surface. MEHT is active in deeply located tissues of the body [247], so therefore the usual activity against fibrotic structures is expected anyway. Due to its repairing action, the mEHT therapy could be in the healing process or also in the rehabilitation period when the infection does not appear. Still, its consequences (primarily pulmonary fibrosis) need care.

Further possible impact of mEHT on fibrosis is developing HSP, which suppresses the fibrotic processes [343], like this is shown in wart healing [344] [345]. Additionally, the positive impact of high-dose vitamin-C [346] may inhibit fibrosis complementing with mEHT, using its intensive attack of viral infected cells' membranes. Clinical study shows successful complementary treatment for lung cancer with high dose vitamin-C [347]. Lung effusion is also one of the patient's remaining negative states cured of the SARS-CoV-2 viral disease. mEHT also offers a solution to this problem [348].

The above effects present the complex behavior of mEHT therapy. Low-frequency modulation mEHT on a high-frequency carrier [232] allows penetration into the entire lung, attacking the virally infected cells in. The demodulated signal promotes the restoration of the cells' homeostatic balance by loading the redistribution. It forces the process to maintain equilibrium [349] forms multiple regulation loops to support the homeostatic control of the body (**Figure 18**).

4. Discussion

Like we learned in malignant diseases, the SARS-CoV-2 coronavirus infection exhibits a complex phenomenon by upsetting the healthy homeostatic balance. It means that the processes in developing conditions are stochastic (probabilities of events dependent on time). They have promoters and suppressors, and their equilibria decide the fate of the infection. The cumulative dose of viral exposure and the efficacy of the local innate immune response (natural IgA and IgM antibodies, mannose-binding lectin) form the most important equilibrium in the first 10 - 15 days of infection. When the virus can block the primary innate defense immunity, it could rapidly spread from the upper respiratory tract to the alveoli, replicating without local protection. This phenomenon causes pneumonia and clinically induces a high antigen concentration. The delayed and strong adaptive immune response (high-affinity IgM and IgG antibodies) that follows causes unstoppable inflammation and generates a cytokine storm, which requires mainly intensive care and is fatal in some cases [176]. Balancing physical activity also affects: low or moderate physical activity can be helpful, but extreme action can facilitate the virus's shedding. The same problem could arise in the case of oral respiration with hyperventilation during the incubation processes. The virus bypasses the immune barrier and determines the rapid development of the disease. This well-presented spatio-temporal harmony (balance of the viral load, repetitive infection, timing of immune actions, concurrent effects of personal

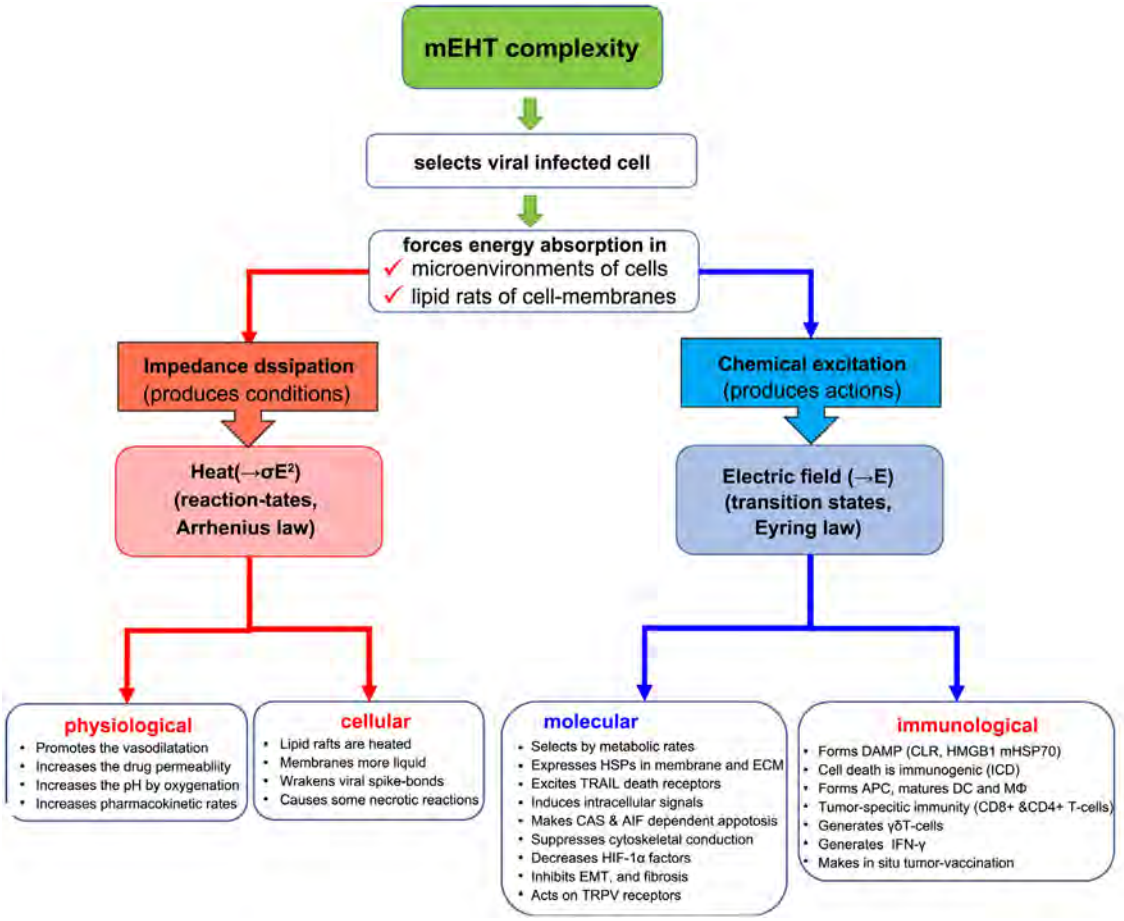

Figure 18. The complexity of mEHT is its two balancing and interaction branches of actions. The conditional heating (depends on square of the field strength) prepares the physiological and cellular conditions, while the electric effects (linearly proportional with field strength) act on molecular level supporting the immune processes.

immune regulations, etc.) of the development of infection decides the fate of the patient.

Consequently, understanding the complex process of infection development is essential for the medical care, prevention, treatment, and rehabilitation of patients. The COVID-19 disease has many unusual aspects compared to other respiratory viral infections. The severe lymphopenia, which causes a deficiency in the immune regulation processes, and a cytokine storm with extensive activation of cytokine-secreting cells with innate and adaptive immune mechanisms, is special, leading to acute respiratory distress syndrome and multiple organ failure [350]. Laboratory evidence from clinical patients showed that a specific T-cell response against SARS-CoV-2 is essential for recognizing and destroying infected cells [351], and the measurement of these could inform the design of prophylactic vaccines and immunotherapy for the future.

Most of the current drug developments are strongly connected to some chosen molecular products. My current proposal opens a new approach with the bioelectromagnetic method. It supports the complex processes of regulation and

control and the restoration of the natural homeostatic balance. This proposed paradigm shifts from current drug-focused developments to bioelectromagnetics. Besides, the change proposes a shift from the product-oriented to the process-oriented approach. This strategic objective has historically been proven in the fights against dangerous enemies. The winning strategy seeks out and attacks the weak side of the "enemy" and avoids having too much confrontation with their strong positions. Applying in the COVID-19 fight case, we must attack the infection's weak side (violation of collective regulation), instead of the viral force (reproductive capacity). My new strategy proposal is biophysical. The mEHT which composes novel advantages:

1) It "rides" the high-frequency carrier, which carries this information in depth, which would not be possible only with this low frequency through the insulating layers, including the tissues, applicators, and boluses.

2) The applied modulation uses appropriate time-fractal series, which promote the correct signal processes in cells after the plasma membrane demodulates the signal. The time-fractal represents the spatio-temporal complexity of healthy homeostasis, maintaining the necessary systemic equilibrium, despite the disturbing local balances.

These novelties, as I described above, could solve many problems connected to the complex control. The homeostatic balance of the immune system is essential. The flexible adaptability of SARS-CoV-2 avoids any homeostatic regulations that make it complex indeed. Our task is supporting the natural processes to find a way of repairing the lost control. The *in situ* generated ICD provides genetic information for APC and forms CD8+ T-cells may be one of the solutions. The transferred information is specific to the actual infected cell and, regardless of the mutation, serves as a feedback mechanism to destroy it. This is an opportunity to target and try to kill cells infected by viruses. Through this mechanism, mEHT treatment could interrupt or at least slow down the rate of viral replication, the delay of which may be essential in preparing for adaptive immune defense. Slower replication activity can retain mild disease does not evolve to severe stages. The complex cooperation of mEHT with the innate and adaptive immune system causes a systemic effect (abscopal) from the local treatment site throughout the body [352]. The method had shown preclinically [353] and clinically [225] eliciting an adaptive immune response in oncology. DAMP induces targeted apoptosis leading to ICD by creating molecular clusters and systemic effects (tumor vaccination, patented [354]). And expectedly could lead to vaccination against viral infection, as occurs in malignant cases.

The inhibitory effect of mEHT against COVID-19 is hypothesized due to its immunological and biophysical selection of cells that create apoptotic signal transduction in infected cells. The process uses bioelectromagnetic effects and takes into account complex regulatory needs. The actions of mEHT in the later stages help the complex fight for healing. The method we propose can generate a virus-specific immune response electromagnetically *in situ*.

Challenges of the Therapeutic Paradigm and Management of the Therapy

The clinical management of the disease is complex and needs right-time decisions about the applied treatments [355]. The adequately sequenced treatment series could synergistically increase the patient's chance of cure. This is also related to the fact that when the treatment starts in the early stages of infection, it may significantly slow down the infection's exacerbation, which can provide sufficient time to develop an adaptive immune response, which can be aided by DAMP-ICD processes.

At the time of development, infection with the SARS-CoV-2 virus can be divided essentially into two phases, separated by basic immune processes [350]. The two phases, innate and adaptive immune reactions [356], occur superimposed and accompanied by cytokine waves [357]. The applied mEHT must be adjusted to the treatment periods (**Figure 19**). It is sometimes performed successfully when the patient remains asymptomatic, or the symptoms are so mild that the patient does not recognize them.

The clinical intention is to prevent the development of a severe disease even in the first phase when the patient still shows mild symptoms. A problem arises when the viral load dose is too high or the innate immune response is too weak to exceed that dose. Then rapid progress of shortness of breath dominates the symptoms [358]. When the disease worsens in the second stage, the adaptive immune system's activity will be decisive [356]. The immune-activated high cytokine production in the second wave typically creates a cytokine storm that primarily requires active medical attention and sometimes treatment in the patient's ICU [359]. Leukocyte-mediated antiviral responses again need a balance in a dual role, as they can help counter the effects of the SARS coronavirus and cause severe pneumonia. The dose of the virus and the timing of the processes can be crucial in preventing infection, which again requires only dynamic stochastic considerations. The direct way considers the complex dynamism of using the different drugs in their regulation of equilibrium. When the therapy uses them in the appropriate time sequences and taking care of homeostatic regulation and its temporal factors, success will not be lacking.

The INF-mediated immunological dynamics became the guiding factor [360] to find the optimal and adaptive treatment. The favorable balance of DAMP in antiviral activity requires close monitoring and patient adjustment. The dose to form the various immuno-active molecules must be adjusted to cytokines' concentration, which helps avoid over-regulation, leading to a septic storm. Developing fibrotic processes is one of the clinically most problematic tendencies. In the intermediate stage of viral infection (weeks 2 - 5), fibrosis signs are already shown: fibrin deposition and infiltration of inflammatory cells and fibroblasts in the epithelial cells of the alveolar parts. In the later stage (weeks 6 to 8), the lung tissue becomes very fibrotic with collagen deposits.

The fibrosis treatment could be artificial respiration in case of shortness of

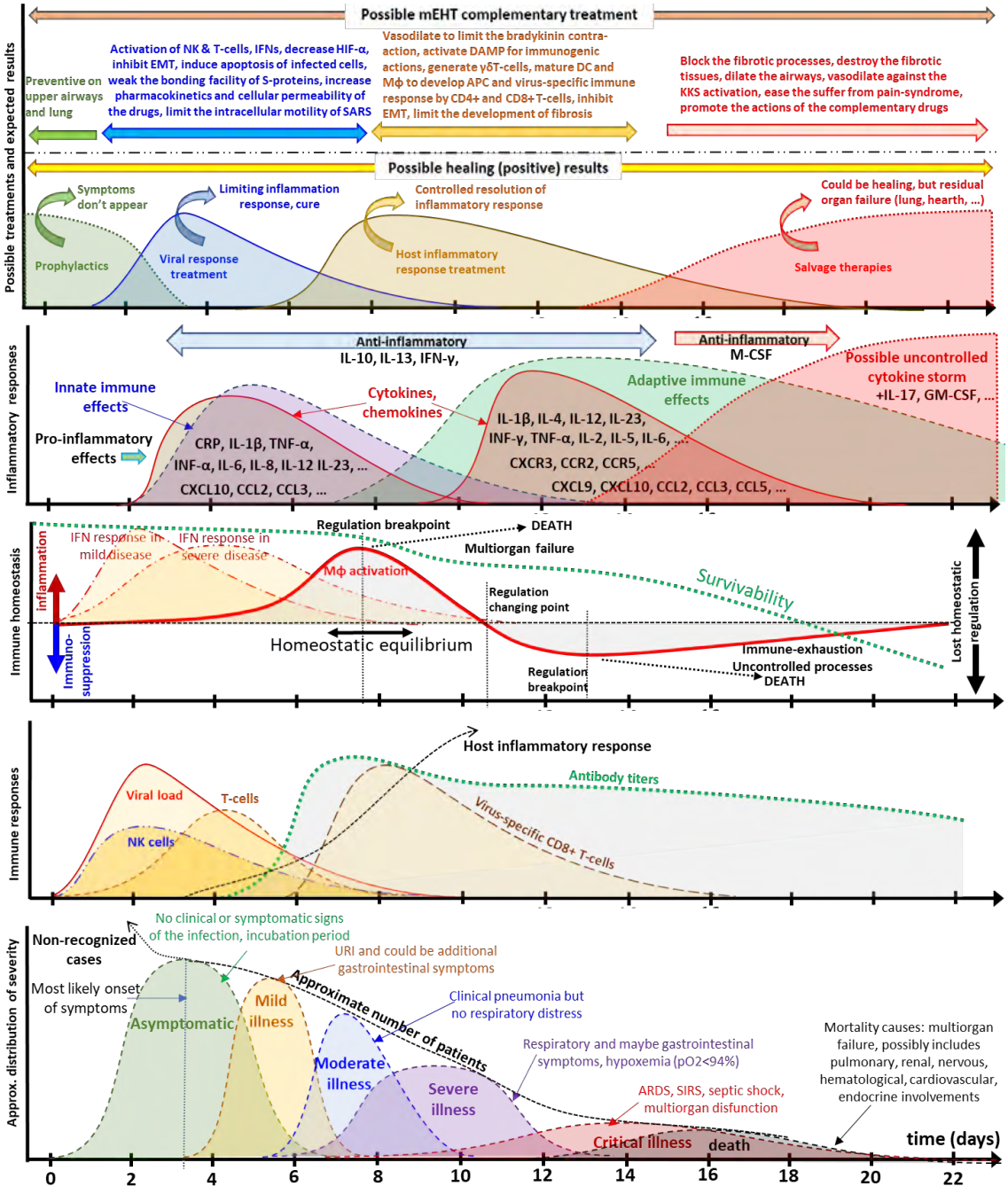

Figure 19. The distribution of the various characters of SARS-CoV-2 infection and treatment possibilities during the infection. Note the distributions are probabilistic, do not cover individual cases. The individual conditions depend on various factors, including the dose of the viral load, the patient's environment, the habits and diets, the "prepared" protection of the immune system, etc. Due to the considerable individual differences, the distributions are normalized as much as was possible. The intervals are approximate like the distributors are also estimates. Distributions are composed in their most probable form using the results [199] [355] [361]-[369]. The disappearance of antibodies against SARS-CoV-2 was also measured [370], but others measured the opposite; the antibody protection exists for at least two years [371].

breath. In less severe cases, this is done simply by intubation with tubular dosing of oxygen, but in more severe cases with mechanically forced ventilation, "posi-

tive end-expiratory pressure" (PEEP) is applied [372]. Although this procedure saves lives, strong mechanical interaction can cause serious side effects [373]. Lung damage caused by mechanical ventilation can develop into additional ALI [332]. These changes' underlying mechanisms may be an epithelial-mesenchymal transition (EMT), and the release of profibrotic mediators caused by cell stretching and mechanical ventilation [335]. Aggravating ALI could also induce pulmonary fibrosis. In the period of infection, the SARS-CoV-2 virus progressively replicates in the upper respiratory tract. Extensive mechanical ventilation can facilitate the direct penetration of high concentrations of the SARS-CoV-2 virus from the URI into the lower respiratory tract, eliciting the effects of neutralizing possible antibodies on the mucosa. Intensive PEEP may be associated with strong functional effects; hyperinflation, and significant hypercapnia (hypercarbia) caused by ventilation of dead parts and occurs to reduce hypoxia [374]. With ventilation, the risk of lung injury is high; most mechanically ventilated patients develop severe ARDS [375]. The detrimental effects of mechanical ventilation can further exacerbate the patient's condition, which is mediated by cellular, molecular mechanisms involved in mechanical stress-induced lung damage. However, patient selection for PEEP treatment is also not straightforward, as the additional extent of viral lung injury limits patients' choice. In contrast, pulmonary hypertension is usually not a clinically relevant factor in the screening process, causing physiological problems during treatment.

Due to the possible damages, the use of "preventive" PEEP is not recommended [376]. Use it only in case when it is necessary indeed. After intubation oxygen supply, an assisted breathing associated with intubation should be used. In this phase, the patient could be treated by mEHT to ease the symptoms by freeing the airways with dilatation and painless relaxing. Accordingly, PEEP mechanical ventilation should only be used in insufficient critical respiration and should be used as carefully as possible. The adverse effects of PEEP could be severe, leading to worsening the patient's condition. The risk/benefit ratio of PEEP-induced lung injury may be higher than without this mechanical support. The strategy has to be well adapted to the patient [377]. When necessary, the PEEP treatment must be kept to the minimum, which enough for patient breathing. The analysis of data shows attention to the technical data shows. This usually means that the application of PEEP is airway occlusion pressure $P_{0.1} < -4$ cm H_2O or the expected pressure generated by respiratory muscles $P_{mus} > 15$ cm H_2O, or expected transpulmonary respiration > 17 cm H_2O) [149]. The position of the patient is also an important factor to evaluate in the actual case and stage. The proposed prone position [378] needs to be applied in the proper time-course [379]; otherwise, it could cause damages [380].

Approximately one-third of the patients experienced persistent lung abnormalities after being cured of SARS-CoV-1 and MERS' acute disease. Furthermore, approximately one-third of patients infected with SARS-CoV-2 develop acute idiopathic pulmonary fibrosis (IPF) even after improvement and discharge from the hospital [381] [382]. Consequently, strict follow-up observation is ne-

cessary after 3 - 6 months of the healing process completed in the hospital to warn of the potential hidden risk of developing IPF. Post-treatment care should prevent, cure, or at least block the further development of the disease's consequences, mainly the problems of fibrotic processes. The antifibrotic treatment of mEHT, like we shown above, could be considered during, as well as it could be a useful approach in post-cure time (Figure 20).

In the second wave of the pandemic, more and more patients have relapsed with persistent symptoms, especially myalgia, intense fatigue, a sensation of fever, shortness of breath, chest tightness, tachycardia, headaches, and anxiety [383]. Regardless of the severity of the disease, avoiding permanent ARDS, the damage could significantly reduce the patient's quality of life. The 8 - 12 weeks after hospitalization complains are pretty common. 74% of patients had persistent symptoms (notably breathlessness and excessive fatigue) [384] in the UK. In an observational cohort study, 78% of patients who had recovered from COVID-19 had abnormal findings on cardiovascular MRI (median of 71 days after diagnosis), and 36% reported dyspnoea and unusual fatigue [385]. The three or more weeks of primary care after the presence of symptoms have proposed guidelines [386]. Nevertheless, the research on the reasons for the long-term care is warranted, together with the rising questions about the consequent morbidities like diabetes, metabolic disorder of interstitial lung-disease [387].

The reinfection of cured patients is also possible [388], so follow-up is reasonable. Returning to the analogy of military strategy: the possibility of winning a war lies in the new technologies, the new weapons that are beyond the enemy's

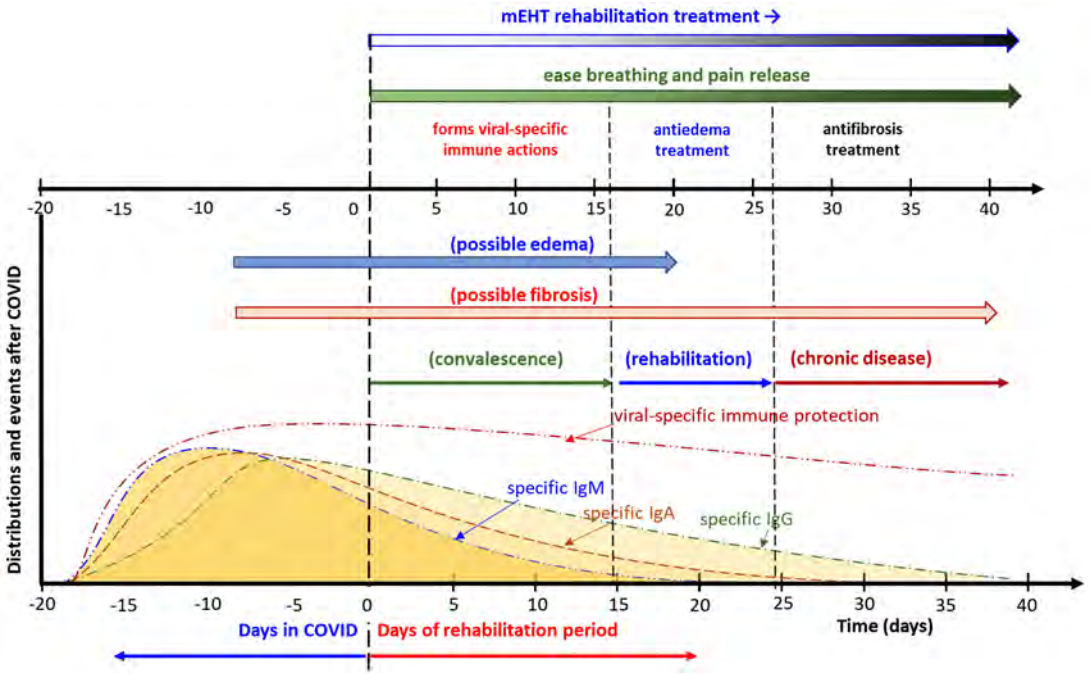

Figure 20. The possible rehabilitation treatment of mEHT. The treatment may be used successfully for the convalescent period against the remaining fibrosis and edema.

expectations. Chemical machinery is embedded and regulated in complex ways in living objects, developed and optimized by evolution over millions of years. We have to use those effects and technology against COVID, which is above specially chosen chemical reactions. We need a deductive (holistic) approach, which considers the system, and deduces the details from the complete unit [389]. Our presented hypothesis below gives a proposal to solve this challenge.

5. Conclusions

The human system has a complex regulatory mechanism controlled by various homeostatic actions to maintain the dynamic balance of the living organism. The self-similar structuring [76] develops an intrinsic self-time [169], regulating any developmental process's complex effects in the organism. Responses must consider this complexity, taking care of events' timing and the formulation of a balance. The balance determines the immune/autoimmune developments, the viral dose's effect concerning the immune developments, and the dangerous cytokine storm. The mEHT method, with its fractal physiology considerations, could help you find the best treatment option. I am convinced that the complexity of the treatment could only manage the disease's complexity. Expectations about a "miraculous" and unique curative effect are not realistic.

According to our recent knowledge except us nobody presented bioelectromagnetic treatment proposal to treat the COVID-19 and its consequences in convalescent period of time.

The mEHT method seems to be an optimal complementary treatment for SARS-CoV-2 infection and its consequences. It has special bioelectromagnetic steps to select for virus-infected cells, based on their markedly changed impedance in their cellular microenvironments. Excitation of membrane rafts and receptors induces transmembrane signals that choose apoptotic pathways and form DAMP and ICD, which develop virus-specific immune responses. An appropriate time fractal amplitude modulation attempts to balance the unusual systemic regulations. Time-fractal modulation drives processes in the direction of healthy homeostatic balance, promoting the immune system for vigilance [390]. Allometric fractal considerations help solve structural and metabolic problems of SARS viruses [81]. Mechanistic investigations of the effects of mEHT in related pulmonary fibrotic animal models can be effectively performed using *in vivo* molecular imaging outcomes [391], and X-ray computed tomography fractal dimension analysis [392]. The mEHT acts on the fractal complexity [393]. It uses an allometric approach [394] for the self-similarity [76] of homeostatic systems [59] [395], providing additional support for its action against the formation of IPF.

The mEHT is a possible and feasible treatment to manage the complexity of the therapy. It could be used for three purposes, encompassing all medical activities used in the epidemic. The method could be applied:

1) as prophylactics, when the infection is recognized, but symptoms have not

developed or only weakly developed yet;

2) for the treatment of patients suffering from mild and severe symptoms;

3) for the recovery period, when the individual is discharged from the hospital but needs rehabilitative care.

Our proposal is to use an adequate electromagnetic treatment, which can solve numerous challenges in the SARS-CoV-2 viral infection and its consequences, based on the results obtained by the mEHT applications that have proven to be successful in malignant diseases [396]. We propose the application of a broad set of mEHT actions for the treatment of SARS-CoV-2 infection and its post-treatment syndrome.

Conflicts of Interest

The author declares no conflicts of interest regarding the publication of this paper.

References

[1] Peiris, J.S., Lai, S.T., Poon, L.L. and SARS Study Group (2003) Coronavirus as a Possible Cause of Severe Acute Respiratory Syndrome. *The Lancet*, **361**, 1319-1325. https://doi.org/10.1016/S0140-6736(03)13077-2

[2] Drosten, C., Gunther, S., Preiser, W., *et al.* (2003) Identification of a Novel Coronavirus in Patients with Severe Acute Respiratory Syndrome. *The New England Journal of Medicine*, **348**, 1967-1976. https://doi.org/10.1056/NEJMoa030747

[3] Gorbalenya, A.E., Baker, S.C., Baric, R.S., de Groot, R.J., Drosten, C., Gulyaeva, A.A., *et al.* (2020) The Species Severe Acute Respiratory Syndrome-Related Coronavirus: Classifying 2019-nCoV and Naming It SARS-CoV-2. *Nature Microbiology*, **5**, 536-544. https://doi.org/10.1038/s41564-020-0695-z

[4] *D*ucharme, J. (2020) World Health Organization Declares COVID-19 a "Pandemic". Here's What That Means, time.com. https://time.com/5791661/who-coronavirus-pandemic-declaration/

[5] Barry, C.A. (1983) Pareto Distributions. International Co-Operative Publishing House, Fairland.

[6] Galvani, A.P. and May, R.M. (2005) Epidemiology: Dimensions of Superspreading. *Nature*, **438**, 293-295. https://doi.org/10.1038/438293a

[7] Chin, W.C.B. and Bouffanais, R. (2020) Spatial Super-Spreaders and Super-Susceptibles in Human Movement Networks. https://arxiv.org/abs/2005.05063 https://doi.org/10.1038/s41598-020-75697-z

[8] Bergmann, K. (2014) UV-C Irradiation: A New Viral Inactivation Method for Biopharmaceuticals. *America Pharmaceutical Review*, Thursday, November 20, 2014. https://www.americanpharmaceuticalreview.com/Featured-Articles/169257-UV-C-Irradiation-A-New-Viral-Inactivation-Method-for-Biopharmaceuticals/

[9] Van Doremalen, N., Morris, D.H., Holbrook, M.G., *et al.* (2020) Aerosol and Surface Stability of SARS-CoV-2 as Compared with SARS-CoV-1. *The New England Journal of Medicine*, **382**, 16. https://doi.org/10.1056/NEJMc2004973

[10] Liu, M. (2020) Overlapping and Discrete Aspects of the Pathology of SARS-CoV, MERS-CoV, and 2019-nCoV. *Journal of Medical Virology*, **92**, 491-494.

https://doi.org/10.1002/jmv.25709

[11] Raoult, D., Zumla, A., Locatelli, F., *et al.* (2020) Coronavirus Infections: Epidemiological, Clinical and Immunological Features and Hypotheses. *Cell Stress*, **4**, 66-75. https://doi.org/10.15698/cst2020.04.216

[12] Pathak, N. (2020) The "Great Imitator": How COVID-19 Can Look like Almost Any Condition? https://www.medicinenet.com/the_great_imitator_covid-19_coronavirus-news.htm

[13] Amaghashlag, D., Kandasami, G., Almanasef, M., *et al.* (2020) Review on the Coronavirus Disease (COVID-19) Pandemic: Its Outbreak and Current Status. *International Journal of Clinical Practice*, **74**, e13637. https://doi.org/10.1111/ijcp.13637

[14] Scarpetta, S., Pearson, M., Colombo, F., *et al.* (2020) OECD Treatments and a Vaccine for COVID-19: The Need for Coordinating Policies on R&D, Manufacturing and Access.

[15] Mather, N. (2020) How We Accelerated Clinical Trials in the Age of Coronavirus. *Nature*, **584**, 326. https://doi.org/10.1038/d41586-020-02416-z

[16] Coronavirus Research Database, Stanford University. https://covdb.stanford.edu/search/?study=clinical-studies&virus=SARS-CoV-2

[17] Weinrauch, Y. and Zychlinsky, A. (1999) The Induction of Apoptosis by Bacterial Pathogens. *Annual Review of Microbiology*, **53**, 155-187. https://doi.org/10.1146/annurev.micro.53.1.155

[18] Feys, B.J. and Parker, J.E. (2000) Interplay of Signaling Pathways in Plant Disease Resistance. *Trends in Genetics*, **16**, 4449-4555. https://doi.org/10.1016/S0168-9525(00)02107-7

[19] Jacobson, M.D., Weil, M. and Raff, M.C. (1997) Programmed Cell Death in Animal Development. *Cell*, **88**, 347-354. https://doi.org/10.1016/S0092-8674(00)81873-5

[20] Kerr, J.F., Wyllie, A.H. and Currie, A.R. (1972) Apoptosis: A Basic Biological Phenomenon with Wide-Ranging Implications in Tissue Kinetics. *British Journal of Cancer*, **26**, 239-257. https://doi.org/10.1038/bjc.1972.33

[21] Wyllie, A.H. (1980) Glucocorticoid-Induced Thymocyte Apoptosis Is Associated with Endogenous Endonuclease Activation. *Nature*, **284**, 555-556. https://doi.org/10.1038/284555a0

[22] Núñez, G., Benedict, M.A., Hu, Y. and Inohara, N. (1998) Caspases: The Proteases of the Apoptotic Pathway. *Oncogene*, **17**, 3237-3245. https://doi.org/10.1038/sj.onc.1202581

[23] Kumar, S. (1999) Mechanisms Mediating Caspase Activation in Cell Death. *Cell Death & Differentiation*, **6**, 1060-1066. https://doi.org/10.1038/sj.cdd.4400600

[24] Ganz, T. (2003) Defensins: Antimicrobial Peptides of Innate Immunity. *Nature Reviews Immunology*, **3**, 710-720. https://doi.org/10.1038/nri1180

[25] Yousefifard, M., Zali, A., Ali, K.M., *et al.* (2020) Antiviral Therapy in Management of COVID-19: A Systematic Review on Current Evidence. *Archives of Academic Emergency Medicine*, **8**, e45. https://doi.org/10.1111/ijcp.13557

[26] Nitolescu, G.M., Paunescu, H., Moschos, S.A., *et al.* (2020) Comprehensive Analysis of Drugs to Treat SARS-CoV-2 Infection: Mechanistic Insights into Current Covid-19 Therapies (Review). *International Journal of Molecular Medicine*, **46**, 467-488. https://doi.org/10.3892/ijmm.2020.4608

[27] Callawy, E. (2020) The Race for Coronavirus Vaccines. *Nature*, **580**, 576-577. https://doi.org/10.1038/d41586-020-01221-y

[28] Siemieniuk, R.A.C., Bartoszko, J.J., Ge, L., *et al.* (2020) Drug Treatments for Covid-19: Living Systematic Review and Network Meta-Analysis. *BMJ*, **370**, m2980.

[29] NIH Halts Clinical Trial of Hydroxychloroquine. https://www.nih.gov/news-events/news-releases/nih-halts-clinical-trial-hydroxychloroquine

[30] Chen, C., Huang, J., Cheng, Z., Wu, J., Chen, S., Zhang, Y., *et al.* (2020) Favipiravir versus Arbidol for COVID-19: A Randomized Clinical Trial. https://doi.org/10.1101/2020.03.17.20037432

[31] Grein, J., Ohmagari, N., Shin, D., *et al.* (2020) Compassionate Use of Remdesivir for Patients with Severe COVID-19. *New England Journal of Medicine*, **382**, 2327-2336. https://doi.org/10.1056/NEJMoa2007016

[32] Beigel, J.H., Tomashek, K.M., Dodd, L.E., Mehta, A.K., Zingman, B.S., Kalil, A.C., *et al.* (2020) Remdesivir for the Treatment of Covid-19—Preliminary Report. *New England Journal of Medicine*, **383**, 993. https://doi.org/10.1056/NEJMoa2007764

[33] Sheahan, T.P., Sims, A.C., Leist, S.R., Schäfer, A., Won, J., Brown, A.J., *et al.* (2020) Comparative Therapeutic Efficacy of Remdesivir and Combination Lopinavir, Ritonavir, and Interferon Beta against MERS-CoV. *Nature Communications*, **11**, 222. https://doi.org/10.1038/s41467-019-13940-6

[34] Kim, U.J., Won, E.J., Kee, S.J., Jung, S.I. and Jang, H.C. (2016) Combination Therapy with Lopinavir/Ritonavir, Ribavirin and Interferon-α for Middle East Respiratory Syndrome. *Antiviral Therapy*, **21**, 455-459. https://doi.org/10.3851/IMP3002

[35] del Rio, C. and Malani, P.N. (2019) Novel Coronavirus—Important Information for Clinicians. *JAMA*, **323**, 1039-1040. https://doi.org/10.1001/jama.2020.1490

[36] Lim, J., Jeon, S., Shin, H.Y., Kim, M.J., Seong, Y.M., Lee, W.J., *et al.* (2020) Case of the Index Patient Who Caused Tertiary Transmission of COVID-19 Infection in Korea: The Application of Lopinavir/Ritonavir for the Treatment of COVID-19 Infected Pneumonia Monitored by Quantitative RT-PCR. *Journal of Korean Medical Science*, **35**, e79. https://doi.org/10.3346/jkms.2020.35.e89

[37] Cao, B., *et al.* (2020) A Trial of Lopinavir-Ritonavir in Adults Hospitalized with Severe Covid-19. *The New England Journal of Medicine*, **382**, 1787-1799. https://doi.org/10.1056/NEJMoa2001282

[38] Jawhara, S. (2020) Could Intravenous Immunoglobulin Collected from Recovered Coronavirus Patients Protect against COVID-19 and Strengthen the Immune System of New Patients? *International Journal of Molecular Sciences*, **21**, 2272. https://doi.org/10.3390/ijms21072272

[39] Luo, P., Liu, Y., Qiu, L., Liu, X., Liu, D. and Li, J. (2020) Tocilizumab Treatment in COVID-19: A Single Center Experience. *Journal of Medical Virology*, **92**, 814-848. https://doi.org/10.1002/jmv.25801

[40] Ledford, H. (2020) US Widens Access to Covid-19 Plasma—Despite Lack of Data. *Nature*, **584**, 505. https://doi.org/10.1038/d41586-020-02324-2

[41] Sullivan, H.C. and Roback, J.D. (2020) Convalescent Plasma: Therapeutic Hope or Hopeless Strategy in the SARS-CoV-2 Pandemic. *Transfusion Medicine Reviews*, **34**, 145-150. https://doi.org/10.1016/j.tmrv.2020.04.001

[42] Cohrane-Targeted Update: Safety and Efficacy of Hydroxychloroquine or Chloroquine for Treatment of Covid-19. https://www.who.int/publications/m/item/targeted-update-safety-and-efficacy-of-hydroxychloroquine-or-chloroquine-for-treatment-of-covid-19

[43] Zhou, Y., Chen, V., Shannon, C.P., *et al.* (2020) Interferon-α2b Treatment for Co-

vid-19. *Frontiers in Immunology*, **11**, 1061.
https://doi.org/10.3389/fimmu.2020.01061

[44] Fu, W., Liu, Y., Xia, L., *et al.* (2020) A Clinical Pilot Study on the Safety and Efficacy of Aerosol Inhalation Treatment of IFN-κ plus TFF2 in Patients with Moderate COVID-19. *EClinicalMedicine*, **25**, Article ID: 100478.
https://doi.org/10.1016/j.eclinm.2020.100478

[45] Krammer, F. (2020) SARS-CoV-2 Vaccines in Development. *Nature*, **586**, 516-527.
https://doi.org/10.1038/s41586-020-2798-3

[46] Li, W., Schafer, A., Kulkarni, S.S., *et al.* (2020) High Potency of a Bivalent Human VH Domain in SARS-CoV-2 Animal Models. *Cell*, **183**, 429-441.e16.
https://doi.org/10.1016/j.cell.2020.09.007

[47] Logunov, D.Y., Dolzhikova, I.V., Zubkova, O.V., *et al.* (2020) Safety and Immunogenicity of an rAd26 and rAd5 Vector-Based Heterologous Prime-Boost Covid-19 Vaccine in Two Formulations: Two Open, Non-Randomised Phase 1/2 Studies from Russia. *The Lancet*, **396**, 887-897.
https://doi.org/10.1016/S0140-6736(20)31866-3

[48] Burki, T.K. (2020) The Russian Vaccine for COVID-19. *The Lancet Respiratory Medicine*, **8**, E85-E86. https://doi.org/10.1016/S2213-2600(20)30402-1

[49] Bar-Zeev, N. and Inglesby, T. (2020) COVID-19 Vaccines: Early Success and Remaining Challenges. *The Lancet*, **396**, 868-869.
https://doi.org/10.1016/S0140-6736(20)31867-5

[50] Coronavirus: Oxford University Vaccine Trial Paused after Participant Falls Ill.
https://www.bbc.com/news/world-54082192

[51] Foster, R. and Mundell, E.J. (2020) Details Emerge on Unexplained Illness in AstraZeneca COVID Vaccine Trial. Medical Press.
https://medicalxpress.com/news/2020-09-emerge-unexplained-illness-astrazeneca-covid.html

[52] Cyranoski, D. and Malapaty, S. (2020) Relief as Coronavirus Vaccine Trials Restart—But Transparency Concerns Remain. *Nature*, **585**, 331-332.
https://doi.org/10.1038/d41586-020-02633-6

[53] Pan, H.-C., Peto, R., Karim, Q.A., Alejandria, M., Henao-Restrepo, A.M., García, C.H., Kieny, M.-P., Malekzadeh, R., Murthy, S., Preziosi, M.-P., Reddy, S., Periago, M.R., Sathiyamoorthy, V., Røttingen, J.-A., Swaminathan, S. and WHO Solidarity Trial Consortium (2020) Repurposed Antiviral Drugs for COVID-19-Interim WHO Solidarity Trial Results.

[54] Fox, M. (2020) Johnson & Johnson Pauses Covid-19 Vaccine Trial after "Unexplained Illness".
https://edition.cnn.com/2020/10/12/health/johnson-coronavirus-vaccine-pause-bn/index.html

[55] Lovelace, B. and Farr, C. (2020) U.S. Pauses Eli Lilly's Trial of a Coronavirus Antibody Treatment over Safety Concerns.
https://www.cnbc.com/2020/10/13/us-pauses-eli-lillys-trial-of-a-coronavirus-antibody-treatment-over-safety-concerns.html

[56] Horby, P., Lim, W.S., Emberson, J.R., *et al.* (2020) The Recovery Collaborative Group, Dexamethasone in Hospitalized Patients with Covid-19—Preliminary Report. *NEJM*.

[57] Wolf, Y.I., Katsnelson, M.I. and Koonin, E.V. (2018) Physical Foundations of Biological Complexity. *PNAS*, **115**, E8678-E8687.
https://doi.org/10.1073/pnas.1807890115

[58] Wu, M. and Higgs, P.G. (2012) The Origin of Life Is a Spatially Localized Stochastic Transition. *Biology Direct*, **7**, 42. https://doi.org/10.1186/1745-6150-7-42

[59] Hegyi, G., Vincze, Gy. and Szasz, A. (2012) On the Dynamic Equilibrium in Homeostasis. *Open Journal of Biophysics*, **2**, 64-71. https://doi.org/10.4236/ojbiphy.2012.23009

[60] Modell, H., Cliff, W., Michael, J., *et al.* (2015) A Physiologist's View of Homeostasis. *Advances in Physiology Education*, **39**, 259-266. https://doi.org/10.1152/advan.00107.2015

[61] Billman, G.E. (2020) Homeostasis: The Underappreciated and Far Too Often Ignored Central Organizing Principle of Physiology. *Frontiers in Physiology*, **11**, 200. https://doi.org/10.3389/fphys.2020.00200

[62] Eskov, V.M., Filatova, O.E., Eskov, V.V., *et al.* (2017) The Evolution of the Idea of Homeostasis: Determinism, Stochastics, and Chaos—Self-Organization. *Biophysics*, **62**, 809-820. https://doi.org/10.1134/S0006350917050074

[63] von Bertalanffy, K.L. (1934) Untersuchungen über die Gesetzlichkeit des Wachstums. I. Allgemeine Grundlagen der Theorie; mathematische und physiologische Gesetzlichkeiten des Wachstums bei Wassertieren. *Wilhelm Roux' Archive für Entwicklungsmechanik der Organismen*, **131**, 613-652. https://doi.org/10.1007/BF00650112

[64] Jakubik, J., Randáková, A., Rudajev, V., *et al.* (2019) Application and Limitations of Fitting of the Operational Model to Determine Relative Efficacies of Agonists. *Scientific Reports*, **9**, Article No. 4637. https://doi.org/10.1038/s41598-019-40993-w

[65] Turing, A.M. (1952) The Chemical Basis of Morphogenesis. *Philosophical Transactions of the Royal Society of London*, *Series B*, *Biological Sciences*, **237**, 37-72. https://doi.org/10.1098/rstb.1952.0012

[66] Aronson, J.K. (2016) The Hitchhiker's Guide to Clinical Pharmacology, Pharmacodynamics: How Drugs Work. https://www.cebm.net/wp-content/uploads/2016/05/Pharmacodynamics-How-drugs-work.pdf

[67] Wierman, M.J. (2010) An Introduction to Mathematics of Uncertainty. Hoors Program, Creighton University, College of Arts and Sciences, Omaha. http://typo3.creighton.edu/fileadmin/user/CCAS/programs/fuzzy_math/docs/MOU.pdf

[68] Nurgali, K., Jagoe, R.T. and Abalo, R. (2018) Editorial-Adverse Effects of Cancer Chemotherapy: Anything New to Improve Tolerance and Reduce Sequelae? *Frontiers in Pharmacology*, **9**, 245. https://doi.org/10.3389/fphar.2018.00245

[69] Devaux, C. and Schoepffler, P. (1979) Side-Effects of Mixed Agonist-Antagonist Analgesics Used in Sequential Anaesthesia. *British Journal of Clinical Pharmacology*, **7**, 323S-326S. https://doi.org/10.1111/j.1365-2125.1979.tb04708.x

[70] Rosenberg, S.M. and Queitsch, C. (2014) Combating Evolution to Fight Disease. *Science*, **343**, 1088-1089. https://doi.org/10.1126/science.1247472

[71] West, B.J. (2006) Where Medicine Went Wrong: Rediscovering the Path to Complexity. World Scientific, London. https://doi.org/10.1142/6175

[72] Pei, Y. (2015) From Determinism and Probability to Chaos: Chaotic Evolution towards Philosophy and Methodology of Chaotic Optimization. *The Scientific World Journal*, **2015**, Article ID: 704587. https://doi.org/10.1155/2015/704587

[73] Brown, J.H. and West, G.B. (2000) Scaling in Biology, Santa Fe Institute Studies in the Sciences of Complexity. Oxford University Press, Oxford.

[74] Calder, W.A. (1996) Size, Function and Life History. Dover Publications, Inc., Mineola, New York.

[75] Cohen, I.R. and Harel, D. (2007) Explaining a Complex Living System: Dynamics, Multi-Scaling and Emergence. *Journal of the Royal Society Interface*, **4**, 175-182. https://doi.org/10.1098/rsif.2006.0173

[76] Szasz, O., Szigeti, Gy.P. and Szasz, A. (2017) On the Self-Similarity in Biological Processes. *Open Journal of Biophysics*, **7**, 183-196. https://doi.org/10.4236/ojbiphy.2017.74014

[77] Walleczek, J. (2000) Self-Organized Biological Dynamics & Nonlinear Control. Cambridge Univ. Press, Cambridge. https://doi.org/10.1017/CBO9780511535338

[78] West, B.J. (1990) Fractal Physiology and Chaos in Medicine. World Scientific, Singapore, London.

[79] Bassingthwaighte, J.B., Leibovitch, L.S. and West, B.J. (1994) Fractal Physiology. Oxford Univ. Press, New York, Oxford. https://doi.org/10.1007/978-1-4614-7572-9

[80] Sego, T.J., Gianlupi, J.F., Aponte-Serrano, J., *et al.* (2020) A Modular Framework for Multiscale Multicellular Spatial Modeling of Viral Infection, Immune Response and Drug Therapy Timing and Efficacy in Epithelial Tissues. https://doi.org/10.1101/2020.04.27.064139

[81] He, J.-H. (2008) Fatalness of Virus Depends upon Its Cell Fractal Geometry. *Chaos, Solitons and Fractals*, **38**, 1390-1393. https://doi.org/10.1016/j.chaos.2008.04.018

[82] Frolich, H. (1988) Biological Coherence and Response to External Stimuli. Springer Verlag, Berlin Heidelberg. https://doi.org/10.1007/978-3-642-73309-3

[83] Szendro, P., Vincze, G. and Szasz, A. (2001) Pink Noise Behaviour of the Bio-Systems. *European Biophysics Journal*, **30**, 227-231. https://doi.org/10.1007/s002490100143

[84] Mode, C.J., Durrett, R., Klebaner, F., *et al.* (2013) Applications of Stochastic Processes in Biology and Medicine. *International Journal of Stochastic Analysis*, **2013**, Article ID: 790625. https://doi.org/10.1155/2013/790625

[85] Thimann, K.V. (1956) Promotion and Inhibition: Twin Themes of Physiology. *American Naturalist*, **90**, 145-162. https://doi.org/10.1086/281921

[86] Nickson, C., Iwashyna, J. and Young, P. (2020) COVID-19: Keeping the Baby in the Bath. https://litfl.com/covid-19-keeping-the-baby-in-the-bath

[87] Ortiz-Prado, E., Simbana-Rivera, K., Gomez-Barreno, L., *et al.* (2020) Clinical, Molecular and Epidemiological Characterization of the SARS-CoV-2 Virus and the Coronavirus Disease 2019 (COVID-19), a Comprehensive Literature Review. *Diagnostic Microbiology and Infectious Disease*, **98**, Article ID: 115094. https://doi.org/10.1016/j.diagmicrobio.2020.115094

[88] Chen, I.-Y., Chang, S.-C., Wu, H.-Y., *et al.* (2010) Upregulation of the Chemokine (C-C Motif) Ligand 2 via a Severe Acute Respiratory Syndrome Coronavirus Spike-ACE2 Signaling Pathway. *Journal of Virology*, **84**, 7703-7712. https://doi.org/10.1128/JVI.02560-09

[89] Verdecchia, P., Cavallini, C., Spanevello, A., *et al.* (2020) The Pivotal Link between ACE2 Deficiency and SARS-CoV-2 Infection. *European Journal of Internal Medicine*, **76**, 14-20. https://doi.org/10.1016/j.ejim.2020.04.037

[90] Chung, M.K., Karnik, S., Saef, J., *et al.* (2020) SARS-CoV-2 and ACE2: The Biology and Clinical Data Settling the ARB and ACEI Controversy. *EBioMedicine*, **58**, Article ID: 102907. https://doi.org/10.1016/j.ebiom.2020.102907

[91] Belouzard, S., Millet, J.K., Licitra, B.N., *et al.* (2012) Mechanisms of Coronavirus

Cell Entry Mediated by the Viras Spike Protein. *Viruses*, **4**, 1011-1033. https://doi.org/10.3390/v4061011

[92] Breidenbach, J.D., Dude, P., Gosh, S., *et al.* (2020) Impact of Comorbidities on SARS-CoV-2 Viral Entry-Related Genes. *Journal of Personalized Medicine*, **10**, 146. https://doi.org/10.3390/jpm10040146

[93] Hoffman, M., Kleine-Weber, H., Schroeder, S., *et al.* (2020) SARS-CoV-2 Cell Entry Depends on ACE2 and TMPRSS2 and Is Blocked by a Clinically Proven Protease Inhibitor. *Cell*, **181**, 271-280. https://doi.org/10.1016/j.cell.2020.02.052

[94] Heurich, A., Hofmann-Winkler, H., Giere, S., *et al.* (2020) TMPRSS2 and ADAM17 Cleave ACE2 Differentially and Only Proteolysis by TMPRSS2 Augments Entry Driven by the Severe Acute Respiratory Syndrome Coronavirus Spike Protein. *Journal of Virology*, **88**, 1293-1307. https://doi.org/10.1128/JVI.02202-13

[95] Ou, X., Liu, Y., Lei, X., *et al.* (2020) Characterization of Spike Glycoprotein of SARS-CoV-2 on Virus Entry and Its Immune Cross-Reactivity with SARS-CoV. *Nature Communications*, **11**, 1620. https://doi.org/10.1038/s41467-020-15562-9

[96] Kim, S.Y., Jin, W., Sood, A., Montgomery, D.W., Grant, O.C., Fuster, M.M., Fu, L., Dordick, J.S., Woods, R.J., Zhang, F., *et al.* (2020) Characterization of Heparin and Severe Acute Respiratory Syndrome-Related Coronavirus 2 (SARS-CoV-2) Spike Glycoprotein Binding Interactions. *Antiviral Research*, **181**, Article ID: 104873. https://doi.org/10.1016/j.antiviral.2020.104873

[97] Hudak, A., Szilak, L. and Letoha, T. (2020) Contribution of Syndecans to the Cellular Entry of SARS-CoV-2. *Research Square*. https://doi.org/10.21203/rs.3.rs-70340/v1

[98] Schött, U., Solomon, C., Fries, D., *et al.* (2016) The Endothelial Glycocalyx and Its Disruption, Protection and Regeneration: A Narrative Review. *Scandinavian Journal of Trauma, Resuscitation and Emergency Medicine*, **24**, 48. https://doi.org/10.1186/s13049-016-0239-y

[99] de Haan, C.A., Haijema, B.J., Schellen, P., Wichgers Schreur, P., te Lintelo, E., Vennema, H. and Rottier, P.J. (2018) Cleavage of Group 1 Coronavirus Spike Proteins: How Furin Cleavage Is Traded off against Heparan Sulfate Binding upon Cell Culture Adaptation. *Journal of Virology*, **82**, 6078-6083. https://doi.org/10.1128/JVI.00074-08

[100] Ren, L., Zhang, Y., Li, J., *et al.* (2015) Genetic Drift of Human Coronavirus OC43 Spike Gene during Adaptive Evolution. *Scientific Reports*, **5**, Article No. 11451. https://doi.org/10.1038/srep11451

[101] Bermejo-Jambrina, M., Eder, J., Kaptein, T.M., *et al.* (2020) SARS-CoV-2 Infection and Transmission Depends on Heparan Sulfates and Is Blocked by Low Molecular Weight Heparins. https://doi.org/10.1101/2020.08.18.255810

[102] Negri, E.M., Piloto, B.M., Morinaga, L.K., *et al.* (2020) Heparin Therapy Improving Hypoxia in COVID-19 Patients a Case Series. https://doi.org/10.1101/2020.04.15.20067017

[103] Thachil, J. (2020) The Versatile Heparin in COVID-19. *Journal of Thrombosis and Haemostasis*, **18**, 1020-1022. https://doi.org/10.1111/jth.14821

[104] Park, P.W. (2020) Extracellular Matrix: Surface Proteoglycans. In: *Encyclopedia of Respiratory Medicine*, 2nd Edition, Elsevier, Amsterdam, 1-8. https://doi.org/10.1016/B978-0-12-801238-3.11650-2

[105] Shang, J., Wan, Y., Luo, C., *et al.* (2020) Cell Entry Mechanisms of SARS-CoV-2. *PNAS*, **117**, 11727-11734. https://doi.org/10.1073/pnas.2003138117

[106] Terali, K., Baddal, B. and Gulcan, H.O. (2020) Prioritizing Potential ACE2 Inhibitors in the COVID-19 Pandemic: Insights from a Molecular Mechanics-Assisted Structure-Based Virtual Screening Experiment. *Journal of Molecular Graphics and Modelling*, **100**, Article ID: 107697. https://doi.org/10.1016/j.jmgm.2020.107697

[107] Goldberg, A. (2020) ACE2 in COVID-19: Is It Friend or Foe? Labtag Blog. https://blog.labtag.com/ace2-in-covid-19-is-it-friend-or-foe

[108] Guan, W.-J., Ni, Z.-Y., Liang, W.-H., *et al.* (2020) Clinical Characteristics of Coronavirus Disease 2019 in China. *The New England Journal of Medicine*, **382**, 1708-1720. https://doi.org/10.1056/NEJMoa2002032

[109] Crackower, M.A., Sarao, R., Oliveira-dos-Santos, A.J., Da Costa, J., Zhang, L., *et al.* (2002) Angiotensin-Converting Enzyme 2 Is an Essential Regulator of Heart Function. *Nature*, **417**, 822-828. https://doi.org/10.1038/nature00786

[110] Turner, A.J. (2015) ACE2 Cell Biology, Regulation, and Physiological Functions. In: *The Protective Arm of the Renin-Angiotensin System* (*RAS*), Elsevier, Amsterdam, 185-189, Chapter 25. https://doi.org/10.1016/B978-0-12-801364-9.00025-0

[111] Banu, N., Panikar, S.S., Leal, L.R., *et al.* (2020) Protective Role of ACE2 and Its Downregulation in SARS-CoV-2 Infection Leading to Macrophage Activation Syndrome: Therapeutic Implications. *Life Sciences*, **256**, Article ID: 117905. https://doi.org/10.1016/j.lfs.2020.117905

[112] Gonzalez-Villalobos, R.A., Shen, X.Z., Bernstein, E.A., Janjulia, T., Taylor, B., Giani, J.F., *et al.* (2013) Rediscovering ACE: Novel Insights into the Many Roles of the Angiotensin-Converting Enzyme. *Journal of Molecular Medicine*, **91**, 1143-1154. https://doi.org/10.1007/s00109-013-1051-z

[113] Cheng, H., Wang, Y. and Wang, G. (2020) Organ-Protective Effect of Angiotensin-Converting Enzyme 2 and Its Effect on the Prognosis of COVID-19. *Journal of Medical Virology*, **92**, 726-730. https://doi.org/10.1002/jmv.25785

[114] Bernstrein, K.E., Khan, Z., Giani, J.F., *et al.* (2017) Angiotensin-Converting Enzyme in Innate and Adaptive Immunity. *Nature Reviews Nephrology*, **14**, 325-336. https://doi.org/10.1038/nrneph.2018.15

[115] Bosso, M., Thanaraj, T.A., Abu-Farha, M., Alanbaei, M., *et al.* (2020) The Two Faces of ACE2: The Role of ACE2 Receptor and Its Polymorphysms in Hyperthension and COVID-19. *Molecular Therapy—Methods and Clinical Development*, **18**, 321-327. https://doi.org/10.1016/j.omtm.2020.06.017

[116] Tsioufis, C., Dimitriadis, K. and Tousoulis, D. (2020) The Interplay of Hypertension, ACE-2 and SARS-CoV-2: Emerging Data as the "Ariadne's Thread" for the "Labyrinth" of COVID-19. *Hellenic Journal of Cardiology*, **61**, 31-33. https://doi.org/10.1016/j.hjc.2020.05.003

[117] Devaux, C.A., Rolain, J.-M. and Raoult, D. (2020) ACE2 Receptor Polymorphism: Susceptibility to SARS-CoV-2, Hypertension, Multi-Organ Failure, and COVID-19 Disease Outcome. *Journal of Microbiology, Immunology and Infection*, **53**, 425-435. https://doi.org/10.1016/j.jmii.2020.04.015

[118] Ruiz, C.M.T., Balarin, Spadotto, M.A., Tanaka, S.C.S., Silva Mota da, V.I., Trovó de, M.A.B., *et al.* (2018) Polycystic Ovarian Syndrome: rs1799752 Polymorphism of ACE Gene. *Revista da Associação Médica Brasileira*, **64**, 1017-1022. https://doi.org/10.1590/1806-9282.64.11.1017

[119] Zheng, H. and Cao, J.J. (2020) Angiotensin-Converting Enzyme Gene Polymorphism and Severe Lung Injury in Patients with Coronavirus Disease 2019. *The American Journal of Pathology*, **190**, 1-5. https://doi.org/10.1016/j.ajpath.2020.07.009

[120] Reynolds, H.R., Adhikari, S., Pulgarin, C., Troxel, A.B., Iturrate, E., Johnson, S.B., Hausvater, A., Newman, J.D., Berger, J.S., Bangalore, S., *et al.* (2020) Renin- Angiotensin-Aldosterone System Inhibitors and Risk of Covid-19. *The New England Journal of Medicine*, **382**, 2441-2448. https://doi.org/10.1056/NEJMoa2008975

[121] Vaduganathan, M., Vardeny, O., Michel, T., McMurray, J.J.V., Pfeffer, M.A. and Solomon, S.D. (2020). Renin-Angiotensin-Aldosterone System Inhibitors in Patients with Covid-19. *The New England Journal of Medicine*, **382**, 1653-1659. https://doi.org/10.1056/NEJMsr2005760

[122] Li, Y., Zhou, W., Yang, L., *et al.* (2020) Physiological and Pathological Regulation of ACE2, the SARS-CoV-2 Receptor. *Pharmacological Research*, **1587**, Article ID: 104833. https://doi.org/10.1016/j.phrs.2020.104833

[123] Kalberg, J., Chong, D.S.Y. and Lai, W.Y.Y. (2004) Do Men Have a Higher Case Fatality Rate of Severe Acute Respiratory Syndrome than Women Do? *American Journal of Epidemiology*, **159**, 229-231. https://doi.org/10.1093/aje/kwh056

[124] Chakravarty, D., Nair, S.S., Hammouda, N., *et al.* (2020) Sex Differences in SARS-CoV-2 Infection Rates and the Potential Link to Prostate Cancer. *Communications Biology*, **3**, 374. https://doi.org/10.1038/s42003-020-1088-9

[125] Poletti, P., Tirani, M., Cereda, D., *et al.* (2020) Age-Specific SARS-CoV-2 Infection Fatality Ratio and Associated Risk Factors, Italy, February to April 2020. *Eurosurveillance*, **25**, pii=2001383. https://doi.org/10.2807/1560-7917.ES.2020.25.31.2001383

[126] Zhang, J., Wu, J., Sun, X., *et al.* (2020) Association of Hypertension with the Severity of SARS-CoV-2 Infection: A Meta-Analysis. *Epidemiology and Infection*, **148**, e106. https://doi.org/10.1017/S095026882000117X

[127] Mazucanti, C.H. and Egan, J.M. (2020) SARS-CoV-2 Disease Severity and Diabetes: Why the Connection and What Is to Be Done? *Immunity and Ageing*, **17**, 21. https://doi.org/10.1186/s12979-020-00192-y

[128] Nishiga, M., Wang, D.W., Han, Y., *et al.* (2020) COVID-19 and Cardiovascular Disease: From Basic Mechanisms to Clinical Perspectives. *Nature Reviews Cardiology*, **17**, 543-558. https://doi.org/10.1038/s41569-020-0413-9

[129] Schultze, A., Walker, A.J., MacKenna, B., *et al.* (2020) Risk of COVID-19-Related Death among Patients with Chronic Obstructive Pulmonary Disease or Asthma Prescribed Inhaled Corticosteroids: An Observational Cohort Study Using the OpenSAFELY Platform. *The Lancet Respiratory Medicine*, **8**, 1106-112. https://doi.org/10.1016/S2213-2600(20)30415-X

[130] Wu, V.-C., Hsueh, P.-R., Lin, W.-C., *et al.* (2014) Acute Renal Failure in SARS Patients: More than Rhabdomyoliysis. *Nephrology Dialysis Transplantation*, **19**, 3180-3182. https://doi.org/10.1093/ndt/gfh436

[131] Rubino, F., Amiel, S.A., Zimmet, P., *et al.* (2020) New-Onset Diabetes in Covid-19. *New England Journal of Medicine*, **383**, 789-790. https://doi.org/10.1056/NEJMc2018688

[132] Malapaty, S. (2020) Evidence Suggests the Coronavirus Might Trigger Diabetes. *Nature*, **583**, 16-17. https://doi.org/10.1038/d41586-020-01891-8

[133] Diao, B., Wang, C., Wang, R., *et al.* (2020) Human Kidney Is a Target for Novel Severe Acute Respiratory Syndrome Coronavirus 2 (SARS-CoV-2) Infection. https://doi.org/10.1101/2020.03.04.20031120

[134] Madjid, M., Safavi-Naeini, P., Solomon, S., *et al.* (2020) Potential Effects of Coronaviruses on the Cardiovascular System—A Review. *JAMA Cardiology*, **5**, 831-840.

https://doi.org/10.1001/jamacardio.2020.1286

[135] Puelles, V.G., Lütgehetmann, M., Lindenmeyer, M.T., *et al.* (2020) Multiorgan and Renal Tropism of SARS-CoV-2. *The New England Journal of Medicine*, **383**, 590-592. https://doi.org/10.1056/NEJMc2011400

[136] Radzikowska, U., Ding, M., Tan, G., *et al.* (2020) Distribution of ACE2, CD147, CD26, and Other SARS-CoV-2 Associated Molecules in Tissues and Immune Cells in Health and in Asthma, COPD, Obesity, Hypertension, and COVID-19 Risk Factors. *Allergy*, **75**, 2829-2845. https://doi.org/10.1111/all.14429

[137] Tian, S.F., Hu, W.D., Niu, L., *et al.* (2020) Pulmonary Pathology of Early Phase 2019 Novel Coronavirus (COVID-19) Pneumonia in Two Patients with Lung Cancer. *Journal of Thoracic Oncology*, **15**, 700-704.
https://doi.org/10.1016/j.jtho.2020.02.010
https://pubmed.ncbi.nlm.nih.gov/32114094

[138] Crowley, S.D. and Rudemiller, N.P. (2017) Immunologic Effects of the Renin-Angiotensin System. *Journal of the American Society of Nephrology*, **28**, 1350-1361. https://doi.org/10.1681/ASN.2016101066

[139] Silhol, F., Sarlon, G., Deharo, J.-C., *et al.* (2020) Downregulation of ACE2 Induces Overstimulation of the Renin-Angiotensin System in COVID-19: Should We Block the Renin-Angiotensin System? *Hypertension Research*, **43**, 854-856.
https://doi.org/10.1038/s41440-020-0476-3

[140] Fountain, J.H. and Lappin, S.L. (2020) Physiology, Renin Angiotensin System.
https://www.ncbi.nlm.nih.gov/books/NBK470410/?report=printable

[141] Luo, H., Wang, X., Chen, C., *et al.* (2015) Oxidative Stress Causes Imbalance of Renal Renin Angiotensin System (RAS) Components and Hyperthension in Obese Zucker Rats. *Journal of the American Heart Association*, **4**, e001559.
https://doi.org/10.1161/JAHA.114.001559

[142] Dambic, V., Pojatic, D., Stazic, A., *et al.* (2020) Significance of the Renin-Angiotensin System in Clinical Conditions. In: Kibel, A., Ed., *Selected Chapter from the Renin-Angiotensin System*, IntechOpen, London.
https://doi.org/10.5772/intechopen.92309

[143] Tolouian, R., Vahed, S.Z., Ghiyasvand, S., *et al.* (2020) COVID-19 Interactions with Angiotensin-Converting Enzyme 2 (ACE2) and the Kinin System: Looking at a Potential Treatment. *Journal of Renal Injury Prevention*, **9**, e19.
https://doi.org/10.34172/jrip.2020.19

[144] Tschope, C., Schultheiss, H.-P. and Walther, T. (2002) Multiple Interactions between Renin-Angiotensin and the Kallikrein-Kinin Systems: Role of ACE Inhibition and AT1 Receptor Blockade. *Journal of Cardiovascular Pharmacology*, **39**, 478-487.
https://doi.org/10.1097/00005344-200204000-00003

[145] Sidarta-Oliveira, D., Jara, C.P., Ferruzzi, A.J., *et al.* (2020) SARS-CoV-2 Receptor Is Co-Expressed with Elements of the Kinin-Kallikrein, Renin-Angiotensin and Coagulation Systems in Alveolar Cells. https://doi.org/10.1101/2020.06.02.20120634

[146] Zuo, W., Zhao, X. and Chen, Y.-G. (2020) SARS Coronavirus and Lung Fibrosis. In: Lal, S.K., Ed., *Molecular Biology of the SARS-Coronavirus*, Springer-Verlag, Berlin, Chapter 15, 247-258. https://doi.org/10.1007/978-3-642-03683-5_15

[147] Golias, Ch., Charalabopoulos, A., Stagikas, D., *et al.* (2007) The Kinin System—Bradykinin: Biological Effects and Clinical Implications. Multiple Role of the Kinin System—Bradykinin. *Hippokratia*, **11**, 124-128.

[148] Garvin, M.R., Alvarez, C., Miller, J.I., *et al.* (2020) A Mechanistic Model and Thera-

peutic Interventions for COVID-19 Involving a RAS-Mediated Bradykinin Storm. *eLife*, **9**, e59177. https://doi.org/10.7554/eLife.59177

[149] van de Veerdonk, F.L., Netea, M.G., van Deuren, M., *et al.* (2020) Kinins and Cytokines in COVID-19: A Comprehensive Pathophysiological Approach. https://doi.org/10.20944/preprints202004.0023.v1

[150] Delpino, M.V. and Quarleri, J. (2020) SARS-CoV-2 Pathogenesis: Imbalance in the Renin-Angiotensin System Favors Lung Fibrosis. *Frontiers in Cellular Infection Microbiology*, **10**, 340. https://doi.org/10.3389/fcimb.2020.00340

[151] Cereceda, R. and Beswick, E. (2020) A Supercomputer Analysed Data on COVID-19 and Helped Come Up with This New Hypothesis. Euronews. https://www.euronews.com/2020/09/05/a-supercomputer-analysed-data-on-covid-19-and-helped-come-up-with-this-new-hypothesis

[152] Kaplan, A.P. (2008) Angioedema. *WAO Journal*, **1**, 103-113. https://doi.org/10.1097/WOX.0b013e31817aecbe

[153] Meini, S., Zanichelli, A., Sbrojavacca, R., *et al.* (2020) Understanding the Pathophysiology of COVID-19? Could the Contact System Be the Key? *Frontiers in Immunology*, **11**, 2014. https://doi.org/10.3389/fimmu.2020.02014

[154] LaRusch, G.A., Mahdi, F., Shariat-Madar, Z., Adams, G., Sitrin, R.G., Zhang, W.M., *et al.* (2010) Factor XII Stimulates ERK1/2 and Akt through uPAR, Integrins, and the EGFR to Initiate Angiogenesis. *Blood*, **115**, 5111-5120. https://doi.org/10.1182/blood-2009-08-236430

[155] Wujak, L., Didiasova, M., Zakrzewicz, D., Frey, H., Schasfer, L. and Wygrecka, M. (2015) Heparan Sulfate Proteoglycans Mediate Factor XIIa Binding to the Cell Surface. *Journal of Biological Chemistry*, **290**, 7027-7039. https://doi.org/10.1074/jbc.M114.606343

[156] Yong, S.J. (2020) Overlooked Receptors in Covid-19: What ACE2 Alone Cannot Explain. https://medium.com/microbial-instincts/overlooked-receptors-could-explain-quirks-of-covid-19-that-ace2-alone-cannot-9470817f59d0

[157] Wang, K., Chen, W., Zhou, Y.-S., *et al.* (2020) SARS-CoV-2 Invades Host Cells via a Novel Route: CD147-Spike Protein. https://doi.org/10.1101/2020.03.14.988345

[158] Ulrich, H. and Pillat, M.M. (2020) CD147 as a Target for COVID-19 Treatment: Suggested Effects of Azithromycin and Stem Cell Engagement. *Stem Cell Reviews and Reports*, **16**, 434-440. https://doi.org/10.1007/s12015-020-09976-7

[159] (2020) CD147 a New Target of SARS-CoV-2 Invasion. *Cusabio*. https://www.cusabio.com/c-20985.html

[160] Xiong, L., Edwards, C.K. and Zhou, L. (2014) The Biological Function and Clinical Utilization of CD147 in Human Diseases: A Review of the Current Scientific Literature. *International Journal of Molecular Sciences*, **15**, 17411-17441. https://doi.org/10.3390/ijms151017411

[161] Luan, J., Zhao, Y., Zhang, Y., *et al.* (2017) CD147 Blockade as a Potential and Novel Treatment of Graft Rejection. *Molecular Medicine Reports*, **16**, 4593-4602. https://doi.org/10.3892/mmr.2017.7201

[162] Kendrick, A.A., Schafer, J., Dzieciatkowska, M., *et al.* (2016) CD147: A Small Molecule Transporter Ancillary Protein at the Crossroad of Multiple Hallmarks of Cancer and Metabolic Reprogramming. *Oncotarget*, **8**, 6742-6762. https://doi.org/10.18632/oncotarget.14272

[163] Li, X., Zhang, Y., Ma, W., *et al.* (2020) Enhanced Glucose Metabolism Mediated by

CD147 Contributes to Immunesupression in Hepatocellular Carcinoma. *Cancer Immunology, Immunotherapy*, **69**, 535-548. https://doi.org/10.1007/s00262-019-02457-y

[164] Huang, Q., Li, J., Xing, J., Li, W., Li, H., Ke, X., Zhang, J., Ren, T., Shang, Y., Yang, H., Jiang, J. and Chen, Z. (2014) CD147 Promotes Reprogramming of Glucose Metabolism and Cell Proliferation in HCC Cells by Inhibiting p53-Dependent Signaling Pathway. *Journal of Hepatology*, **61**, 859-866. https://doi.org/10.1016/j.jhep.2014.04.035

[165] Vassilaki, N. and Frakolaki, E. (2017) Virus-Host Interactions under Hypoxia. *Microbes and Infection*, **19**, 193-203. https://doi.org/10.1016/j.micinf.2016.10.004

[166] Domingo, P., Mur, I., Pomar, V., Corominas, H., Casademont, J. and de Benito, N. (2020) The Four Horsemen of a Viral Apocalypse: The Pathogenesis of SARS-CoV-2 Infection (COVID-19). *EBioMedicine*, **58**, Article ID: 102887. https://doi.org/10.1016/j.ebiom.2020.102887

[167] Du, L., He, Y., Zhou, Y., Liu, S., Zheng, B.-J. and Jiang, S. (2009) The Spike Protein of SARS-CoV—A Target for Vaccine and Therapeutic Development. *Nature Reviews Microbiology*, **7**, 226-236. https://doi.org/10.1038/nrmicro2090

[168] Walls, A.C., Park, Y.-J., Tortorici, M.A., *et al.* (2020) Structure, Function, and Antigenicity of the SARS-CoV-2 Spike Glycoprotein. *Cell*, **180**, 281-292. https://doi.org/10.1016/j.cell.2020.02.058

[169] Szasz, O., Szigeti, G.P. and Szasz, A. (2019) The Intrinsic Self-Time of Biosystems. *Open Journal of Biophysics*, **9**, 131-145.

[170] Longo, G. and Montevil, M. (2014) Perspectives on Organisms, Biological Time, Symmetries and Singularities. Springer-Verlag, Berlin, Heidelberg.

[171] Wang, F., Zhang, H. and Sun, Z. (2020) The Laboratory Tests and Host Immunity of COVID-19 Patients with Different Severity of Illness. *JCI Insight*, **5**, e137799. https://doi.org/10.1172/jci.insight.137799

[172] Banoun, H. (2020) Evolution of SARS-CoV-2 in Relation to the Host Immune System. https://papers.ssrn.com/sol3/papers.cfm?abstract_id=3637909 https://doi.org/10.2139/ssrn.3637909

[173] Sun, X., Wang, T., Cai, D., *et al.* (2020) Cytokine Storm in the Early Stages of Covid-19 Pneumonia. *Cytokine and Growth Factor Reviews*, **53**, 38-42. https://doi.org/10.1016/j.cytogfr.2020.04.002

[174] McMillan, P. and Uhal, B.D. (2020) COVID-19—A Theory of Autoimmunity to ACE-2. *MOJ Immunology*, **7**, 17-19.

[175] Mahmudpour, M., Roozbeh, J., Kehavarz, M., *et al.* (2020) COVID-19 Cytokine Storm—The Anger of Inflammation. *Cytokine*, **133**, Article ID: 155151. https://doi.org/10.1016/j.cyto.2020.155151

[176] Channappanavar, R. and Perlman, S. (2017) Pathogenic Human Coronavirus Infections: Causes and Consequences of Citokine Storm and Immunopathology. *Seminars in Immunopathology*, **39**, 529-539. https://doi.org/10.1007/s00281-017-0629-x

[177] Maisch, B. (2019) Cardio-Immunology of Myocarditis: Focus on Immune Mechanisms and Treatment Options. *Frontiers in Cardiovascular Medicine*, **6**, 48. https://doi.org/10.3389/fcvm.2019.00048

[178] Anoop, U.R. and Verma, K. (2020) Pulmonary Edema in COVID19—A Neural Hypothesis. *ACS Chemical Neuroscience*, **11**, 2048-2050. https://doi.org/10.1021/acschemneuro.0c00370

[179] MsGrath, B.A., Wallace, S. and Goswamy, J. (2020) Laryngeal Oedema Associated

with COVID-19 Complicating Airway Management. *Anaesthesia*, **75**, 972. https://doi.org/10.1111/anae.15092

[180] Tse, G.M.-K., To, K.-F., Chan, P.K.-S., *et al.* (2014) Pulmonary Pathological Features in Coronavirus Associated Severe Acute Respiratory Syndrome (SARS). *Journal of Clinical Pathology*, **57**, 260-265. https://doi.org/10.1136/jcp.2003.013276

[181] Luks, A.M., Freer, L., Grissom, C.K., *et al.* (2020) COVID-19 Lung Injury Is Not High Altitude Pulmonary Edema. *High Altitude Medicine and Biology*, **21**, 192-193. https://doi.org/10.1089/ham.2020.0055

[182] Zhu, Z., Tang, J., Chai, X., *et al.* (2020) How to Differentiate COVID-19 Pneumonia from Heart Failure with Computed Tomography at Initial Medical Contact during Epidemic Period. https://doi.org/10.1101/2020.03.04.20031047

[183] Gattinoni, L., Coppola, S., Cressoni, M., Busana, M., Rossi, S. and Chiumello, D. (2020) Covid-19 Does Not Lead to a "Typical" Acute Respiratory Distress Syndrome. *American Journal of Respiratory and Critical Care Medicine*, **201**, 1299-1300. https://doi.org/10.1164/rccm.202003-0817LE

[184] Okada, H., Yoshida, S., Hara, A., *et al.* (2020) Vascular Endothelial Injury Exacerbates Coronavirus Disease 2019: The Role of Endothelial Glycocalyx Protection. *Microcirculation*, e12654. https://doi.org/10.1111/micc.12654

[185] Lang, M., Som, A., Carey, D., *et al.* (2020) Pulmonary Vascular Manifestations of COVID-19 Pneumonia. *Radiology*: *Cardiothoracic Imaging*, **2**, e200277. https://doi.org/10.1148/ryct.2020200277

[186] Coperchini, F., Chiovato, L., Croce, L., *et al.* (2020) The Cytokine Storm in COVID-19: An Overview of the Involvement of the Chemokine/Chemokine-Receptor System. *Cytokine and Growth Factor Reviews*, **53**, 25-32. https://doi.org/10.1016/j.cytogfr.2020.05.003

[187] Maisch, B. (2020) SARS-CoV-2 as Potential Cause of Cardiac Inflammation and Heart Failure. Is It the Virus, Hyperinflammation, or MODS? *Herz*, **45**, 321-322. https://doi.org/10.1007/s00059-020-04925-z

[188] Huertas, A., Montani, D., Savale, L., *et al.* (2020) Endothelial Cell Dysfunction: A Major Player in SARS-CoV-2 Infection (COVID-19)? *European Respiratory Journal*, **56**, Article ID: 2001634. https://doi.org/10.1183/13993003.01634-2020

[189] Arteriograph, Interesting Facts—Innovative Method to Ease Arterial Stiffness Measurement. https://www.tensiomed.com/interesting-facts

[190] De Andrea, M., Ravera, R., Gioia, D., Gariglio, M. and Landolfo, S. (2002) The Interferon System: An Overview. *European Journal of Paediatric Neurology*, **6**, A41-A46. https://doi.org/10.1053/ejpn.2002.0573

[191] Parkin, J. and Cohen, B. (2001) An Overview of the Immune System. *The Lancet*, **357**, 1777-1789. https://doi.org/10.1016/S0140-6736(00)04904-7

[192] Liu, J., Zheng, X., Tong, Q., Li, W., Wang, B., Sutter, K., *et al.* (2020) Overlapping and Discrete Aspects of the Pathology and Pathogenesis of the Emerging Human Pathogenic Coronaviruses SARS-CoV, MERS-CoV, and 2019-nCoV. *Journal of Medical Virology*, **92**, 491-494. https://doi.org/10.1002/jmv.25709

[193] Xu, Z., Shi, L., Wang, Y., Zhang, J., Huang, L., Zhang, C., *et al.* (2020) Pathological Findings of COVID-19 Associated with Acute Respiratory Distress Syndrome. *The Lancet Respiratory Medicine*, **8**, 420-422. https://doi.org/10.1016/S2213-2600(20)30076-X

[194] Pacha, O., Sallman, M.A. and Evans, S.E. (2020) COVID-19: A Case for Inhibiting IL-17? *Nature Reviews*, *Immunology*, **20**, 345-346. https://doi.org/10.1038/s41577-020-0328-z

[195] Haller, O., Kochs, G. and Weber, F. (2007) Interferon, Mx, and Viral Countermeasures. *Cytokine & Growth Factor Reviews*, **18**, 425-433. https://doi.org/10.1016/j.cytogfr.2007.06.001

[196] Seder, R.A., Gazzinelli, R., Sher, A. and Paul, W.E. (1993) Interleukin 12 Acts Directly on CD4+ T Cells to Enhance Priming for Interferon γ Production and Diminishes Interleukin 4 Inhibition of Such Priming. *Proceedings of the National Academy of Sciences of the United States of America*, **90**, 10188-10192. https://doi.org/10.1073/pnas.90.21.10188

[197] Karupiah, G., Xie, Y.-W., Buller, M.L., *et al.* (1993) Inhibition of Viral Replication by Interferon-γ-Induced Nitric Oxide Synthase. *Science*, **261**, 1445-1448. https://doi.org/10.1126/science.7690156

[198] Hu, X., Li, W.P., Meng, C., *et al.* (2003) Inhibition of IFN-γ Signaling by Glucocorticoids. *The Journal of Immunology*, **170**, 4833-4839. https://doi.org/10.4049/jimmunol.170.9.4833

[199] Liu, P.P., Blet, A., Symth, D., *et al.* (2020) The Science Underlying COVID-19. *Circulation*, **142**, 68-78. https://doi.org/10.4049/jimmunol.170.9.4833

[200] Ong, E.Z., Chan, Y.F.Z., Leong, W.Y., Lee, N.M.Y., Kalimuddin, S., Mohideen, S.M.H., Chan, K.S., Tan, A.T., Bertoletti, A., Ooi, E.E. and Low, J.G.H. (2020) A Dynamic Immune Response Shapes COVID-19 Progression. *Cell Host & Microbe*, **27**, 879-882. https://doi.org/10.1016/j.chom.2020.03.021

[201] Caruana, G., Croxatto, A., Coste, A.T., *et al.* (2020) Diagnostic Strategies for SARS-CoV-2 Infection and Interpretation of Microbiological Results. *Clinical Microbiology and Infection*, **26**, 1178-1182. https://doi.org/10.1016/j.cmi.2020.06.019

[202] Skevaki, C., Fragkou, P.C., Cheng, C., *et al.* (2020) Laboratory Characteristics of Patients Infected with the Novel SARS-CoV-2 Virus. *Journal of Infection*, **81**, 205-212. https://doi.org/10.1016/j.jinf.2020.06.039

[203] Ruiz de Morales, J.M.G., Puig, L., Dauden, E., *et al.* (2019) Critical Role of Interleukin (IL)-17 in Inflammatory and Immune Disorders: An Updated Review of the Evidence Focusing in Controversies. *Autoimmunity Reviews*. https://doi.org/10.1016/j.autrev.2019.102429

[204] Fu, Y., Cheng, Y. and Wu, Y. (2020) Understanding SARS CoV-2-Mediated Inflammatory Responses: From Mechanisms to Potential Therapeutic Tools. *Virologica Sinica*, **35**, 266-271. https://doi.org/10.1007/s12250-020-00207-4

[205] Yale University (2020) Common Cold Combats Influenza. https://healthcare-in-europe.com/en/news/common-cold-combats-influenza.html

[206] Wu, A., Mihaylova, V.T., Landry, M.L., *et al.* (2020) Interference between Rhinovirus and Influenza A Virus: A Clinical Data Analysis and Experimental Infection Study. *The Lancet Microbe*.

[207] Turner, R.B., Felton, A., Kosak, K., *et al.* (1986) Prevention of Experimental Coronavirus Colds with Intranasal Alpha-2b Interferon. *The Journal of Infectious Diseases*, **154**, 443-447. https://doi.org/10.1093/infdis/154.3.443

[208] Manduffie, D. (2020) Scientists Say the Common Cold Can Keep the Flu at Bay. Can It Do the Same for Covid-19? https://www.courthousenews.com/scientists-say-the-common-cold-can-keep-the-flu-at-bay-can-it-do-the-same-for-covid-19

[209] Sette, A. and Crotty, S. (2020) Pre-Existing Immunity to SARS-CoV-2: The Knowns and Unknowns. *Nature Reviews, Immunology*. https://doi.org/10.1038/s41577-020-00430-w

[210] Foxman, E.F., Storer, J.A., Fitzgerald, M.E., *et al.* (2015) Temperature-Dependent Innate Defense against the Common Cold Virus Limits Viral Replication at Warm Temperature in Mouse Airway Cells. *PNAS*, **112**, 827-832. https://doi.org/10.1073/pnas.1411030112

[211] Brenner, I.K.M., Castellani, J.W., Gabaree, C., *et al.* (1999) Immune Changes in Humans during Cold Exposure: Effects of Prior Heating and Exercise. *Journal of Applied Physiology*, **87**, 699-710. https://doi.org/10.1152/jappl.1999.87.2.699

[212] Kamat, S. and Kumari, M. (2020) BCG against SARS-CoV-2: Second Youth of an Old Age Vaccine? *Frontiers in Pharmacology*. https://doi.org/10.3389/fphar.2020.01050

[213] Luke, A., O'Neill, J. and Netea, M.G. (2020) BCG-Induced Trained Immunity: Can It Offer Protection against COVID-19? *Nature Reviews/Immunology*. https://doi.org/10.1038/s41577-020-0337-y

[214] Chumakov, K., Benn, C.S., Aaby, P., Kottilil, S. and Gallo, R. (2020) Can Existing Live Vaccines Prevent COVID-19? *Science*, **368**, 1187-1188. https://doi.org/10.1126/science.abc4262

[215] Baragona, S. (2020) TB, Measles, Polio Vaccines Might Fight COVID-19. https://www.voanews.com/covid-19-pandemic/tb-measles-polio-vaccines-might-fight-covid-19

[216] Fidel, P.L. and Noverr, M.C. (2020) Could an Unrelated Live Attenuated Vaccine Serve as a Preventive Measure to Dampen Septic Inflammation Associated with COVID-19 Infection? *mBio*, **11**, e00907-20. https://doi.org/10.1128/mBio.00907-20

[217] Imami, A.S., O'Donovan, S.M., Creeden, J.F., Wu, X., Eby, H., McCullumsmith, C.B., Uvnäs-Moberg, K., McCullumsmith, R.E. and Andari, E. (2020) Oxytocin's Anti-Inflammatory and Proimmune Functions in COVID-19: A Transcriptomic Signature-Based Approach. *Physiological Genomics*, **52**, 401-407. https://doi.org/10.1152/physiolgenomics.00095.2020

[218] Voronov, S., Zueva, N., Orlov, V., *et al.* (2002) Temperature-Induced Selective Death of the C-Domain within Angiotensin-Converting Enzyme Molecule. *FEBS Letters*, **522**, 77-82. https://doi.org/10.1016/S0014-5793(02)02888-0

[219] Tharakan, S, Nomoto, K., Miyashita, S., *et al.* (2020) Body Temperature Correlates with Mortality in COVID-19 Patients. *Critical Care*, **24**, 298. https://doi.org/10.1186/s13054-020-03045-8

[220] Kang, D. and Ellgen, C. (2020) The Role of Temperature in COVID-19 Disease Severity and Transmission Rates. http://www.preprints.org https://doi.org/10.20944/preprints202005.0070.v1

[221] Szasz, A., Szasz, N. and Szasz, O. (2010) Oncothermia—Principles and Practices. Springer Science, Heidelberg. http://www.springer.com/gp/book/9789048194971 https://doi.org/10.1007/978-90-481-9498-8

[222] Chi, K.-H. (2020) Tumour-Directed Immunotherapy: Clinical Results of Radiotherapy with Modulated Electro-Hyperthermia. In: Szasz, A., Ed., *Challenges and Solutions of Oncological Hyperthermia*, Cambridge Scholars, Newcastle upon Tyne, Ch. 12, 206-226. https://www.cambridgescholars.com/challenges-and-solutions-of-oncological-hyperthermia

[223] Pang, L.K.C. (2012) Clinical Research on Integrative Treatment of Colon Carcinoma with Oncothermia and Clifford TCM Immune Booster. *Oncothermia Journal*, **5**, 24-41.

[224] Krenacs, T. and Benyo, Z. (2017) Tumor Specific Stress and Immune Response In-

duced by Modulated Electrohyperthermia in Relation to Tumor Metabolic Profiles. *Oncothermia Journal*, **20**, 264-272.

[225] Szasz, A.M., Minnaar, C.A., Szentmartoni, Gy., *et al.* (2019) Review of the Clinical Evidences of Modulated Electro-Hyperthermia (mEHT) Method: An Update for the Practicing Oncologist. *Frontiers in Oncology*, **9**, Article No. 1012. https://doi.org/10.3389/fonc.2019.01012

[226] Szasz, A.M., Arkosy, P., Arrojo, E.E., *et al.* (2020) Guidelines for Local Hyperthermia Treatment in Oncology. In: Szasz, A., Ed., *Challenges and Solutions of Oncological Hyperthermia*, Cambridge Scholars, Newcastle upon Tyne, Ch. 2, 32-71.

[227] Minnaar, C.A., Kotzen, J.A., Naidoo, T., *et al.* (2020) Analysis of the Effects of mEHT on the Treatment-Related Toxicity and Quality of Life of HIV-Positive Cervical Cancer Patients. *International Journal of Hyperthermia*, **37**, 263-272. https://doi.org/10.1080/02656736.2020.1737253

[228] Minnaar, C.A., Szasz, A.M., Arrojo, E., Lee, S.-Y., Giorentini, G., Borbenyi, E., *et al.* (2020) Summary and Update of the Method Modulated Electro-Hyperthermia. *Oncothermia Journal*, Special Edition, 49-130. https://oncotherm.com/sites/oncotherm/files/2020-09/specialedition01_1.pdf

[229] Szasz, A. (2020) Towards the Immunogenic Hyperthermic Action: Modulated Electro-Hyperthermia. *Clinical Oncology and Research*, *Science Repository*, **3**, 5-6. https://doi.org/10.31487/j.COR.2020.09.07

[230] Minnaar, C.A., Baeyens, A., Aeni, O.A., *et al.* (2019) Defining Characteristics of Nodal Disease on PET/CT Scans in Patients with HIV-Positive and -Negative Locally Advanced Cervical Cancer in South Africa. *Tomography*, **5**, 339-345. https://doi.org/10.18383/j.tom.2019.00017

[231] Minnaar, C.A., Kotzen, J.A., Ayeni, O.A., *et al.* (2019) The Effect of Modulated Electro-Hyperthermia on Local Disease Control in HIV-Positive and -Negative Cervical Cancer Women in South Africa: Early Results from a Phase III Randomized Controlled Trial. *PLoS ONE*, **14**, e0217894. https://doi.org/10.1371/journal.pone.0217894

[232] Szasz, A. (2015) Bioelectromagnetic Paradigm of Cancer Treatment Oncothermia. In: Rosch, P.J., Ed., *Bioelectromagnetic and Subtle Energy Medicine*, CRC Press, Taylor & Francis Group, Boca Raton, 323-336.

[233] Szasz, A. and Szasz, O. (2013) Oncothermia Protocol. *Oncothermia Journal*, **8**, 13-45. https://doi.org/10.1155/2013/159570 https://oncotherm.com/sites/oncotherm/files/2019-10/Oncothermia%20protocol.pdf

[234] Minnaar, C.A., Szasz, A.M., Arrojo, E., Lee, S.-Y., Giorentini, G., Borbenyi, E., *et al.* (2020) Summary and Update of the Method Modulated Electro-Hyperthermia. *Oncothermia Journal*, Special Edition, 49-130. https://oncotherm.com/sites/oncotherm/files/2020-09/specialedition01_1.pdf

[235] Szasz, O., Szasz, A.M. Minnaar, C. and Szasz, A. (2017) Heating Preciosity—Trends in Modern Oncological Hyperthermia. *Open Journal of Biophysics*, **7**, 116-144. https://doi.org/10.4236/ojbiphy.2017.73010

[236] Sanchez, E.L. and Lagunoff, M. (2015) Viral Activation of Cellular Metabolism. *Virology*, **479-480**, 609-618. https://doi.org/10.1016/j.virol.2015.02.038

[237] Mayer, K.A., Stöckl, J., Zlabinger, G.J., *et al.* (2019) Hijacking the Supplies: Metabolism as a Novel Facet of Virus-Host Interaction. *Frontiers in Immunology*, **10**, 1533. https://doi.org/10.3389/fimmu.2019.01533

[238] Thaker, S.K., Ch'ng, J. and Christofk, H.R. (2019) Viral Hijacking of Cellular Meta-

bolism. *BMC Biology*, **17**, 59. https://doi.org/10.1186/s12915-019-0678-9

[239] Andocs, G., Rehman, M.U., Zhao, Q.L., Papp, E., Kondo, T. and Szasz, A. (2015) Nanoheating without Artificial Nanoparticles Part II. Experimental Support of the Nanoheating Concept of the Modulated Electro-Hyperthermia Method, Using U937 Cell Suspension Model. *Biology and Medicine*, **7**, 1-9. https://doi.org/10.4172/0974-8369.1000247

[240] Szasz, O. and Szasz, A. (2014) Oncothermia—Nano-Heating Paradigm. *Journal of Cancer Science and Therapy*, **6**, 4. https://doi.org/10.4172/1948-5956.1000259

[241] Hegyi, G., Szigeti, G.P. and Szasz, A. (2013) Hyperthermia versus Oncothermia: Cellular Effects in Complementary Cancer Therapy. *Evidence-Based Complementary and Alternative Medicine*, **2013**, Article ID: 672873. https://doi.org/10.1155/2013/672873

[242] Conti, C., De Marco, A., Mastromarino, P., *et al.* (1999) Antiviral Effect of Hyperthermic Treatment in Rhinovirus Infection. *Antimicrobial Agents and Chemotherapy*, **43**, 822-829. https://doi.org/10.1128/AAC.43.4.822

[243] Szasz, A., Vincze, Gy., Szasz, O. and Szasz, N. (2003) An Energy Analysis of Extracellular Hyperthermia. *Magneto- and Electro-Biology*, **22**, 103-115. https://doi.org/10.1081/JBC-120024620

[244] Szasz, O., Szasz, A.M., Minnaar, C. and Szasz, A. (2017) Heating Preciosity—Trends in Modern Oncological Hyperthermia. *Open Journal of Biophysics*, **7**, 116-144. https://doi.org/10.4236/ojbiphy.2017.73010

[245] Wust, P., Kortum, B., Strauss, U., Nadobny, J., Zschaeck, S., Beck, M., *et al.* (2020) Non-Thermal Effects of Radiofrequency Electromagnetic Fields. *Scientific Reports*, **10**, Article No. 13488. https://doi.org/10.1038/s41598-020-69561-3

[246] Szasz, A. (2019) Thermal and Nonthermal Effects of Radiofrequency on Living State and Applications as an Adjuvant with Radiation Therapy. *Journal of Radiation and Cancer Research*, **10**, 1-17. https://doi.org/10.4103/jrcr.jrcr_25_18

[247] Szasz, O., Szigeti, Gy.P., Vancsik, T. and Szasz, A. (2018) Hyperthermia Dosing and Depth of Effect. *Open Journal of Biophysics*, **8**, 31-48. https://doi.org/10.4236/ojbiphy.2018.81004

[248] Simons, K. and Sampaio, L. (2011) Membrane Organization and Lipid Rafts. *Cold Spring Harbor Perspectives in Biology*, **3**, a004697. https://doi.org/10.1101/cshperspect.a004697

[249] Simons, K. and Toomre, D. (2000) Lipid Rafts and Signal Transduction. *Nature Reviews Molecular Cell Biology*, **1**, 31-41. https://doi.org/10.1038/35036052

[250] Rajendran, L. and Simons, K. (2005) Lipid Rafts and Membrane Dynamics. *Journal of Cell Science*, **118**, 1099-1102. https://doi.org/10.1242/jcs.01681

[251] Vincze, Gy., Szigeti, Gy., Andocs, G. and Szasz, A. (2015) Nanoheating without Artificial Nanoparticles. *Biology and Medicine*, **7**, 4.

[252] Papp, E., Vancsik, T., Kiss, E. and Szasz, O. (2017) Energy Absorption by the Membrane Rafts in the Modulated Electro-Hyperthermia (mEHT). *Open Journal of Biophysics*, **7**, 216-229. https://doi.org/10.4236/ojbiphy.2017.74016

[253] Prasad, B., Kim, S., Cho, W., *et al.* (2018) Effect of Tumor Properties on Energy Absorption, Temperature Mapping, and Thermal Dose in 13,56-MHz Radiofrequency Hyperthermia. *Journal of Thermal Biology*, **74**, 281-289. https://doi.org/10.1016/j.jtherbio.2018.04.007

[254] Nagy, G., Meggyeshazi, N. and Szasz, O. (2013) Deep Temperature Measurements in Oncothermia Processes. *Conference Papers in Medicine*, **2013**, Article ID:

685264. https://doi.org/10.1155/2013/685264

[255] Csoboz, B., Balogh, G.E., Kusz, E., *et al.* (2013) Membrane Fluidity Matters: Hyperthermia from the Aspects of Lipids and Membranes. *International Journal of Hyperthermia*, **29**, 491-499. https://doi.org/10.3109/02656736.2013.808765

[256] Li, G.-M., Li, Y.-G., Yamate, M., *et al.* (2007) Lipid Rafts Play an Important Role in the Early Stage of Severe Acute Respiratory Syndrome-Coronavirus Life Cycle. *Microbes and Infection*, **9**, 96-102. https://doi.org/10.1016/j.micinf.2006.10.015

[257] Manes, S., del Real, G. and Martinez, A. (2003) Pathogens: Raft Hijackers. *Nature Reviews Immunology*, **3**, 557-568. https://doi.org/10.1038/nri1129

[258] Takahashi, T. and Suzuki, T. (2009) Role of Membrane Rafts in Viral Infection. *The Open Dermatology Journal*, **3**, 178-194. https://doi.org/10.2174/1874372200903010178

[259] Baglivo, M., Baronio, M., Natalini, G., *et al.* (2020) Natural Small Molecules as Inhibitors of Coronavirus Lipid Dependent Attachment to Host Cells: A Possible Strategy for Reducing SARS-COV-2 Infectivity? *Acta BioMedica*, **91**, 161-164.

[260] Wang, T.T., Lien, C.Z., Liu, S., *et al.* (2020) Effective Heat Inactivation of SARS-CoV-2. https://doi.org/10.1101/2020.04.29.20085498

[261] Kiss, B., Kis, Z., Palyi, B., *et al.* (2020) Topography, Spike Dynamics and Nanomechanics of Individual Native SARS-CoV-2 Virions. https://doi.org/10.1101/2020.09.17.302380

[262] Lee, Y.-N., Chen, L.-K., Ma, H.-C., *et al.* (2005) Thermal Aggregation of SARS-CoV Membrane Protein. *Journal of Virological Methods*, **129**, 152-161. https://doi.org/10.1016/j.jviromet.2005.05.022

[263] Maruyama, H., Kimura, T., Liu, H., *et al.* (2018) Influenza Virus Replication Raises the Temperature of Cells. *Virus Research*. https://doi.org/10.1016/j.virusres.2018.09.011

[264] De Maio, A. (1999) Heat Shock Proteins: Facts, Thoughts, and Dreams. *Shock*, **11**, 1-12. https://doi.org/10.1097/00024382-199901000-00001

[265] Feder, M.E. and Hofmann, G.E. (1999) Heat-Shock Proteins, Molecular Chaperones, and the Stress Response: Evolutionary and Ecological Physiology. *Annual Review of Physiology*, **61**, 243-282. https://doi.org/10.1146/annurev.physiol.61.1.243

[266] Santoro, M.G. (2000) Heat Shock Factors and the Control of the Stress Response. *Biochemical Pharmacology*, **59**, 55-63. https://doi.org/10.1016/S0006-2952(99)00299-3

[267] Blank, M. (2012) Evidence for Stress Response. https://bioinitiative.org/wp-content/uploads/pdfs/sec07_2007_Evidence_for_Stress_Response.pdf

[268] Milani, A., Basirnejad, M. and Bolhassani, A. (2019) Heat-Shock Proteins in Diagnosis and Treatment: An Overview of Different Biochemical and Immunological Functions. *Immunotherapy*, **11**, 215-239. https://doi.org/10.2217/imt-2018-0105

[269] Kregel, K.C. (2002) Molecular Biology of Thermoregulation Invited Review: Heat Shock Proteins: Modifying Factors in Physiological Stress Responses and Acquired Thermotolerance. *Journal of Applied Physiology*, **92**, 2177-2186. https://doi.org/10.1152/japplphysiol.01267.2001

[270] De Marco, A. and Santoro, M.G. (1193) Antiviral Effect of Short Hyperthermic Treatment at Specific Stages of Vesicular Stomatitis Virus Replication Cycle. *Journal of General Virology*, **74**, 1685-1690. https://doi.org/10.1099/0022-1317-74-8-1685

[271] Yerusameli, A., Karman, S. and Lwoff, A. (1982) Treatment of Perennial Allergic Rhinitis by Local Hyperthermia. *Proceedings of the National Academy of Sciences of the United States of America*, **79**, 4766-4769. https://doi.org/10.1073/pnas.79.15.4766

[272] Roulston, A., Marcellus, R.C. and Branton, P.E. (1999) Viruses and Apoptosis. *Annual Review of Microbiology*, **53**, 577-628. https://doi.org/10.1146/annurev.micro.53.1.577

[273] Hardwick, J.M. (2001) Apoptosis in Viral Pathogenesis. *Cell Death & Differentiation*, **8**, 109-110. https://doi.org/10.1038/sj.cdd.4400820

[274] Benedict, C.A., Norris, P.S. and Ware, C.F. (2002) To Kill or Be Killed: Viral Evasion of Apoptosis. *Nature Immunology*, **3**, 1013-1018. https://doi.org/10.1038/ni1102-1013

[275] Wan, Y., Song, D., Li, H., *et al.* (2020) Stress Proteins: The Biological Functions in Virus Infection, Present and Challenges for Target-Based Antiviral Drug Development. *Signal Transduction and Targeted Therapy*, **5**, 125. https://doi.org/10.1038/s41392-020-00233-4

[276] Ren, L., Yang, R., Gou, L., *et al.* (2005) Apoptosis Induced by the SARS-Associated Coronavirus in Vero Cells Is Replication-Dependent and Involves Caspase. *DNA and Cell Biology*, **24**, 496-502. https://doi.org/10.1089/dna.2005.24.496

[277] Fung, T.S. and Liu, D.X. (2014) Coronavirus Infection, ER Stress, Apoptosis and Innate Immunity. *Frontiers in Microbiology*, **5**, 296. https://doi.org/10.3389/fmicb.2014.00296

[278] Tan, Y.-X., Tan, T.H.P., Lee, M.J.-R., *et al.* (2007) Induction of Apoptosis by the Severe Acute Respiratory Syndrome Coronavirus 7a Protein Is Dependent on Its Interaction with the Bcl-XL Protein. *Journal of Virology*, **81**, 6346-6355. https://doi.org/10.1128/JVI.00090-07

[279] Andocs, G., Renner, H., Balogh, L., Fonyad, L., Jakab, C. and Szasz, A. (2009) Strong Synergy of Heat and Modulated Electro-Magnetic Field in Tumor Cell Killing, Study of HT29 Xenograft Tumors in a Nude Mice Model. *Strahlentherapie und Onkologie*, **185**, 120-126. https://doi.org/10.1007/s00066-009-1903-1

[280] Meggyeshazi, N., Andocs, G. and Krenacs, T. (2013) Programmed Cell Death Induced by Modulated Electro-Hyperthermia. *Conference Papers in Medicine*, **2013**, Article ID: 187835. https://doi.org/10.1155/2013/249563

[281] Cummins, N. and Badley, A. (2009) The Trail to Viral Pathogenesis: The Good, the Bad and the Ugly. *Current Molecular Medicine*, **9**, 495-505. https://doi.org/10.2174/156652409788167078

[282] Peteranderi, C. and Herold, S. (2017) The Impact of the Interferon/TNF-Related Apoptosis-Inducing Ligand Signaling Axis on Disease Progression in Respiratory Viral Infection and Beyond. *Frontiers in Immunology*, **8**, 313. https://doi.org/10.3389/fimmu.2017.00313

[283] Lugade, A.A., Sorensen, E.W., Gerber, S.A., Moran, J.P., Frelinger, J.G. and Lord, E.M. (2008) Radiation-Induced IFN-Gamma Production within the Tumor Microenvironment Influences Antitumor Immunity. *The Journal of Immunology*, **180**, 3132-3139. https://doi.org/10.4049/jimmunol.180.5.3132

[284] Tsang, Y.-W., Huang, C.-C., Yang, K.-L., Chi, M.-S., Chiang, H.-C., Wang, Y.-S., Andocs, G., Szasz, A., Li, W.-T. and Chi, K.-H. (2015) Improving Immunological Tumor Microenvironment Using Electro-Hyperthermia Followed by Dendritic Cell Immunotherapy. *BMC Cancer*, **15**, 708. https://doi.org/10.1186/s12885-015-1690-2

[285] Vancsik, T., Kovago, Cs., Kiss, E., *et al.* (2018) Modulated Electro-Hyperthermia

Induced Loco-Regional and Systemic Tumor Destruction in Colorectal Cancer Allografts. *Journal of Cancer*, **9**, 41-53. https://doi.org/10.7150/jca.21520

[286] Meggyeshazi, N., Andocs, G., Balogh, L., *et al.* (2014) DNA Fragmentation and Caspase-Independent Programmed Cell Death by Modulated Electrohyperthermia. *Strahlentherapie und Onkologie*, **190**, 815-822. https://doi.org/10.1007/s00066-014-0617-1

[287] Andocs, G., Rehman, M.U., Zhao, Q.-L., Tabuchi, Y., Kanamori, M. and Kondo, T. (2016) Comparison of Biological Effects of Modulated Electro-Hyperthermia and Conventional Heat Treatment in Human Lymphoma U937 Cell. *Cell Death Discovery* (*Nature Publishing Group*), **2**, 16039. https://doi.org/10.1038/cddiscovery.2016.39

[288] Forika, G., Balogh, A., Vancsik, T., Zalatnai, A., *et al.* (2020) Modulated Electro-Hyperthermia Resolves Radioresistance of Panc1 Pancreas Adenocarcinoma and Promotes DNA Damage and Apoptosis *in Vitro*. *International Journal of Molecular Sciences*, **21**, 5100. https://pubmed.ncbi.nlm.nih.gov/32707717 https://doi.org/10.3390/ijms21145100

[289] Kao, P.H.-J., Chen, C.-H., Chang, Y.-W., *et al.* (2020) Relationship between Energy Dosage and Apoptotic Cell Death by Modulated Electro-Hyperthermia. *Scientific Reports*, **10**, Article No. 8936. https://doi.org/10.1038/s41598-020-65823-2 https://www.nature.com/articles/s41598-020-65823-2

[290] Graner, M.W. (2016) HSP90 and Immune Modulation in Cancer. *Advances in Cancer Research*, **129**, 191-224. https://doi.org/10.1016/bs.acr.2015.10.001

[291] Murshid, A., Gong, J. and Calderwood, K. (2012) Role of Heat Shock Proteins in Antigen Cross Presentation. *Frontiers in Immunology*, **3**, 63. https://doi.org/10.3389/fimmu.2012.00063

[292] Yang, K.-L., Huang, C.-C., Chi, M.-S., Chiang, H.-C., Wang, Y.-S., Andocs, G., *et al.* (2016) *In Vitro* Comparison of Conventional Hyperthermia and Modulated Electro-Hyperthermia. *Oncotarget*, **7**, 84082-84092. https://doi.org/10.18632/oncotarget.11444

[293] Meggyeshazi, N. (2015) Studies on Modulated Electrohyperthermia Induced Tumor Cell Death in a Colorectal Carcinoma Model. Thesis, Pathological Sciences Doctoral School, Semmelweis University, Budapest. http://repo.lib.semmelweis.hu/handle/123456789/3956

[294] Andocs, G., Meggyeshazi, N., Balogh, L., *et al.* (2014) Upregulation of Heat Shock Proteins and the Promotion of Damage-Associated Molecular Pattern Signals in a Colorectal Cancer Model by Modulated Electrohyperthermia. *Cell Stress and Chaperones*, **20**, 37-46. https://doi.org/10.1007/s12192-014-0523-6

[295] Qin, W., Akutsu, Y., Andocs, G., *et al.* (2014) Modulated Electro-Hyperthermia Enhances Dendritic Cell Therapy through an Abscopal Effect in Mice. *Oncology Reports*, **32**, 2373-2379. https://doi.org/10.3892/or.2014.3500

[296] Binder, R.J. (2014) Functions of Heat Shock Proteins in Pathways of the Innate and Adaptive Immune System. *Journal of Immunology*, **193**, 5765-5771. https://doi.org/10.4049/jimmunol.1401417

[297] Deffit, S.N. and Blum, J.S. (2015) A Central Role for HSC70 in Regulating Antigen Trafficking and MHC Class II Presentation. *Molecular Immunology*, **68**, 85-88. https://doi.org/10.1016/j.molimm.2015.04.007

[298] Hernandez, C., Huebener, P. and Schwabe, R.F. (2016) Damage-Associated Molecular Patterns in Cancer: A Double-Edged Sword. *Oncogene*, **35**, 5931-5941. https://doi.org/10.1038/onc.2016.104

[299] Keep, O., Galluzzi, L., Senovilla, L., *et al.* (2009) Viral Subversion of Immunogenic Cell Death. *Cell Cycle*, **8**, 860-869. https://doi.org/10.4161/cc.8.6.7939

[300] Klune, J.R., Dhuper, R., Cardinal, J., *et al.* (2008) HMGB1: Endogenous Danger Signaling. *Molecular Medicine*, **14**, 476-484. https://doi.org/10.2119/2008-00034.Klune

[301] Foel, D. (2007) Mechanisms of Disease: A "DAMP" View of Inflammatory Arthritis. *Nature Clinical Practice Rheumatology*, **3**, 382-390. https://doi.org/10.1038/ncprheum0531

[302] Bosteels, C., Neyt, K., Vanheerswynghels, M., *et al.* (2020) Inflammatory Type 2 cDCs Acquire Features of cDC1s and Macrophages to Orchestrate Immunity to Respiratory Virus Infection. *Immunity*, **52**, 1039-1056. https://doi.org/10.1016/j.immuni.2020.04.005

[303] Xu, Z., Yang, Y., Zhou, J., *et al.* (2019) Role of Plasma Calreticulin in the Prediction of Severity in Septic Patients. *Disease Makers*, **2019**, Article ID: 8792640. https://doi.org/10.1155/2019/8792640

[304] Gold, L.I., Eggleton, P., Sweetwyne, M.T., Van Duyn, L.B., Greives, M.R., Naylor, S.-M., Michalak, M. and Murphy-Ullrich, J.E. (2009) Calreticulin: Non-Endoplamic Reticulum Functions in Physiology and Disease. *FASEB*, **24**, 665-683. https://doi.org/10.1096/fj.09-145482

[305] Andersson, U., Ottestad, W. and Tracey, K.J. (2020) Extracellular HMGB1: A Therapeutic Target in Severe Pulmonary Inflammation Including COVID-19? *Molecular Medicine*, **26**, 42. https://doi.org/10.1186/s10020-020-00172-4

[306] Derer, A., Deloch, L., Rubner, Y., *et al.* (2015) Radio-Immunotherapy-Induced Immunogenic Cancer Cells as Basis for Induction of Systemic Anti-Tumor Immune Responses—Pre-Clinical Evidence and Ongoing Clinical Applications. *Frontiers in Immunology*, **6**, 505. https://doi.org/10.3389/fimmu.2015.00505

[307] Stagg, A.J. and Knight, S.C. (2001) Antigen-Presenting Cells. http://labs.icb.ufmg.br/lbcd/pages2/bernardo/Bernardo/Artigos/Antigen-presenting%20Cells.pdf https://doi.org/10.1038/npg.els.0000903

[308] Chi, K.-H. (2018) Tumor-Directed Immunotherapy: Combined Radiotherapy and Oncothermia. *Oncothermia Journal*, **24**, 196-235.

[309] Holtmeier, W. and Kabelitz, D. (2005) $\gamma\delta$ T Cells Link Innate and Adaptive Immune Responses, Mechanisms of Epithelial Defense. *Chemical Immunology and Allergy*, **86**, 151-183. https://doi.org/10.1159/000086659

[310] Coronavirus and the Cytoskeleton, Cytoskeleton, Inc. https://www.cytoskeleton.com/coronavirus-newsletter

[311] Simpson, C. and Yamauchi, Y. (2020) Microtubules in Influenza Virus Entry and Egress. *Viruses*, **12**, 117-136. https://doi.org/10.3390/v12010117

[312] Lv, X., Li, Z., Guan, J., Hu, S., Zhang, J., Lan, Y., Zhao, K., Lu, H., Song, D., He, H., Gao, F. and Hea, W. (2019) Porcine Hemagglutinating Encephalomyelitis Virus Activation of the Integrin a5b1-FAK-Cofilin Pathway Causes Cytoskeletal Rearrangement to Promote Its Invasion of N2a Cells. *Journal of Virology*, **93**, e01736-18. https://doi.org/10.1128/JVI.01736-18

[313] Rüdiger, A.-T., Mayrhofer, P., Ma-Lauer, Y., Pohlentz, G., Muthing, J., Brunn, von A. and Schwegmann-Wessels, C. (2016) Tubulins Interact with Porcine and Human S Proteins of the Genus Alphacoronavirus and Support Successful Assembly and Release of Infectious Viral Particles. *Virology*, **497**, 185-197. https://doi.org/10.1016/j.virol.2016.07.022

[314] Ward, B.M. (Yu2011) The Taking of the Cytoskeleton One Two Three: How Viruses Utilize the Cytoskeleton during Egress. *Virology*, **411**, 244-250. https://doi.org/10.1016/j.virol.2010.12.024

[315] Vincze, Gy., Szigeti, Gy.P. and Szasz, A. (2016) Reorganization of the Cytoskeleton. *Journal of Advances in Biology*, **9**, 1872-1882. https://cirworld.com/index.php/jab/article/view/4059

[316] Vincze, Gy. and Szasz, A. (2015) Reorganization of Actin Filaments and Microtubules by Outside Electric Field. *Journal of Advances in Biology*, **8**, 1514-1518.

[317] Marchetti, M. (2020) COVID-19-Driven Endothelial Damage: Complement, HIF-1, and ABL2 Are Potential Pathways of Damage and Targets for Cure. *Annals of Hematology*, **99**, 1701-1707. https://doi.org/10.1007/s00277-020-04138-8

[318] Whyte, M.K.B. and Walmsley, S.R. (2014) The Regulation of Pulmonary Inflammation by the Hypoxia-Inducible Factor-Hydroxylase Oxygen-Sensing Pathway. *Annals of the American Thoracic Society*, **11**, S271-S276. https://doi.org/10.1513/AnnalsATS.201403-108AW

[319] Zhang, R., Wu, Y., Zhao, M., *et al.* (2009) Role of HIF-1alpha in the Regulation ACE and ACE2 Expression in Hypoxic Human Pulmonary Artery Smooth Muscle Cells. *American Journal of Physiology—Lung Cellular and Molecular Physiology*, **297**, L631-L640. https://doi.org/10.1152/ajplung.90415.2008

[320] Arias-Reyes, C., Zubieta-DeUrioste, N., Poma-Machicao, L., *et al.* (2020) Does the Pathogenesis of SAR-CoV-2 Virus Decrease at High-Altitude? *Respiratory Physiology & Neurobiology*, **22**, Article ID: 103443. https://doi.org/10.1016/j.resp.2020.103443

[321] Joyce, K.E., Weaver, S.R. and Lucas, S.J.E. (2020) Geographic Components of SARS-CoV-2 Expansion: A Hypothesis. *Journal of Applied Physiology*, **129**, 257-262. https://doi.org/10.1152/japplphysiol.00362.2020

[322] Afsar, B., Kanbay, M. and Afsar, R.E. (2020) Hypoxia Inducible Factor-1 Protects against COVID-19: A Hypothesis. *Medical Hypotheses*, **143**, Article ID: 109857. https://doi.org/10.1016/j.mehy.2020.109857

[323] Rubio-Casillas, A. (2020) Does SARS CoV 2 Virus Induce Hypoxia to Increase Its Replication?

[324] Kim, W., Kim, M.S., Kim, H.J., *et al.* (2017) Role of HIF-1α in Response of Tumors to a Combination of Hyperthermia and Radiation *in Vivo*. *International Journal of Hyperthermia*, **34**, 276-283. https://doi.org/10.1080/02656736.2017.1335440

[325] Mathivanan, S., Devesa, I., Changeux, J.-P., *et al.* (2016) Bradykinin Induces TRPV1 Exocytotic Recruitment in Peptidergic Nociceptors. *Frontiers in Pharmacology*, **7**, 178. https://doi.org/10.3389/fphar.2016.00178

[326] Jia, Y. and Lee, L.-Y. (2007) Role of TRPV Antagonists in Respiratory Diseases. *Biochimica et Biophysica Acta*, **1772**, 915-927. https://doi.org/10.1016/j.bbadis.2007.01.013

[327] Dietrich, A. (2019) Modulators of Transient Receptor Potential (TRP) Channels as Therapeutic Options for Lung Disease. *Pharmaceuticals*, **12**, 23. https://doi.org/10.3390/ph12010023

[328] Kuebler, W.M., Jordt, S.-E. and Liedtke, W.B. (2020) Urgent Reconsideration of Lung Edema as a Preventable Outcome in COVID-19: Inhibition of TRPV4 Represents a Promising and Feasible Approach. *American Journal of Physiology—Lung Cellular and Molecular Physiology*, **318**, L1239-L1243. https://doi.org/10.1152/ajplung.00161.2020

[329] Lee, S.-Y., Kim, J.-H., Han, Y.-H., *et al.* (2018) The Effect of Modulated Electro-Hyperthermia on Temperature and Blood Flow in Human Cervical Carcinoma. *International Journal of Hyperthermia*. https://doi.org/10.1080/02656736.2018.1423709

[330] Batawi, S., Tarazan, N., Al-Raddadi, R., *et al.* (2019) Quality of Life Reported by Survivors after Hospitalization for Middle East Respiratory Syndrome (MERS). *Health and Quality of Life Outcomes*, **17**, 101. https://doi.org/10.1186/s12955-019-1165-2

[331] Ngai, J.C., Ko, F.W., Ng, S.S., To, K.W., Tong, M. and Hui, D.S. (2010) The Long-Term Impact of Severe Acute Respiratory Syndrome on Pulmonary Function, Exercise Capacity and Health Status. *Respirology*, **15**, 543-550. https://doi.org/10.1111/j.1440-1843.2010.01720.x

[332] Gurkan, O.U., O'Donnell, C., Brower, R., *et al.* (2003) Differential Effects of Mechanical Ventilatory Strategy on Lung Injury and Systemic Organ Inflammation in Mice. *American Journal of Physiology—Lung Cellular and Molecular Physiology*, **285**, L710-L718. https://doi.org/10.1152/ajplung.00044.2003

[333] Kalluri, R. and Weinberg, R.A. (2009) The Basics of Epithelial-Mesenchymal Transition. *Journal of Clinical Investigation*, **119**, 1420-1428. https://doi.org/10.1172/JCI39104

[334] Lee, K.A. and Nelson, C.M. (2012) New Insights into the Regulation of Epithelial-Mesenchymal Transition and Tissue Fibrosis. *International Review of Cell and Molecular Biology*, **294**, 171-221. https://doi.org/10.1016/B978-0-12-394305-7.00004-5

[335] Cabrera-Benítez, N.E., Parotto, M., Post, M., *et al.* (2012) Mechanical Stress Induces Lung Fibrosis by Epithelial-Mesenchymal Transition. *Critical Care Medicine*, **40**, 510-517. https://doi.org/10.1097/CCM.0b013e31822f09d7

[336] Hill, C., Jones, M.G., Davies, D.E., *et al.* (2019) Epithelial-Mesenchymal Transition Contributes to Pulmonary Fibrosis via Aberrant Epithelial/Fibroblastic Cross-Talk. *Journal of Lung Health and Diseases*, **3**, 31-35. https://doi.org/10.29245/2689-999X/2019/2.1149

[337] Szasz, O., Szigeti, Gy.P., Szasz, A. and Benyo, Z. (2018) Role of Electrical Forces in Angiogenesis. *Open Journal of Biophysics*, **8**, 49-67. https://doi.org/10.4236/ojbiphy.2018.82005

[338] Ballerini, M., Baronzio, G.F., Capito, G., Szasz, O. and Cassutti, V. (2013) Androtherm Application for the Peyronie's Disease. *Conference Papers in Medicine*, **2013**, Article ID: 962349. http://www.hindawi.com/archive/2013/962349 https://doi.org/10.1155/2013/962349

[339] Hegyi, G., Molnar, I., Mate, A. and Petrovics, G. (2017) Targeted Radiofrequency Treatment—Oncothermia Application in Non Oncological Diseases as Special Physiotherapy to Delay the Progressive Development. *Clinical Practice*, **14**, 73-77. https://doi.org/10.4172/clinical-practice.100098

[340] Jeung, T.-S., Ma, S.-Y., Choi, J., *et al.* (2015) Results of Oncothermia Combined with Operation, Chemotherapy and Radiation Therapy for Primary, Recurrent and Metastatic Sarcoma. *Case Reports in Clinical Medicine*, **4**, 157-168. http://www.scirp.org/journal/PaperInformation.aspx?PaperID=56280 https://doi.org/10.4236/crcm.2015.45033

[341] DaSilva, R.M.V., Barichello, P.A., Medeiros, M.L., *et al.* (2013) Effect of Capacitive Radiofrequency on the Fibrosis of Patients with Cellulitis. *Dermatology Research and Practice*, **2013**, Article ID: 715829. https://doi.org/10.1155/2013/715829

[342] de Araujo, A.R., Soares, V.P.C., da Silva, F.S., *et al.* (2014) Radiofrequency for the Treatment of Skin Laxity: Mith or Truth. *Anais Brasileiros de Dermatologia*, **90**, 707-721. https://doi.org/10.1590/abd1806-4841.20153605

[343] Hagiwarra, S., Iwasasa, H., Matsumoto, S., *et al.* (2007) Association between Heat Stress Protein 70 Induction and Decreased Pulmonary Fibrosis in an Animal Model of Acute Lung Injury. *Lung*, **185**, 287-293. https://doi.org/10.1007/s00408-007-9018-x

[344] Ren, Y., Huo, W., Qi, R.-Q., *et al.* (2015) Intensive Local Thermotherapy Cleared Extensive Viral Warts in a Patient with Systemic Lupus Erythematosus. *International Journal of Hyperthermia*, **31**, 5-7. https://doi.org/10.3109/02656736.2014.993339

[345] Li, X., Zhang, C., Hong, Y., *et al.* (2012) Local Hyperthermia Treatment of Extensive Viral Warts in Darier Disease: A Case Report and Literature Review. *International Journal of Hyperthermia*, **28**, 451-455. https://doi.org/10.3109/02656736.2012.677929

[346] Fischer, H., Schwarzer, C. and Illek, B. (2003) Vitamin C Controls the Cystic Fibrosis Transmembrane Conductance Regulator Chloride Channel. *PNAS*, **101**, 3691-3696. https://doi.org/10.1073/pnas.0308393100

[347] Ou, J., Zhu, X., Zhang, H., *et al.* (2020) A Retrospective Study of Gemcitabine and Carboplatin with or without Intravenous Vitamin C on Patients with Advanced Triple-Negative Breast Cancer. *Integrative Cancer Therapies*, **19**, 1-7. https://doi.org/10.1177/1534735419895591

[348] Szasz, O., Szigeti, Gy.P. and Szasz, A.M. (2017) Electrokinetics of Temperature for Development and Treatment of Effusions. *Advances in Bioscience and Biotechnology*, **8**, 434-449. https://doi.org/10.4236/abb.2017.811032

[349] Szasz, A., Vincze, Gy., Szigeti, Gy. and Szasz, O. (2017) Internal Charge Redistribution and Currents in Cancerous Lesions. *Journal of Advances in Biology*, **10**, 2061-2079. http://cirworld.com/index.php/jab/article/view/6328/6283

[350] Akdis, M., Sokolowska, M., O'Mahony, L., *et al.* (2020) Immune Response to SARS-CoV-2 and Mechanisms of Immunopathological Changes in COVID-19. *Allergy*, **75**, 1564-1581. https://doi.org/10.1111/all.14364

[351] Rokni, M., Ghasemi, V. and Tavakoli, Z. (2020) Immune Responses and Pathogenesis of SARS-CoV-2 during an Outbreak in Iran: Comparison with SARS and MERS. *Reviews in Medical Virology*, **30**, e2107. https://doi.org/10.1002/rmv.2107

[352] Minnaar, C.A., Kotzen, J.A., Ayeni, O.A., *et al.* (2020) Potentiation of the Abscopal Effect by Modulated Electro-Hyperthermia in Locally Advanced Cervical Cancer Patients. *Frontiers in Oncology*, **10**, 1-8. https://doi.org/10.3389/fonc.2020.00376

[353] Krenacs, T., Meggyeshazi, N., Forika, G., *et al.* (2020) Modulated Electro- Hyperthermia-Induced Tumor Damage Mechanisms Revealed in Cancer Models. *International Journal of Molecular Sciences*, **21**, 6270. https://doi.org/10.3390/ijms21176270

[354] Patents on Tumor-Vaccination. a) EP 2703001 A1, Europe (2014) http://www.google.com/patents/EP2703001A1?cl=en;
b) US 2015/0217099 A1, USA (2015) http://www.freepatentsonline.com/20150217099.pdf;
c) 2013 307 344, Australia (2016) http://www.ipaustralia.com.au/applicant/xax-kft/patents/AU2013307344/;
d) KR 10-1714281, South Korea (2017) https://patents.google.com/patent/KR101714281B1/en

e) CA 2,879,739, Canada (2017)
http://www.google.com/patents/CA2879739C?cl=en.

[355] Lopez-Collazo, E., Avendano-Ortiz, J., Martin-Quiros, A., *et al.* (2020) Immune Response and COVID-19: A Mirror Image of Sepsis. *International Journal of Biological Sciences*, **16**, 2479-2489. https://doi.org/10.7150/ijbs.48400

[356] Bootman, M., Golding, J. and Male, D.K. (2020) How Does the Human Body Fight a Viral Infection? Open Learn.
https://www.open.edu/openlearn/science-maths-technology/biology/how-does-the-human-body-fight-viral-infection

[357] Garcia, L.F. (2020) Immune Response, Inflammation, and the Clinical Spectrum of COVID-19. *Frontiers in Immunology*, **11**, 1441.
https://doi.org/10.3389/fimmu.2020.01441

[358] Fu, L., Wang, B., Yuan, T., *et al.* (2020) Clinical Characteristics of Coronavirus Disease 2019 (COVID-19) in China: A Systematic Review and Meta-Analysis. *Journal of Infection*, **80**, 656-665. https://doi.org/10.1016/j.jinf.2020.03.041

[359] Mehta, P., McAuley, D., Brown, M., *et al.* (2020) COVID-19: Consider Cytokine Storm Syndromes and Immunosuppression. *The Lancet*, **395**, 1033-1034.
https://doi.org/10.1016/S0140-6736(20)30628-0

[360] Shahabinezhad, F., Mosaddeghi, P., Negahdaripour, M., *et al.* (2020) Therapeutic Approaches for Covid-19 Based on the Dynamics of Interferon-Mediated Immune Responses. https://doi.org/10.20944/preprints202003.0206.v1

[361] Matched Antigen Pairs of SARS-CoV-2 Serology Test Development. Creative Diagnostics.
https://www.creative-diagnostics.com/news-matched-antigen-pair-for-sars-cov-2-serology-test-development-86.htm

[362] Chakravarthy, K.V. (2012) Investigating the Adaptive Immune Response in Influenza and Secondary Bacterial Pneumonia and Nanoparticle Based Therapeutic Delivery. PhD Dissertation, Department of Microbiology and Immunology, State University of New York, Buffalo.
https://www.researchgate.net/publication/258694611_Investigating_the_adaptive_immune_response_in_influenza_and_secondary_bacterial_pneumonia_and_nanoparticle_based_therapeutic_delivery

[363] Long, Q.-X., Liu, B.-Z., Deng, H.-J., *et al.* (2020) Antibody Responses to SARS-CoV-2 in Patients with COVID-19. *Nature Medicine*, **26**, 845-848.
https://doi.org/10.1038/s41591-020-0897-1

[364] Zhang, W., Du, R.-H., Li, B., *et al.* (2020) Molecular and Serological Investigation of 2019-nCoV Infected Patients: Implication of Multiple Shedding Routes. *Emerging Microbes & Infections*, **9**, 386-389. https://doi.org/10.1080/22221751.2020.1729071

[365] Zhao, J., Yuan, Q., Wang, H., *et al.* (2020) Antibody Responses to SARS-CoV-2 in Patients of Novel Coronavirus Disease 2019. *Clinical Infectious Diseases*, ciaa344.
https://doi.org/10.1093/cid/ciaa344

[366] Guo, L., Ren, L., Yang, S., *et al.* (2020) Profiling Early Humoral Response to Diagnose Novel Coronavirus Disease (COVID-19). *Clinical Infectious Diseases*, ciaa310.

[367] Liu, L., Liu, W., Zeng, Y., *et al.* (2020) A Preliminary Study on Serological 1 Assay for Severe Acute Respiratory Syndrome Coronavirus 2 (SARS-CoV-2) in 238 Admitted Hospital Patients. *Microbes and Infection*, **22**, 206-211.
https://doi.org/10.1016/j.micinf.2020.05.008

[368] Sethuraman, N., Jeremiah, S.S. and Ryo, A. (2020) Interpreting Diagnostic Tests for SARS-CoV-2. *JAMA*, **323**, 2249-2251. https://doi.org/10.1001/jama.2020.8259

[369] Chen, J., Lau, Y.F., Lamirande, E.W., Paddock, C.D., Bartlett, J.H., Zaki, S.R. and Subbarao, K. (2010) Cellular Immune Responses to Severe Acute Respiratory Syndrome Coronavirus (SARS-CoV) Infection in Senescent BALB/c Mice: CD4+ T Cells Are Important in Control of SARS-CoV Infection. *Journal of Virology*, **84**, 1289-1301. https://doi.org/10.1128/JVI.01281-09

[370] Liu, A., Wang, W., Zhao, X., *et al.* (2020) Disappearance of Antibodies to SARS-CoV-2 in a Covid-19 Patient after Recovery. *Clinical Microbiology and Infection*. https://doi.org/10.1016/j.cmi.2020.07.009

[371] Mo, H., Zeng, G., Ren, X., *et al.* (2006) Longitudinal Profile of Antibodies against SARS-Coronavirus in SARS Patients and Their Clinical Significance. *Respirology*, **11**, 49-53. https://doi.org/10.1111/j.1440-1843.2006.00783.x

[372] Fan, E., Beitler, J.R., Brochard, L., *et al.* (2020) COVID-19-Associated Acute Respiratory Distress Syndrome: Is a Different Approach to Management Warranted? *The Lancet Respiratory Medicine*, **8**, 816-821. https://doi.org/10.1016/S2213-2600(20)30304-0

[373] Vargas, M., Sutherasan, Y., Gregoretti, C., *et al.* (2020) PEEP Role in ICU and Operating Room: From Pathophysiology to Clinical Practice. *The Scientific World Journal*, **2014**, Article ID: 852356. https://doi.org/10.1155/2014/852356

[374] Ranieri, M.V., Macia, L., Fiore, T., *et al.* (1995) Cardiorespiratory Effects of Positive End-Expiratory Pressure during Progressive Tidal Volume Reduction (Permissive Hypercapnia) in Patients with Acute Respiratory Distress Syndrome. *Anesthesiology*, **83**, 710-720. https://doi.org/10.1097/00000542-199510000-00010

[375] Zhu, N., Zhang, D., Wang, W., *et al.* (2020) A Novel Coronavirus from Patients with Pneumonia in China, 2019. *New England Journal of Medicine*, **382**, 727-733. https://doi.org/10.1056/NEJMoa2001017

[376] Tsolaki, V., Siempos, I., Magira, E., *et al.* (2020) PEEP Levels in COVID-19 Pneumonia. *Critical Care*, **24**, 303. https://doi.org/10.1186/s13054-020-03049-4

[377] Walkey, A.J., Del Sorbo, L., Hodgson, C.L., *et al.* (2017) Higher PEEP versus Lower PEEP Strategies for Patients with Acute Respiratory Distress Syndrome. *Annals of the American Thoracic Society*, **14**, S297-S303. https://doi.org/10.1513/AnnalsATS.201704-338OT

[378] Roesthuis, L., van den Berg, M. and van der Hoeven (2020) Advanced Respiratory Monitoring in COVID-19 Patient: Use Less PEEP. *Critical Care*, **24**, 230. https://doi.org/10.1186/s13054-020-02953-z

[379] Marini, J.J. and Gattinoni, L. (2020) Management of COVID-19 Respiratory Distress. *JAMA*, **323**, 2329-2330. https://doi.org/10.1001/jama.2020.6825

[380] Vashist, R. and Duggal, A. (2020) Respiratory Failure in Patients Infected with SARS-CoV-2. *CCJM*. https://doi.org/10.3949/ccjm.87a.ccc025

[381] Reed, J. and Hutchinson, S. (2020) Coronavirus: Warning Thousands Could Be Left with Lung Damage. *BBC News*. https://www.bbc.com/news/health-53065340

[382] George, P.M., Wells, A.U. and Jenkins, R.G. (2020) Pulmonary Fibrosis and COVID-19: The Potential Role for Antifibrotic Therapy. *The Lancet Respiratory Medicine*, **8**, 807-815. https://doi.org/10.1016/S2213-2600(20)30225-3

[383] Davido, B., Seang, S., Tubiana, R. and de Truchis, P. (2020) Post-COVID-19 Chronic Symptoms: A Post-Infectious Entity? *Clinical Microbiology and Infection*. https://doi.org/10.1016/j.cmi.2020.09.001

[384] Arnold, D.T., Hamilton, F.W., Milne, A., Morley, A., Viner, J., Attwood, M., Noel, A., Gunning, S., Hatrick, J., Hamilton, S., Elvers, K.T., Hyams, C., Bibby, A., Moran,

E., Adamali, H., Dodd, J., Maskell, N.A. and Barratt, S. (2020) Patient Outcomes after Hospitalisation with COVID-19 and Implications for Follow-Up; Results from a Prospective UK Cohort. https://doi.org/10.1101/2020.08.12.20173526

[385] Puntmann, V.O., Carerj, M.L., Wieters, I., *et al.* (2020) Outcomes of Cardiovascular Magnetic Resonance Imaging in Patients Recently Recovered from Coronavirus Disease 2019 (COVID-19). *JAMA Cardiology*, **5**, 1265-1273. https://doi.org/10.1001/jamacardio.2020.3557

[386] Greenhalgh, T., Knight, M., A'Court, C., Buxton, M. and Husain, L. (2020) Management of Post-Acute Covid-19 in Primary Care. *BMJ*, **370**, m3026. https://doi.org/10.1136/bmj.m3026

[387] Yelin, D., Wirtheim, E., Vetter, P., Kalil, A.C., Bruchfeld, J., Runold, M., Guaraldi, G., Mussini, C., Gudiol, C., Pujol, M., Bandera, A., Scudeller, L., Paul, M., Kaiser, L. and Leibovici, L. (2020) Long-Term Consequences of COVID-19: Research Needs. *The Lancet Infection*, **20**, 1115-1117. https://doi.org/10.1016/S1473-3099(20)30701-5

[388] Gousseff, M., Penot, P., Gallay, L., *et al.* (2020) Clinical Recurrences of COVID-19 Symptoms after Recovery: Viral Relapse, Reinfection or Inflammatory Rebound? *Journal of Infection*, **81**, 816-846. https://doi.org/10.1016/j.jinf.2020.06.073

[389] Matricardi, P.M., Dal Negro, R.W. and Nisini, R. (2020) The First, Holistic Model for COVID19: Implications for Prevention, Diagnosis, and Public Health Measures. *Pediatric Allergy and Immunology*, 1-17. https://doi.org/10.1111/pai.13271

[390] Szasz, A. and Szasz, O. (2020) Time-Fractal Modulation of Modulated Electro-Hyperthermia (mEHT). In: Szasz, A., Ed., *Challenges and Solutions of Oncological Hyperthermia*, Cambridge Scholars, Newcastle upon Tyne, Ch. 17, 377-415.

[391] Cunha, L., Szigeti, K., Mathé, D. and Metello, L.F. (2014) The Role of Molecular Imaging in Modern Drug Development. *Drug Discovery Today*, **19**, 936-948. https://doi.org/10.1016/j.drudis.2014.01.003

[392] Szigeti, K., Szabó, T., Korom, C., Czibak, I., Horváth, I., Veres, D.S., Gyöngyi, Z., Karlinger, K., Bergmann, R., Pócsik, M., Budán, F. and Máthé, D. (2016) Radiomics-Based Differentiation of Lung Disease Models Generated by Polluted Air Based on X-Ray Computed Tomography Data. *BMC Medical Imaging*, **16**, 14. https://doi.org/10.1186/s12880-016-0118-z

[393] Szasz, A. (2014) Oncothermia: Complex Therapy by EM and Fractal Physiology. 31*th URSI General Assembly and Scientific Symposium* (*URSI GASS*), Beijing, 20 October 2014, 1-4. https://doi.org/10.1109/URSIGASS.2014.6930100

[394] Szasz, O., Vincze, G., Szigeti, G.P., Benyo, Z. and Szasz, A. (2018) An Allometric Approach of Tumor-Angiogenesis. *Medical Hypothesis*, **116**, 74-78. https://doi.org/10.1016/j.mehy.2018.03.015

[395] Hegyi, G., Vincze, Gy. and Szasz, A. (2020) Thermodynamic Description of Living Homeostasis. In: George, T.F., Ed., *New Insights into Physical Science*, Vol. 1, Book Publisher International, London, Chapter 10, 1-13. http://www.bookpi.org/bookstore/product/new-insights-into-physical-science-vol-1

[396] Szasz, A., Iluri, N. and Szasz, O. (2013) Local Hyperthermia in Oncology—To Choose or Not to Choose? In: Huilgol, N., Ed., *Hyperthermia*, InTech, London, Ch. 1, 1-82. https://doi.org/10.5772/52208

Scientific Research Publishing

Open Journal of Biophysics, 2021, 11, 68-132
https://www.scirp.org/journal/ojbiphy
ISSN Online: 2164-5396
ISSN Print: 2164-5388

Approaching Complexity: Hyperthermia Dose and Its Possible Measurement in Oncology

Oliver Szasz, Andras Szasz

Biotechnics Department, St. Istvan University, Budaörs, Hungary
Email: biotech@gek.szie.hu

How to cite this paper: Szasz, O. and Szasz, A. (2021) Approaching Complexity: Hyperthermia Dose and Its Possible Measurement in Oncology. *Open Journal of Biophysics*, **11**, 68-132.
https://doi.org/10.4236/ojbiphy.2021.111002

Received: November 13, 2020
Accepted: January 24, 2021
Published: January 27, 2021

Abstract

A heuristic stochastic solution of the Pennes equation is developed in this paper by applying the self-organizing, self-similar behaviour of living structures. The stochastic solution has a probability distribution that fits well with the dynamic changes in the living objects concerned and eliminates the problem of the deterministic behaviour of the Pennes approach. The solution employs the Weibull two-parametric distribution which offers satisfactory delivery of the rate of temperature change by time. Applying the method to malignant tumours obtains certain benefits, increasing the efficacy of the distortion of the cancerous cells and avoiding doing harm to the healthy cells. Due to the robust heterogeneity of these living systems, we used thermal and bioelectromagnetic effects to distinguish the malignant defects, selecting them from the healthy cells. On a selective basis, we propose an optimal protocol using the provided energy optimally such that molecular changes destroy the malignant cells without a noticeable effect on their healthy counterparts.

Keywords

Self-Organizing, Self-Similarity, Avrami-Function, Weibull-Distribution, Temperature, Specific Absorption Rate (SAR)

1. Introduction

Hyperthermia has had a long and bumpy history from the dawn of human medicine. The overall body temperature has long served as the basic reference by which to measure the systemic hyperthermic effect of various conditions, including natural and artificial impacts. Localized heating, however, was not so easy to understand. The body's thermal homeostatic control regulates the blood-perfusion to prevent a sustained increase allowing for a rapid reduction in temperature, provided no further energy was provided from a local ener-

gy-source. The blood which has a cooling action on the local tissue, also has a heating effect on the whole system as the heat is transferred through the circulation to the rest of the body tissues

However, the process of heat distribution in the body is not a simple thermodynamic process. Living organisms are highly heterogenic and have complex interconnections and feedback regulations within. The non-linearly increasing blood-flow (*BF*) [1] for the regulation of rising temperature does not only act as a thermodynamical heat-exchanger. The blood delivers life-supporting molecules, such as oxygen and nutrients, as well as various regulating species such as circulation cells (like immune cells), proteins (like cytokines, chemokines, erythrocytes, etc.) and molecules (like carbon dioxide, various ions, etc.), for the chemical actions required for the processes of living. The thus intensified oxygen delivery supports the radiosensitivity of tissues. This effect is well established in radiotherapeutics. Moreover, the vasodilation and better perfusion through the vessel walls and the cell-membranes as a result of increased heat, together with the increased reaction rate of the chemicals, supports the action of chemotherapies. On the other hand, in massive tumours, the neo-angiogenic arteries do not vasodilate, as they lack musculature in their vessel walls [2].

The malignant tissues are different in their structure, cellular network, metabolic processes, and energy- and alkaline balances from their healthy counterparts. These particular biophysical differences determine the reaction to heating [3]. The bloodstream counteracts the overheating, regulating the flow capacity of the vessels as a result of physiological feedback cycles. The elevation of the temperature can cause vasoconstriction in certain tumours, reversing the development of blood perfusion and modifying the heat conduction [4]. The same increase in temperature in the neighbouring healthy tissue causes vasodilatation, with a corresponding rapid growth in its relative blood perfusion and heat conduction [5]. The change of blood-perfusion can result in a heat trap [6], helping us to selectively increase the temperature in the area of already-limited perfusion [7] caused by the higher internal pressure of the tumour [8]. The blood-flow (*BF*) of tumour tissue behaves in a different way with respect to temperature than its healthy counterpart [9]. Due to the missing musculature of the neo-angiogenic arteries, tumours are not able to react in the same way as the normal vessels in an adult body, and so the *BF* can decrease as a result of heating [10]. The relative *BF* can even drop below that of healthy vessels [11] and the dynamism of the various tissues changes [12]. The increasing temperature can change local immune-reactions and the immune-status of the heated volume. A temperature of over 40˚C downregulates the natural killer cell cytotoxicity [13], and other immune actions can be weakened too [14].

A mandatory parameter of all medical interventions is dosage, by which the desired effects and active changes are measured and controlled. Hyperthermia, by definition, involves a temperature increase, so the use of the temperature as a dosing parameter appears to be evident. However, for the regulative control of

dose, we expect a volume/mass dependence of the applied unit, such that a half-dose could be applied for half the mass, with the size of the target determining the applied dose. The challenge is that the temperature does not satisfy this elementary supposition; it does not depend on the size of the target. If we apply temperature as a dose and have a certain temperature in a volume, then half of that volume will have the same temperature and, indeed, any portion of the volume will also have the same value of temperature because the temperature is the measure of an energy average. The challenge of dosage is a barrier to the acceptance of hyperthermia in oncology [15]. The solution could lie in defining a reference point [16] chosen for necrotic tissue damage. It is observed that a temperature of 43˚C causes satisfactory necrosis in vitro in cell-culture of Chinese Hamster ovary tumour-cells [17].

The living object is a complex, mostly chemical piece of "machinery", where the temperature is one of the overall regulating factors. We can use the temperature dependence of the general chemical reaction rate (Arrhenius law [18]), which is also applicable in biology [19], where the Boltzmann distribution exists [20]. The dose was chosen according to this concept [21], and was later defined as "cumulative equivalent minutes at 43˚C" (*CEM*43˚C). The location of a phase transition within the cells is expected to be in the lipid membranes [22] [23] [24]. This cellular phase transition supports the choice of 43˚C, as the base temperature is at approximately 42.5˚C [25]. The break characterizing this phase transition is observed clinically, too [26] [27].

While the challenge associated with the dose was overcome by fixing the dose of hyperthermia, another barrier in the acceptance of hyperthermia was highlighted. The *BF* causes an unstable situation in the locally heated tumour due to its active cooling as it travels from the unheated body through the tumour. Additional to their extreme heterogeneity, most tumours create inhomogeneities in temperature in the tumour which is increased by the competitive thermal actions between the external heating and the blood-cooling in the capillary levels too. Isothermal equality, which is mandatory for the dosing, is therefore not guaranteed. The solution was to add an additional measure to the *CEM*43˚C unit in which the character of the inhomogeneity is conveyed by a special notation, *Tx*, denoting the percentage *x* in the target volume having temperature *T*: *CEM*43˚C *Tx*. Presently this is the widely applied "official" dosage unit of hyperthermia applications in oncology. A new, temperature related dose is emerging, the TRISE, which correlates with the complete remission of the patients [28].

2. Method

The temperature development (measured in ˚C) is interconnected with the specific absorption rate (*SAR*):

$$SAR = \frac{\text{absorbed power}}{\text{mass which absorbsit}}\left[\frac{\text{Watt}}{\text{kg}} = \frac{\text{W}}{\text{kg}}\right] \tag{1}$$

(The expressions in the [ ] brackets denote the SI units of the value). The energy

absorption creates the increase in temperature, and the *SAR* characterizes the dynamism of the absorbed energy

$$\text{Power} = \frac{\text{absorbed energy}}{\text{time period of absorption}} \left[\frac{\text{Joule}}{\text{second}} = \frac{\text{J}}{\text{s}} = \text{W} \right] \tag{2}$$

The temperature change (ΔT) depends on the absorbed energy in the heated mass. The absorbed energy is determined by the absorbed power, the *SAR* multiplied by the duration of its action providing the energy absorption in the target, so the absorbed energy is the sum of the products of the *SAR* and its actual duration:

$$\frac{\text{energy}}{\text{mass}} = E(t) = \sum_0^t SAR \cdot \tau = SAR \cdot t \left[\frac{\text{J}}{\text{kg}} \right] \tag{3}$$

where t is the duration of constant *SAR* value. The $SAR = SAR(\tau)$ usually depends on the time; consequently the energy is the integral of the $SAR(\tau)$ by τ time until t application time:

$$E(t) = \int_0^t SAR(\tau)\,\mathrm{d}\tau \left[\frac{\text{J}}{\text{kg}} \right] \tag{4}$$

The energy absorption naturally depends on the specifics of the character of the matter (c, specific heat), showing how much energy is necessary to heat up 1 kg of given material by 1˚C:

$$c = \frac{\text{energy}}{\text{mass} \cdot {}^\circ\text{C}}, \left[\frac{\text{J}}{\text{kg} \cdot {}^\circ\text{C}} \right] \tag{5}$$

Hence the temperature rise of the tissue with specific heat c during the time period Δt is:

$$c\Delta T \sim \frac{\text{power}}{\text{mass}} \Delta t, \left[\frac{\text{W} \cdot \text{s}}{\text{kg}} = \frac{\text{J}}{\text{kg}} \right] \tag{6}$$

and consequently

$$c \frac{\Delta T}{\Delta t} = \frac{\text{power}}{\text{mass}} = SAR \left[\frac{\text{W}}{\text{kg}} \right] \tag{7}$$

However, the heating situation is more complicated because the local heat is conducted away by the *BF*, which acts as a heat-sink of the absorbed *SAR*. The specific heat of the blood is c_b and the effective blood perfusion rate is $w_b \left[\frac{\text{ml}}{100\ \text{g} \cdot \text{min}} \text{ or } \frac{1}{6} \times 10^{-6} \frac{\text{m}^3}{\text{kg} \cdot \text{s}} \right]$, which is the blood flow through the vasculature of the given volume per unit tissue-mass per unit time. In most cases, the tissue is considered to be equal in size to the complete volume of the micro-circulatory system. According to this approximation, the unit of the blood-perfusion transferred is approximately described by $\left[\frac{\text{ml}}{100\ \text{g} \cdot \text{min}} \cong \frac{1}{100 \times 60} \frac{1}{\text{s}} = \frac{1}{6} \times 10^{-3} \frac{1}{\text{s}} \right]$. When we apply the above consideration for SI units, we get: $\left[\frac{\text{m}^3}{\text{kg} \cdot \text{s}} \cong 10^{-3} \frac{1}{\text{s}} \right]$. The error in

this is $\frac{\rho_b}{\rho}<1\%$, where ρ_b and ρ are the density of the blood and the surrounding tissue, respectively.) The blood density $\rho_b, \left[\frac{\text{kg}}{\text{m}^3}\right]$ sinks energy thus:

$$\text{cooling} = -c_b \rho_b w_b \Delta T, \quad \left[\frac{\text{J}}{\text{kg}\cdot^\circ\text{C}}\cdot\frac{\text{kg}}{\text{m}^3}\cdot\frac{1}{\text{s}}\cdot^\circ\text{C} = \frac{\text{W}}{\text{m}^3}\right] \tag{8}$$

Due to the regulatory role of the blood in thermal homeostasis, the W_b depends on the temperature: $W_b = W_b(T)$. The thermal role of the *BF* requires a massive thermal pool which keeps the base temperature constant (body temperature, $T_{body} = 36.5[^\circ\text{C}]$). Various heat exchanges with the environment ensure the stability of the base temperature. We can therefore introduce a parameter f [29] such that:

$$f = \begin{bmatrix} 1 & \text{when no heat loss} \\ 0 & \text{when only heat loss} \end{bmatrix} \tag{9}$$

The $f=1$ condition means all metabolic energy is used for the reactions associated with life, while $f=0$ means the metabolic energy does not support life; it is radiated to the environment as heat. Naturally, both are extremes, $f=1$ being impossible because the living state is an open system, and $f=0$ because life needs energy for itself. For human adults at rest $f \cong 0.15$ [30], so the heat exchange is intensive enough even though there is intense local heating. This is an important factor when the blood-cooling by *BF* is considered, the heat being effectively radiated out, showing that the blood is able to maintain its cooling efficacy.

A further complication is the heat-diffusion in the tissues, by which the temperature spreads by time even without blood-circulation. This naturally depends on the gradient of the temperature in the space, given by $grad(T) = \frac{\text{d}T}{\text{d}\boldsymbol{x}}$, where $\frac{\text{d}T}{\text{d}\boldsymbol{x}}, \left[\frac{^\circ\text{C}}{\text{m}}\right]$ is the temperature change $\text{d}T$ in the space interval $\text{d}\boldsymbol{x}$ calculated in all directions (all directions being designated by the bold lettering). This gradient will be the driving force of the smearing of the temperature in the space, so its change in the space characterizes the thermal diffusion:

$$k\frac{\text{d}\left[\boldsymbol{grad}(T)\right]}{\text{d}\boldsymbol{x}} = k\left[\frac{\text{d}^2T}{\text{d}x^2}+\frac{\text{d}^2T}{\text{d}y^2}+\frac{\text{d}^2T}{\text{d}z^2}\right] = k\nabla T, \quad \left[\frac{\text{J}}{\text{m}\cdot^\circ\text{C}}\cdot\frac{^\circ\text{C}}{\text{m}^2} = \frac{\text{J}}{\text{m}^3}\right] \tag{10}$$

where the sign "∇" symbolizes the thermal diffusion process in all three (x, y, z) dimensions of the space, centred around the actually chosen $\boldsymbol{x}$ point, and where $k, \left[\frac{\text{W}}{\text{m}\cdot^\circ\text{C}}\right]$ is the coefficient of the heat-diffusion. ("∇T" therefore, demonstrates the temperature spreading in all three dimensions). One more factor modifies the energy balance: the increased metabolic rate by temperature $\sim q_0 \rho 1.1^{(\Delta T)}\left[\frac{\text{W}}{\text{m}^3}\right]$ [31], where q_0 is the basal metabolic rate $q_0 = BMR, \left[\frac{\text{W}}{\text{kg}}\right]$.

The *BMR* has allometric scaling [32], which allows the determination of the *BMR* depending on the body-mass [33].

Considering the above terms, the equation which describes the heating process is: (Pennes equation [34])

$$\rho_h c\frac{\partial T}{\partial t} = \rho_h SAR - c_b\rho_b w_b\left(T\right)\left(\Delta T\right) - k_h\nabla^2 T + q_0\rho 1.1^{(\Delta T)} \tag{11}$$

The analytical solution of this partial differential equation is a difficult task. The first approach uses the Green-function [35] [36] and the Green heat kernel function [37], and approaches an analytical solution [38]. The point source Green function solution [39] can simulate the highly localised heating using a nanoparticle or thin needle. Heating by 915 MHz from the skin's surface was calculated. Interestingly, when the *BF* has spatial inhomogeneity due to the cooling bolus on the surface, it produces a bump in the temperature development by depth [40].

Despite the possibility of the analytical solution of the Pennes equation, it is not widely applied in practical use. Its complicated mathematics deters many physicians from using it, but in fact, the complicated mathematical calculation is not necessary. Numerical methods are precise enough for efficient use [41]. Using small differences (small steps of developing processes, denoted with Δ), instead of the differential approach, is entirely compatible with the homeostatic control, which does not allow sudden, very rapid changes, even when the controlling signals are rapid. Clinical standards average the *SAR* in the MHz range of frequencies over a six-minute period [42]. As a consequence, the differences can be used instead of derivatives in practical approaches. Hence the complete balance of treated healthy tissue is:

$$\begin{aligned}\rho_h c\frac{\Delta T}{\Delta t} &= \rho_h SAR - c_b\rho_b w_b\left(T\right)\left(\Delta T\right)\\ &\quad - k_h\left(\frac{\Delta\left(\frac{\Delta T}{\Delta x}\boldsymbol{i}+\frac{\Delta T}{\Delta y}\boldsymbol{j}+\frac{\Delta T}{\Delta z}\boldsymbol{k}\right)}{\Delta x}\right) + q_0\rho 1.1^{(\Delta T)}\end{aligned} \tag{12}$$

where $\boldsymbol{i}, \boldsymbol{j}$ and $\boldsymbol{k}$ are the unit vectors in the 3D dimensions *x*, *y* and *z*, and the equation is written using the SI units $\left[\frac{\mathrm{W}}{\mathrm{m}^3}\right]$.

The characteristic constants used, collected from various pieces of literature, are: $\rho_{tumoqur} = \rho_t = 1050\left[\frac{\mathrm{kg}}{\mathrm{m}^3}\right]$, $\rho_{blood} = \rho_b = 1060\left[\frac{\mathrm{kg}}{\mathrm{m}^3}\right]$, $\rho_{healthy} = \rho_h = 1190\left[\frac{\mathrm{kg}}{\mathrm{m}^3}\right]$, $q_0 = 368\left[\frac{\mathrm{W}}{\mathrm{m}^3}\right] \approx 0.37\left[\frac{\mathrm{W}}{\mathrm{kg}}\right]$, [43]; or $q_0 \approx 1\left[\frac{\mathrm{W}}{\mathrm{kg}}\right] \cong 1000\left[\frac{\mathrm{W}}{\mathrm{m}^3}\right]$, [44]; $c_t = 3639\left[\frac{\mathrm{J}}{\mathrm{kg}\cdot{}^\circ\mathrm{C}}\right]$; $c_b = 3840\left[\frac{\mathrm{J}}{\mathrm{kg}\cdot{}^\circ\mathrm{C}}\right]$, [45]; $c_h = 3800\left[\frac{\mathrm{J}}{\mathrm{kg}\cdot{}^\circ\mathrm{C}}\right]$, [46]; $k_t = 0.56\left[\frac{\mathrm{W}}{\mathrm{m}\cdot{}^\circ\mathrm{C}}\right]$; $k_h = 0.56\left[\frac{\mathrm{W}}{\mathrm{m}\cdot{}^\circ\mathrm{C}}\right]$;

$W_{b\text{-}tumour} = \rho_b w_{bt} = 1.8\left[\frac{\text{kg}}{\text{m}^3 \cdot \text{s}}\right]$; $W_{b\text{-}healthy} = \rho_b w_{bh} = 3.6\left[\frac{\text{kg}}{\text{m}^3 \cdot \text{s}}\right]$; [47] [48]. Data may vary by organs [49].

It is evident that the *BF* can fundamentally modify the calculations. The measurements of the *BF* in clinical practice give inconsistent results measured even in the same patient. The person's actual state, comfort level, stresses, and environmental and social factors cause deviations in the skin condition, modifying the results of the measurements, so the uncertainty is clinically inherent [50].

The $SAR\left[\frac{\text{W}}{\text{kg}}\right]$ identifies the power intake per unit mass from outside energy sources. The critical fact is that the electromagnetic non-ionizing heating processes dominantly use electric fields, pumping considerable energy into the larger target. The *SAR* depends on the conductivity ($\sigma\left[\frac{1}{\Omega \cdot \text{m}}\right]$) and the allied electric field ($\Xi\left[\frac{\text{V}}{\text{m}}\right]$):

$$\rho SAR = \sigma \Xi^2 \left[\frac{\text{W}}{\text{m}^3}\right] \tag{13}$$

when the electric field is sinusoidal then its peak value has to be divided by $\sqrt{2}$ to obtain the average. Consequently, in practical use, [51]:

$$SAR = \frac{\sigma}{2\rho} \Xi^2 \left[\frac{\text{W}}{\text{kg}}\right] \tag{14}$$

The most substantial challenge in the calculation of the absorbed energy is the high heterogeneity of the absorption process. The human target is heterogenic in the thermal, electrical and structural aspects.

Additional to the static challenges, the heterogeneity appears in the dynamism of the transports non-linearly, as well as in the various chemical reactions that consume energy in the living target. Consequently, the parameters in (11) and (14) are time (t) and space (x) dependent so the correct equations, taking into consideration the heterogeneity in micro and macro ranges, are in reality very complicated. The Pennes equation with spatiotemporal (x,t) dependences is:

$$\begin{aligned} &\rho_h(x,t)c(x,t)\frac{\partial T(x,t)}{\partial t} \\ &= \rho_h(x,t)SAR(x,t) - c_b\rho_b w_b(T,x,t)\left(\Delta T(x,t)\right) \\ &\quad - k_h(x)\nabla^2 T(x,t) + q_0(x,t)\rho(x,t)1.1^{\left(\Delta T(x,t)\right)} \end{aligned} \tag{15}$$

and the external energy-pumped is:

$$SAR(x,t) = \frac{\sigma(x,t)}{2\rho(x,t)} \Xi^2(x,t)\left[\frac{\text{W}}{\text{kg}}\right] \tag{16}$$

Due to the complications, we usually simplify the situation with rational assumptions:

1) The metabolic addition in the heating phases will be negligible compared to

the incoming *SAR*, so it is not considered in most of the calculations. The neglection can be explained according to the principal of the optimization of living processes in their adaption to environmental challenges. The consequence of the life-optimization of energy transfers via chemical reactions minimizes thermodynamic losses [52] [53]. However, hyperthermia increases biochemical reaction rates [54] and, therefore, the metabolic rate as well. The rapid growth and higher metabolism of tumours typically yield tumour temperatures higher than the surrounding healthy baseline temperature [55]. When the metabolic addition is more than 5% on top of the *SAR*, we include it in the calculation.

2) In a tumour situation, the main macroscopic heterogeneity is between the tumour and its healthy environment. The parameters at the surface of the tumour do not jump but have a slope, depending on the kind of the tumour and its stage. The gradient is mostly created by the homeostatic control of the *BF*.

3) The macroscopic spatiotemporal dependence of the densities (ρ), specific absorption rates (c) and conductivity (σ) is weak, usually it is less than 5% in both the tumorous and healthy tissues. Consequently, in practical calculations, we consider these parameters as constants in the specific tissues, distinguishing only the tumorous and non-tumorous mass. Detailed reviews and discussions on tumour-blood-flow affecting the applied temperature are available [56] [57].

4) The largest heterogeneity, however, is microscopic. The tissue contains inherently different electrolytes separated by membranes and other structures (such as vessel-walls, node-walls, etc.). In tumours, the malignant cells and their microenvironment dominate the heterogenic behaviour. The microscopic heterogeneity can be specially targeted, choosing the proper frequency for selection [58] [59]. The frequency dispersion by the various components of the microscopic tissue environments will be discussed later.

The homeostasic functions characterize the local stability of the living system, having very complex feedback mechanisms which secure the stability against a relatively wide-range of perturbations. The homeostasis is not static. It is a self-organized dynamic process that has no static state at all. The system is energetically open. Its rigid, static state is death. The complexity of the dynamic behaviour guarantees robust stability, so the system is in a homeodynamic position rather than homeostatic.

The complexity of the dynamic interaction represents a feedback regulation of the system at every level of its structure. The complex system cannot be considered as a sum of its distinct parts. The whole is more than the sum of the parts; the interactions are largely non-linear; the system is energetically open and has adaptive exchanges with its environment. The approach to describing it must be analytic and not synthetic. Considerations regarding the complexity create huge challenges in the development of the calculations, the attempted solutions to which typically uses a synthesis of the parts, which could be calculated. However, this calculation strategy does not work. The analysis must consider the complexity.

We could overcome the above difficulties by considering one of the robust behaviours of this complexity: the self-organization and its consequent self-similarity [60]. The complexities of the living structures have a universal behaviour: they are self-organized [61]. Recent decades have seen the development of various approaches describing the complexity of systems on the basis of self-organization [62] [63]. A great many studies deal with fractal physiology [64] [65], describing biological self-organization [66]. This peculiar structure is built up according to relatively simple rules based on self-similarity [67]. The dynamism of the structure is determined by the symmetries of the system [68], and constructs a self-managed spatiotemporal fractal network [69] [70], leading to a common bioscaling behaviour of living material [71]. As a result, the similarity of living species [72] allows allometric scaling in 24 orders of magnitude from the smallest to the largest bio objects [73].

Living systems are open dynamic structures, completing random stationary stochastic self-organizing activities [74]. The self-organizing technique generates a spatiotemporal fractal structure, which is self-similar both in space and time [75]. The emerging fields of bio-scaling [32] [76] [77], and network analysis [78] [79] extend detailed analyses. The characteristic stochastic (probability) behaviour of living matter is related to the intrinsic bifurcation in the entirety of the living organization. The basic bifurcation mechanism could be represented by a non-linear double-well potential of chemical reactions [80] [81], generating a chaotic arrangement.

The self-organized self-similarity describes and defines living objects [82] according to the universality of their complex feedback mechanisms to control the actual dynamic equilibrium, that is, their homeostasis. The progression of life involves non-linear and non-equilibrial thermodynamic and chemodynamic consequences including fractal structures and phase transitions like in non-living systems. We may use the robust self-similar actions in solving the heating process in a stochastic way.

To calculate the temperature development over time, let us introduce a stochastic variable θ defined by measurements on the cohort of individuals. θ is the time taken to reach thermal homeostasis, a saturation in the temperature development (the time to the stage when $\frac{\Delta T}{\Delta t} \cong 0$). The deterministic approach gives modelling facilities for the interpretation of data, but the reality is stochastic, determined by the probabilities of events, and no deterministic decisions can be made. Deterministic models could give information about the large-scale average nature of the dynamism, but the details will be hidden. The stochastic description describes the reality in a very general way and provides a good tool for the design and analysis of experiments. The introduced θ stochastically describes the personal and individual differences in obtaining $\frac{\Delta T}{\Delta t} \cong 0$ conditions during the time of treatment. It shows the variation in the control of thermal homeostasis (TH) according to the subject of an individual treatment; see **Figure 1**.

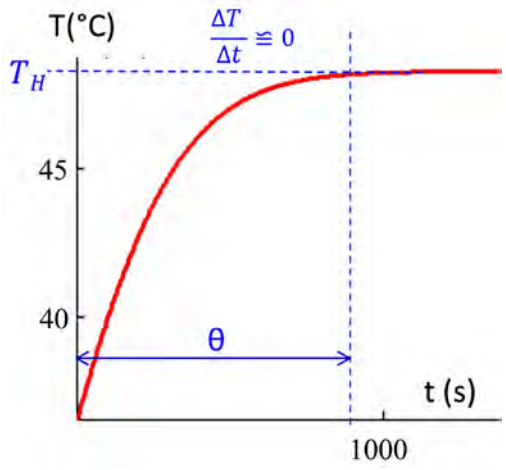

Figure 1. The *TH* state fixes a temperature value T_H, where the curve saturates, and the thermal homeostasis keeps the temperature constant $\left(\frac{\Delta T}{\Delta t} \cong 0\right)$. The stochastic time-parameter θ of the individual heating characterizes the time when the *TH* happens.

The distribution function of *TH* is the probability of the θ time being less than or equal to time *t*, namely

$$p_{TH}(t) = P\{\theta \le t\} \tag{17}$$

Thus, the probability distribution of dynamic equilibrium (temperature development function, the time of control of the development (*C*)) can be defined by the probability of the equilibrium θ time being higher than *t*, which can be expressed in the form

$$p_C(t) = 1 - p_{TH}(t) = P\{\theta > t\} \tag{18}$$

The density function of the dynamic control distribution function is a derivative of $p_C(t)$:

$$f(t) = \frac{\mathrm{d}p_C(t)}{\mathrm{d}t} \tag{19}$$

The $f(t)$ is the density of the probability of θ, therefore, the average θ is:

$$\langle\theta\rangle = \int_0^\infty t f(t)\,\mathrm{d}t = \int_0^\infty p_C(t)\,\mathrm{d}t \tag{20}$$

Let us introduce a function of the rate at which a loss of control occurs at $(t+\Delta t)$: $h(t)$. This failure-rate refers to when the thermal homeostasis cannot control the heating process. It is a "hazard" that θ does not describe the homeostatic process. The $h(t)$ is the "uncontrolled rate" or "out of control rate". The $h(t)\mathrm{d}t$ rate measures the probability of the failures during the *t* length of control-time of the evolving process to *TH*. Therefore, the probability that in the case of a *t* length of time to *TH*, loss of control occurs at $(t+\Delta t)$ is:

$$h(t)\Delta t = 1 - \frac{p_C(t+\Delta t)}{p_C(t)} = -\frac{\mathrm{d}\frac{p_C(t)}{\mathrm{d}t}}{p_C(t)}\Delta t = -\frac{\frac{\mathrm{d}\left[1-p_{TH}(t)\right]}{\mathrm{d}t}}{p_C(t)}\Delta t = \frac{f(t)}{p_C(t)}\Delta t \tag{21}$$

Hence:

$$h(t) = -\frac{\mathrm{d}\dfrac{p_C(t)}{\mathrm{d}t}}{p_C(t)} = \frac{f(t)}{p_C(t)} \tag{22}$$

It's cumulative form is:

$$H(t) = \int_0^t h(\tau)\,\mathrm{d}\tau = -\ln\left(p_C(t)\right) \tag{23}$$

and consequently:

$$p_C(t) = \mathrm{e}^{-H(t)} \tag{24}$$

As we discussed above, the inherent property of living objects is self-organization and the consequent self-similarity [60]. This could be the basis of the proper parameterization of homeostatic thermal control, and likewise of the control of the *TH*. Taking this self-similarity into consideration, the failure rate in (22) must be a self-similar time function [83], mirrored by a scaling, shown as follows:

$$h(t) = \alpha t^{\beta} \tag{25}$$

Its self-similarity is obvious because it gives the same function by a magnification of any number m:

$$h(mt) = \alpha(mt)^{\beta} = m^{\beta}\alpha t^{\beta} = m^{\beta}h(t) \tag{26}$$

The survival probability distribution function from (23) and (24) is:

$$p_C(t) = \mathrm{e}^{-\int_0^t h(\tau)\mathrm{d}\tau} \tag{27}$$

The self-similar failure rate (hazard function) is:

$$H(t) = \int_0^t \alpha\tau^{\beta}\,\mathrm{d}\tau = \frac{\alpha}{\beta+1}t^{\beta+1} \tag{28}$$

Substituting (28) with survival (27), we get:

$$p_C(t) = \mathrm{e}^{-\int_0^t \alpha\tau^{\beta}\mathrm{d}\tau} = \mathrm{e}^{-\frac{\alpha}{\beta+1}t^{\beta+1}} \tag{29}$$

Introducing

$$t_0 = \left(\frac{n}{\alpha}\right)^{\frac{1}{n}} \text{ and } n = \beta + 1 \tag{30}$$

we hence arrive at:

$$p_C(t) = \mathrm{e}^{-\left(\frac{t}{t_0}\right)^n} \tag{31}$$

which has two parameters for one curve, t_0 being the scale parameter, which is the natural scale of the time-function variation, and n being the shape parameter. Consequently, the thermal homeostatic distribution function $p_{TH}(t)$ by (17) and (18) is the well-known cumulative form of the two-parametric Weibull distribution ($W(t)$) [84]:

$$p_{TH}(t) = W(t) = 1 - e^{-\left(\frac{t}{t_0}\right)^n} = 1 - p_C(t) \tag{32}$$

with the additional conditions that $t \geq 0$, $W(t) = 0$ when $t < 0$. The inverse function, when the time t is calculated from a given probability p is:

$$t = W_{inv}(p) = t_0 \left(-\ln(1-p)\right)^{\frac{1}{n}} \tag{33}$$

The full regulation and controlling processes are essentially, inherently dynamic, so it is better to use the term "homeodynamics" instead of "homeostasis" [85]. A broad-spectrum of self-organized structures could be described with the $W(t)$ function, among these structures gene expression data [86] and neural networks [87]. A consequence of the widely applicable universality of behaviour, general ontogenic growth [88] also allows the deduction of the Weibull distribution [89]. Importantly, the information traffic on networks also has self-similar fractal behaviour as described by the Weibull distribution [90], which also allows the self-organizing dynamic approach for the stabilizing regulation of the system. We may conclude that self-organizing and self-similarity are universal laws fingerprinted in the fractal description and can be described by a cumulative Weibull distribution $W(t)$.

Note, that we have preciously applied a mathematical transformation which unified the physical models of biological processes and self-similar processes with the help of an appropriate comparative function [83]. Choosing the Avrami-like comparative function, the mathematical model of the processes will be described by the Avrami-equation [91]. This unusual universality is a consequence of the self-organized behaviour of the homeodynamic conditions of life, and the general analogy of self-organized processes can be a fruitful heuristic method in biological model-calculations. The Avrami describes some living phenomena well [92] [93], and the equation is connected to the self-similarity and dynamism of the living structures [87]. The Avrami-equation has the following form, which is identical to the Weibull distribution using Weibull function (WF):

$$1 - W(t) = WF(t) = e^{-\left(\frac{t}{t_0}\right)^n} \tag{34}$$

The shape parameter is usually $n > 1$, having the same shape as the psychometric function [94], a consequence of the Weber-Fechner law. In the case that $n = 1$, WF is a simple exponential function, and where $n < 1$, the decrease is faster than an exponential decrease.

The case in which $n = 1$ is a simple, very frequently occurring behaviour of stand-alone systems, satisfying the basic rule of self-regulation by negative feedback: the change of the property Θ over time is negatively proportional to the value of the property Θ. In mathematical form:

$$\frac{d\Theta(t)}{dt} = -c \cdot \Theta(t) \tag{35}$$

The solution is exponential decay:

$$\Theta(t) = \Theta(0)\mathrm{e}^{-ct} \tag{36}$$

where c is a constant and $\Theta(0)$ is the starting $\Theta(t)$ value ($t = 0$). When the starting $\Theta(0) = 0$, then the solution is a decreasing function from $\Theta(0)$:

$$\Theta(t) = \Theta(0)\left(1 - \mathrm{e}^{-ct}\right) = \Theta(0)\left(1 - \mathrm{e}^{-\left(\frac{t}{t_0}\right)}\right) \tag{37}$$

where $t_0 = \frac{1}{c}$. This is the form of $W(t)$ at $n = 1$. By the growth of $n > 1$, the complexity of the interaction grows. The equation modifies, thus:

$$\frac{\mathrm{d}\Theta(t)}{\mathrm{d}t} = -c \cdot t^{n-1}\left(\Theta(0) - \Theta(t)\right) \tag{38}$$

and the solution is:

$$\Theta(t) = \Theta(0)\left(1 - \mathrm{e}^{-\left(\frac{t}{t_0}\right)^n}\right) \tag{39}$$

where $t_0 = \left(\frac{n}{c}\right)^{\frac{1}{n}}$. The solution in (39) is identical to that in (37) at the limit of $n = 1$.

It is clear that the shape factor n characterizes the complexity of the function. The initial change is a power function and is not linear. The changes in the $WF(t)$ function are shown in Figure 2. The limit $\lim_{n\to\infty} WF(t)$ is a step function at $t = t_0$, while the $\lim_{n\to\infty} WF(t) = \frac{\Theta(0)}{\mathrm{e}} \cong 0.368 \cdot \Theta(0)$ is constant.

The mean, the median, and the inflection points are frequently used in the practical evaluation, as shown in Figure 3:

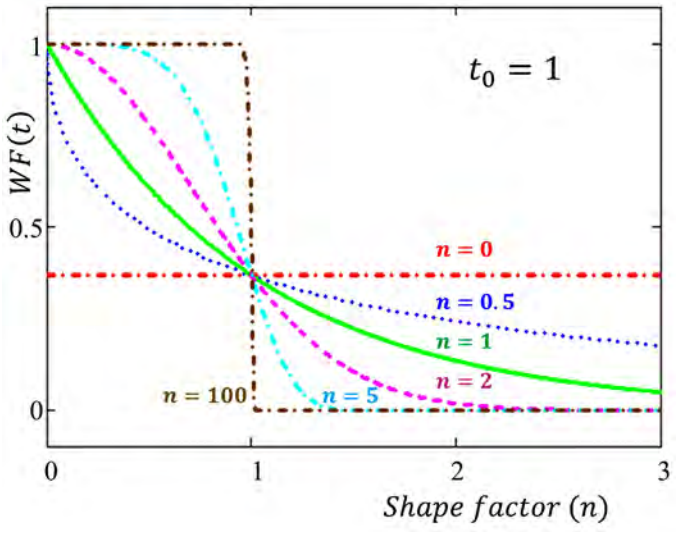

Figure 2. The changes in $WF(t)$ by n, measured in self-time units ($t_0 = 1$).

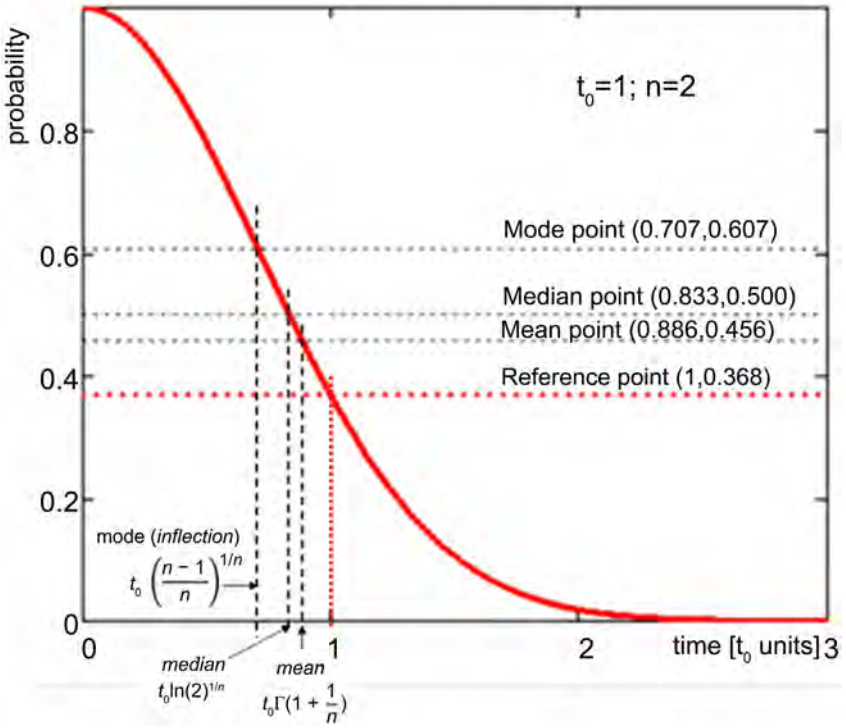

Figure 3. The noteworthy points of *WF*, when $t_0 = 1$ and $n = 2$. The reference point is $\frac{1}{e} \cong 0.37$, when $t = t_0$. The inflection point marks the mode, the change of the sign of the growth of the derivative of the function.

$$\begin{aligned} &\text{median}\left[p_S(t)\right] = t_0\left[\ln(2)\right]^{\frac{1}{n}} \\ &\text{mean}\left[p_S(t)\right] = t_0\int_0^{\infty} e^{-x}x^{\frac{1}{n}}dx = t_0\Gamma\left(1+\frac{1}{n}\right) \\ &\text{mode}\left[p_S(t)\right] = t_0\left[\frac{n-1}{n}\right]^{\frac{1}{n}} \end{aligned} \tag{40}$$

The values of the median, mode and mean when $t_0 = 1$ and $n = 2$ are 0.5, 0.607 and 0.456, respectively. The quantile of the *WF* function is ≈0.632, and it is independent from the value of *n*. All the notable points are proportional to t_0, and consequently, $t_0 = 1$ is chosen for the natural unit of the elapsed time. The value of t_0 characterizes the self-time of the living system, which is responsible for the individual complexity (personal variation) of the living unit [95]. Thermodynamic optimizing introduces variation in self-time, on the basis of constant entropy production over time [96]. Self-time is connected to allometry [97], and it scales with the allometric factor, which is usually $\alpha \approx \frac{3}{4}$, the power rule of which is strongly supported by various physiological times [98]. The real observed coordination time and the self-time are strictly connected, and their values are transformed into each other [95]. The changes of self-time in the various parameter-pairs of *WF* are shown in **Figure 4**.

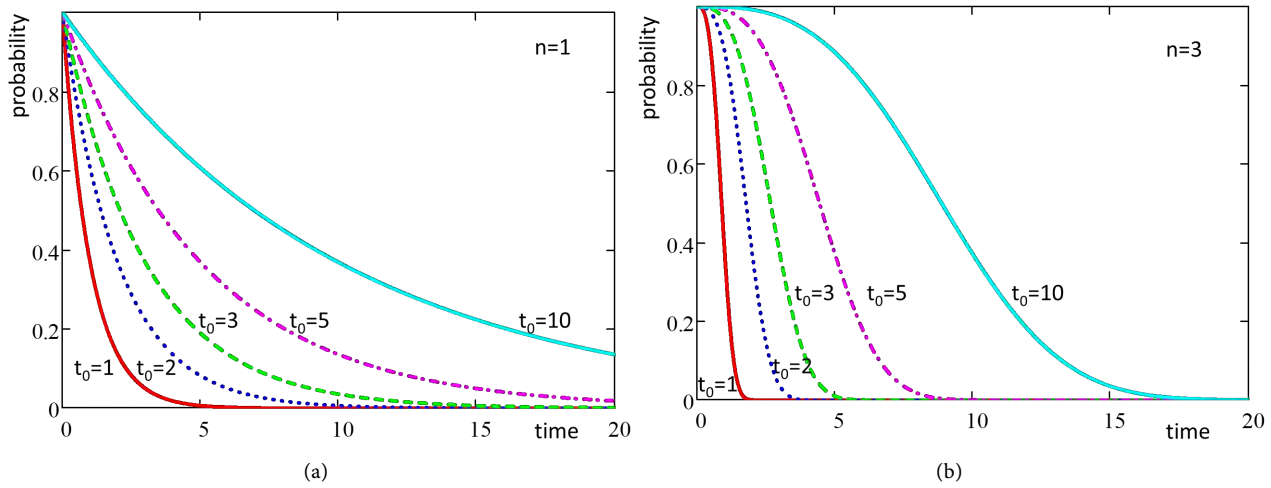

Figure 4. WF with various parameters: (a) changing t_0 (scale parameter) in simple exponential conditions, (the shape parameter is $n=1$); (b) the shape parameter differs from the exponential, containing extended complexity ($n=3$).

The energy absorption of living objects follows the rule of complexity, and the temperature development depends on it. The complex structure determines the heat-conduction, the dynamic feedback properties, and the steady-state saturation and stabilization of the temperature, providing a constant *SAR* value. We assume that the complex behaviour of the *WF* describes the absorption and wash-out processes well, and without a complicated solution of the Pennes Equation (15) we may describe the hyperthermia process by temperature development in a complex system.

3. Results

The *WF* function is assumed to describe the complex heating process over time in conditions of thermal homeostasis. Consequently, the entire velocity v_T of the change of the temperature could be described with the *WF*:

$$WF(t) \propto \frac{\Delta T}{\Delta t} = v_T \tag{41}$$

The letter $\propto$ means that v_T behaves in the same way as $WF(t)$ does. It denotes only a character of heating and not equality, because the values of $WF(t)$ are limited ($0 \le WF(t) \le 1$). The character v_T is a multiplicative factor of the real reaction when the system reaches its heating maximum at the *TH* in time t_{TH} then $WF(t_{TH}) = 1$. In this approach, the development of the temperature behaves like the sum of $WF(t)\Delta t$ terms:

$$\sum WF(t)\Delta t \propto \Delta T \tag{42}$$

In analytical form, using (34) and referring to the body temperature (T_{body}) as the base-line:

$$T(t) - T_{body} \propto \int_0^t \exp\left(-\left(\frac{\tau}{t_0}\right)^n\right) \mathrm{d}\tau \tag{43}$$

Hence **Figure 5** shows the graphical measure of the temperature.

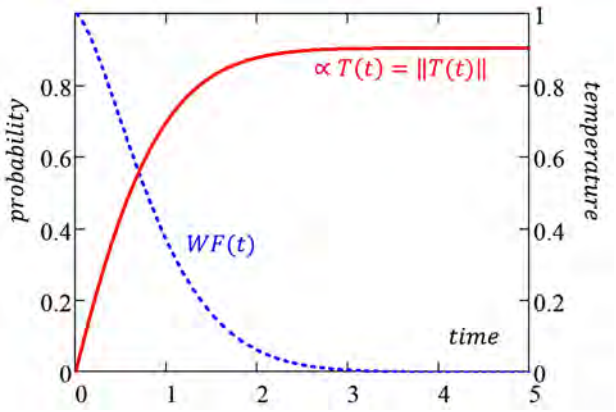

Figure 5. The approximation of temperature development (solid line) by the *WF* (dashed line). The parameters are $n = 1.48$ and $t_0 = 1$. The unit of time is t_0. The temperature development is a relative form (it is normalized) of the real temperature, so it is denoted by $\|T(t)\|$ in the curve.

The normalization of $\|T(t)\|$ can be determined from the saturation value (the T_H value) of the actual homeodynamic case. The *TH* condition reduces the Pennes Equation (11) thus:

$$c_b \rho_b w_b (T)(\Delta T) + k_h \nabla^2 T = \rho SAR + q_0 \rho 1.1^{(\Delta T)} \tag{44}$$

because in this state $\frac{\partial T}{\partial t} \cong \frac{\Delta T}{\Delta t} = 0$. As we discussed, the metabolic term $q_0 \rho 1.1^{(\Delta T)}$ is negligible compared to ρSAR. The diffusion term is also small compared to the *BF*, which is an effective heat exchanger. Hence these approximative steps reduce (44) to:

$$c_b \rho_b w_b (T)(\Delta T) = \rho SAR \Rightarrow T - T_{body} = \frac{\rho SAR}{c_b \rho_b w_b (T)} \tag{45}$$

The density ρ characterizes the healthy (ρ_h) or tumorous (ρ_t) tissue, depending on the absorption volume under investigation. Also, the *BF* changes as well, depending on whether we consider a healthy (w_{bh}) or tumorous (w_{bt}) target. An early study has shown that an internal temperature change (mild fever) causes a sudden increase in the heat conductance of healthy tissues [99] due to, after passing a threshold, the *BF* delivering seven times more power (up from 21 W/K to 150 W/K with an increase in body temperature of <1˚C). Later it was shown that the development is not a step-function but a power function. For the temperature-dependent *BF* we use the results obtained by a nonlinear three-dimensional heat-transfer model [100]. The obtained functions for prostate and surrounding tissues are:

For healthy muscle

$$\rho_{bm} w_{bm} (T) = \begin{cases} 0.45 + 3.55 \exp\left(-\frac{(T-45)^2}{12} \right) & \text{if } T \le 45 \\ 4 & \text{if } T > 45 \end{cases} \tag{46}$$

for healthy adipose tissue

$$\rho_{ba} w_{ba}(T) = \begin{cases} 0.36 + 0.36 \exp\left(-\dfrac{(T-45)^2}{12}\right) & \text{if } T \le 45 \\ 0.72 & \text{if } T > 45 \end{cases} \tag{47}$$

for tumour tissue

$$\rho_{bt} w_{bt}(T) = \begin{cases} 0.833 & \text{if } T < 37 \\ 0.833 - \dfrac{(T-37)^{4.8}}{5438} & \text{if } 37 \le T \le 42 \\ 0.416 & \text{if } T > 42 \end{cases} \tag{48}$$

The graphs of these solutions are shown in Figure 6. The vasoconstriction of tumour-tissue is expected from finite elements calculations too, modelling the human prostate [101].

With increasing temperature, the tumour serves as an effective heat-trap due to the *BF* within barely increasing [102], so the heat-sinking effect seen in healthy tissue is absent. The characteristic difference between the absolute *BF* of a tumour and healthy tissue has been observed by others, too [103] [104]. Due to the angiogenetic effect, the size of the tumour also affects the *BF*. This depends on the tumour-weight by negative logarithmic function [105].

Equations (46)-(48) allow the determination of the T_H from (45). When there is forwarded power applied (P_{fwr}), and the complete heated mass is M containing m_t and m_h tumour and healthy masses, then $M = m_t + m_h$. Assuming an equal *SAR* throughout the volume of *M*, we may calculate the SAR taking into account the reflected power (P_{refl}) and the efficacy (η), which is calculated from the various losses by the technical realization; we get:

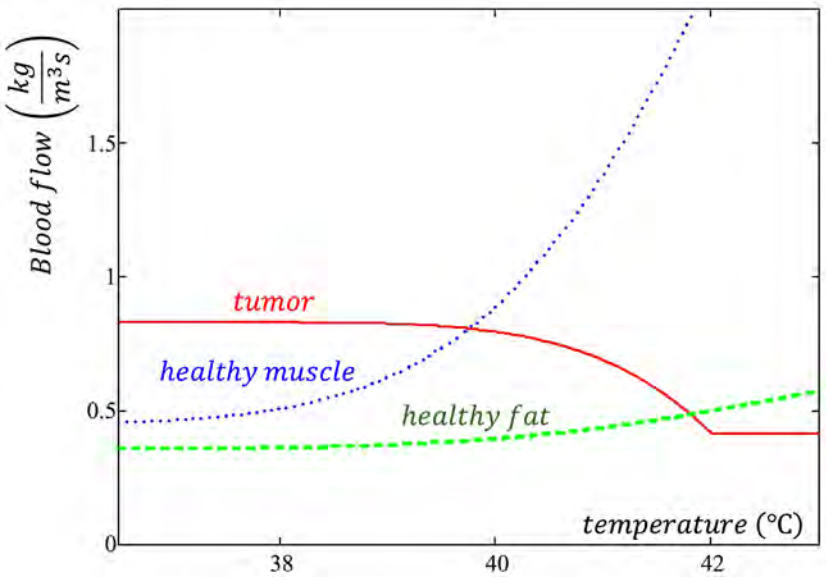

Figure 6. The modelled blood flow by temperature variation [104]. Tumorous tissue (solid line), healthy muscle (dotted line), healthy fatty tissue (dashed line).

$$SAR = \frac{\left(P_{fwr} - P_{refl}\right)\eta}{m_t + m_h} \tag{49}$$

Using (46) and (48) for muscle and tumour, respectively, we may calculate the T_H, solving Equation (45). Denoting the roots of tumour and muscle T_H by T_t and T_m, we can construct the final T_H by supposing a complete isothermal *TH* condition:

$$T_H = \frac{m_t T_t + m_h T_m}{m_t + m_h} \tag{50}$$

Knowing this T_H value, the temperature gain is $T_{gain} = T_H - T_{body}$, and so, using the normalized $\|T(t)\|$, the curve of temperature growth can be obtained:

$$T(t) = T_{body} + \frac{\|T(t)\|}{T_H} T_{gain} \tag{51}$$

This curve captures all the complex interactions arising from the structure of the heated volume. The two parameters n and t_0 contain the stochastic complexity characterizing the *WF* of the system, so the diffusivity is also included in the pool of the complexity.

Let us make the calculation for the capacitive coupling of modulated electro-hyperthermia (mEHT, trade name oncothermia [106]), with actual values of *WF* parameters $n = 1.48$ and $t_0 = 1$. We will assume the following parameters:

The diameter of the applicator $D_{app} = 0.2$ m, $P_{fwr} = 150$ W, $P_{refl} = 3\ \mathrm{W}(2\%)$, $\eta = 0.85$, depth of the tumour $h_t = 0.1$ m, the size of the tumor $s_t = 0.1 \times 0.05 \times 0.1 = 0.5 \times 10^{-3}\,\mathrm{m}^3 = 0.5\ell$, the body thickness in the supine position at the belly $d_{body} = 0.2$ m, and size of the entire affected volume $s_V = 9.05 \times 10^{-3}\,\mathrm{m}^3 = 9.05\ell$.

The calculated values are: $m_t = 0.595$ kg; $m_h = 9.5$ kg; $SAR = 12.377 \frac{\mathrm{W}}{\mathrm{m}^3}$. The obtained T_H temperatures $T_t = 45.89^{\circ}\mathrm{C}$; $T_h = 40.32^{\circ}\mathrm{C}$, and consequently $T_H = 40.65^{\circ}\mathrm{C}$; hence $T_{gain} = 4.15^{\circ}\mathrm{C}$. The metabolic addition has no role in this approximation. The temperature grows as shown in **Figure 7**.

The metabolic addition is $381 \frac{\mathrm{W}}{\mathrm{m}^3} = 0.38 \frac{\mathrm{W}}{\mathrm{kg}}$, [43]. For simplicity, we count the metabolic rate as equal in the tumour and healthy tissue, because the same volume, where the tumour has less malignant cells due to the increased volume of extracellular electrolyte [107], as well as its volume having certain necrotic parts. Consequently, with the already higher than healthy metabolic rate of the tumour-cells, their metabolic activity in the unit-volume is equal to that in the healthy volume. The overall metabolic activity is 3% of the applied *SAR*, so it could be counted in the calculation. In this case, the determined T_H values are: $T_t = 47.10^{\circ}\mathrm{C}$; $T_h = 40.44^{\circ}\mathrm{C}$, and consequently $T_H = 40.85^{\circ}\mathrm{C}$; hence $T_{gain} = 4.35^{\circ}\mathrm{C}$, which is 0.2˚C higher with metabolic addition than without it. In a more general estimation, we use the metabolic part of the $\frac{\Delta T(t)}{\Delta t}$ change:

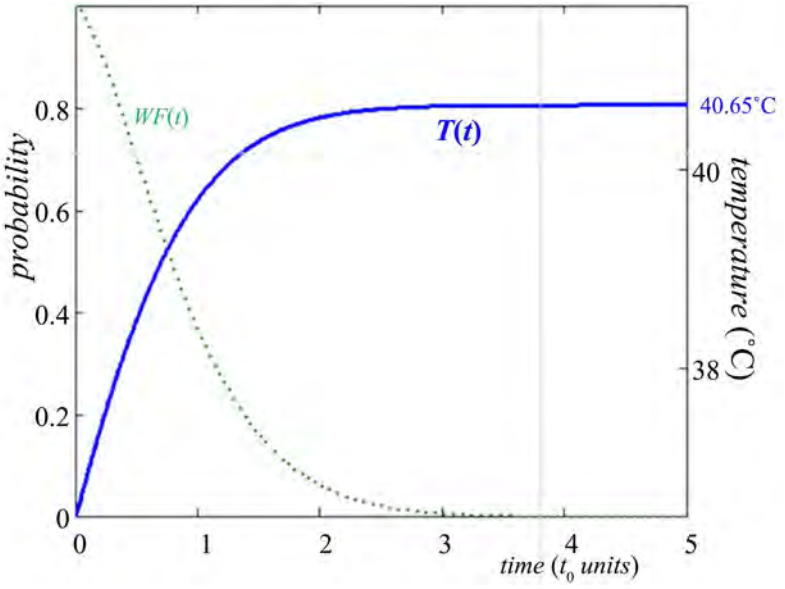

Figure 7. The temperature development of the tumour (right-hand axis) $m_t = 0.595$ kg and $m_h = 9.5$ kg by the WF approximation ($n = 1.48, t_0 = 1$) calculated for mEHT. ($P_{fwr} = 150$ W , $P_{refl} = 3\,\mathrm{W}(2\%)$, $\eta = 0.85$). Other parameters in the calculation are in the text.

$$\rho_h c \frac{\Delta T(t)}{\Delta t} = q_0 \rho_t \cdot 1.1^{(\Delta T(t))} \Rightarrow \Delta T(t) \cong \frac{q_0 \rho_t}{\rho_h c} 1.1^{(\Delta T(t))} \Delta t \tag{52}$$

In the case of a 6˚C temperature increase during the entire $t = 1$ h period of treatment, the metabolic addition is $\Delta T \le 0.5$˚C . Consequently, ignoring it is correct.

The beginning of the heating process is quasi-adiabatic, due to the relatively slow processes of the homeostatic feedback [108] [109]. This situation means that at the beginning of the heating, the energy entirely heats the target without other components of the energy balance.

$$q_0 \rho 1.1^{(\Delta T)} - c_b \rho_b w_b (T)(\Delta T) - k_h \nabla^2 T \cong 0 \tag{53}$$

Hence the task at the start of the heating is to determine the slope of the starting curve from (15):

$$\rho_h c \frac{\partial T}{\partial t} \approx \rho_h SAR \Rightarrow \frac{\Delta T}{\Delta t} = \frac{SAR}{c} \tag{54}$$

This approximation is allowed up until it reaches the non-linearity shown in the curve, numerically calculated for the above data; see **Figure 8**.

The activation of the various feedback mechanisms, like the *BF*, the metabolic rate, and the heat-conduction, causes the curve to deviate from the linear slope. The variation of the forwarded power changes the curves, and the appropriate equilibrium temperature is shown in **Figure 9**.

The change of the t_0 self-time changes the shape of the heating curve, but the final temperature in equilibrium remains constant; see **Figure 10**.

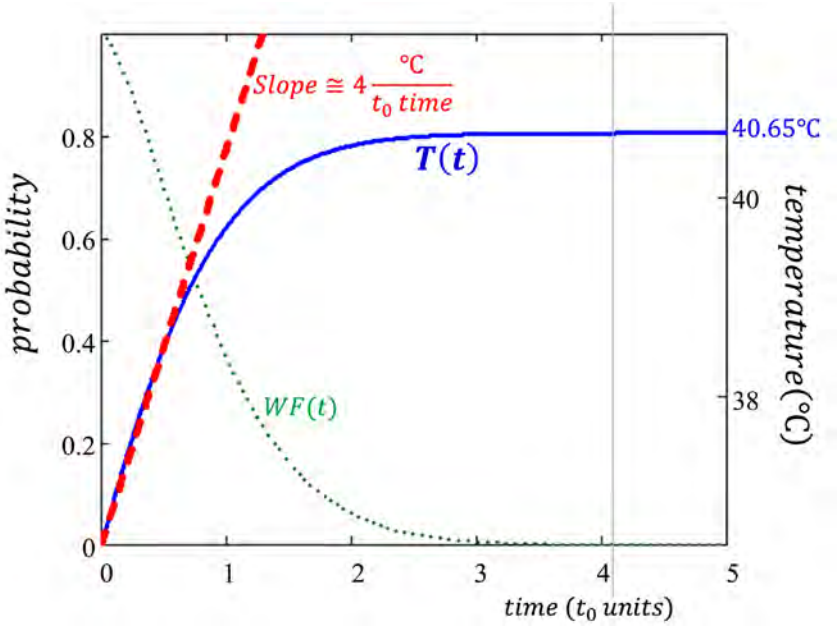

Figure 8. The linear slope of $T(t)$ at start (dashed line, right-hand axis). The temperature development of the tumour $m_t = 0.595$ kg calculated for mEHT ($P_{fwr} = 150$ W, $P_{refl} = 3\ \mathrm{W}(2\%)$, $\eta = 0.85$). Other parameters in the calculation are in the text.

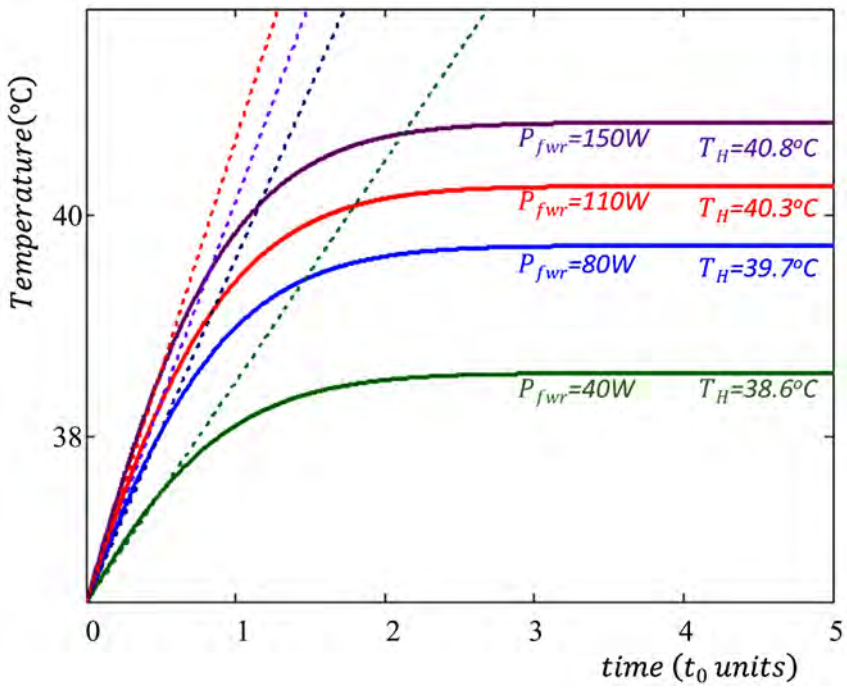

Figure 9. The temperature development (solid lines) of the tumour $m_t = 0.595$ kg by various forwarded powers, calculated for mEHT ($P_{refl} = 3\ \mathrm{W}(2\%)$, $\eta = 0.85$). The slopes are shown (dashed line). Other parameters in the calculation are in the text.

The change of the n shape-factor does not effect as robustly as the scale factor did; see Figure 11.

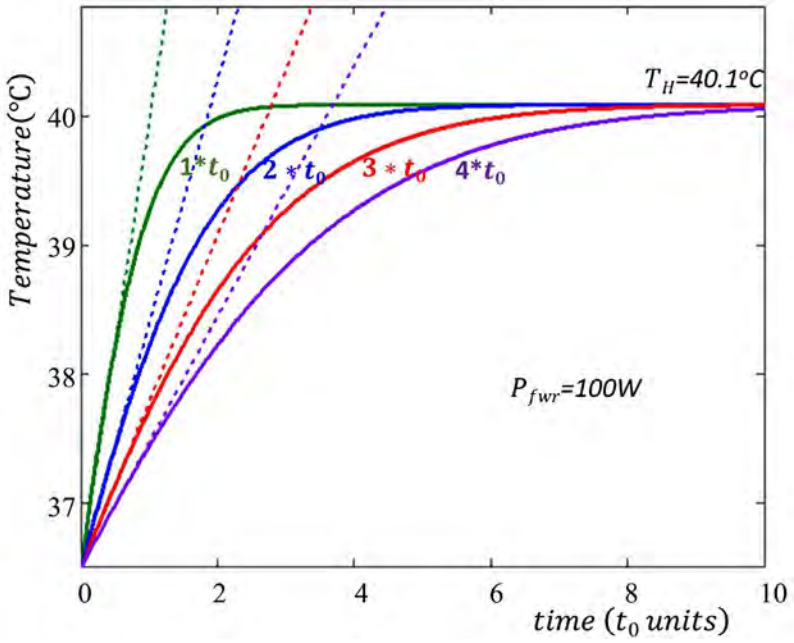

Figure 10. The temperature development (solid lines) of the tumour $m_t = 0.595$ kg by various time-constants, calculated for mEHT. ($P_{fwr} = 100$ W , $P_{refl} = 3\ \mathrm{W}(2\%)$, $\eta = 0.85$). Other parameters in the calculation are in the text.

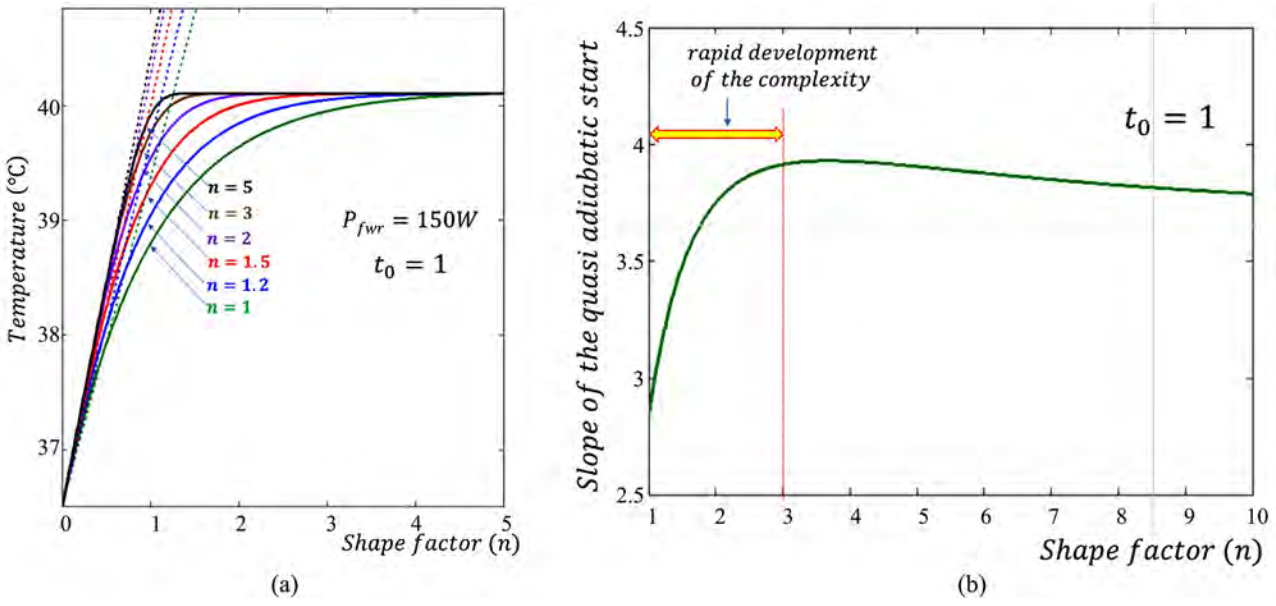

Figure 11. The effect of developing complexity by growing shape factor n: (a) temperature development; (b) change to the starting, quasi adiabatic slope value by n ($P_{fwr} = 150$ W , $P_{refl} = 3\ \mathrm{W}(2\%)$, $\eta = 0.85$).

The shape-factor n, which characterizes the complexity by (39), is distinguishable from the simple, single feedback mechanism ($n = 1$). While complexity develops (n increases) the adiabatic slope starts changing considerably in the $1 \le n \le 3$ interval, but afterwards the change is not considerable.

When the power is switched off, $SAR = 0$, the system cools down as a result

of its complex interactions, and Equation (11) reduces to the form where the complex interactions in (54) derive the change of the temperature:

$$\rho_h c \frac{\partial T}{\partial t} = -c_b \rho_b w_b (T)(\Delta T) - k_h \nabla^2 T + q_0 \rho 1.1^{(\Delta T)} \tag{55}$$

The washout time, driven by the *BF*, is different for thermal processes and the clearance of molecules (like radiofarmacons, tracers or blood-delivered molecules or particles). The main difference is in the mechanisms of diffusion, which are different for various blood-delivered particles or molecules and for heat. The thermal washout is also a complex process mainly driven by the *BF*, but not determined by it alone. In investigations of the clearance of tracers, it is clearly shown that in reality the clearance (wash-out) tightly depends on *BF*, but these parameters are not equal, instantaneous mixing with metabolic changes and diffusion breaking the unity. Also, the metabolic heat does not have a direct action on the clearance, while the thermal washout is directly modified by it.

A "similarity" can be observed in the washout of tracers [110], which is a rescaling of the time, showing similar scaling behaviour as we have seen in the heat-up process. The scaling of washout "similarity" is present in the wash-in of tracers as well [111]. An important observation in contrast material studies is that the enhancement of the contrast material decreases with temperature growth, while it increases with the thermal cooling coefficient; see **Figure 12** [112]. The main message of this is that the high variability of the *BF* by tumour entities, as well as the tumours having massively heterogenic *BF*, form a gradient from the centre to the periphery.

In most of the examinations, the diffusion and metabolic parts are neglected for simplicity, and the temperature dependence of the *BF* not being considered, so the following equation remains to be investigated:

$$\rho_h c \frac{\mathrm{d}T}{\mathrm{d}t} = -c_b \rho_b w_b \left(T - T_{body}\right) \tag{56}$$

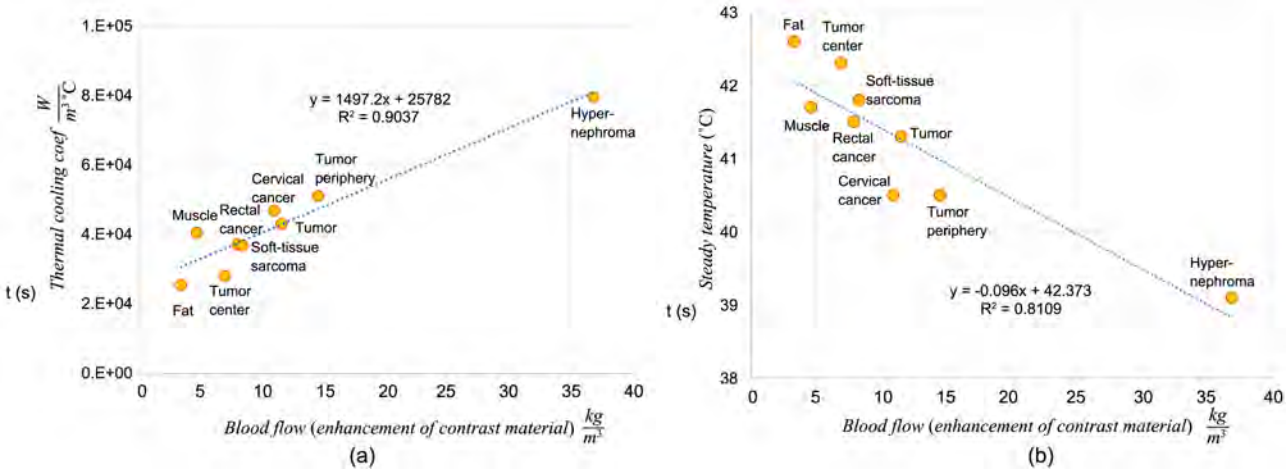

Figure 12. The effect of *BF* on the thermal coefficient and the steady temperature measured in different tumours. It is important to note that the tumour-periphery has the highest *BF*. The *BF* was measured with the concentration of the contrast material.

The starting temperature is T_H and so the analytical solution is exponential:

$$T(t) = \left(T_H - T_{body}\right) e^{-\frac{t}{t_0}} + T_{body} \quad \text{where } t_0 = \frac{c\rho_h}{c_b \rho_b w_b} \tag{57}$$

It is a simple exponential equation, which is a special case of *WF*, when $n = 1$. In general, neglecting the time-dependent metabolic addition, the thermal cooling is exponential; see **Figure 13**. The initial slope of the curve characterizes the quasi-adiabatic energy-take-off again, so it describes the given conditions determined by the blood flow.

The thermal washout (cooling rate) measurement validated Equation (57) in the given circumstances, and the guessed washout time, (when the $t = t_0$) is about 6.5 min, cooling down from 42˚C after 30 - 60 min microwave heating [113]. This approximation was made based on the measurement of the first 3 min, while the cooling to the T_{body} required a longer time. The washout depends on the measured tissue and other conditions; see **Figure 14**.

The time of thermal washout can be modified by changing the metabolic rate by lowering the temperature, causing a longer tail to the washout function in time. Consequently, with a longer $t_0' > t_0$ the value will be added to the simple exponential, which depends on the decreased metabolism resulting from the cooling process. This additional effect will have a time-lag because of the actual physiological time of metabolic reaction. Due to the physiological self-time, which is approximated as the thermal washout physiological time, this time-lag will be nearly 6 min.

The thermal self-cooling mechanism also has complex behaviour, because it too depends only on the simple unchanged *BF*. The *BF* depends on the temperature, as well as the heat-conduction, the surface cooling with the environment, and other physiological factors (like sweating, control by the hair, stress-status).

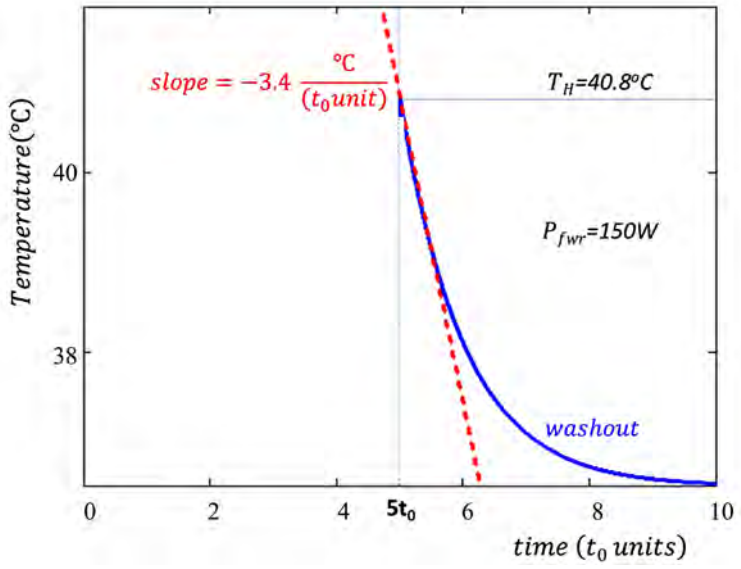

Figure 13. The exponential thermal cooling (washout) of the heated target (solid line). The quasi-adiabatic fit is shown (dashed line).

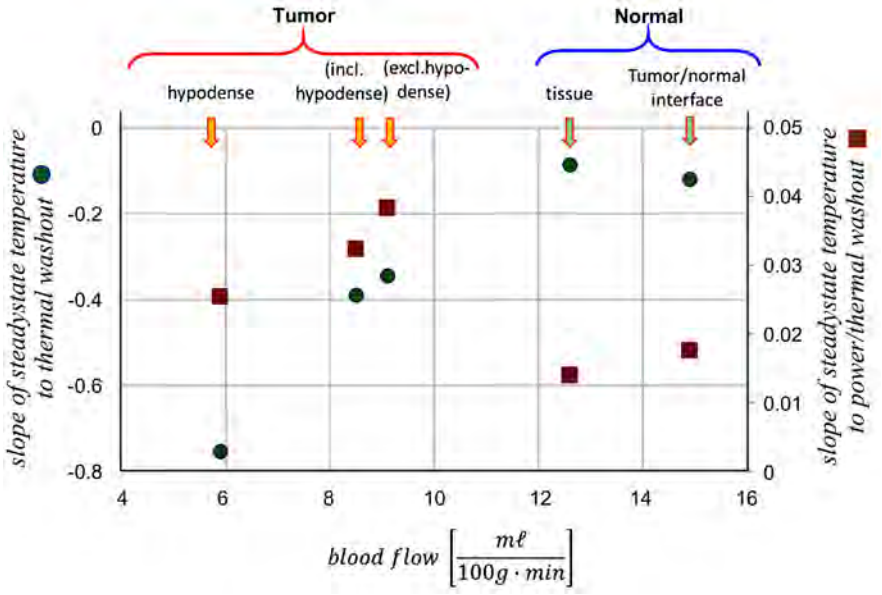

Figure 14. The slopes of the linear fit of the blood-flow vs the washout time of various tissues [117]. (● slope of steady-state temperature vs thermal washout; ▪ the slope of the steady-state temperature vs $\frac{\text{power}}{\text{theraml washout}}$.)

The decreasing temperature causes slower *BF* and lessens the other regulatory actions off the cooling rate, so the cooling will have a longer tail than the exponential ($WF\ n = 1$) alone. This complexity again induces the application of the integrative *WF* instead of the simple exponential. The integral of *WF* with the parameter $n > 1$ is shown in Figure 15.

The complete heat-up and cool-down temperature development are shown in Figure 16. Both the heating and cooling have a quasi-adiabatic fit to the linear slope covering the curve for pretty long sections. Still, the slopes differ, due to the separate mechanisms and conditions. The heating starts from body temperature, while the cooling starts higher, from the homeostatic one. The conditions of the *BF* and other factors change, which cause the deviations from linearity during the thermal processes. The heating linearity deviates by *SAR*-promoted intensified activities of *BF*, heat-diffusion, and metabolic rate, so the thermal conditions are forced by energy-absorption. In the cooling period, the system is alone, and with no constraints, the *BF*, the metabolic rate, and the temperature decrease. The heating has an $n > 1$ condition, depending on the structure of the target, and the self-organized network, which absorbs the energy, while during cooling $n \approx 1$.

The curve changes characteristics with the applied *SAR* values. Calculating the *SAR* from the power situation, we have temperature curves for different applied power; see Figure 17.

4. Discussion

The original Pennes Equation (11) describes a non-equilibrial heat-flow when

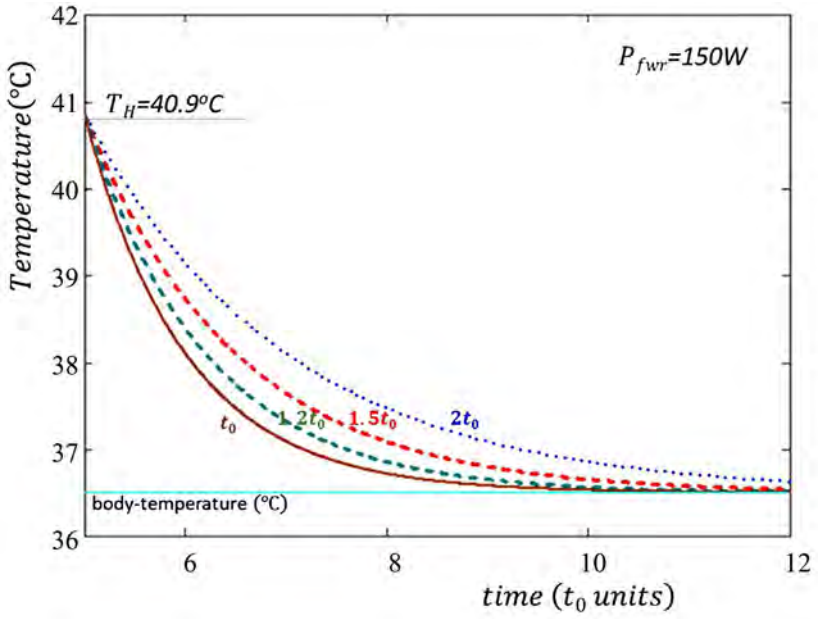

Figure 15. The long-tail washout function due to the complexity of cooling.

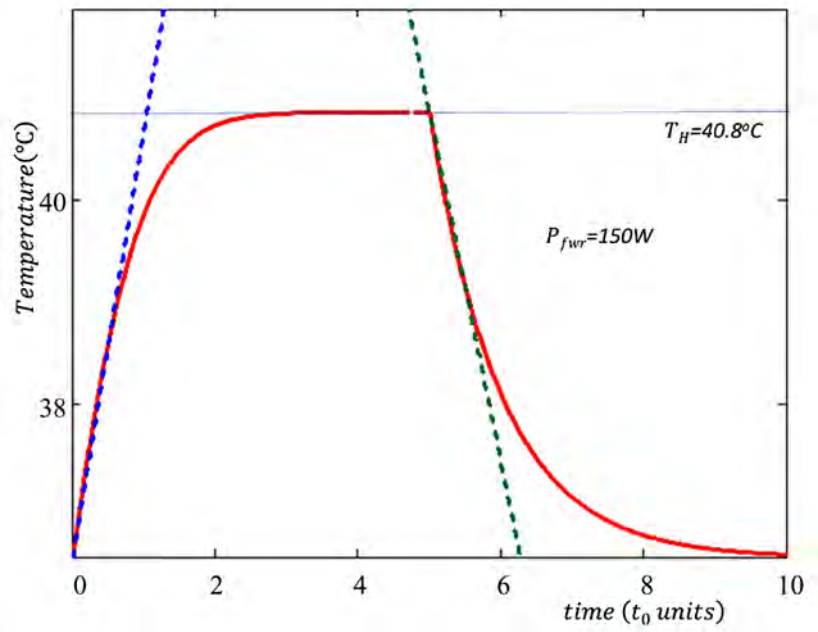

Figure 16. The complete temperature history of heating and the self-cooling by thermal homeostasis after the switching off of power-absorption.

the temperature is the only driving force, and the parameters are constants, independent of the temperature. The temperature definition supposes a system in which the participating units are independent, and only their mechanical energy changes by growing energy-intake. This has a temperature distribution [114], and supposes no interactions between the participating units (called an ideal gas). The Pennes equation is correct and usable, since the internal energy depends exclusively on the temperature, for which numerous model-calculations have been

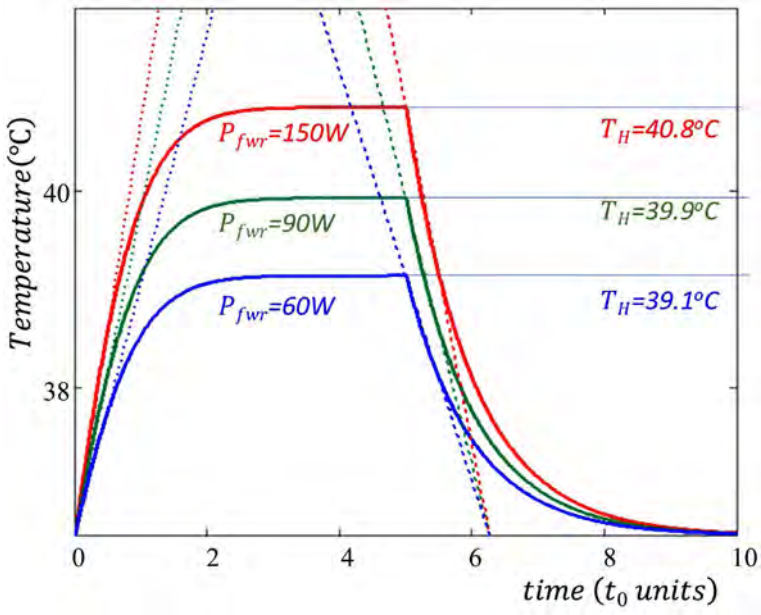

Figure 17. The temperature development by the applied power.

provided [115] [116] [117] [118]. To tackle time-dependent transient problems, some solutions have been published [39] [119].

Nevertheless, in reality, these are temperature-dependent values, and furthermore, their temperature functions are non-linear due to their complexly interconnected functions. The non-linear complexity of homeostasis is a game-changer for the discussion of (11).

Naturally, living objects are not such systems. Interactions with homeostatic functions must be considered, modifying the energy distribution in the heated matter. This type of energy utilization is missing from the Pennes bioheat-equation, leading to the above application of *WF* to represent the homeostatic complexity. The main basic constants, the *BF*, the densities, the specific heat values, the coefficient of the heat-diffusion and the metabolic rate represent the main constants in (11), but as a consequence of the homeostatic interactions, these parameters are also altered, which we denoted by the spatio-temporal functions in (15).

The complexity of the task is extended with the inhomogeneous breaks on the curves when phase transition happens. As a consequence of energy-induced structural changes, enzyme-assisted phase transitions are frequent in the homeostatic system. The massive number of these structural transitions (entropy changes in micro-environment of the molecules) gives us the possibility to handle them as a distribution, and we are again in the realm of the self-similarity self-ordering idea described by *WF*.

Hyperthermia in oncology is devoted to destroying the malignant cells as selectively as possible. The Weibull distribution is used with success for the self-organized malignancy in space and time [120]. Cancer breaks the network of normal cells. The cooperative harmony of the tissue changes to non-cooperative competitiveness. It forms a new complex structure non-linearly, far from ther-

modynamic equilibrium, but also self-organized. It could be described as a dynamic phase transition from healthy to cancerous [121], described with a clear analogy to phase transitions in a lifeless phenomenon. The self-organized biological development of tumours intrinsically developing in a healthy environment, the tumour-development deriving from that environment and showing the universal law of growth [122] [123], $W(t)$ is preferred to describe malignant diseases too.

The heating not only effects the temperature growth but also naturally causes physical changes. The structure of the tissue will not remain the same as it was before. The structural rearrangements will be temperature-dependent, and also energy-consuming. When the energy causes the phase to change, the temperature does not change; only the structure changes. This is like when water is being heated and it reaches 100˚C, and for a period the system expends all its energy to turn the liquid to gas (structural transition), while the temperature does not change during this process. The process is naturally thermal, but the temperature does not change. When the structural rearrangement is complete, the temperature starts to rise again as the energy intake continues. A similar effect occurs with ionizing radiation therapy when we expect the breaking of the DNA strands, which absorbs energy. The energy which is not used for this bonding break causes an increase in temperature, which would be an adverse effect in radiation therapy.

Some special papers have been devoted to modifying the Pennes-like equations [124] [125] [126] [127], but none have yet to consider the energy used in the distortion of the actual arrangements. The energy could be used solely to bring about chemical changes (distortion of the molecules and restructuring of the arrangements) in oncological hyperthermia. The temperature will not be changed locally when the energy is consumed for structural change. The temperature is only a condition (when the change happens) but not a measure of the change itself. The Pennes equation could be generalized [128] considering the cellular destruction and the structural rearrangements [129].

The introduction of a WF assisted solution offers the possibility to measure this structural change from the temperature development curve. The WF as the velocity of temperature change (41) has a development which is described by the probability distribution function (PDF) as the derivative of the WF which we used:

$$\frac{\mathrm{d}v(t)}{\mathrm{d}t}=\frac{\mathrm{d}W(t)}{\mathrm{d}t}=WF_{PDF}(t)=\begin{cases}\dfrac{n}{t_0}\left(\dfrac{t}{t_0}\right)^{n-1}\mathrm{e}^{-\left(\frac{t}{t_0}\right)^n} & \text{if } t\geq 0\\ 0 & \text{if } t<0\end{cases} \tag{58}$$

First, the velocity changes very rapidly and then, after a peak, it decreases; with homeostatic control, the reaction of the body activates (**Figure 18**). This distribution determines the change of temperature (the WF function), which determines the temperature curve (the $T(t)$ function), as shown in **Figure 7**.

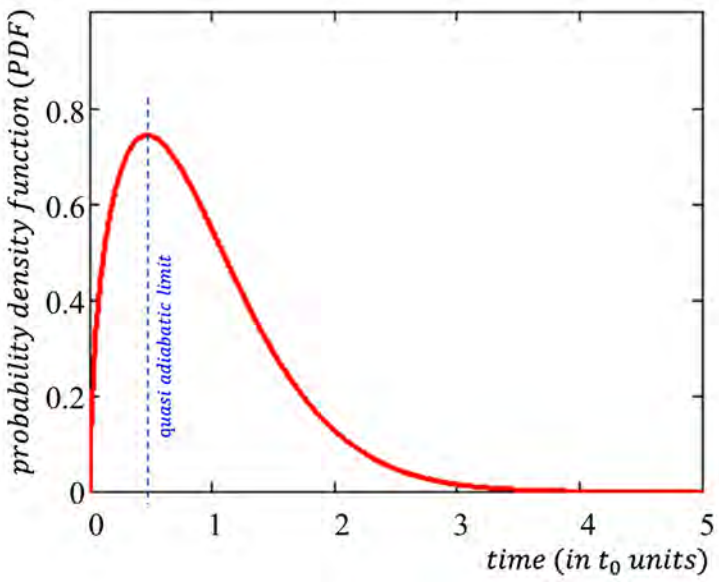

Figure 18. The power-density function of *WF*. The maximum of the PDF curve is the approximate limit of the quasi adiabatic heating (see text).

The PDF curve shows the change in velocity of the temperature growth. The curve starts with the rapid increase in temperature until reaching its peak. The comparatively very rapid growth could be considered the quasi-adiabatic process, which determines the starting slope in Figure 8, and so determines the certainty of the slope.

A simple approach of *WF* parameters could be obtained from the measured temperature plot by time [130]. Two helpful points have to be noted, as shown in Figure 19. The point x_m marks the highest point where the linear fit of the quasi-adiabatic slope ($\frac{\Delta T}{\Delta t}$) follows the measured curve, and x_H is determined by the point at which the temperature reaches a steady state (homeostatic equilibrium). These are measured in real-time (in seconds), and are different of course for tumorous and for healthy plots, which are denoted by the additional subscripts *t* and *h*, respectively. We show these values in Figure 19.

The x_m point fits the mode of the distribution function because it corresponds to the peak of the change of velocity (Figure 18), while the x_H point denotes when the *WF* decreased to below an error value, which we decide on as 1%. Recognizing these values, we get:

$$x_m = t_0\left(\frac{n-1}{n}\right)^{1/n} \quad \text{and} \quad x_H = t_0 \exp\left(\frac{\ln\left(-\ln(0.01)\right)}{n}\right) \tag{59}$$

Both parameters of the original *WF* could be determined from the two equations of (59). In doing this, we are able to use the original t_0 units for exact evaluations. Note, x_H marks a point from the stochastic approach, which was denoted by θ at the introduction of the *WF*; see Figure 1. The difference seen in Figure 19 between the tumorous and healthy temperature plots follows the selectivity of

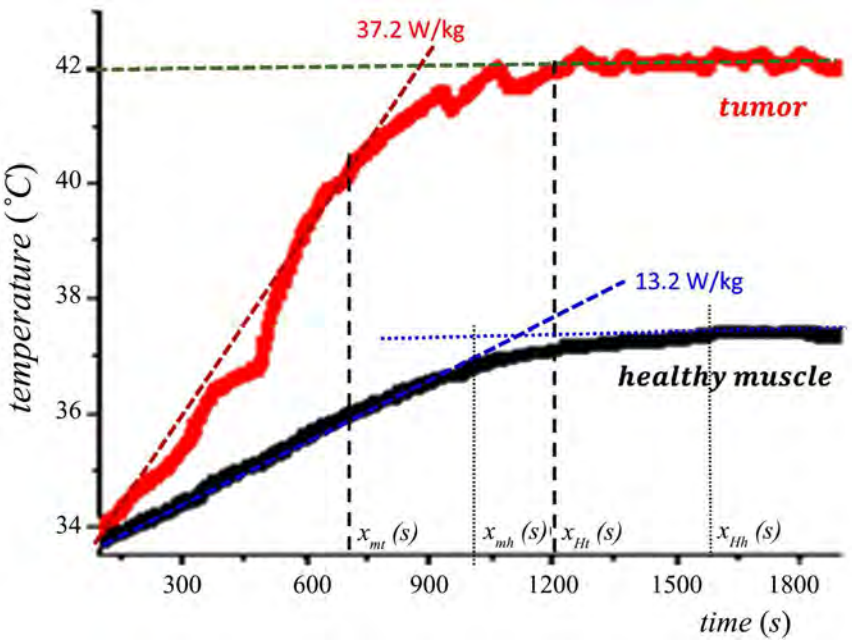

Figure 19. The measured temperature plot is a preclinical measurement [130].

the treatment, which can be quantified by the starting slopes as well as by the specific differences of the parameters $\left(x_{mt}-x_{mh}\right)$ and $\left(x_{Ht}-x_{Hh}\right)$.

The t_0 point can be determined by simple geometric fitting. We know that the value of t_0 is always at the point where $1/\mathrm{e}\cong 0.368$, so having a slope with this value on the temperature plot determines the position of t_0, as shown in **Figure 20**. The angle of the specific slope which we use is 0.353 [rad] or 20.2˚. This simple approximation directly determines the conversion of time to t_0. Note, the derivative of WF at the t_0 point $\frac{\mathrm{d}W\left(t_0\right)}{\mathrm{d}t}=-\left(\frac{1}{\mathrm{e}}\right)\frac{n}{t_0}\cong -0.368\frac{n}{t_0}$ differs by multiplication with $\frac{n}{t_0}$ from the same-point derivative of the temperature plot, $\frac{\mathrm{d}W\left(t_0\right)}{\mathrm{d}t}=-\left(\frac{1}{\mathrm{e}}\right)\frac{n}{t_0}\cong -0.368\frac{n}{t_0}$.

The comparison of the results of **Figure 10** and **Figure 11** shows that the scale factor t_0 causes a massive change in the quasi-adiabatic starting slope, while the shape factor n causes only a minor change. The difference mirrors their roles in homeostatic (homeodynamic) control: the t_0 scale factor depends on the dynamic processes in the regulation, principally on BF, while the n shape factor primarily reflects the structural differences. In this way, the shape parameter follows one of the major factors of the complexity in the temperature development, the BF, which changes non-linearly with the temperature [131]. The non-Newtonian behaviour [132], and the flow-state, which can cause the negative impedance of BF [133], alters the non-linearity by temperature. The difference in angiogenesis between the tumour and healthy vessel network [134] could also affect the temperature dependence of the BF. The attractive idea of our present approach is the

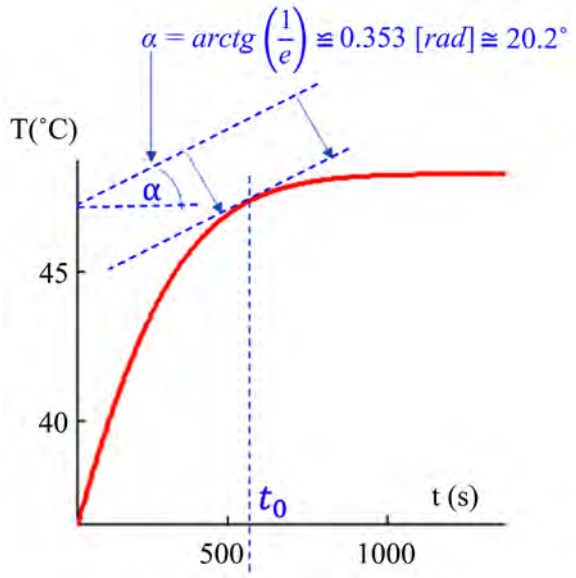

Figure 20. A simple geometric fitting to determine the t_0 unit (see text). Calculating with (59) could perfectly control this approximate fit.

stochastic considerations, so these effects are well presented in the personal differences in the heating reactions, which are considered in the personalized fit of *WF* approach; the complex package in *WF* considers all, even small, modifications.

The assumption is ordinarily that the temperature reaches the homeostatic state by a rigorously monotonic function. This could be incorrect, however, when the homeostatic control is achieved too late, or when it does not have enough cooling capacity to compensate for the heating energy [135]. When saturation occurs earlier than the negative physiological feedback to regulate it, an overshoot can happen, or an equilibrium may not be formed due to the massive energy input (Figure 21). The uncontrolled absorption leads to ablation. Such overshooting and ablation (burning) situations are beyond the possibilities of these present considerations. The complexity described by *WF* is valid only in near stationary developments.

When phase transition does not occur (like when heating water from 0˚C to 100˚C at normal pressure), the temperature plot is linear across its full range, but keeping a constant temperature at the phase transition (100˚C) and then continuing linearly with another slope, corresponding to the thermal parameters of the new phase (Figure 22).

Note the development of the temperature in the case of heating pure water. Here a fraction of the power applied to humans in local hyperthermia could heat up the same mass of the water from 36˚C to 45˚C (Figure 23).

Living objects, of course, do not have the same behaviour as pure water. The water phantom is far from correct in comparison to a living reality. The water phantom is homogenous, having only non-homogenous heating due to the exponential decay of the electromagnetic energy-absorption by depth [136], which

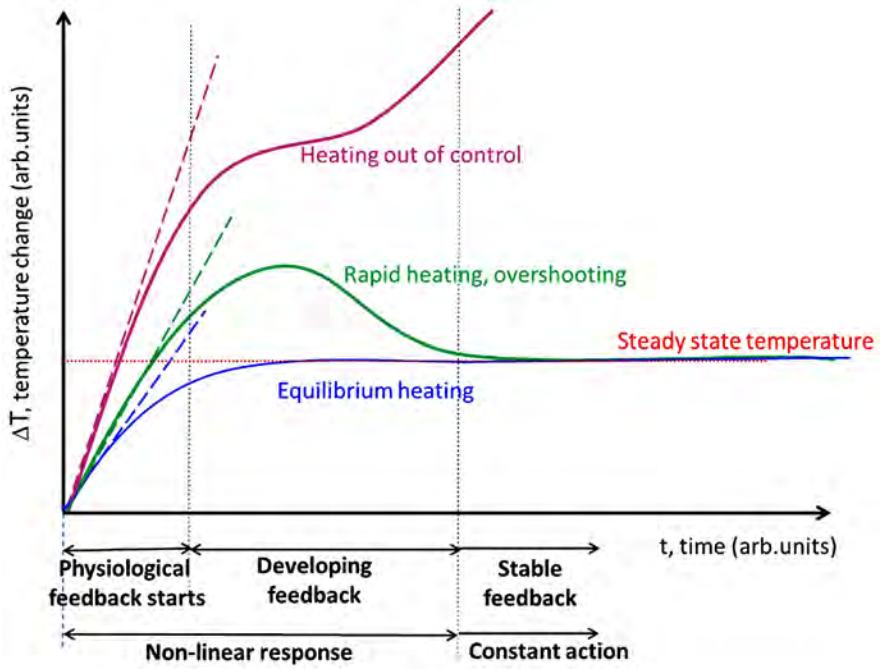

Figure 21. Relation of the absorbed energy to the homeostatic thermal regulation. The timing and the energy-compensation balance the actual shape of the temperature plot.

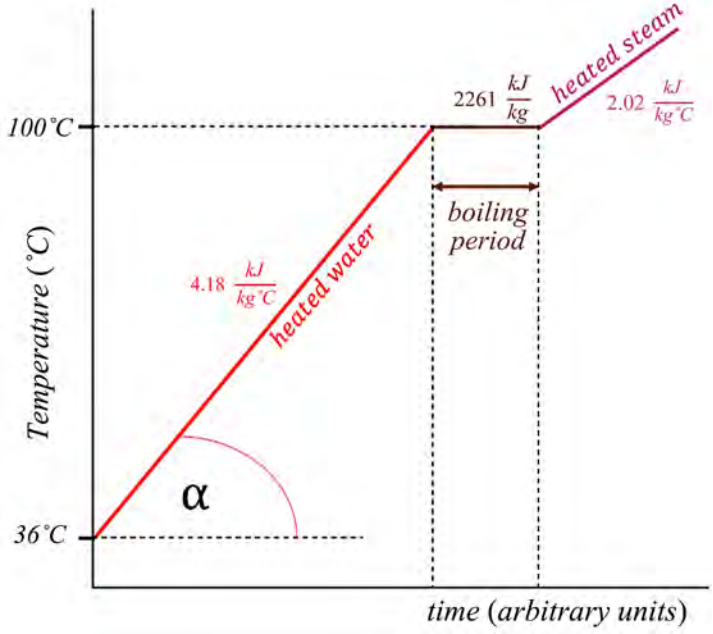

Figure 22. Heating of simple water phantom, temperature vs time. The phase transition at 100˚C happens at a constant temperature, while the elapsed time develops.

may initialize mas-transports by temperature gradient in the volume. The exponential decay sharply, and inversely depends on the wavelength [137]. The attenuation of the power absorption of human tissues differs from water [138]; nevertheless, the penetration remains exponential with various rates of decrease in the variety of tissues.

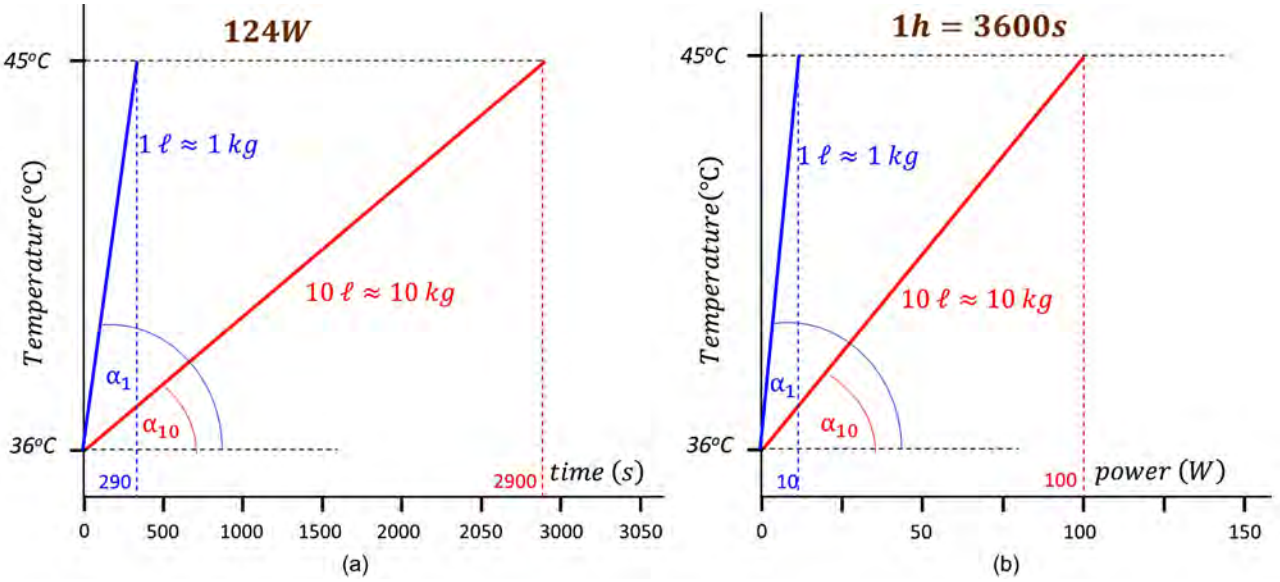

Figure 23. The heating of the water phantom only: (a) 124 W is applied (using 150 W forwarded but calculating 3% reflected power and 85% efficacy of heating) and heats up ten litres of water from 36˚C to 45˚C in a duration of less than an hour, while a volume of 1 litre needs only less than 5 min; (b) ten litres of water reaches the desired 45˚C within one hour with 100 W absorbed power, while one litre needs only 10 W to elevate the temperature from 36˚C to 45˚C.

A living structure represents an inherent decisional heterogeneity, having a large number of electrolytes separated by various walls and membranes. Consequently, both the thermal and electromagnetic parameters vividly change in the macroscopic and microscopic ranges and the homogeneous *SAR* is illusory. The self-organized structure drives the organization of the heterogeneity, forming fractal behaviour [139]. The self-organized self-similar structure present both in space and time [75], develops spatio-temporal behaviour of the tissues. The concentration of the electrolytes dynamically changes due to their energetically open structure, which initializes the dynamism of the system. The living dynamism performs random stationary stochastic self-organizing processes [74] [140] as a consequence of its self-similar stochastic behaviour. It fluctuates by a particular noise (called pink-noise, or temporal fractal noise) [141] [142], a fingerprint of the self-organizing [143], representing a general behaviour of living biomaterial [70].

Together with the macro heterogeneity, the tumour is also massively diverse on a microscopic level. The *BF* in the tumour has a threshold between the vasodilation and vasoconstriction. The threshold depends on the temperature, and is usually at an interval between 39˚C and 43˚C [11]. The angio-change is independent of the general inhomogeneity of the tissue but depends on the type of the tumour and its stage. The angio-reaction will change the temperature development, due to the massive change of *BF* from the vasodilated situation to the low-*BF* vasoconstriction. The drop in *BF* increases the temperature due to the lowered cooling capacity. The quasi-adiabatic slope jumps in the vasoconstrictive stage of the tumour, and the same *SAR* generates a greater temperature development per unit time [135].

Further microscopic heterogeneity is observed on a molecular level. The structural disruption and rearrangements use a part of the energy without any considerable change of temperature. Where the energy concentrates on the structural order, the points on the temperature plot by time remain approximately at the same temperature values, despite the continuously absorbed *SAR* accompanied by the approximately constant temperature as we expect during phase transitions. The *SAR* at these points is dominantly consumed by the structural energy and not for the heating of the tumour's environment.

The heterogeneities influence temperature development, and such a linear temperature development, as we have in the case of water (**Figure 23**) is unrealistic in the human body. The macroscopic temperature is roughly like that seen in **Figure 8**, presenting a linear slope only at the beginning of the heating when the heat is not yet spreading intensively by diffusion, and the blood-flow regulation has a lag. However, the simple picture has a fine-structure depending on the dynamism of the heat-diffusion and the blood-flow and other regulating components like metabolism. The initial linear slope starts curving downwards, and after a maximum, the temperature decreases (**Figure 24**). The intensification of the blood-flow causes this "bump" in temperature and it is visible only when the time-lagging feedback appears at the end of the period of intensively rising temperature. Note, the break of the linearity could be earlier in preclinical measurements (see **Figure 19**), where the homeostatic reactions are quicker. The thermal homeostatic function keeps the temperature unchanged (T_{H2}) and is the first saturation period, where the vasodilatation/vasoconstriction transition balances approximately constant value in the tumour (see the tumour-curve up to 39˚C in **Figure 6**), After this point, the temperature might stabilize at another level for a short time due to the balance (T_{H1}), or, if the homeostatic regulation cannot stabilize the equilibrium, it might start to grow continuously. The vasoconstriction could easily develop additional necrotic volumes lacking blood-flow regulation such that the temperature could grow in those regions rapidly. While the forwarded *SAR* does not chage; its hetereogenic absorption changes, but varies from the temperature development primarily because of the heterogeneity of *BF*. The applied *SAR* is constant, while the absorbed energy grows but not as rapidly as expected, because the blood-cooling takes energy away in the system. The energy absorption changes at the vasodilatation/vasoconstriction transition.

The homeostatic "bump" modifies the temperature development at all variations of the power, too (**Figure 25**), but the slope of the quasi-adiabatic linear-fit at the beginning does not change until the very slow temperature increase when the time-lag of the homeostatic control modifies the starting slope as well. We assume that the homeostatic cooling switches on smoothly by a Gaussian distribution and with an amplitude factor A:

$$\frac{A}{\sigma\sqrt{2\pi}}\exp\left[-\left(\frac{t-\mu}{\sigma\sqrt{2}}\right)^2\right] \tag{60}$$

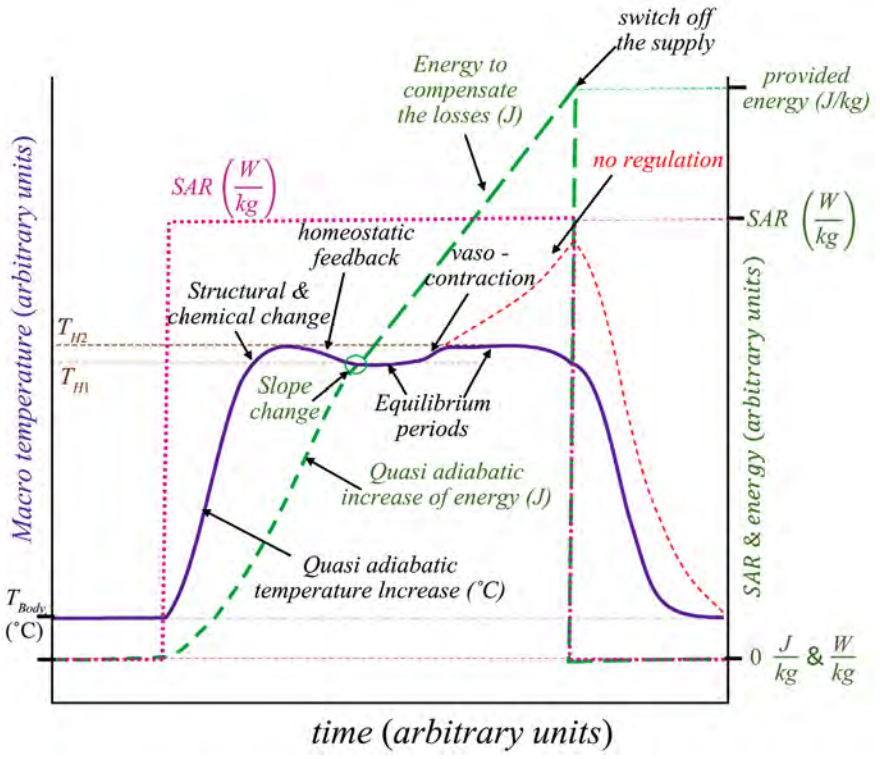

Figure 24. The possible fine structure of the development of temperature in macroscopic steps. The important factor of the figure is the time-lag of the various effects. Here all the possible effects are shown, not all of which will necessarily be active in the actual energy-absorption.

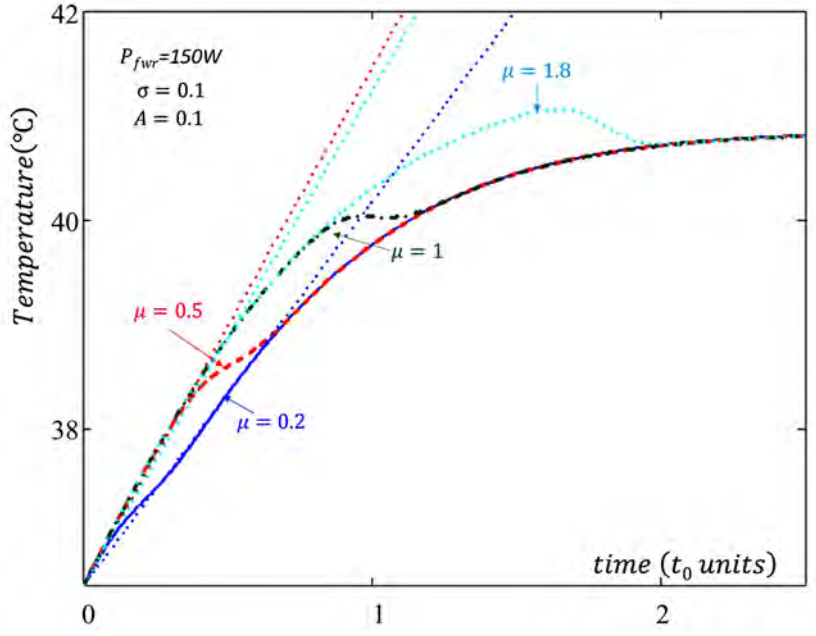

Figure 25. The homeostatic regulation could become active with different time-lags μ.

which is equal with WF when $t_0 = \sigma\sqrt{2}$ and $n = 2$. The time-lag of the start of this feedback is included in the μ, and the "smoothness" is in the t_0. The shape

does not change, $n=2$. The time-lag $\mu=0.2$ shows an early homeostatic reaction, which regulation requires a high velocity of *BF*. In animal experiments where the heart-rate is higher than in humans, because of the allometric scaling, a short time-lag is frequent, as we see in preclinical experiments [130]; see **Figure 19**. Different time-lags have been used under various conditions in calculations [43].

The thermal and electromagnetic heterogeneity allow two different ways of handling the energy-absorption of the living material: make a complete average of the microscopic deviations, regarding this as equal in the target, or use the biophysical differences accepting the micro-variations to select the malignant cells. The first approach considers the entire volume in focus as being like homogeneous matter, and it is heated irrespective of the differences in the micro-environments, while the second one concentrates on malignant cells as the direct aim of the study. The two approaches fundamentally define the performance of the actual treatment. When the target is regarded as homogeneous, its full mass represents the energy-absorber, requesting such energy as is enough for this task. The micro-selection however demands much lower energy consumption, the intended target of the energy absorption being only a fraction of that in the homogeneous approach. The selection of the energy absorption specifies the efficacy of the actual treatment.

The isothermal, homogeneous heating of a local tumour does not reach stable thermal equilibrium, because the non-linear reaction of the feedback mechanisms opposes the heating action, so an instable equilibrium forms a steady-state situation. In this process, the target develops new thermal inhomogeneities, because the cooling action of the blood is not equally distributed in the volume of the focus. As a consequence, clinical practice divides patients into "heatable" or "non-heatable" categories [144]. The selection is based on the possibility of the temperature increase in the actual location by local/regional treatment failing to reach the desired temperature in the target. The "non-heatable" cases could have the same *SAR* as the "heatable" ones, but their intensive homeostatic control blocks the marked temperature increase. We have to accept the real situation: the technical difficulty of the focussing of temperature is not identical with that of the focussing of *SAR*. The temperature depends on various processes, and naturally changes by elapsed time, spreading over the neighbouring volume.

The final goal of the energy-absorption is not a simple heating; the intention is to destroy the malignancy. Naturally, chemical and structural changes happen in the process of the cell dying. An overall, isothermal heating could complete this task, pumping much more energy into the target than necessary for the elimination of the cancer cells, heating up all the parts, even those which trigger the counter-actions of the thermal control. The isothermal approach requires extra energy to compensate for the forced physio-regulation attempting to restore thermal homeostasis. The homogeneous heating induces intensive BF and so risks the development of life-threatening micro and macrometastases, by the in-

tensification of the delivery of the circulating tumour cells, worsening the life-prognosis. Multiple isothermal hyperthermia studies have shown effective and significant local control of the treated tumour, but at the same time present a decreased overall survival among others for breast carcinoma [145] [146], for non-small-cell lung cancer [147] [148], for uterine cervix cancer [149] [150], and even for the easily "heatable" surface tumours [151].

However, the thermal and electronic parameters differ between the tumour and the healthy environment, allowing the microscopic selection of biophysical origin. The variation of these parameters modifies the macro and microstructures of the tissue, varying the heterogeneity of the energy absorption. Malignant cells metabolize intensively, supporting their proliferation [152]. Their increased glucose metabolism can be measured by positron emission tomography (PET) [153]. The extra metabolic activity increases the ionic concentration in the vicinity, increasing the conductivity of that region [154], also detectable by imaging [155]. The changing of the networking arrangement microscopically causes the loss of the healthy cooperative connections with neighbouring cells, constructing a largely different fractal structure [156]. The malignant cells break their intercellular bonds [157] and junctions [158], and individually "combat" all other cells for metabolic energy. Measurement of the growing disorder in cancer came with the first imaging of a lesion [159], proving the increase of the dielectric constant in the microenvironment of the cells [160]. This decreases the complex electric impedance of the microenvironment of the tumour cells, channeling the radiofrequency (*RF*) current to their location [161], allowing their selection by electromagnetic means [162].

The energy of the current primarily heats up the lipid rafts on the membrane of the cancer cells [163]. The membrane rafts are groups of clustered transmembrane proteins fixed by lipid-protein interactions [164]. A dominant part of the transmembrane proteins is clustered in raft domains. The rafts collect dynamic proteins [165], and have high lateral mobility in the membrane [166]. The size of these clusters is in the nano-range; depending on the ratio of protein to lipid content, different ranges of their horizontal diameters have been measured: 10 - 100 nm [167]; 25 - 700 nm [168]; 100 - 200 nm [169]. The width of the membrane is 5 nm [170], but the thickness of rafts, due to their transmembrane proteins, is larger. An interesting result [216] is that the temperature increase of the nanoparticle is proportional to the square of its radius, which gives an easy comparison of the temperature using the sizes of the particles. The size of rafts is 6 - 50 nm, and the large rafts dominate the protein content of the membrane [171]. The malignant cells lose their intercellular connections, and the formerly connected transmembrane proteins form rafts, which are significantly denser in the membrane of cancer-cells than in their noncancerous counterparts [172].

The extracellular matrix (ECM) and the cellular membrane absorb the main part of the energy in the MHz region of *RF* [173]. The water content of the ECM interacts with the membrane [174], having variant bonds [175], and importantly

alters the membrane effect, showing a low *SAR* but high voltage drop [176], which can help the signal's excitation of the raft proteins [177]. The electrostatic charge of the membrane attracts the ions from the ECM, the effect of which is sufficient to establish a transmembrane potential [178].

The primary targets to absorb the well-chosen *RF* on the membrane of the selected malignant cells are the transmembrane proteins located in the rafts. The β/δ frequency dispersion [179] promotes the focusing of the energy on the lipid-protein interactions at the applied 10^7 Hz frequency range. Nearly ten times higher conductivity was measured at transmembrane proteins [180]. Models of added protein domains with different concentrations in the lipid layer showed between one and three orders of magnitude higher conductivity in the presence of protein fractions than the lipid membrane alone [181]. These electric impedance differences guide the *RF* to the rafts [182]. The thermal effect is limited to nanoscopic local "points", the rafts, which are most sensitive to any lethal attack on malignant cells, which is the basis of the mEHT method. The well-chosen *RF* current [183] uses a 13.56 MHz carrier frequency according to the medical standards. An appropriate time-fractal modulation is applied [184], which is essential to obtaining the proper selection effect. (The technical description can be found elsewhere [185] [186]). In this way, mEHT targets the lipid-protein interactions that can cause specific energy-absorption in the membrane rafts, which carry many signal-receptors and are involved in multiple functional signal pathways [182].

Many observations have been made on various electromagnetic energy-absorptions, aside from those regarding temperature changes. The electric field promotes cellular fusion at low [187], and high [188] frequencies; a field-strength-dependent haemolytic effect has been observed resulting from RF exposure [189], as has the activation of ion-channels at the cellular membrane [190], membrane-mediated Ca^{2+} signalling effects on the immune system [191], and the induction of transmembrane Ca^{2+} by alternating current (low-frequency electromagnetic fields [LFEMF]) [192]. The biological effects of LFEMF have raised significant interest and debate in the past. Numerous reviews [193] [194] and articles report the responses of biological matter to LFEMF [195]-[203]. These observations realize the entropy change (structural and chemical alterations), which due to the energy absorption, are clearly thermal, but the temperature is only a condition and does not change during the process [204].

The strength of electric field $\Xi(t)$ determines the energy delivery by the electromagnetic energy supplies, and determines the *SAR* in the media of ρ density and σ conductivity (assuming homogeneous target):

$$SAR(t) = \frac{\sigma}{2\rho}\Xi(t)^2\left[\frac{\mathrm{W}}{\mathrm{kg}}\right] \tag{61}$$

Note, the σ thermal conductivity varies non-linearly by temperature [205]. Radiating the homogeneous resistive media with R resistance by P power, and

the thickness of the target being d, we may calculate the $\Xi(t)$ field:

$$\Xi(t)=\frac{\sqrt{R\cdot P}}{d}\left[\frac{\mathrm{V}}{\mathrm{m}}\right] \tag{62}$$

If the energy delivery is sinusoidal, the average of the $\langle\Xi\rangle=\frac{\Xi}{\sqrt{2}}$, so the effective electric field is:

$$\Xi_{eff}(t)=\frac{\sqrt{R\cdot P}}{d\sqrt{2}} \tag{63}$$

when the target resistance is $R=50\,\Omega$, and the applied power is $P=150\ \mathrm{W}$, and $\sigma=0.75\ \mathrm{S/m}=1/\Omega\cdot\mathrm{m}$, the SAR from (61) and (62) is:

$$SAR(t)=\frac{\sigma}{2\rho}\frac{R\cdot P}{d}\cong 45\left[\frac{\mathrm{W}}{\mathrm{kg}}\right] \tag{64) (65}$$

The provided energy inversely depends on the mass of the target and linearly by the duration of the SAR. For example, the energy in ablation techniques to gain high temperature needs extremely high SAR (in the range of 10 - 100 kW/kg [206]), but it targets only a relatively small mass, so the absorbed energy is small. Local hyperthermia with isothermal intent uses a relatively large SAR compared to the selective method, to heat the mass as homogeneously as possible. However, these treatments can create unwanted hot-spots [207] depending on the technical realization and the actual conditions of the patient, causing very frequent complaints during the treatment [208].

In heterogenic matter, when we select the absorption target inside the volume, and the mass ratio of the selected mass m to the total M is ξ, the SAR concentrates on the selected part with a value of $\xi=\frac{m}{M}$ higher. So when nanoparticles (NPs) are chosen there, and its concentration is a 50 mg mass in 1 kg, the corresponding SAR in our numerical example (65) is $SAR_{nano}\cong 1.8\times10^{5}\frac{\mathrm{W}}{\mathrm{kg}}=180\frac{\mathrm{kW}}{\mathrm{kg}}$, and when the energy pump is sinusoidally periodic, according to (63) it becomes halved: 90 kW/kg.

Usually, the SAR value in nano-heating is even higher, ranging from 100 to 500 kW/kg [209]. These values are 1000 times higher than local hyperthermia uses but correspond well with the absorbed power in a nano-selective heating solution of membrane rafts.

The mEHT method could be used to heat injected artificial nanoparticles together with exciting the intrinsic membrane rafts. When injecting gold nanoparticles in the tissue the energy absorption is focused on both nano-centres, and the temperature grows by the diffuse heating from these [210]. However, the apoptotic cell-distortion, which is the hallmark of mEHT action, was decreased, probably because of the sharing of the energy between the membrane rafts and the gold nanoparticles; however, the heating was active in both situations.

The selective heating of mEHT uses the membrane's peculiarities for the excitation of the transmembrane proteins by energy absorption of the chosen cells. The absorbed energy at the membrane sharply depends on the electric field conditions in the membrane and its immediate vicinity. The double phospholipid membrane structure modifies the applied electric field. The temperature gradient is one of the driving forces of the signal propagation that starts at the outer membrane of the cell as extrinsic excitation. The excitation requires energy absorption and changes the molecular structure, involving the bound water. The effects cause thermal changes, but not in a temperature-dependent manner [128] [211]. The action is like a first-order phase transition with latent energy exchange at constant (transition) temperature.

The absorbed bound water on the membrane has an important role in the *SAR* and electric field distribution [176]. The modification distinguishes the intra- and extracellular electrolytes and the membrane itself, as well as the outer and inner sides of the membrane water-absorption layer [176]; see **Figure 26**.

Heating of the transmembrane protein clusters (rafts) shows different patterns than in the phospholipid membrane [182]. The water bound to the protein increases the altogether otherwise high average dielectric constant of the raft [212]. A precise model calculation [182] shows the electric loss density jump on the raft (**Figure 27**) with a rapid change on the membrane surfaces on both sides. Two calculations were made: in the homogenous approach the two sides of the raft

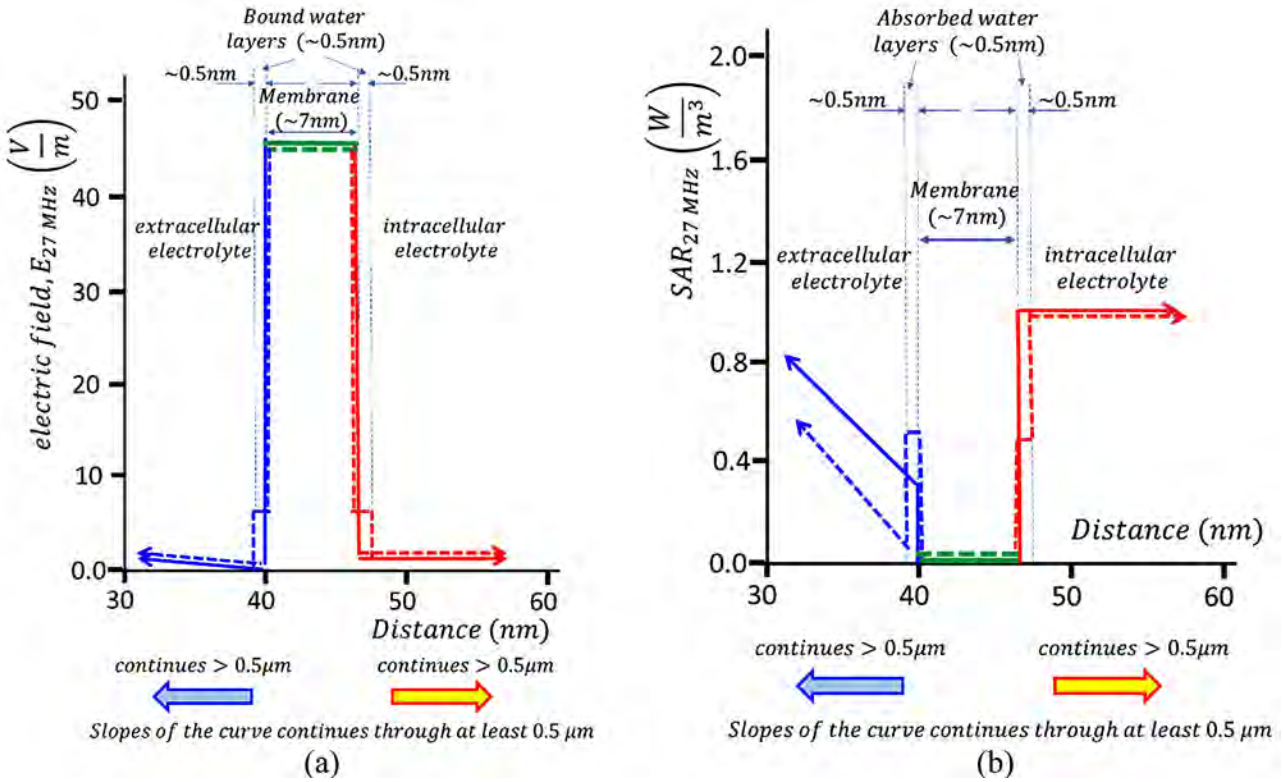

Figure 26. Comparison of the free membrane (solid lines) and membrane-bounded water (dashed line) electric field (a) and the *SAR* (b) at 27 MHz in spherical cell-model (It is modified to same scales from [176]).

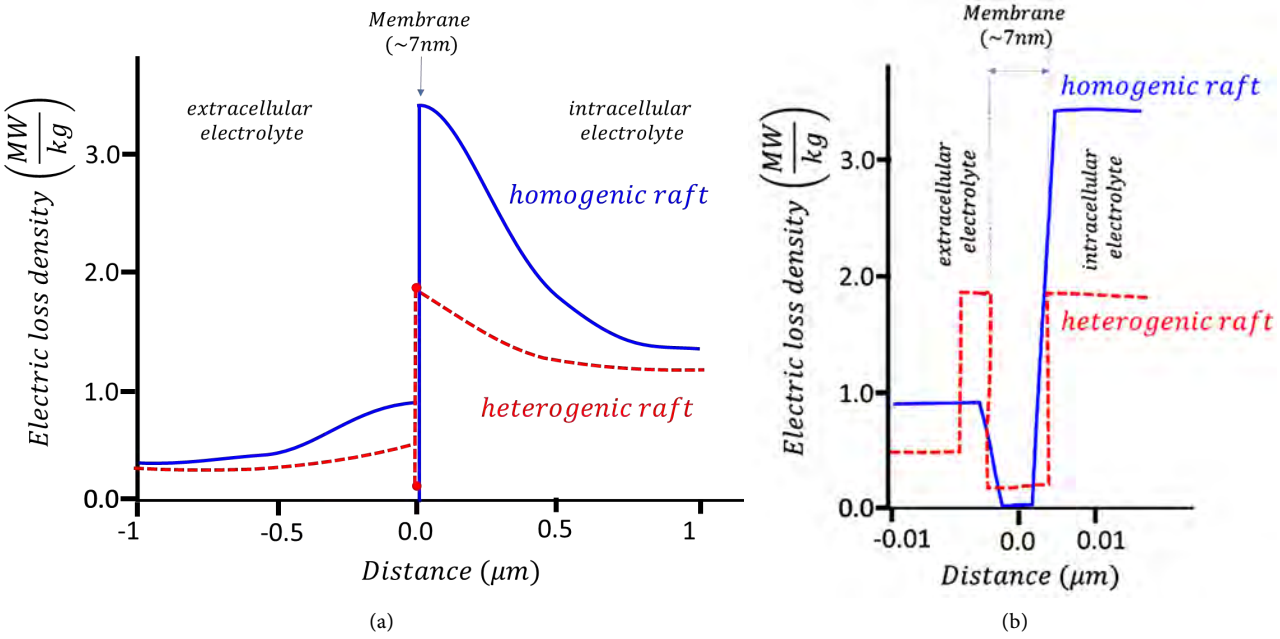

Figure 27. The electric energy loss density near the membrane of the cell in a spot of the raft under homogenous (solid line) and complex heterogenic (dashed line) assumptions: (a) The environment of the membrane; (b) Enlarged membrane area.

are identical, while in the complex, heterogenic one, the outer side has higher conductivity due to the difference of the electrolyte composition of the cytoplasm and the extracellular matrix (ECM), and the inner part has a lower dielectric constant, due to the complex connections inside the cell. The energy loss density is higher in the ECM.

The calculation used $f = 13.56$ MHz frequency and assumed $E_{13.56\,\mathrm{MHz}} = 1.1\times10^{7}\,\frac{\mathrm{V}}{\mathrm{m}} = 11\frac{\mathrm{mV}}{\mathrm{nm}}$, consequently having 55 mV membrane potential in the thickness of $d_{membrane} = 5$ nm. This potential is lower than the healthy cell usually has, but the malignancy lowers the membrane potential in most cases [213]. The heterogenic complexity decreases the jump of electric loss density, which is clearly followed by the local *SAR* (**Figure 28**).

The temperature development on the surface of the membrane is the same on both sides; but macroscopically (distant from the surface), the temperature is lower in the ECM than in the cytoplasm (**Figure 29**).

The temperature of the rafts affects the ECM in its immediate vicinity only. A similar size gold nanoparticle with radius $r_n = 30$ nm, absorbing $I_0 = 10^4\,\frac{\mathrm{W}}{\mathrm{m}^2}$ energy flux, was heated up by 4˚C in surrounding water, and at a distance of 70 nm from its surface, the gain of temperature practically vanished [214]. This rapid disappearance of the temperature in the vicinity of the nanoparticle supports the approximation in which we ignored the diffusion part of the Pennes equation, to simplify its solution. This approach is valid in nanoscopic energy-absorption only, which is realized in the mEHT too.

The excitation of the rafts needs extra energy, and structural changes happen,

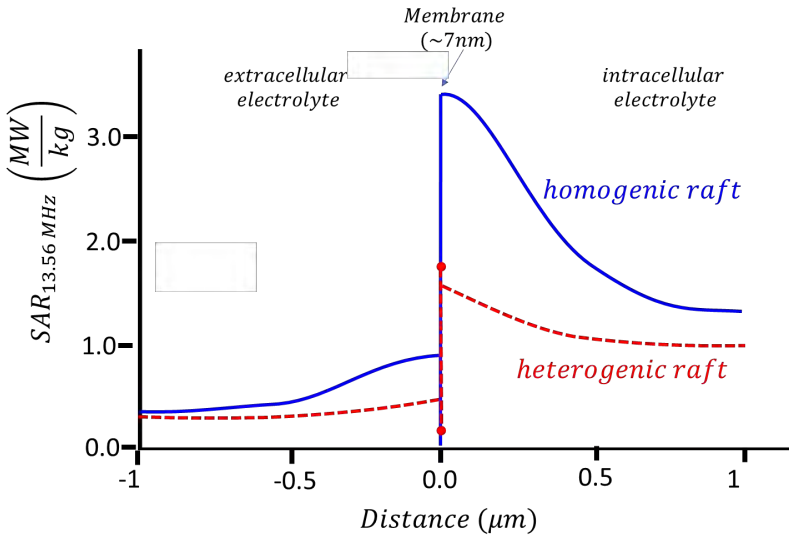

Figure 28. The provided *SAR* to the membrane area, in a spot of the raft under homogenous (solid line) and complex heterogenic (dashed line) assumptions.

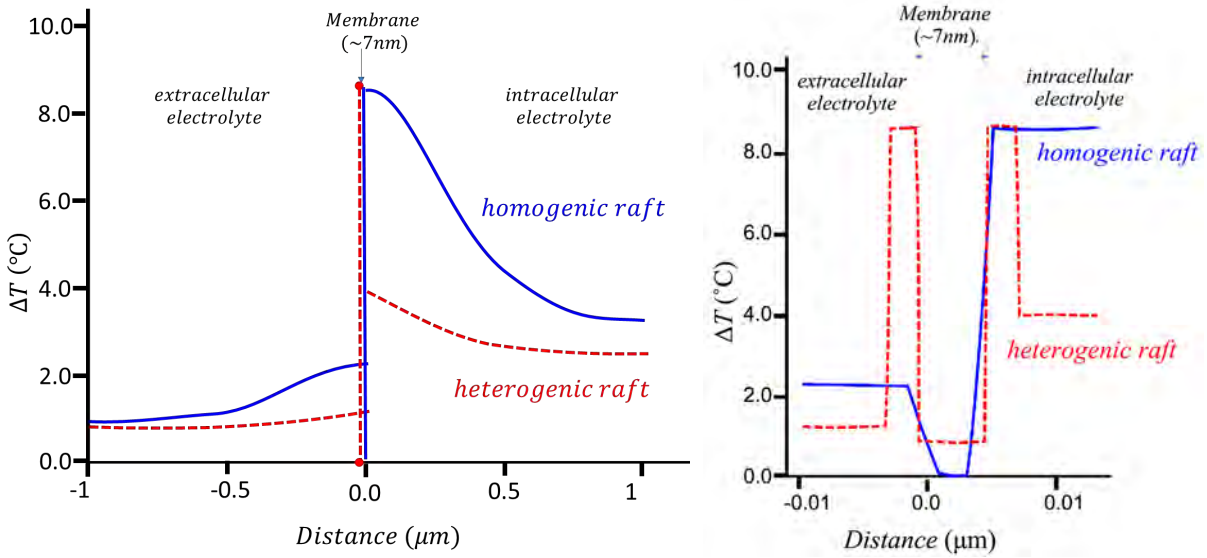

Figure 29. The developed temperature in a spot of the raft under homogenous (solid line) and complex heterogenic (dashed line) assumptions: (a) The environment of the membrane; (b) Enlarged membrane area.

which rearranges the giant membrane vehicles [215] and could modify the cell membrane [216]. The membrane phase transition can be modelled experimentally too, when the Arrhenius dependence breaks in both the resistivity and capacity parts of the lipid bilayer [217] (**Figure 30**). This again needs a local, microscopic increase in the absorbed energy, which appears microscopically.

The energy absorption of membrane rafts realizes heterogenic energy absorption, which follows the natural heterogeneities of the living matter. While the homogeneous concept intensifies the quick physiological regulation, the heterogenic selection has less strength to trigger the immediate feedback of regulation

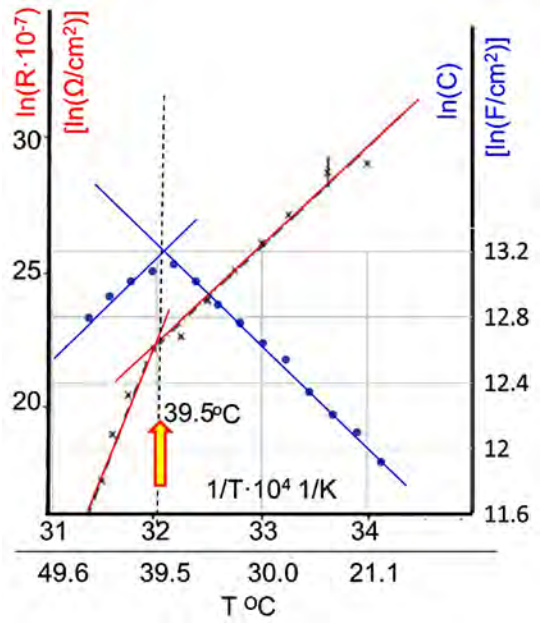

Figure 30. Arrhenius-like plots of the resistance and capacity of the membrane. It shows a phase transition at the temperature of 39.5˚C (● The capacitive x the resistive plot).

mechanisms. The physiological reaction appears later when the small heated substances heat up their environment, attracting the reaction of the general control. The temperature development in the microscopic range has many similarities with the macroscopic pattern but has a certain difference in the absorbed *SAR* (**Figure 31**). The absorbed *SAR* transfers one state to the other one, and the change of temperature is a "side effect": the excess part of the constant systemic *SAR* heats up. The spread of heat energy by time keeps the energy-replacement macroscopic, and gradually less energy will be selectively taken by the rafts, which constitute only a minimal fraction of the total mass of the tumour. There are two possible phase transitions that happen: one is for the chemical changes to produce signals and its structural consequences; the other one is the phase transition of the lipid membrane. Their temperatures are denoted by T_{ch} and T_{mem}, respectively. Both transitions are temperature-dependent, so when the raft does not heat up to the transition temperatures, these will not occur. When the transition happens, the temperature remains constant until it finishes. Afterwards, the temperature increases as usual until the *SAR* switches off. When the rafts absorb the constant average, which heats the entire mass, its temperature will be equal to its environment. The selection disappears due to the homeostatic equilibrium. However, in this state, the energy-absorption in the target acts only to replace the energy being carried away by heat-exchange with the environment of the target and also the environmental conditions of the human body.

The constant *SAR* is macroscopic; the active absorption at the microscopic level is different, being deducted from the average *SAR*, and the remaining power heating the lesion, as is shown in a hypothetical situation in **Figure 31**. The *SAR* value which is required to maintain a chosen temperature changes. The

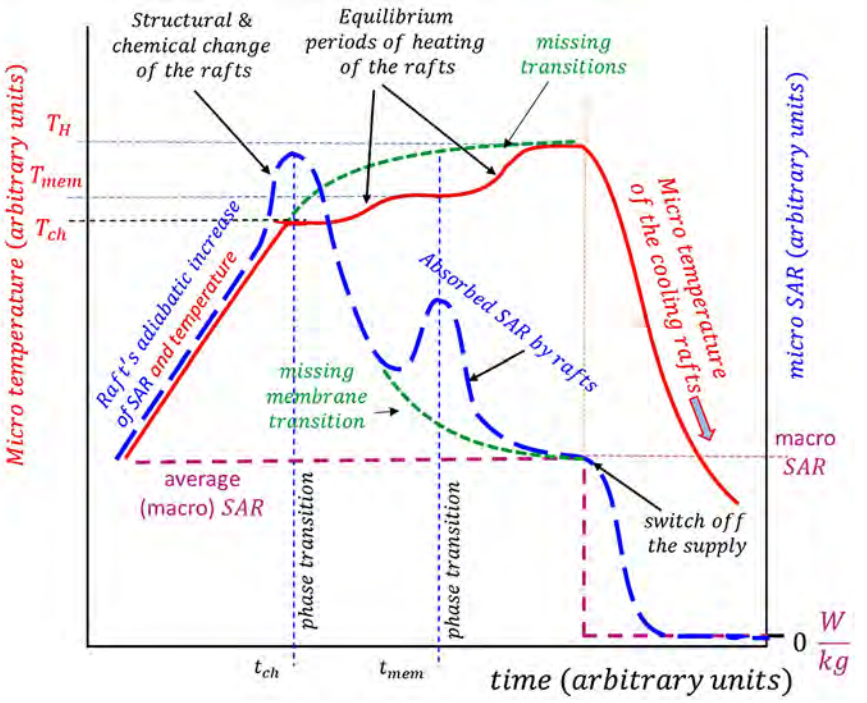

Figure 31. The temperature development and the *SAR* in the microscopic range (For explanation, see the text).

continuously growing temperature reaches definite values at which the energy requirement is higher than the general adiabatic need, as we showed by time development in Figure 31. The points at which the required micro (*mSAR*) changes, in order to energize the micro processes, are: the chemical phase transition T_{ch}, the membrane phase transition T_{mem} and the switching off of the supply after reaching the T_H homeostatic equilibrium, Figure 31. The first, chemical phase transitions, modify the microscopic energy consumption through chemical processes (signal excitation, signal transduction, protein structural changes), and usually we do not take the temperature so high as that at which the membrane phase transition happens (>42˚C). The change of *mSAR* vs temperature development shows a double peak pattern when the temperature goes over 42˚C, and afterward, the temperature grows directly with the constant average *SAR* in the target (Figure 32; it becomes a homogenous situation, the rafts having the same average *SAR* as the wider environment, which is in thermal equilibrium. The system temperature grows until reaching the homeostatic point and remains at this temperature until the switching off of the *SAR*. This is the stage at which the system has constant temperature due to the constant *SAR* replacement of lost energy.

Changes of *mSAR* by temperature depend on the demand for energy in the studied region. This changes not only with the phase transitions but also due to the homeostatic mechanisms, and in the end, the raft is heated in the same way as its environment.

Understanding these heating processes, the optimal strategy is to keep the growth

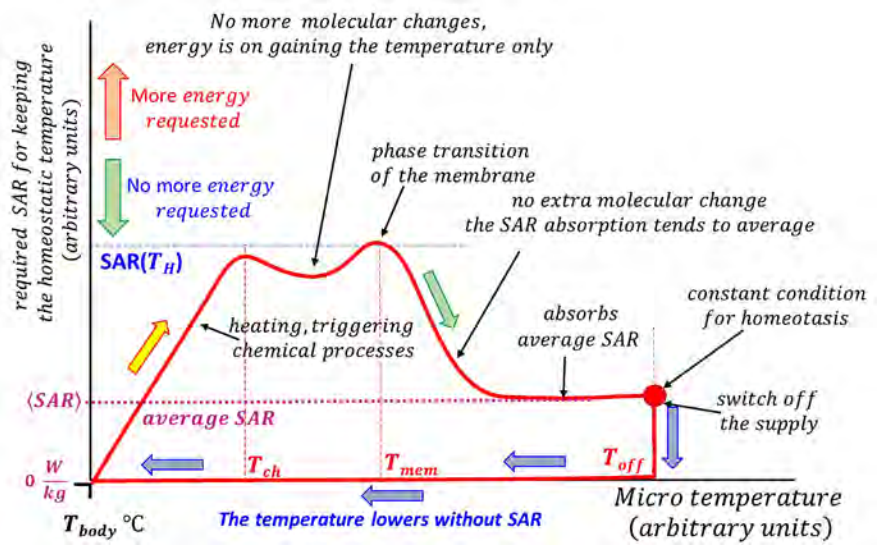

Figure 32. The required *SAR* values vs temperature in the micro-region of selectively heated rafts. The red dot before the switching off of the *SAR* represents the equilibrium when both the *SAR* and the temperature are constant. The provided absorbed energy is only replacing the loss by cooling to the environment.

of temperature continuous, so to maintain the condition where $\frac{\Delta T}{\Delta t}=\frac{1}{c}SAR$. The well-developed treatment protocol makes use of step-up heating when the linear $\frac{\Delta T}{\Delta t}$ slope dominates (**Figure 33**).

When the temperature development deviates from the slope, going to be stationary another so called constant perfusion rate model could be introduced, when the Pennes' Equation (11) reduced to:

$$\rho_h c_h \frac{\partial T}{\partial t}=\rho_h SAR-c_b\rho_b w_b\left(T\right)\left(\Delta T\right) \tag{66}$$

The solution of (66):

$$\Delta T=\frac{\rho_h SAR}{c_b\rho_b w_b\left(T\right)}\left(1-\mathrm{e}^{-\left(\frac{t}{\tau_{cp}}\right)}\right) \tag{67}$$

where

$$\tau_{cp}=\frac{c_h\rho_h}{c_b\rho_b w_b\left(T\right)} \tag{68}$$

Is the time-constant of the constant perfusion model, and $\tau_{cp}\cong t_0$ when t is large, corresponding with the stationery solution of (57). Using realistic parameters we get $\tau_{cp}\cong 7$ min. So the temperature rise will be different, **Figure 34**.

In the case of gradual step-up heating the simplified Pennes equation:

$$\begin{aligned}&\rho c\frac{\partial T}{\partial t}+c_b\rho_b w_b\left(T-T_b\right)=p\left(t\right),\rho c\cong c_b\rho_b,\\&p\left(t\right)=p_0\left(H_1\left(t\right)+H_1\left(t-\Theta\right)+H_1\left(t-2\Theta\right)+\cdots+H_1\left(t-n\Theta\right)\right)\end{aligned} \tag{69}$$

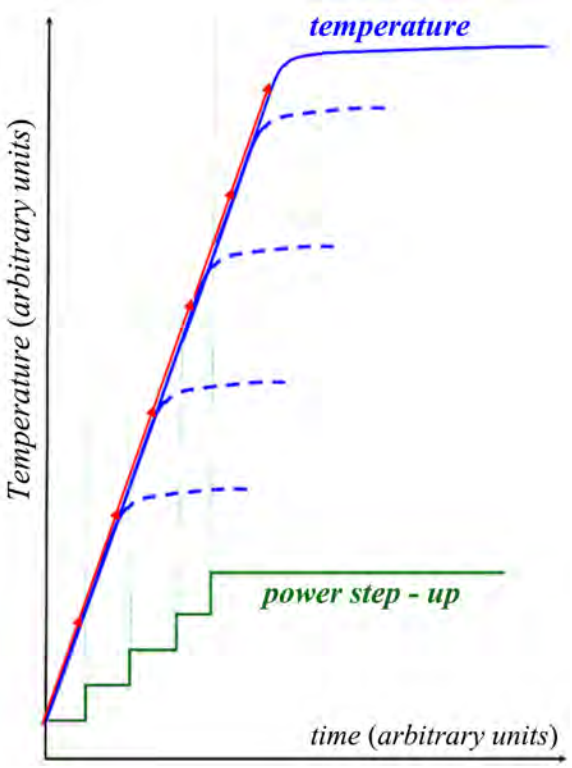

Figure 33. The temperature development by the step-up in the time period, when the curve is in the quasi-adiabatic line.

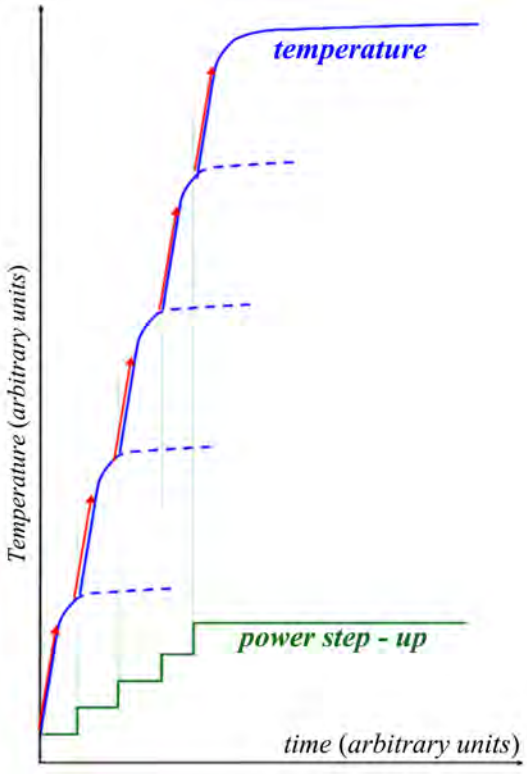

Figure 34. The temperature development by the step-up in the period out of the constant perfusion model, Note, at the end the temperature could grow higher than in Figure 33.

where $H_1(t)$ is the Heaviside unit-jump function, p_0 is the jump of *SAR* (assumed equal tranches!) and Θ is the time between the two jumps on.

So, we get:

$$\frac{\partial \Delta T}{\partial t}+\frac{1}{\tau}\Delta T=\frac{p(t)}{\rho c},\qquad \tau=w_b^{-1} \tag{70}$$

Using Laplace transformation:

$$\Delta T(s)=\frac{\tau}{\rho c}\frac{1}{1+s\tau}p(s),\qquad p(s)=p_0\frac{1}{s}\left(1+\mathrm{e}^{-s\Theta}+\mathrm{e}^{-s2\Theta}+\cdots+\mathrm{e}^{-sn\Theta}\right) \tag{71}$$

We get by inverse Laplace transformation the time-function of the temperature rise:

$$\Delta T(t)=\frac{\tau}{\rho c}p_0\left[\left(1-\mathrm{e}^{-\frac{t}{\tau}}\right)H_1(t)+\left(1-\mathrm{e}^{-\frac{t-\Theta}{\tau}}\right)H_1(t-\Theta)+\left(1-\mathrm{e}^{-\frac{t-2\Theta}{\tau}}\right)H_1(t-2\Theta)+\cdots+\left(1-\mathrm{e}^{-\frac{t-n\Theta}{\tau}}\right)H_1(t-n\Theta)\right] \tag{72}$$

Note, $p_0=SAR$, in simple one-step heating, like it was used in (54). This is physically simple: in every Θ time a new exponential function starts and added to the previous time-function Figure 35.

The time-derivative function of (72) is:

$$\frac{\mathrm{d}\Delta T}{\mathrm{d}t}=\frac{p_0}{\rho c}\left[\mathrm{e}^{-\frac{t}{\tau}}H_1(t)+\mathrm{e}^{-\frac{t-\Theta}{\tau}}H_1(t-\Theta)+\mathrm{e}^{-\frac{t-2\Theta}{\tau}}H_1(t-2\Theta)+\cdots+\mathrm{e}^{-\frac{t-n\Theta}{\tau}}H_1(t-n\Theta)\right] \tag{73}$$

The right-side derivatives of the time-dependent temperature of (72) show the newly started targeting:

$$\left.\frac{\mathrm{d}\Delta T}{\mathrm{d}t}\right|_{t=+0}=\frac{p_0}{\rho c},\ \left.\frac{\mathrm{d}\Delta T}{\mathrm{d}t}\right|_{t\to+\Theta}=\frac{p_0}{\rho c}\left(1+\mathrm{e}^{-\frac{\Theta}{\tau}}\right),\cdots,\ \left.\frac{\mathrm{d}\Delta T}{\mathrm{d}t}\right|_{t\to+n\Theta}=\frac{p_0}{\rho c}\left(1+\mathrm{e}^{-\frac{\Theta}{\tau}}+\mathrm{e}^{-\frac{2\Theta}{\tau}}+\cdots+\mathrm{e}^{-\frac{n\Theta}{\tau}}\right) \tag{74}$$

It is simply the identical restart of the SAR process, when the time Θ is longer than the τ blood-perfusion time-constant. In this case all the jumps could be described independently. Using the practical units in physiology:

$$\left.\frac{\Delta T}{t}\right|_{t=0}=\frac{\tau}{\rho c}p_0\left(1-\mathrm{e}^{-\frac{t}{\tau}}\right)\cong\frac{p_0}{\rho c}$$
$$\text{in practical units}:\left.\frac{\Delta T}{t}\right|_{t=0}\left[C^0/\min[]\frac{SAR[\mathrm{W/kg}]}{c}\frac{SAR[\mathrm{W/kg}]}{67}\right] \tag{75}$$

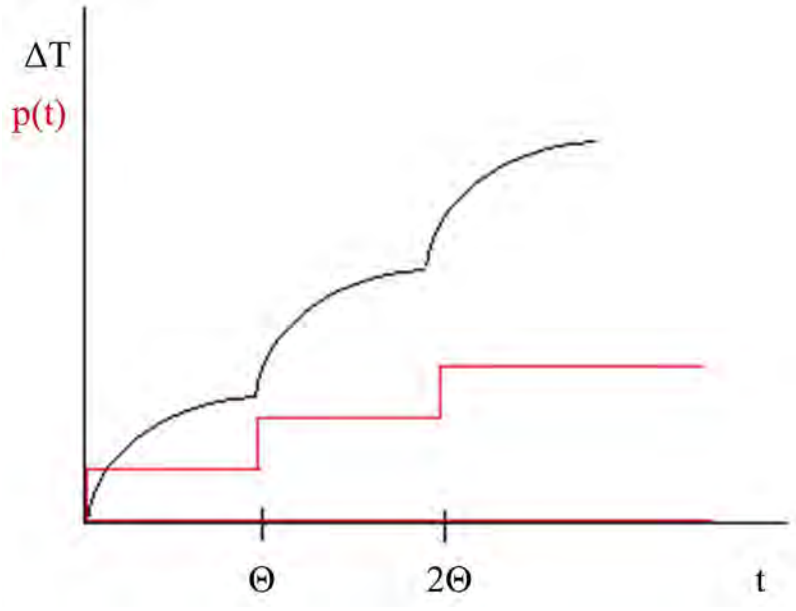

Figure 35. The time-function of temperature in case of step-up jumps of *SAR*.

with the above calculated (75).

When the incident power is terminated, the blood-perfusion starts to cool the target (clearance of temperature). This could be described by the Pennes equation too:

$$\frac{\partial\left(T-T_b\right)}{\partial t}+\frac{1}{\tau}\left(T-T_b\right)=0, \qquad \tau=w_b^{-1} \tag{76}$$

Its solution is:

$$\Delta T\left(t\right)=\left(T-T_b\right)=\frac{\tau}{\rho c}p_0\mathrm{e}^{-\frac{t}{\tau}}, \tag{77}$$

From $\Delta T\left(t\right)$ function the τ blood-perfusion time-constant could be determined, and so we get w_b too by (57) and (70). The clearance temperature (the speed of cooling) is:

$$\left.\frac{\mathrm{d}\Delta T}{\mathrm{d}t}\right|_{t=0}=-\frac{p_0}{\rho c} \tag{78}$$

which is in its absolute value identical with (54) (after stationary heating, and so the target is in thermal-equilibrium). Using again the physiology units, we get:

$$\left.\frac{\mathrm{d}\Delta T}{\mathrm{d}t}\right|_{t=0}\left[C^0/\min[]\frac{SAR\left[\mathrm{W/kg}\right]}{67}\right] \tag{79}$$

The results have to be generalized, recognizing, that the living target changes during the heating in its multiple parameters, including the thermal and the electrical ones. This changes the blood-perfusion as well as the complete temperature rise, despite the constant power provided, the SAR will change too. Due to this instead of (72) we use

$$\Delta T(t)=\frac{1}{\rho c}\left[\tau_0 p_0\left(1-\mathrm{e}^{-\frac{t}{\tau}}\right)H_1(t)+\tau_1 p_1\left(1-\mathrm{e}^{-\frac{t-\Theta}{\tau}}\right)H_1(t-\Theta)\right.$$
$$+\tau_2 p_2\left(1-\mathrm{e}^{-\frac{t-2\Theta}{\tau}}\right)H_1(t-2\Theta)+\cdots \tag{80}$$
$$\left.+\tau_n p_n\left(1-\mathrm{e}^{-\frac{t-n\Theta}{\tau}}\right)H_1(t-n\Theta)\right]$$

and consequently instead of (73):

$$\frac{\mathrm{d}\Delta T}{\mathrm{d}t}=\frac{1}{\rho c}\left[p_0\mathrm{e}^{-\frac{t}{\tau}}H_1(t)+p_1\mathrm{e}^{-\frac{t-\Theta}{\tau}}H_1(t-\Theta)\right.$$
$$\left.+p_2\mathrm{e}^{-\frac{t-2\Theta}{\tau}}H_1(t-2\Theta)+\cdots+p_n\mathrm{e}^{-\frac{t-n\Theta}{\tau}}H_1(t-n\Theta)\right] \tag{81}$$

The right derivatives of the curve in (81):

$$\left.\frac{\mathrm{d}\Delta T}{\mathrm{d}t}\right|_{t=+0}=\frac{p_0}{\rho c},\left.\frac{\mathrm{d}\Delta T}{\mathrm{d}t}\right|_{t\to+\Theta}=\frac{p_1}{\rho c}\left(1+\mathrm{e}^{-\frac{\Theta}{\tau_0}}\right),\cdots,$$
$$\left.\frac{\mathrm{d}\Delta T}{\mathrm{d}t}\right|_{t\to+n\Theta}=\frac{p_0}{\rho c}\left(1+\mathrm{e}^{-\frac{\Theta}{\tau_0}}+\mathrm{e}^{-\frac{2\Theta}{\tau_1}}+\cdots+\mathrm{e}^{-\frac{n\Theta}{\tau_{n-1}}}\right) \tag{82}$$

And again, when the switching time Θ is much longer the largest blood-perfusion time-constant, than we may use again the approximation (75):

$$\left.\frac{\mathrm{d}\Delta T}{\mathrm{d}t}\right|_{t=+0,\cdots,+n\Theta}\left[C^0/\min[]\frac{SAR_0[\mathrm{W/kg}]}{67}\right]$$
$$\left.\frac{\mathrm{d}\Delta T}{\mathrm{d}t}\right|_{t=+\Theta}\left[C^0/\min[]\frac{SAR_1[\mathrm{W/kg}]}{67}\right] \tag{83}$$
$$\left.\frac{\mathrm{d}\Delta T}{\mathrm{d}t}\right|_{+n\Theta}\left[C^0/\min[]\frac{SAR_n[\mathrm{W/kg}]}{67}\right]$$

The realization of the strategy of blocking the development of thermal spreading could be more effective when the linear period of $\frac{\Delta T}{\Delta t}$ is carefully managed and the system cooled down before the spread of the heat starts. The concept could be completed by the cutting of the heating curve, which could be done at various points of the temperature development (Figure 36).

The straight-line sided triangle at the early cut looks the most controllable situation, stopping the heating at the end-point when the linear slope fits. Technically the appropriate pulsing of the SAR follows the optimizing rule well (Figure 37). This protocol does not change, or changes by only a little, the overall temperature, so all the energy is concentrated on the selected rafts.

Note, the selective, non-isothermal energy-absorption is similar to the ionizing radiation concept when the selection is directed at the breaking of DNA. The heat and temperature gain which they produce during treatment are adverse effects, and the protocols try to avoid them. The dose in the ionizing radiation is

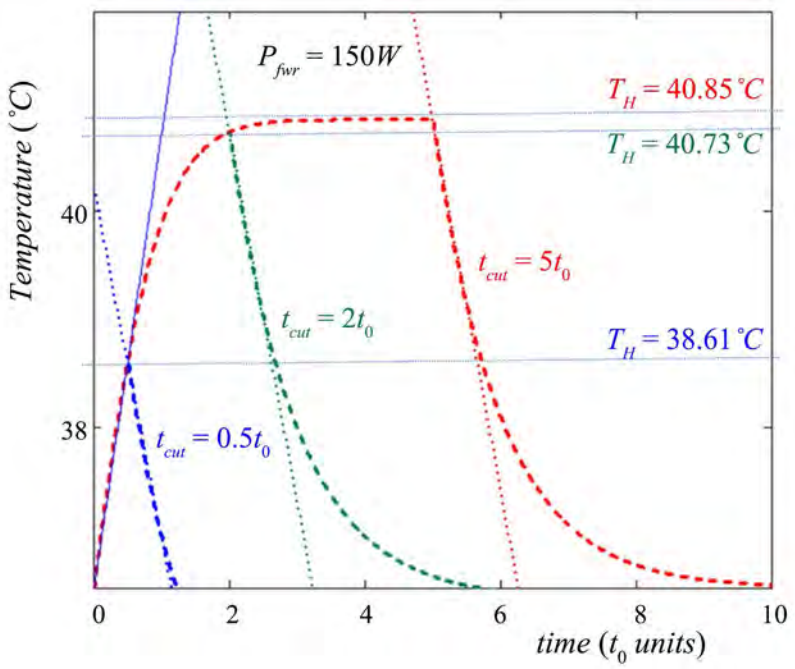

Figure 36. The temperature development terminated in different stages of the process.

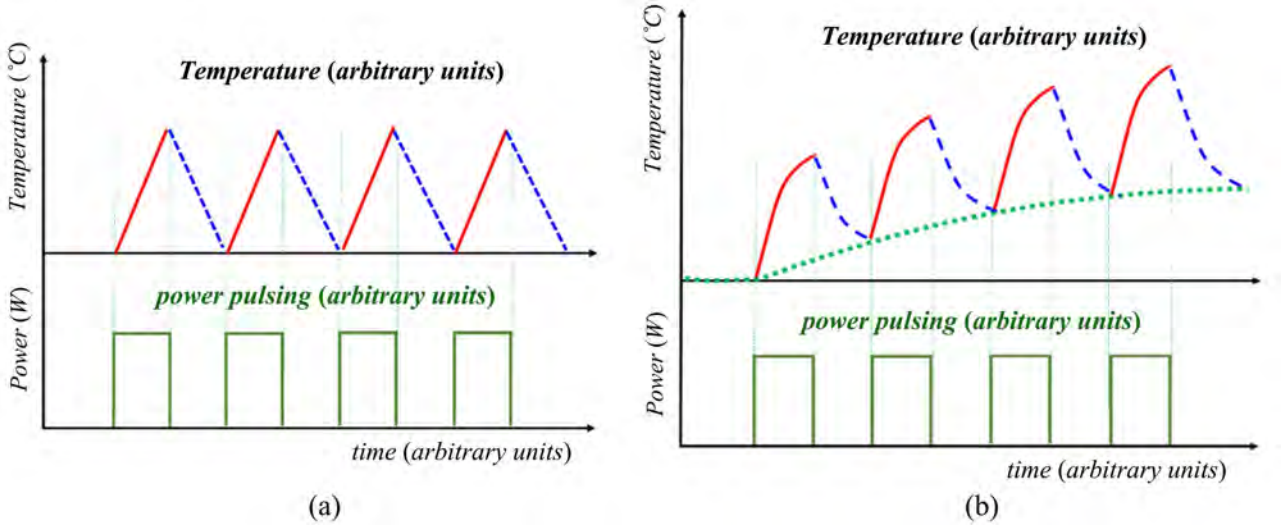

Figure 37. Temperature development by the appropriately pulsed power, providing step-up: (a) Terminated before the non-linear period starts; (b) Terminated after the non-linear period starts.

the Gray Gy = J/kg, which is the measure of the absorbed energy, by (3), and in time-dependent power by (4). The dose of the radiotherapy treatment-cycle is the sum of the fractional doses in the process. We may introduce the same in hyperthermia with regard to the absorbed energy:

$$E_{dose}\left(t_{\Sigma}\right) = \sum_{i=1}^{N} \int_{0}^{t_i} SAR(\tau)\,\mathrm{d}\tau \tag{84}$$

where N is the number of treatments in the actual cycle, t_i is the time of the i-th treatment and

$$t_{\Sigma} = t_1 + t_2 + \cdots + t_{N-1} + t_N = \sum_{i=1}^{N} t_i \tag{85}$$

is the entire treatment time in the cycle.

The evaluation of $SAR(\tau)$ in a selective mode of hyperthermia counts the energy absorbed in the target irrespective of the kind of source, so the specific energy unit Gy could be applied in the non-ionizing radiation too. The energy which is provided by ionizing radiation (IR) triggers biological mechanisms, which are mostly the rupturing of DNA, while the desired effects are different in non-ionizing applications (nIR). We may observe contrary interests in using the absorbed energy in these therapies [3]. In the ionizing strategy, the distortion of the DNA strands is the goal, and the heat-production during this process is an adverse effect. In nIR hyperthermia, it is the other way round, and the heat production becomes the goal of the treatment. While the IR treatment is of short duration, the nIR is significantly longer, and while the physiological control mechanisms have no role in IR, these have an important role in nIR applications. Both treatments are electromagnetic, but IR has a frequency a few billion times higher and also has much shorter duration of treatment than nIR.

5. Verification

The preclinical verification of the dose and its temperature dependence shows the practical applicability of the above model-calculation. Phantom experiments [218], and in vitro cell-culture measurements show the apoptotic efficacy [219] [220] of mEHT, and the temperature mapping gives also a hint, that the above considerations are realistic [221]. The pulsed power application is measured [222] and verifies the advantage of the increased efficacy of such heating method [223]. The clinical applications have a well-defined protocol [224] and guideline [225] with the step-up heating requirements, and the clinical results validate the usage of the step-up heating model [226].

The present considerations are valid for solid tumours, where the Pennes-equation is effective. The selective activation of the haematological cancers is in progress.

6. Conclusion

Considering the homeostatic self-similarity, we have shown a stochastic heuristic solution of the Pennes equation and its applicability in hyperthermia treatments in oncology. Weibull parametric distribution with satisfactory refinement can solve the problem of the description of the heating of the body, without the complications involved in solving the Pennes equation. This solution is stochastic, having a probability distribution which fits much more to the dynamic changes in the living objects, and eliminates the problem of the deterministic behaviour of the Pennes approach. The introduced selective heating allows focusing upon the malignant cells using the thermal and bioelectromagnetic heterogeneity of the tumorous lesions. The solution allows the introduction of a

protocol that most optimally uses the provided energy for molecular changes, destroying the malignant cells without a noticeable effect on their healthy counterparts. The present considerations are valid for solid tumors, where the Pennes-equation is effective. The selective activation of the haematological cancers is in progress.

Conflicts of Interest

The authors declare no conflicts of interest regarding the publication of this paper.

References

[1] Vaupel, P. and Hammersen, F. (1982) Mikrozirkulation in malignen Tumoren. Karger, Basel.

[2] Vaupel, P. (1990) Pathophysiological Mechanism of Hyperthermia in Cancer Therapy. In: Gautherie, M., Ed., *Methods of Hyperthermia Control*, *Biological Basis of Oncologic Thermotherapy*. *Clinical Thermology* (*Subseries Thermotherapy*), Springer Verlag, Berlin, Heidelberg, 73-134. https://doi.org/10.1007/978-3-642-74939-1_2

[3] Szasz, A. (2019) Thermal and Nonthermal Effects of Radiofrequency on Living State and Applications as an Adjuvant with Radiation Therapy. *Journal of Radiation and Cancer Research*, **10**, 1-17. https://doi.org/10.4103/jrcr.jrcr_25_18

[4] Vaupel, P., Kallinowski, F. and Okunieff, P. (1989) Blood Flow, Oxygen and Nutrient Supply, and Microenvironment of Human Tumours: A Review. *Cancer Research*, **49**, 6449-6465.

[5] Song, C.W., Choi, I.B., Nah, B.S., Sahu, S.K. and Osborn, J.L. (1995) Microvasculature and Perfusion in Normal Tissues and Tumours. In: Seegenschmiedt, M.H., Fessenden, P. and Vernon, C.C., Eds., *Thermoradiometry and Thermochemotherapy*, Vol. 1, Springer-Verlag, Berlin Heidelberg, 139-156. https://doi.org/10.1007/978-3-642-57858-8_7

[6] Takana, Y. (2001) Thermal Responses of Microcirculation and Modification of Tumour BF in Treating the Tumours. In: Kosaka, M., Sugahara, T., Schmidt, K.L. and Simon, E., Eds., *Theoretical and Experimental Basis of Hyperthermia*. *Thermotherapy for Neoplasia*, *Inflammation*, *and Pain*, Springer Verlag, Tokyo, 408-419. https://doi.org/10.1007/978-4-431-67035-3_45

[7] Song, C.W., Park, H. and Griffin, R.J. (2001) Theoretical and Experimental Basis of Hyperthermia. In: Kosaka, M., Sugahara, T., Schmidt, K.L., *et al.*, Eds., *Thermotherapy for Neoplasia*, *Inflammation*, *and Pain*, Springer Verlag, Tokyo, 394-407. https://doi.org/10.1007/978-4-431-67035-3_44

[8] Wu, M., Frieboes, H.B., McDougall, S.R., *et al.* (2013) The Effect of Interstitial Pressure on Tumor Growth: Coupling with the Blood and Lymphatic Vascular Systems. *Journal of Theoretical Biology*, **320**, 131-151. https://doi.org/10.1016/j.jtbi.2012.11.031

[9] Song, C.W., Lokshina, A., Rhee, J.G., *et al.* (1984) Implication of BF in Hyperthermic Treatment of Tumours. *IEEE Transactions on Biomedical Engineering*, **31**, 9-16. https://doi.org/10.1109/TBME.1984.325364

[10] Jain, R.K. (1988) Determinants of Tumor Blood Flow: A Review. *Cancer Research*, **48**, 2641-2658.

[11] Song, C.W. (1984) Effect of Local Hyperthermia on Blood Flow and Microenvironment: A Review. *Cancer Research* (*Suppl.*), **44**, 4721s-4730s.

[12] Dudar, T.E. and Jain, R.K. (1984) Differential Response of Normal and Tumour Microcirculation to Hyperthermia. *Cancer Research*, **44**, 605-612.

[13] Hietanen, T., Kapanaen, M. and Kellokumpu-Legtinen, P.L. (2016) Restoring Natural Killer Cell Cytotoxicity after Hyperthermia Alone or Combined with Radiotherapy. *Anticancer Research*, **36**, 555-564.

[14] Beachy, S.H. and Repasky, E.A. (2011) Toward Establishment of Temperature Thresholds for Immunological Impact of Heat Exposure in Humans. *International Journal of Hyperthermia*, **27**, 344-352. https://doi.org/10.3109/02656736.2011.562873

[15] Jones, E., Thrall, D., Dewhirst, M.W. and Vujaskovic, Z. (2006) Prospective Thermal Dosimetry: The Key to Hyperthermia's Future. *International Journal of Hyperthermia*, **22**, 247-253. https://doi.org/10.1080/02656730600765072

[16] Fatehi, D., van der Zee, J., van der Wal, E., *et al.* (2006) Temperature Data Analysis for 22 Patients with Advanced Cervical Carcinoma Treated in Rotterdam Using Radiotherapy, Hyperthermia and Chemotherapy: A Reference Point Is Needed. *International Journal of Hyperthermia*, **22**, 353-363. https://doi.org/10.1080/02656730600715796

[17] Separeto, S.A. and Dewey, W.C. (1984) Thermal Dose Determination in Cancer Therapy. *International Journal of Radiation Oncology*, *Biology*, *Physics*, **10**, 787-800. https://doi.org/10.1016/0360-3016(84)90379-1

[18] Arrhenius, S. (1915) Quantitative Laws in Biological Chemistry. G. Bell, London. https://doi.org/10.5962/bhl.title.22817

[19] Jackson, M.B. (2006) Molecular and Cellular Biophysics. Cambridge University Press, Cambridge. https://doi.org/10.1017/CBO9780511754869

[20] Nelson, P. (2004) Biological Physics. WH Freeman and Company, New York.

[21] Perez, C.A. and Sapareto, S.A. (1984) Thermal Dose Expression in Clinical Hyperthermia and Correlation with Tumor Response/Control. *Cancer Research*, **44**, 4818s-4825s.

[22] Feo, F., Canuto, R.A. and Garcea, R. (1976) Lipid Phase Transition and Breaks in the Arrhenius Plots of Membrane-Bound Enzymes in Mitochondria from Normal Rat Liver and Hepatoma AH-130. *FEBS Letters*, **72**, 262-266. https://doi.org/10.1016/0014-5793(76)80982-9

[23] Overath, P., Schairer, H.U. and Stoffel, W. (1970) Correlation of *in Vivo* and *in Vitro* Phase Transitions of Membrane Lipids in *Escherichia coli*. *Proceedings of the National Academy of Sciences*, **67**, 606-312. https://doi.org/10.1073/pnas.67.2.606

[24] Watson, K., Bertoli, E. and Griffiths, D.E. (1975) Phase Transitions in Yeast Mithochondrial Membranes. *Biochemical Journal*, **146**, 401-407. https://doi.org/10.1042/bj1460401

[25] Dewey, W.C., Hopwood, L.E., Sapareto, S.A., *et al.* (1977) Cellular Response to Combination of Hyperthermia and Radiation. *Radiology*, **123**, 463-474. https://doi.org/10.1148/123.2.463

[26] Lindholm, C.-E. (1992) Hyperthermia and Radiotherapy. PhD Thesis, Lund University, Malmo.

[27] Hafstrom, L., Rudenstam, C.M., Blomquist, E., *et al.* (1991) Regional Hyperthermic Perfusion with Melphalan after Surgery for Recurrent Malignant Melanoma of the Extremities. Swedish Melanoma Study Group. *Journal of Clinical Oncology*, **9**,

2091-2094. https://doi.org/10.1200/JCO.1991.9.12.2091

[28] Franckena, M., Fatehi, D., de Bruijne, M., Canters, R.A.M., van Norden, Y., Mens, J.W., van Rhoon, G.C. and van der Zee, J. (2009) Hyperthermia Dose-Effect Relationship in 420 Patients with Cervical Cancer Treated with Combined Radiotherapy and Hyperthermia. *European Journal of Cancer*, **45**, 1969-1978. https://doi.org/10.1016/j.ejca.2009.03.009

[29] Ballesteros, F.J., Martinez, V.J., Luque, B., *et al.* (2018) On the Thermodynamic Origin of Metabolic Scaling. *Scientific Reports*, **8**, Article No. 1448. https://doi.org/10.1038/s41598-018-30973-x

[30] Zotin, A.I. (2010) Thermodynamic Bases of Biological Processes. Cambridge Univ. Press, Cambridge.

[31] Matay, G. and Zombory, L. (2000) Physiological Effects of Radiofrequency Radiation and Their Application for Medical Biology. Muegyetemi Kiado, Budapest, 80.

[32] Brown, J.H., West, G.B. and Enquist, B.J. (2005) Yes, West, Brown and Enquist's Model of Allometric Scaling Is Both Mathematically Correct and Biologically Relevant. *Functional Ecology*, **19**, 735-738. https://doi.org/10.1111/j.1365-2435.2005.01022.x

[33] Fristoe, T.S., Burger, J.R., Balk, M.A., *et al.* (2015) Metabolic Heat Production and Thermal Conductance Are Mass-Independent Adaptations to Thermal Environment in Birds and Mammals. *PNAS*, **112**, 15934-15939. https://doi.org/10.1073/pnas.1521662112

[34] Pennes, H.H. (1948) Analysis of Tissue and Arterial Blood Temperatures in the Resting Human Forearm. *Journal of Applied Physics*, **1**, 93-122. https://doi.org/10.1152/jappl.1948.1.2.93

[35] Deng, Z.-S. and Liu, J. (2012) Analytical Solutions to 3-D Bioheat Transfer Problems with or without Phase Change. In: *Heat Transfer Phenomena and Applications*, Intech, Rijeka, Chapter 8, 205-242. https://doi.org/10.5772/52963

[36] Giordano, M.A., Gutierrez, G. and Rinaldi, C. (2010) Fundamental Solutions to the Bioheat Equation and Their Application to Magnetic Fluid Hyperthermia. *International Journal of Hyperthermia*, **26**, 475-484.

[37] Cundin, L.X., Roach, W.P. and Millenbaugh, N. (2009) Empirical Comparison of Pennes' Bio-Heat Equation. *Proceedings of SPIE*, **7175**, 717516-717519. https://doi.org/10.1117/12.805577

[38] Lakhssassi, A., Kengne, E. and Semmaoui, H. (2010) Modified Pennes' Equation Modelling Bio-Heat Transfer in Living Tissues: Analytical and Numerical Analysis. *Natural Science*, **2**, 1375-1385. https://doi.org/10.4236/ns.2010.212168

[39] Gao, B., Langer, S. and Corry, P.M. (1995) Application of the Time-Dependent Green's Function and Fourier Transforms to the Solution of the Bioheat Equation. *International Journal of Hypertension*, **11**, 267-285. https://doi.org/10.3109/02656739509022462

[40] Van der Gaag, M.L., De Bruijne, M., Samaras, T., van der Zee, J. and Van Rhoon, G. (2006) Development of a Guideline for the Water Bolus Temperature in Superficial Hyperthermia. *International Journal of Hyperthermia*, **22**, 637-656. https://doi.org/10.1080/02656730601074409

[41] Liu, K.-C. and Tu, F.-J. (2019) Numerical Solution of a Bioheat Transfer Problem with Transient Blood Temperature. *International Journal of Computational Methods*, **16**, Article ID: 1843001. https://doi.org/10.1142/S0219876218430016

[42] (2006) IEEE C95.1. IEEE Standard for Safety Levels with Respect to Human Expo-

sure to Radio Frequency Electromagnetic Fields, 3 kHz to 300 GHz; IEEE Std C95.1-2005. IEEE, Piscataway.

[43] Ma, J., Yang, X., Sun, Y., *et al.* (2019) Thermal Damage in Three-Dimensional Vivo Bio-Tissues Induced by Moving Heat Sources in Laser Therapy. *Scientific Reports*, **9**, Article No. 10987. https://doi.org/10.1038/s41598-019-47435-7

[44] Thermal Conditions, CUErgo, Cornell University Ergonomics Web. http://ergo.human.cornell.edu/studentdownloads/DEA3500notes/Thermal/thcondnotes.html

[45] Van Haaren, P.M.A., Hulshof, M.C.C.M., Kok, H.P., *et al.* (2008) Relation between Body Size and Temperatures during Locoregional Hyperthermia of Oesophageal Cancer Patients. *International Journal of Hypertension*, **24**, 663-674. https://doi.org/10.1080/02656730802210448

[46] Giering, K., Lamprecht, I. and Minet, O. (1996) Specific Heat Capacities of Human and Animal Tissues. *Proceedings of SPIE—The International Society for Optical Engineering*, Vol. 2624, 178-188. https://doi.org/10.1117/12.229547

[47] de Greef, M. (2012) Loco-Regional Hyperthermia Treatment Planning: Optimisation under Uncertainty. Dutch Cancer Society, Amsterdam.

[48] ESHO Taskgroup Committee (1992) Treatment Planning and Modelling in Hyperthermia, a Task Group Report of the European Society for Hyperthermic Oncology. Tor Vergata, Rome.

[49] Kok, H.P., Van Haaren, P.M.A., Van de Kamer, J.B., *et al.* (2005) High-Resolution Temperature-Based Optimization for Hyperthermia Treatment Planning. *Physics in Medicine and Biology*, **50**, 3127-3141. https://doi.org/10.1088/0031-9155/50/13/011

[50] Newman, W.H., Lele, P.P. and Bowman, H.P. (1990) Limitations and Significance of Thermal Washout Data Obtained during Microwave and Ultrasound Hyperthermia. *International Journal of Hypertension*, **6**, 771-784. https://doi.org/10.3109/02656739009140824

[51] Kodera, S. and Hirata, A. (2018) Comparison of Thermal Response for RF Exposure in Human and Rat Models. *International Journal of Environmental Research and Public Health*, **15**, 2320. https://doi.org/10.3390/ijerph15102320

[52] Vincze, Gy. and Szasz, A. (2011) On the Extremum Properties of Thermodynamic Steady State in Non-Linear Systems. In: Piraján, J.C.M., Ed., *Thermodynamics—Physical Chemistry of Aqueous Systems*, IntechOpen, London, 241-316. http://www.intechopen.com/books/thermodynamics-physical-chemistry-of-aqueous-systems/on-the-extremum-properties-of-thermodynamic-steady-state-in-non-linear-systems https://doi.org/10.5772/21871

[53] Vincze, Gy. and Szasz, A. (2019) New Look at an Old Principle: An Alternative Formulation of the Theorem of Minimum Entropy Production. *Journal of Advances in Physics*, **16**, 508-517. https://doi.org/10.24297/jap.v16i1.8516

[54] Weiss, T.F. (1996) Cellular Biophysics. Transport, Vol 1. MIT Press, Cambridge.

[55] Head, J.F., Wang, F., Lipari, C.A., *et al.* (2000) The Important Role of Infrared Imaging in Breast Cancer. *IEEE Engineering in Medicine and Biology Magazine*, **19**, 52-57. https://doi.org/10.1109/51.844380

[56] Baronzio, G.F., Gramaglia, A., Baronzio, A., *et al.* (2006) Influence of Tumor Microenvironment on Thermoresponse: Biologic and Clinical Implications. In: Baronzio, G.F. and Hager, E.D., Eds., *Hyperthermia in Cancer Treatment: A Primer*, Landes Bioscience, Springer Science, New York, 62-86.

[57] Kelleher, D.K. and Vaupel, P. (2006) Vascular Effects of Localized Hyperthermia. In: Baronzio, G.F. and Hager, E.D., Eds., *Hyperthermia in Cancer Treatment: A Primer*, Landes Biosceince, Springer Science, New York, 94-104.

[58] Schwan, H.P. (1957) Electrical Properties of Tissue and Cell Suspensions. *Advances in Biological and Medical Physics*, **5**, 147-209. https://doi.org/10.1016/B978-1-4832-3111-2.50008-0

[59] Pethig, R. and Kell, D.B. (1987) The Passive Electrical Properties of Biological Systems: Their Significance in Physiology, Biophysics and Biotechnology. *Physics in Medicine and Biology*, **32**, 933-977. https://doi.org/10.1088/0031-9155/32/8/001

[60] Kurakin, A. (2011) The Self-Organizing Fractal Theory as a Universal Discovery Method: The Phenomenon of Life. *Theoretical Biology and Medical Modelling*, **8**, 4. https://doi.org/10.1186/1742-4682-8-4

[61] Walleczek, J. (2000) Self-Organized Biological Dynamics & Nonlinear Control. Cambridge University Press, Cambridge. https://doi.org/10.1017/CBO9780511535338

[62] Haken, H. (1987) Self-Organization and Information. *Physica Scripta*, **35**, 247-254. https://doi.org/10.1088/0031-8949/35/3/006

[63] Sornette, D. (2000) Chaos, Fractals, Self-Organization and Disorder: Concepts and Tools. Springer Verlag, Berlin, Los Angeles.

[64] Deering, W. and West, B.J. (1992) Fractal Physiology. *IEEE Engineering in Medicine and Biology*, **11**, 40-46. https://doi.org/10.1109/51.139035

[65] West, B.J. (1990) Fractal Physiology and Chaos in Medicine. World Scientific, Singapore, London.

[66] Kauffman, S.A. (1993) The Origins of Order: Self-Organization and Selection in Evolution. Oxford University Press, New York, Oxford. https://doi.org/10.1007/978-94-015-8054-0_8

[67] Brummer, A.B., Savage, van M. and Enquist, B.J. (2017) A General Model for Metabolic Scaling in Self-Similar Asymmetric Networks. *PLOS Computational Biology*, **13**, e1005394. https://doi.org/10.1371/journal.pcbi.1005394

[68] Ochiai, T., Nacher, J.C. and Akutsu, T. (2018) Symmetry and Dynamics in Living Organisms: The Self-Similarity Principle Governs Gene Expression Dynamics.

[69] Bassingthwaighte, J.B., Leibovitch, L.S. and West, B.J. (1994) Fractal Physiology. Oxford Univ. Press, New York, Oxford. https://doi.org/10.1007/978-1-4614-7572-9

[70] Musha, T. and Sawada, Y. (1994) Physics of the Living State. IOS Press, Amsterdam.

[71] Glazier, D.S. (2014) Metabolic Scaling in Complex Living Systems. *Systems*, **2**, 451-540. https://doi.org/10.3390/systems2040451

[72] Scheffer, M. and Nes, V.E.H. (2006) Self-Organized Similarity, the Evolutionary Emergence of Groups of Similar Species. *PNAS*, **103**, 6230-6235. https://doi.org/10.1073/pnas.0508024103

[73] West, G.B., Woodruf, W.H. and Born, J.H. (2002) Allometric Scaling of Metabolic Rate from Molecules and Mitochondria to Cells and Mammals. *Proceedings of the National Academy of Sciences of the United States of America*, **99**, 2473-2478. https://doi.org/10.1073/pnas.012579799

[74] Li, W. (1989) Spatial 1/f Spectra in Open Dynamical Systems. *Europhysics Letters*, **10**, 395-400. https://doi.org/10.1209/0295-5075/10/5/001

[75] Schlesinger, M.S. (1987) Fractal Time and 1/f Noise in Complex Systems. *Annals of the New York Academy of Sciences*, **504**, 214-228.

https://doi.org/10.1111/j.1749-6632.1987.tb48734.x

[76] Brown, J.H. and West, G.B. (2000) Scaling in Biology. Oxford University Press, Oxford.

[77] West, G.B. and Brown, J.H. (2005) The Origin of Allometric Scaling Laws in Biology from Genomes to Ecosystems: Towards a Quantitative Unifying Theory of Biological Structure and Organization. *Journal of Experimental Biology*, **208**, 1575-1592. https://doi.org/10.1242/jeb.01589

[78] Aon, M.A., Saks, V. and Schlattner, U. (2014) Systems Biology of Metabolic and Signaling Networks: Energy, Mass and Information Transfer. Springer Series in Biophysics No. 16. Springer, Berlin. https://doi.org/10.1007/978-3-642-38505-6

[79] Song, C., Havlin, S. and Makse, H.A. (2005) Self-Similarity of Complex Networks. *Letters to Nature*, **433**, 392-395. https://doi.org/10.1038/nature03248

[80] Frohlich, H. (1983) Coherence in Biology. In: Frohlich, H. and Kremer, F., Eds., *Coherent Excitations in Biological Systems*, Springer Verlag, Berlin, Heidelberg, 1-5. https://doi.org/10.1007/978-3-642-69186-7_1

[81] Frohlich, H. (1988) Biological Coherence and Response to External Stimuli. Springer Verlag, Berlin, Heidelberg. https://doi.org/10.1007/978-3-642-73309-3

[82] Camazine, S., Deneubourg, J.L., Franks, N.R., *et al.* (2003) Self-Organization in Biological Systems. Princeton Studies in Complexity. Princeton Univ. Press, Princeton, Oxford.

[83] Szasz, O., Szigeti, Gy.P. and Szasz, A. (2017) On the Self-Similarity in Biological Processes. *Open Journal of Biophysics*, **7**, 183-196. https://doi.org/10.4236/ojbiphy.2017.74014

[84] Weibull, W. (1951). A Statistical Distribution Function of Wide Applicability. *Journal of Applied Mathematics*, **18**, 293-297.

[85] Lloyd, D., Aon, M.A. and Cortassa, S. (2001) Why Homeodynamics, Not Homeostasis? *The Scientific World*, **1**, 133-145. https://doi.org/10.1100/tsw.2001.20

[86] Wang, H., Wang, Z., Li, X., *et al.* (2011) A Robust Approach Based on Weibull Distribution for Clustering Gene Expression Data. *Algorithms for Molecular Biology*, **6**, 14. https://doi.org/10.1186/1748-7188-6-14

[87] Hesse, J. and Gross, T. (2014) Self-Organized Criticality as a Fundamental Property of Neural Systems. *Frontiers in Systems Neuroscience*, **8**, 166. https://doi.org/10.3389/fnsys.2014.00166

[88] West, G.B., Brown, J.H. and Enquist, B.J. (2001) A General Model for Ontogenetic Growth. *Nature*, **413**, 628-631. https://doi.org/10.1038/35098076

[89] Pugno, N.M. (2005) On the Statistical Law of Life. https://arxiv.org/ftp/q-bio/papers/0503/0503011.pdf

[90] Sharkovsky, S. and Grab, E. (2011) Modelling Self-Similar Traffic in Networks. *RTU 52nd International Scientific Conference*, Riga, 13-15 October 2011.

[91] Avrami, M.A. (1939) Kinetics of Phase Change. I General Theory. *The Journal of Chemical Physics*, **7**, 1103.

[92] Cope, F.W. (1977) Detection of Phase Transitions and Cooperative Interactions by Avrami Analysis of Sigmoid Biological Time Curves for Muscle, Nerve, Growth, Firefly, and Infrared Phosphorescence, of Green Leaves, Melanin and Cytochrome C. *Physiological Chemistry and Physics*, **9**, 443-459.

[93] Cope, F.W. (1980) Avrami Analysis of Electrical Switching in Hydrated Melanin Suggest Dependence on a Phase Transition. *Physiological Chemistry and Physics*,

12, 537-538.

[94] May, K.A. and Solomon, J.A. (2013) Four Theorems on the Psychometric Function. *PLoS ONE*, **8**, e74815. https://doi.org/10.1371/journal.pone.0074815

[95] Szasz, O., Szigeti, G.P. and Szasz, A. (2019) The Intrinsic Self-Time of Biosystems. *Open Journal of Biophysics*, **9**, 131-145.

[96] Andresen, B., Shiner, J.S. and Uehlinger, D.E. (2002) Allometric Scaling and Maximum Efficiency in Physiological Eigen Time. *Proceedings of the National Academy of Sciences of the United States of America*, **90**, 5822-5824. https://doi.org/10.1073/pnas.082633699

[97] Brown, J.H. and West, G.B. (2000) Scaling in Biology. Oxford University Press, Oxford.

[98] Gunther, B. and Morgado, E. (2005) Allometric Scaling of Biological Rhythms in Mammals. *Biological Research*, **38**, 207-212. https://doi.org/10.4067/S0716-97602005000200010

[99] Benzinger, T.H. (1959) On Physical Heat Regulation and the Sense of Temperature in Man. Proceedings *of the National Academy of Sciences of the United States of America*, **45**, 645-659. https://doi.org/10.1073/pnas.45.4.645

[100] Erdmann, B., Lang, J. and Seebass, M. (1998) Optimization of Temperature Distributions for Regional Hyperthermia Based on a Nonlinear Heat Transfer Model. *Annals of the New York Academy of Sciences*, **858**, 36-46. https://doi.org/10.1111/j.1749-6632.1998.tb10138.x

[101] Tompkins, D.T., Vanderby, R., Klein, S.A., Beckman, W.A., Steeves, R.A., Frey, D.M. and Palival, B.R. (1994) Temperature-Dependent versus Constant-Rate Blood Perfusion Modelling in Ferromagnetic Thermoseed Hyperthermia: Results with a Model of the Human Prostate. *International Journal of Hyperthermia*, **10**, 517-536. https://doi.org/10.3109/02656739409009355

[102] Guy, A.W. and Chou, C.K. (1983) Physical Aspects of Localized Heating by Radio-Waves and Microwaves. In: Storm, K.F., Ed., *Hyperthermia in Cancer Therapy*, GK Hall Medical Publishers, Boston, 279-304.

[103] Gottstein, U. (1969) Störungen des Hirnkreislaufes und zerebralen Stoffwechsels durch Hypoglykämie. In: Quandt, J., Ed., *Die zerebralen Durchblutungsstörungen des Erwachsenenalters*, Volk und Gesundheit, Berlin, 857-867.

[104] Hahn, G.M. (1987) Blood-Flow. In: Field, S.B. and Franconi, C., Eds., *Physics and Technology of Hyperthermia*, NATO ASI Series, Series E: Applied Sciences, Martinus Nijhoff Publishers, Dordrecht, Boston, Lanchester, No. 127, 441-446. https://doi.org/10.1007/978-94-009-3597-6_19

[105] Pence, D.M. and Song, C.W. (1986) Effect of Heat on Blood-Flow. In: Anghileri, L.J. and Robert, J., Eds., *Hyperthermia in Cancer Treatment*, Vol. II, CRC Press Inc., Boca Raton, 1-17. https://doi.org/10.1201/9780429266546-1

[106] Szasz, A., Szasz, O. and Szasz, N. (2010) Oncothermia—Principles and Practices. Springer Verlag, Dordrecht, Heidelberg. https://doi.org/10.1007/978-90-481-9498-8

[107] Silbernagl, S. and Despopoulos, A. (2015) Color Atlas of Physiology. 7th Edition, Georg Thieme Verlag, Stuttgart/New York. https://doi.org/10.1055/b-005-148942

[108] Wildeboer, R., Southern, P. and Pankhurst, Q.A. (2014) On the Reliable Measurement of Specific Absorption Rates and Intrinsic Loss Parameters in Magnetic Hyperthermia Materials. *Journal of Physics D: Applied Physics*, **47**, Article ID: 495003. https://doi.org/10.1088/0022-3727/47/49/495003

[109] Wust, P. (2005) Thermoregulation in Humans—Experiences from Thermotherapy.

Conference in Stuttgart, Nov. 21, 2005.

[110] Bassingthwaighte, J.B. (1977) Physiology and Theory of Tracer Washout Techniques for the Estimation of Myocardial Blood Flow: Flow Estimation from Tracer Washout. *Progress in Cardiovascular Diseases*, **20**, 165-189. https://doi.org/10.1016/0033-0620(77)90019-6

[111] Bassingthwaighte, J.B. (1974) Organ Blood Flow, Wash-In, Washout, and Clearance of Nutrients and Metabolites. *Mayo Clinic Proceedings*, **49**, 248-255.

[112] Feldmann, H.J., Molls, M., Hoederath, A., *et al.* (1992) Blood Flow and Steady State Temperatures in Deep-Seated Tumors and Normal Tissues. *International Journal of Radiation Oncology*, *Biology*, *Physics*, **23**, 1003-1008. https://doi.org/10.1016/0360-3016(92)90906-X

[113] Samulski, T.V., Fessenden, P., Valdagni, R., *et al.* (1987) Correlations of Thermal Washout Rate, Steady State Temperatures, and Tissue Type in Deep Seated Recurrent or Metastatic Tumors. *International Journal of Radiation Oncology*, *Biology*, *Physics*, **13**, 907-916. https://doi.org/10.1016/0360-3016(87)90106-4

[114] Mandl, F. (2008) Statistical Physics. 2nd Edition, Manchester Physics, John Wiley & Sons, Hoboken.

[115] Liu, J. (2000) Temperature Monitoring and Heating Optimization in Cancer Hyperthermia. *Progress in Natural Science*, **10**, 787-793.

[116] Deng, Z.-S. and Liu, J. (2002) Analytical Study on Bioheat Transfer Problems with Spatial or Transient Heating on Skin Surface or inside Biological Bodies. *Journal of Biomechanical Engineering*, **124**, 638-649. https://doi.org/10.1115/1.1516810

[117] Wren, J., Karlsson, M. and Loyd, D. (2001) A Hybrid Equation for Simulation of Perfused Tissue during Thermal Treatment. *International Journal of Hypertension*, **17**, 483-498. https://doi.org/10.1080/02656730110081794

[118] Davalos, R.D., Rubinsky, B. and Mir, L.M. (2003) Theoretical Analysis of the Thermal Effects during *in Vivo* Tissue Electroporation. *Bioelectrochemistry*, **61**, 99-107. https://doi.org/10.1016/j.bioelechem.2003.07.001

[119] Bagaria, H.G. and Johnson, D.T. (2005) Transient Solution to the Bioheat Equation and Optimization for Magnetic Fluid Hyperthermia Treatment. *International Journal of Hyperthermia*, **21**, 57-75. https://doi.org/10.1080/02656730410001726956

[120] Izquierdo-Kulich, E. and Nieto-Villar, J.M. (2013) Morphogenesis and Complexity of the Tumor Patterns. In: Rubio, R.G., Ryazantsev, Y.S., Starov, V.M., Huang, G.-X., Chetverikov, A.P., Arena, P., Nepomnyashchy, A.A., Ferrus, A. and Morozov, E.G., Eds., *Without Bounds: A Scientific Canvas of Nonlinearity and Complex Dynamics*. *Understanding Complex Systems*, Springer-Verlag Berlin Heidelberg, 657-691. https://doi.org/10.1007/978-3-642-34070-3_48

[121] Davies, P.C.W., Demetrius, L. and Tuszynski, J.A. (2011) Cancer as a Dynamical Phase Transition. *Theoretical Biology and Medical Modelling*, **8**, 30. https://doi.org/10.1186/1742-4682-8-30

[122] Bru, A., Albertos, S., Subiza, J.L., García-Asenjo, J.L. and Bru, I. (2003) The Universal Dynamics of Tumor Growth. *Biophysical Journal*, **85**, 2948-2961. https://doi.org/10.1016/S0006-3495(03)74715-8

[123] Guiot, C., Degiorgis, P.G., Delsanto, P.P., Gabriele, P. and Deisboeck, T.S. (2003) Does Tumor Growth Follow a "Universal Law"? *Journal of Theoretical Biology*, **225**, 147-151. https://doi.org/10.1016/S0022-5193(03)00221-2

[124] Wissler, E.H. (1998) Pennes' 1948 Paper Revisited. *Journal of Applied Physiology*, **85**, 35-41. https://doi.org/10.1152/jappl.1998.85.1.35

[125] Nelson, D.A. (1998) Invited Editorial on "Pennes' 1948 Paper Revisited". *Journal of Applied Physiology*, **85**, 2-3. https://doi.org/10.1152/jappl.1998.85.1.2

[126] Charny, C.K., Weinbaum, S. and Levin, R.L. (1990) An Evaluation of the Weinbaum-Jiji Equation for Normal and Hyperthermic Conditions. *Journal of Biomechanical Engineering*, **112**, 80-87. https://doi.org/10.1115/1.2891130

[127] Najarian, S. and Pashaee, A. (2001) Inprovement of the Pennes Equation in the Analysis of Heat Transfer Phenomenon in Blood Perfused Tissues. *Biomedical Sciences Instrumentation*, **37**, 185-190.

[128] Szasz, A. and Vincze, Gy. (2006) Dose Concept of Oncological Hyperthermia: Heat-Equation Considering the Cell Destruction. *Journal of Cancer Research and Therapeutics*, **2**, 171-181. https://doi.org/10.4103/0973-1482.29827

[129] Szasz, A. and Vincze, Gy. (2007) Hyperthermia, a Modality in the Wings. *Journal of Cancer Research and Therapeutics*, **3**, 56-66. https://doi.org/10.4103/0973-1482.31976

[130] Kim, J.-K., Prasad, B. and Kim, S. (2017) Temperature Mapping and Thermal Dose Calculation in Combined Radiation Therapy and 13.56 MHz Radiofrequency Hyperthermia for Tumor Treatment. *Proceedings SPIE* 10047, *Optical Methods for Tumor Treatment and Detection: Mechanisms and Techniques in Photodynamic Therapy XXVI*, Vol. 10047, Article ID: 1004718. https://doi.org/10.1117/12.2253163 http://spie.org/Publications/Proceedings/Paper/10.1117/12.2253163?origin_id=x4318

[131] Boldrini, J.L., Viana, M.P., dos Reis, S.F., *et al.* (2018) A Mathematical Model for Thermoregulation in Endotherms Including Heat Transport by Blood Flow and Thermal Feedback Control Mechanisms: Changes in Coat, Metabolic Rate, Blood Fluxes, Ventilation and Sweating Rates. *Letters in Biomathematics*, **5**, 129-173. https://doi.org/10.1080/23737867.2018.1497458

[132] Vincze, Gy., Szigeti, Gy.P. and Szasz, O. (2016) Non-Newtonian Analysis of Blood Flow. *Journal of Advances in Physics*, **11**, 3470-3481. https://doi.org/10.24297/jap.v11i5.6834

[133] Vincze, Gy., Szigeti, Gy.P. and Szasz, O. (2016) Negative Impedance Interval of Blood Flow in Capillary Bed. *Journal of Advances in Physics*, **11**, 3482-3487. https://doi.org/10.24297/jap.v11i5.365

[134] Szasz, O., Vincze, Gy., Szigeti, Gy.P., *et al.* (2018) An Allometric Approach of Tumor-Angiogenesis. *Medical Hypotheses*, **116**, 74-78. https://doi.org/10.1016/j.mehy.2018.03.015

[135] Szasz, O., Szigeti, Gy.P. and Szasz, A. (2016) Connections between the Specific Absorption Rate and the Local Temperature. *Open Journal of Biophysics*, **6**, 53-74. https://doi.org/10.4236/ojbiphy.2016.63007

[136] Rao, N.N. (1994) Elements of Engineering Electromagnetics. Prentice Hall International, London.

[137] Jackson, J.D. (1999) Classical Electrodynamics. John Wiley & Sons Inc., New York.

[138] Polk, C. and Postow, E. (1996) Handbook of Biological Effects of Electromagnetic Fields. CRC Press, New York, London, Tokyo, 15.

[139] Dissado, L.A. (1990) A Fractal Interpretation of the Dielectric Response of Animal Tissues. *Physics in Medicine and Biology*, **35**, 1487-1503. https://doi.org/10.1088/0031-9155/35/11/005

[140] Goldberger, A.L., Amaral, L.A., Hausdorff, J.M., *et al.* (2002) Fractal Dynamics in Physiology: Alterations with Disease and Aging. *PNAS Colloquium*, **99**, 2466-2472.

https://doi.org/10.1073/pnas.012579499

[141] Szendro, P., Vincze, G. and Szasz, A. (2001) Pink Noise Behaviour of the Bio-Systems. *European Biophysics Journal*, **30**, 227-231. https://doi.org/10.1007/s002490100143

[142] Szendro, P., Vincze, G. and Szasz, A. (2001) Bio-Response on White-Noise Excitation. *Electromagnetic Biology and Medicine*, **20**, 215-229. https://doi.org/10.1081/JBC-100104145

[143] Bak, P., Tang, C. and Wieserfeld, K. (1988) Self-Organized Criticality. *Physical Review A*, **38**, 364-373. https://doi.org/10.1103/PhysRevA.38.364

[144] Jones, E., Dewhirst, M. and Vujaskovic, Z. (2003) Hyperthermia Improves the Complete Response Rate for Superficial Tumours Treated with Radiation: Results of a Prospective Randomized Trial Testing the Thermal Dose Parameter CEM 43°T90. *International Journal of Radiation Oncology*, *Biology*, *Physics*, **57**, S253-S254. https://doi.org/10.1016/S0360-3016(03)01088-5

[145] Vernon, C.C., Hand, J.W., Field, S.B., Machin, D., Whaley, J.B., van der Zee, J., van Putten, W.L.J., van Rhoon, G.C., van Dijk, J.D.P., Gonzalez Gonzalez, D., Liu, F.-F., Goodman, P. and Sherar, M. (1996) Radiotherapy with or without Hyperthermia in the Treatment of Superficial Localized Breast Cancer: Results from Five Randomized Controlled Trials. *International Journal of Radiation Oncology*, *Biology*, *Physics*, **35**, 731-744. https://doi.org/10.1016/0360-3016(96)00154-X

[146] Sherar, M., Liu, F.-F., Pintilie, M., *et al.* (1997) Relationship between Thermal Dose and Outcome in Thermoradiotherapy Treatments for Superficial Recurrences of Breast Cancer: Data from a Phase III Trial. *International Journal of Radiation Oncology*, *Biology*, *Physics*, **39**, 371-380. https://doi.org/10.1016/S0360-3016(97)00333-7

[147] Mitsumori, M., Zeng, Z.F., Oliynychenko, P., *et al.* (2007) Regional Hyperthermia Combined with Radiotherapy for Locally Advanced Non-Small Cell Lung Cancers. *International Journal of Clinical Oncology*, **12**, 192-198. https://doi.org/10.1007/s10147-006-0647-5

[148] Shinn, K.S., Choi, I.B., Kay, C.S., *et al.* (1996) Thermoradiotherapy in the Treatment of Locally Advanced Nonsmall Cell Lung Cancer. *Journal of the Korean Society for Therapeutic Radiology and Oncology*, **14**, 115-122. https://doi.org/10.1016/0169-5002(96)85955-1

[149] Vasanthan, A., Mitsumori, M., Park, J.H., *et al.* (2005) Regional Hyperthermia Combined with Radiotherapy for Uterine Cervical Cancers: A Multi-Institutional Prospective Randomized Trial of the International Atomic Energy Agency. *International Journal of Radiation Oncology*, *Biology*, *Physics*, **61**, 145-153. https://doi.org/10.1016/j.ijrobp.2004.04.057

[150] Zolciak-Siwinska, A., Piotrkowicz, N., Jonska-Gmyrek, J., *et al.* (2013) HDR Brachytherapy Combined with Interstitial Hyperthermia in Locally Advanced Cervical Cancer Patients Initially Treated with Concomitant Radiochemotherapy—A Phase III Study. *Radiotherapy and Oncology*, **109**, 194-199. https://doi.org/10.1016/j.radonc.2013.04.011

[151] Jones, E.L., Oleson, J.R., Prosnitz, L.R., *et al.* (2005) Randomized Trial of Hyperthermia and Radiation for Superficial Tumors. *Journal of Clinical Oncology*, **23**, 3079-3085. https://doi.org/10.1200/JCO.2005.05.520

[152] Vaupel, P.W. and Kelleher, D.K. (1996) Metabolic Status and Reaction to Heat of Normal and Tumour Tissue. In: Seegenschmiedt, M.H., Fessenden, P. and Vernon, C.C., Eds., *Thermo-Radiotherapy and Thermo-Chemotherapy. Biology*, *Physiology*

and Physics, Vol. 1, Springer Verlag, Berlin Heidelberg, 157-176. https://doi.org/10.1007/978-3-642-57858-8_8

[153] Oehr, P., Biersack, H.J. and Coleman, R.E. (2004) PET and PET-CT in Oncology. Springer Verlag, Berlin-Heidelberg. https://doi.org/10.1007/978-3-642-18803-9

[154] Foster, K.R. and Schepps, J.L. (1981) Dielectric Properties of Tumor and Normal Tissues at Radio through Microwave Frequencies. *Journal of Microwave Power*, **16**, 107-119. https://doi.org/10.1080/16070658.1981.11689230

[155] Seersa, I., Beravs, K., Dodd, N.J.F., *et al.* (1997) Electric Current Imaging of Mice Tumors. *MRM*, **37**, 404-409. https://doi.org/10.1002/mrm.1910370318

[156] Landini, G. and Rippin, J.W. (1993) Fractal Dimensions of the Epithelial-Connective Tissue Interfaces in Premalignant and Malignant Epithelial Lesions of the Floor of the Mouth. *Analytical and Quantitative Cytology and Histology*, **15**, 144-149.

[157] Wong, S.H.M, Fang, C.M., Chuah, L.-H., *et al.* (2018) E-Cadherin: Its Dysregulation in Carcinogenesis and Clinical Implications. *Critical Reviews in Oncology/Hematology*, **121**, 11-22. https://doi.org/10.1016/j.critrevonc.2017.11.010

[158] Knights, A.J., Funnel, A.P., Crossley, M. and Pearson, R.C.M. (2012) Holding Tight: Cell Junctions and Cancer Spread. *Trends in Cancer Research*, **8**, 61-69.

[159] Damadian, R. (1971) Tumor Detection by Nuclear Magnetic Resonance. *Science*, **171**, 1151-1153. https://doi.org/10.1126/science.171.3976.1151

[160] Szentgyorgyi, A. (1968) Bioelectronics. A Study on Cellular Regulations, Defense and Cancer. Academy Press, New York, London.

[161] Szasz, A., Vincze, Gy., Szasz, O. and Szasz, N. (2003) An Energy Analysis of Extracellular Hyperthermia. *Magneto- and Electro-Biology*, **22**, 103-115. https://doi.org/10.1081/JBC-120024620

[162] Blad, B. and Baldetorp, B. (1996) Impedance Spectra of Tumour Tissue in Comparison with Normal Tissue; a Possible Clinical Application for Electric Impedance Tomography. *Physiological Measurement*, **17**, A105-A115. https://doi.org/10.1088/0967-3334/17/4A/015

[163] Vincze, Gy., Szigeti, Gy., Andocs, G. and Szasz, A. (2015) Nanoheating without Artificial Nanoparticles. *Biology and Medicine*, **7**, 249.

[164] Thomas, S., Preda-Pais, A., Casares, S. and Brumeanu, T.D. (2004) Analysis of Lipid Rafts in T Cells. *Molecular Immunology*, **41**, 399-409. https://doi.org/10.1016/j.molimm.2004.03.022

[165] Nicolau, D.V., Burrage, K., Parton, R.G. and Hancock, J.F. (2006) Identifying Optimal Lipid Raft Characteristics Required to Promote Nanoscale Protein-Protein Interactions on the Plasma Membrane. *Journal of Molecular Cell Biology*, **26**, 313-323. https://doi.org/10.1128/MCB.26.1.313-323.2006

[166] Nicolson, G.L. (2014) The Fluid—Mosaic Model of Membrane Structure: Still Relevant to Understanding the Structure, Function and Dynamics of Biological Membranes after More than 40 Years. *Biochimica et Biophysica Acta*, **1838**, 1451-1466. https://doi.org/10.1016/j.bbamem.2013.10.019

[167] Gramse, G., Dols-Perez, A., Edwards, M.A., Fumagalli, L. and Gomila, G. (2013) Nanoscale Measurement of the Dielectric Constant of Supported Lipid Bilayers in Aqueous Solutions with Electrostatic Force Microscopy. *Journal of Biophysics*, **104**, 1257-1262. https://doi.org/10.1016/j.bpj.2013.02.011

[168] Dharia, S. (2011) Spatially and Temporally Resolving Radio-Frequency Changes in Effective Cell Membrane Capacitance. PhD Theses, University of Utah, Salt Lake City.

[169] Pike, L.J. (2003) Lipid Rafts: Bringing Order to Chaos. *The Journal of Lipid Research*, **44**, 655-667. https://doi.org/10.1194/jlr.R200021-JLR200

[170] Andersen, O.S., Koeppe, I.I. and Roger, E. (2007) Bilayer Thickness and Membrane Protein Function: An Energetic Perspective. *Annual Review of Biophysics and Biomolecular Structure*, **36**, 107-130. https://doi.org/10.1146/annurev.biophys.36.040306.132643

[171] Nicolau Dan, V., Burrage, K, Parton, R.G. and Hancock, J.F. (2006) Identifying Optimal Lipid Raft Characteristics Required to Promote Nanoscale Protein-Protein Interactions in the Plasma Membrane. *Molecular and Cellular Biology*, **26**, 313-323

[172] Staunton, J.R., Wirtz, D., Tlsty, T.D., *et al.* (2013) A Physical Sciences Network Characterization of Non-Tumorigenic and Metastatic Cells. *Scientific Reports*, **3**, Article No. 1449. https://doi.org/10.1038/srep01449

[173] Kotnik, T. and Miklavcic, D. (2000) Theoretical Evaluation of the Distributed Power Dissipation in Biological Cells Exposed to Electric Fields. *Bioelectromagnetics*, **21**, 385-394. https://doi.org/10.1002/1521-186X(200007)21:5<385::AID-BEM7>3.0.CO;2-F

[174] Pething, R. (1979) Dielectric and Electronic Properties of Biological Materials. John Wiley and Sons, New York.

[175] Volkov, V.V., Palmer, D.J. and Righini, R. (2007) Distinct Water Species Confined at the Interface of a Phospholipid Membrane. *Physical Review Letters*, **99**, Article ID: 078302. https://doi.org/10.1103/PhysRevLett.99.078302

[176] Liu, L.M. and Cleary, S.F. (1995) Absorbed Energy Distribution from Radiofrequency Electromagnetic Radiation in a Mammalian Cell Model: Effect of Membrane-Bound Water. *Bioelectromagnetics*, **16**, 160-171. https://doi.org/10.1002/bem.2250160304

[177] Hendry, B. (1981) Membrane Physiology and Membrane Excitation. Croom Helm, London. https://doi.org/10.1007/978-1-4615-9766-7

[178] Ma, Y., Poole, K., Goyette, J., *et al.* (2017) Introducing Membrane Charge and Membrane Potential to T Cell Signaling. *Frontiers in Immunology*, **8**, 1513. https://doi.org/10.3389/fimmu.2017.01513

[179] Martinsen, O.G., Grimnes, S. and Schwan, H.P. (2002) Interface Phenomena and Dielectric Properties of Biological Tissue. Corpus ID: 41679856. https://www.semanticscholar.org/paper/INTERFACE-PHENOMENA-AND-DIELECTRIC-PROPERTIES-OF-Martinsen-Grimnes/96e2f6c14dbba2ae5537a8a637b52d486b3925ef

[180] Banerjee, S., Vandenbranden, M. and Ruysschaert, J. (1981) Interaction of Tobacco Mosaic Virus Protein with Lipid Membrane Systems. *FEBS Letters*, **133**, 221-224. https://doi.org/10.1016/0014-5793(81)80510-8

[181] Schubert, D., Bleuel, H., Domninc, B. and Wiedner, G. (1977) Protein-Induced Conductivity Changes in Black Lipid Membranes and Protein Aggregation. *FEBS Letters*, **74**, 47-49. https://doi.org/10.1016/0014-5793(77)80749-7

[182] Papp, E., Vancsik, T., Kiss, E. and Szasz, O. (2017) Energy Absorption by the Membrane Rafts in the Modulated Electro-Hyperthermia (mEHT). *Open Journal of Biophysics*, **7**, 216-229. https://doi.org/10.4236/ojbiphy.2017.74016

[183] Szasz, A., Szasz, O. and Szasz, N. (2001) Electro-Hyperthermia: A New Paradigm in Cancer Therapy. *Deutsche Zeitschrift fur Onkologie*, **33**, 91-99. https://doi.org/10.1055/s-2001-19447

[184] Szasz, O. and Szasz, A. (2013) Burden of Oncothermia: Why Is It Special? *Confe-*

rence Papers in Medicine, **2013**, Article ID: 938689.
https://doi.org/10.1155/2013/938689

[185] Szasz, A. (2015) Bioelectromagnetic Paradigm of Cancer Treatment Oncothermia. In: Rosch, P.J., Ed., *Bioelectromagnetic and Subtle Energy Medicine*, CRC Press, Taylor & Francis Group, London, 323-336.

[186] Szasz, A. (2014) Oncothermia: Complex Therapy by EM and Fractal Physiology. I*EEE General Assembly and Scientific Symposium* (*URSI GASS*), 2014 21*th URSI*, Beijing, 16-23 August 2014, 1-4. https://doi.org/10.1109/URSIGASS.2014.6930100

[187] Sowers, A.E. (1984) Characterisation of Electric Field-Induced Fusion in Erythrocyte Ghost Membranes. *The Journal of Cell Biology*, **99**, 1989-1996.
https://doi.org/10.1083/jcb.99.6.1989

[188] Marszalek, P. and Tsong, T.Y. (1995) Cell Fission and Formation of Mini Cell Bodies by High Frequency Alternating Electric Field. *Biophysical Journal*, **68**, 1218-1221.
https://doi.org/10.1016/S0006-3495(95)80338-3

[189] Cleary, S.F., Liu, L.-M. and Garber, F. (1985) Erythrocyte Haemolysis by Radiofrequency Fields. *Bioelectromagnetics*, **6**, 313-322.
https://doi.org/10.1002/bem.2250060311

[190] Liu, D.-S., Astumian, R.D. and Tsong, T.Y. (1990) Activation of Na+ and K+ Pumping Modes of (Na,K)-ATPase by an Oscillating Electric Field. *The Journal of Biological Chemistry*, **265**, 7260-7267. https://doi.org/10.1016/S0021-9258(19)39108-2

[191] Walleczek, J. (1992) Electromagnetic Field Effects on Cells of the Immune System: The Role of Calcium Signalling. *FASEB Journal*, **6**, 3177-3185.
https://doi.org/10.1096/fasebj.6.13.1397839

[192] Cho, M.R., Thatte, H.S., Silvia, M.T., *et al.* (1999) Transmembrane Calcium Influx Induced by AC Electric Fields. *FASEB Journal*, **13**, 677-683.
https://doi.org/10.1096/fasebj.13.6.677

[193] Ho, M.-W., Popp, F.-A. and Warnke, U. (1994) Bioelectrodynamics and Biocommunication. World Scientific, Singapore, London. https://doi.org/10.1142/2267

[194] Bernardi, P. and D'Inzeo, G. (1989) Physical Mechanisms for Electromagnetic Interaction with Biological Systems. In: Lin, J.C., Ed., *Electromagnetic Interaction with Biological Systems*, Plenum Press, New York, London, 179-214.
https://doi.org/10.1007/978-1-4684-8059-7_9

[195] Markov, M.S. (1994) Biological Effects of Extremely Low Frequency Magnetic Fields. In: Ueno, S., Ed., *Biomagnetic Stimulation*, Plenum Press, New York, London, 91-104.
https://doi.org/10.1007/978-1-4757-9507-3_7

[196] Bauerus, K.C.L., Sommarin, M., Persson, B.R., *et al.* (2003) Interaction between Weak Low Frequency Magnetic Fields and Cell Membranes. *Bioelectromagnetics*, **24**, 395-402. https://doi.org/10.1002/bem.10136

[197] Benett, W.R. (1994) Cancer and Power Lines. *Physics Today*, 23-29.
https://doi.org/10.1063/1.881417

[198] Portier, C.J. and Wolfe, M.S. (1998) Assessment of Health Effects from Exposure to Power-Line Frequency Electric and Magnetic Fields. National Institute of Environmental Health Sciences, Research Triangle Park, NIH Publication No. 98-3981.

[199] Harland, J.D. and Liburdy, R.P. (1997) Environmental Magnetic Fields Inhibit the Anti-Proliferation Action of Tamoxifen and Melatonin in a Human Breast Cancer Cell Line. *Bioelectromagnetics*, **18**, 555-562.
https://doi.org/10.1002/(SICI)1521-186X(1997)18:8<555::AID-BEM4>3.0.CO;2-1

[200] Ahlbom, A., Day, N., Feychting, M., *et al.* (2000) A Pooled Analysis of Magnetic

Fields and Childhood Leukaemia. *British Journal of Cancer*, **83**, 692-698. https://doi.org/10.1054/bjoc.2000.1376

[201] Greenland, S., Sheppard, A.R., Kaune, W.T., *et al.* (2000) A Pooled Analysis of Magnetic Fields, Wire Codes, and Childhood Leukaemia. *Epidemiology*, **11**, 624-634. https://doi.org/10.1097/00001648-200011000-00003

[202] Blackman, C.F., Benane, S.G. and House, D.E. (2001) The Influence of 1.2μT, 60Hz Magnetic Fields on Melatonin- and Tamoxifen-Induced Inhibition of MCF-7 Cell Growth. *Bioelectromagnetics*, **22**, 122-128. https://doi.org/10.1002/1521-186X(200102)22:2<122::AID-BEM1015>3.0.CO;2-V

[203] Glaser, R. (2005) Are Thermoreceptors Responsible for "Non-Thermal" Effects of RF Fields? Edition Wissenschaft Forschungsgemeinschaft Funk e. V. G 14515. Issue No. 21. December 2005.

[204] Zotin, A.A. and Zotin, A.I. (1996) Thermodynamic Bases of Developmental Processes. *Journal of Non-Equilibrium Thermodynamics*, **21**, 307-320. https://doi.org/10.1515/jnet.1996.21.4.307

[205] Lakhssassi, A., Kengne, E. and Semmaoui, H. (2010) Investigation of Nonlinear Temperature Distribution in Biological Tissues by Using Bioheat Transfer Equation of Pennes' Type. *Natural Science*, **2**, 131-138. https://doi.org/10.4236/ns.2010.23022

[206] Chang, I. (2003) Finite Element Analysis of Hepatic Radiofrequency Ablation Probes Using Temperature-Dependent Electrical Conductivity. *BioMedical Engineering OnLine*, **2**, Article No. 12. https://doi.org/10.1186/1475-925X-2-12

[207] Kok, H.P., Navarro, F., Strigari, L., *et al.* (2018) Locoregional Hyperthermia of Deep-Seated Tumours Applied with Capacitive and Radiative Systems: A Simulation Study. *International Journal of Hypertension*, **34**, 714-730. https://doi.org/10.1080/02656736.2018.1448119

[208] Canters, R.A.M., Franckena, M., van der Zee, J. and van Rhoon, G.C. (2011) Optimizing Deep Hyperthermia Treatments: Are Locations of Patient Pain Complaints Correlated with Modelled SAR Peak Locations? *Physics in Medicine and Biology*, **56**, 439-451. https://doi.org/10.1088/0031-9155/56/2/010

[209] Dutz, S. and Hergt, R. (2013) Magnetic Nanoparticle Heating and Heat Transfer on a Microscale: Basic Principles, Realities and Physical Limitations of Hyperthermia for Tumour Therapy. *International Journal of Hypertension*, **29**, 790-800. https://doi.org/10.3109/02656736.2013.822993

[210] Chen, C.-C., Chen, C.-L., Li, J.-J., *et al.* (2019) The Presence of Gold Nanoparticles in Cells Associated with the Cell-Killing Effect of Modulated Electro-Hyperthermia. *ACS Applied Bio Materials*, **2**, 3573-3581. https://doi.org/10.1021/acsabm.9b00453

[211] Szasz, A. (2007) Hyperthermia, a Modality in the Wings. *Journal of Cancer Research and Therapeutics*, **3**, 56-66. https://doi.org/10.4103/0973-1482.31976

[212] Guest, W.C., Cashman, N.R. and Plotkin, S.S. (2011) A Theory for the Anisotropic and Inhomogeneous Dielectric Properties of Proteins. *Physical Chemistry Chemical Physics*, **13**, 6286-6295. https://doi.org/10.1039/c0cp02061c

[213] Yang, M. and Brackenbury, W.J. (2013) Membrane Potential and Cancer Progression. *Frontiers in Physiology*, **4**, 185. https://doi.org/10.3389/fphys.2013.00185

[214] Govorov, A.O. and Richardson, H.H. (2007) Generating Heat with Metal Nanoparticles. *Nanotoday*, **2**, 30-39. https://doi.org/10.1016/S1748-0132(07)70017-8

[215] Johnson, S.A., Stinson, B.M., Go, M.S., *et al.* (2010) Temperature-Dependent Phase Behavior and Protein Partitioning in Giant Plasma Vehicles. *Biochimica et Biophysica Acta*, **1798**, 1427-1435. https://doi.org/10.1016/j.bbamem.2010.03.009

[216] Veatch, S.L., Cicuta, P., Sengupta, P., Honerkamp-Smith, A., Holowka, D. and Baird, B. (2008) Critical Fluctuations in Plasma Membrane Vesicles. *ACS Chemical Biology*, **3**, 287-295. https://doi.org/10.1021/cb800012x

[217] Langner, M., Komorowska, M., Koter, M. and Gomulkiewicz, J. (1984) Phase Transitions in Spherical Bilayer Membranes Prepared of Bulk Erythrocyte Membrane Lipids. *General Physiology and Biophysics*, **3**, 521-526.

[218] Hossain, M.T., Prasad, B., Park, K.S., *et al.* (2016) Simulation and Experimental Evaluation of Selective Heating Characteristics of 13,56 MHz Radiofrequency Hyperthermia in Phantom Models. *International Journal of Precision Engineering and Manufacturing*, **17**, 253-256. https://doi.org/10.1007/s12541-016-0033-9

[219] Andocs, G., Rehman, M.U., Zhao, Q.L., Papp, E., Kondo, T. and Szasz, A. (2015) Nanoheating without Artificial Nanoparticles Part II. Experimental Support of the Nanoheating Concept of the Modulated Electro-Hyperthermia Method, Using U937 Cell Suspension Model. *Biology and Medicine*, **7**, 1-9. https://doi.org/10.4172/0974-8369.1000247

[220] Andocs, G., Rehman, M.U., Zhao, Q.-L., Tabuchi, Y., Kanamori, M. and Kondo, T. (2016) Comparison of Biological Effects of Modulated Electro-Hyperthermia and Conventional Heat Treatment in Human Lymphoma U937 Cell. *Cell Death Discovery*, **2**, Article No. 16039. https://doi.org/10.1038/cddiscovery.2016.39

[221] Prasad, B., Kim, S., Cho, W., *et al.* (2018) Effect of Tumor Properties on Energy Absorption, Temperature Mapping, and Thermal Dose in 13,56-MHz Radiofrequency Hyperthermia. *Journal of Thermal Biology*, **74**, 281-289. https://doi.org/10.1016/j.jtherbio.2018.04.007

[222] Portoro, I., Danics, L. and Veres, D. (2018) Increased Efficacy in Treatment of Glioma by a New Modulated Electro-Hyperthermia (mEHT) Protocol. *Oncothermia Journal*, **24**, 344-356.

[223] Kao, P.H.-J., Chen, C.-H., Chang, Y.-W., *et al.* (2020) Relationship between Energy Dosage and Apoptotic Cell Death by Modulated Electro-Hyperthermia. *Scientific Reports*, **10**, Article No. 8936. https://doi.org/10.1038/s41598-020-65823-2

[224] Fiorentini, G., Sarti, D. and Casadei, V. (2019) Modulated Electro-Hyperthermia (mEHT) [oncothermia®] Protocols as Complementary Treatment. *Oncothermia Journal*, **25**, 85-115.

[225] Szasz, A.M., Arkosy, P., Arrojo, E.E., *et al.* (2020) Guidelines for Local Hyperthermia Treatment in Oncology. In: Szasz, A., Ed., *Challenges and Solutions of Oncological Hyperthermia*, Ch. 2, Cambridge Scholars, Cambridge, 32-71.

[226] Szasz, A.M., Minnaar, C.A., Szentmartoni, Gy., *et al.* (2019) Review of the Clinical Evidences of Modulated Electro-Hyperthermia (mEHT) Method: An Update for the Practicing Oncologist. *Frontiers in Oncology*, **9**, Article No. 1012. https://doi.org/10.3389/fonc.2019.01012

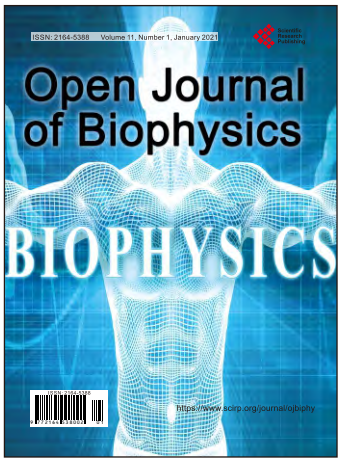

Call for Papers

Open Journal of Biophysics

ISSN Print: 2164-5388 ISSN Online: 2164-5396
https://www.scirp.org/journal/ojbiphy

Open Journal of Biophysics (OJBIPHY) is an international journal dedicated to the latest advancement of biophysics. The goal of this journal is to provide a platform for scientists and academicians all over the world to promote, share, and discuss various new issues and developments in different areas of biophysics.

Subject Coverage

All manuscripts must be prepared in English, and are subject to a rigorous and fair peer-review process. Accepted papers will immediately appear online followed by printed hard copy. The journal publishes original papers including but not limited to the following fields:

- Bioelectromagnetics
- Bioenergetics
- Bioinformatics and Computational Biophysics
- Biological Imaging
- Biomedical Imaging and Bioengineering
- Biophysics of Disease
- Biophysics of Photosynthesis
- Cardiovascular Biophysics
- Cell Biophysics
- Medical Biophysics
- Membrane Biophysics
- Molecular Biophysics and Structural Biology
- Physical Methods
- Physiology and Biophysics of the Inner Ear
- Proteins and Nucleic Acids Biophysics
- Radiobiology
- Receptors and Ionic Channels Biophysics
- Sensory Biophysics and Neurophysiology
- Systems Biophysics
- Theoretical and Mathematical Biophysics

We are also interested in: 1) Short Reports—2-5 page papers where an author can either present an idea with theoretical background but has not yet completed the research needed for a complete paper or preliminary data; 2) Book Reviews—Comments and critiques.

Notes for Intending Authors

Submitted papers should not have been previously published nor be currently under consideration for publication elsewhere. Paper submission will be handled electronically through the website. All papers are refereed through a peer review process. For more details about the submissions, please access the website.

Website and E-Mail

https://www.scirp.org/journal/ojbiphy **E-mail: ojbiphy@scirp.org**

What is SCIRP?

Scientific Research Publishing (SCIRP) is one of the largest Open Access journal publishers. It is currently publishing more than 200 open access, online, peer-reviewed journals covering a wide range of academic disciplines. SCIRP serves the worldwide academic communities and contributes to the progress and application of science with its publication.

What is Open Access?

All original research papers published by SCIRP are made freely and permanently accessible online immediately upon publication. To be able to provide open access journals, SCIRP defrays operation costs from authors and subscription charges only for its printed version. Open access publishing allows an immediate, worldwide, barrier-free, open access to the full text of research papers, which is in the best interests of the scientific community.

- High visibility for maximum global exposure with open access publishing model
- Rigorous peer review of research papers
- Prompt faster publication with less cost
- Guaranteed targeted, multidisciplinary audience

Scientific Research Publishing

Website: https://www.scirp.org

Subscription: sub@scirp.org

Advertisement: service@scirp.org